

AD-A055 658

GENERAL ELECTRIC CO CINCINNATI OHIO AIRCRAFT ENGINE GROUP F/G 21/5
BACKUP CONTROL FOR A VARIABLE CYCLE ENGINE.(U)

DEC 77 H B KAST, G L POPPEL, J E HURTLE

F33615-76-C-2086

UNCLASSIFIED

77AEG-633

AFAPL-TR-77-92

NL

1 OF 3
ADA
055658



FOR FURTHER TRAN

Handwritten scribble
2
JC

AFAPL-TR-77-92

AD A 055658

**BACKUP CONTROL
FOR A VARIABLE CYCLE ENGINE**

Phase 1 Interim Technical Report

AUTHORS:

HOWARD B. KAST
JAMES E. HURTLE
GARY L. POPPEL

GENERAL ELECTRIC COMPANY
1 JIMSON ROAD
CINCINNATI, OHIO 45215

DECEMBER 1977

TECHNICAL REPORT AFAPL-TR-77-92
FINAL REPORT FOR PERIOD AUGUST 1976 - AUGUST 1977

DDC
APR 12 1978
JUN 23 1978
F

AD No. *Handwritten mark*
DC FILE COPY

Approved for public release; distribution unlimited

78 06 21 102

AIR FORCE AERO-PROPULSION LABORATORY
AIR FORCE WRIGHT-AERONAUTICAL LABORATORIES
AIR FORCE SYSTEMS COMMAND
WRIGHT-PATTERSON AIR FORCE BASE, OHIO 45433

NOTICE

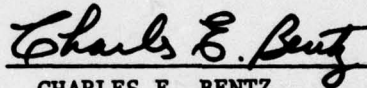
When Government drawings, specifications, or other data are used for any purpose other than in connection with a definitely related Government procurement operation, the United States Government thereby incurs no responsibility nor any obligation whatsoever; and the fact that the government may have formulated, furnished, or in any way supplied the said drawings, specifications, or other data, is not to be regarded by implication or otherwise as in any manner licensing the holder or any other person or corporation, or conveying any rights or permission to manufacture, use, or sell any patented invention that may in any way be related thereto.

This report has been reviewed by the Information Office (OI) and is releasable to the National Technical Information Service (NTIS). At NTIS, it will be available to the general public, including foreign nations.

This technical report has been reviewed and is approved for publication.

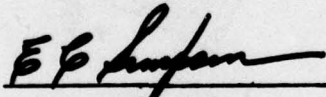


LESTER L. SMALL
Project Engineer
Components Branch



CHARLES E. BENTZ
Tech Area Manager
Components Branch

FOR THE COMMANDER



E. C. SIMPSON
Director
Turbine Engine Division

"If your address has changed, if you wish to be removed from our mailing list, or if the addressee is no longer employed by your organization please notify AFAPL/TBC, W-PAFB, OH 45433 to help us maintain a current mailing list".

Copies of this report should not be returned unless return is required by security considerations, contractual obligations, or notice on a specific document.

UNCLASSIFIED

SECURITY CLASSIFICATION OF THIS PAGE (When Data Entered)

REPORT DOCUMENTATION PAGE		READ INSTRUCTIONS BEFORE COMPLETING FORM	
1. REPORT NUMBER AFAPL-TR-77-92	2. GOVT ACCESSION NO.	3. RECIPIENT'S CATALOG NUMBER	
4. TITLE (and Subtitle) BACKUP CONTROL FOR A VARIABLE CYCLE ENGINE		5. TYPE OF REPORT & PERIOD COVERED Interim Technical Report Aug 76 - Aug 77 on phase 1	
7. AUTHOR(s) Howard B. Kast, Garry L. Poppel James E. Hurtle		6. PERFORMING ORG. REPORT NUMBER 77 AEG 633	
9. PERFORMING ORGANIZATION NAME AND ADDRESS General Electric Company Aircraft Engine Group Cincinnati, Ohio 45215		8. CONTRACT OR GRANT NUMBER(s) F33615-76-C-2086	
11. CONTROLLING OFFICE NAME AND ADDRESS Air Force Aero Propulsion Laboratory (TBC) Wright-Patterson AFB, Ohio 45433		10. PROGRAM ELEMENT, PROJECT, TASK AREA & WORK UNIT NUMBERS Project 3066 Task 306603 W.U. 30660373	
14. MONITORING AGENCY NAME & ADDRESS (if different from Controlling Office) 3066 03		12. REPORT DATE December 1977	
16. DISTRIBUTION STATEMENT (of this Report) Approved for public release; distribution unlimited.		13. NUMBER OF PAGES 192	
17. DISTRIBUTION STATEMENT (of the abstract entered in Block 20, if different from Report)		15. SECURITY CLASS. (of this report) Unclassified	
18. SUPPLEMENTARY NOTES		15a. DECLASSIFICATION/DOWNGRADING SCHEDULE N/A	
19. KEY WORDS (Continue on reverse side if necessary and identify by block number) Backup Control Emergency Control Gas Turbine Engines Control Reliability			
20. ABSTRACT (Continue on reverse side if necessary and identify by block number) The next generation of variable cycle aircraft engines will have an increased complexity associated with the number of controlled engine variables, inherent cycle variability, and inlet-engine-exhaust control integration. This level of engine complexity and the expanding integration of aircraft/engine controls causes a commensurate increase in the control system complexity and capacity. Digital electronics has been identified as the only viable means for meeting these significantly more sophisticated requirements of the future VCE. Although recent digital electronic advances promise new levels of reliability, this is offset by the increased circuitry of the more complex control. Especially in the case of the			

DD FORM 1 JAN 73 1473 EDITION OF 1 NOV 65 IS OBSOLETE

UNCLASSIFIED

SECURITY CLASSIFICATION OF THIS PAGE (When Data Entered)

403 46878 06 21 102 JOB

UNCLASSIFIED

SECURITY CLASSIFICATION OF THIS PAGE(When Data Entered)

single engine aircraft, it is recognized that such variable cycle engines should be equipped with a Backup Control for emergency use.

This report documents the results of Phase I, the trade studies, of the Backup Control for a Variable Cycle Engine program. The trade studies were based on a single engine aircraft, the JTDE-23 engine and a full authority digital electronic primary control system. A minimum 'get home' capability was defined which included completing a takeoff, a minimum climb rate, deceleration from supersonic flight, windmill air start, minimum cruise range, wave-off, landing and safe runway roll. Backup control requirements were determined using the YF17 aircraft data for thrust, the JTDE-23 engine computer model for the variables to be controlled, and the F101 engine and control model for transient performance. Seven backup control approaches were selected for consideration from a list of 48 possibilities. These approaches included hydromechanical, electrical, fluidic and a combination of electrical/hydromechanical technologies. Reliability estimates were made on six controls; and estimated performance, volume, weight, cost analyses and preliminary design studies were made in more detail on three of these approaches. A recommended approach was selected; namely, the hydromechanical backup control using speed demand and fuel flow scheduling. This selection was based on the above analyses and studies, together with a comparison of the technologies, a comparison of parallel versus series type backup/primary control interface and a tabulated evaluation of each backup control's advantages and disadvantages.

ACCESSION for	
NTIS	W. H. Section <input checked="" type="checkbox"/>
DDC	D. H. Section <input type="checkbox"/>
UNANNOUNCED	<input type="checkbox"/>
JUSTICE	
BY	
DISTRIBUTION/AVAILABILITY CODES	
D.	ITAL
A	

UNCLASSIFIED

SECURITY CLASSIFICATION OF THIS PAGE(When Data Entered)

FOREWORD

This report describes a design study effort conducted by the General Electric Company and sponsored by the Air Force Aero Propulsion Laboratory, Air Force Systems Command, Wright-Patterson AFB, Ohio under Project 3066, Task 03 and Work Unit 73 with Lester L. Small, AFAPL/TBC as Project Engineer.

The work reported herein was performed during the report period of August 15, 1976 to August 30, 1977. Ray E. Anderson was the General Electric Program Manager and the technical work was performed under the direction of Howard B. Kast, Engineering Manager. The Engineering Manager was assisted by James E. Hurtle, Gary L. Poppel and Robert P. Wanger.

This report covers Phase I of the Backup Control for a Variable Cycle Engine Program and summarizes the system trade studies and backup control selection. Phase II, a continuation of this program, will involve the design, fabrication and bench testing of the selected backup control.

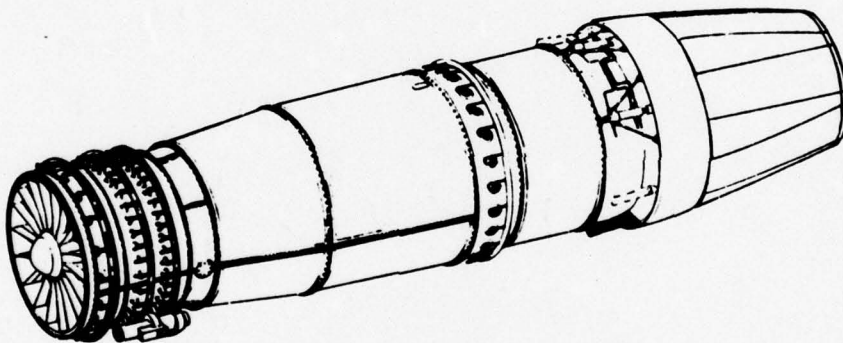


TABLE OF CONTENTS

<u>SECTION</u>	<u>PAGE</u>
I INTRODUCTION	1
II POSSIBLE APPROACHES	3
III SELECTION OF THE RECOMMENDED APPROACH	21
IV CONCLUSIONS	33
V RECOMMENDATIONS	35
APPENDICES - SUPPORTING DATA	39
A STATEMENT OF WORK	39
B DESCRIPTION OF VARIABLE CYCLE ENGINE	41
C SELECTION OF THE AIRCRAFT	43
D DESCRIPTION OF PRIMARY ELECTRONIC CONTROL SYSTEM	44
E DEFINITION OF MINIMUM GET HOME CAPABILITY	50
F OPERATIONAL OBJECTIVES AND CONSTRAINTS	51
G STEADY-STATE AND TRANSIENT ENGINE PERFORMANCE REQUIREMENTS	56
H BACKUP CONTROL REQUIREMENTS	61
I HYDROMECHANICAL BACKUP CONTROL HAVING CORE SPEED SETTING WITH SCHEDULED FUEL FLOW LIMITS IN A PARALLEL CONFIGURATION	88
J HYDROMECHANICAL BACKUP CONTROL HAVING A CORE SPEED SETTING FUNCTION WITH SCHEDULES FUEL FLOW LIMITS IN A SERIES CONFIGURATION	118
K COMBINATION ELECTRICAL/HYDROMECHANICAL APPROACH HAVING FUEL FLOW SETTING FUNCTION WITH FUEL RATE LIMITS IN A SERIES CONFIGURATION	119
L HYDROMECHANICAL BACKUP CONTROL HAVING FUEL FLOW SETTING FUNCTION WITH FUEL RATE LIMITS IN A SERIES CONFIGURATION	153
M HYDROMECHANICAL BACKUP CONTROL HAVING A FUEL FLOW SETTING FUNCTION WITH FUEL RATE LIMITS IN A PARALLEL CONFIGURATION	154

TABLE OF CONTENTS (Concluded)

<u>SECTION</u>		<u>PAGE</u>
N	ELECTRICAL BACKUP CONTROL HAVING CORE SPEED SETTING WITH SPEED RATE LIMITS IN A PARALLEL CONFIGURATION	157
O	FLUIDIC BACKUP CONTROL HAVING FUEL FLOW SETTING FUNCTION WITH FUEL RATE LIMITS IN A SERIES CONFIGURATION	188

LIST OF FIGURES

<u>FIGURE</u>	<u>PAGE</u>
1. Series Arrangement of Primary and Backup Controls	4
2. Parallel or Standby Arrangement of Primary and Backup Controls	5
3. A Matrix Of Backup Control Alternate Approaches	7
4. Hydromechanical Backup Control Schematic	9
5. Schematic for the Combination Electrical/Hydromechanical Backup Control	13
6. Block Diagram for the Electrical Approach	17
7. Fluidic Backup Control for Variable Cycle Engine	19
8. Components Required for a Parallel Redundant Fuel Metering Approach	29
B-1 JTDE-23 Engine	42
D-1 JTDE Control System FADEC	45
D-2 Hydromechanical Backup Control Using W_f/P_{T2}	46
D-3 Servovalve with Fluidic Override	48
D-4 Fluidic Servovalve	48
F-1 Possible Backup Control Inputs and Outputs	53
F-2 Vibration Requirements for Gearbox Mounted Components	54
G-1 Estimated Performance on Backup Control Operation Showing Fan Speed, Percent Increase of Specific Fuel Consumption (SFC) and F_N versus PLA	59
G-2 Operation on Backup Control, Fan Stall Margin and T_{41} vs. PLA	60
H-1 Backup Control Parameters vs. Mach Number, JTDE-23 Cycle Operation on Limits	62
H-2 Variation in T_{41} for Hot and Cold Day	64
H-3 Temperature Limiting on W_f and W_f/P_{T2} Backup Control	65
H-4 Temperature Limiting on W_f , W_f/P_{T2} and W_f/P_{S3} Backup Control	66
H-5 Effect on Turbine Temperature Variation of Adding W_f/P_{S3} Backup Control Mode — T_{41} vs $T_{2.5}$	67
H-6 Effect on Turbine Temperature Variation of Adding W_f/P_{S3} Backup Control Mode — ΔT_{41} vs Mach Number	68

LIST OF FIGURES (Continued)

<u>FIGURE</u>	<u>PAGE</u>
H-7 Overspeed Limit Selection	69
H-8 Temperature Limiting on W_f , W_f/P_{T2} and N_G Backup Control	70
H-9 Backup Control Mode Investigation with Variation in T_{41} as a Function of $T_{2.5}$	71
H-10 Backup Control Mode Investigation with Variation in T_{41} as a Function of Mach Number	72
H-11 Temperature Limiting on W_f and W_f/P_{T2} Backup Control, all Other Variables Failed on Stops	74
H-12 Turbine Temperature Variation Comparison; Nonmanipulated Variables at SLS and Against Stops, W_f/P_{T2} and W_f Backup Modes	75
H-13 Temperature Limiting on N_G Overspeed Limit, All Other Variable Failed on Stops	76
H-14 Corrected Core Speed vs. W_f/P_{T2}	77
H-15 F101 \dot{W}_f vs. W_f , Min Dry to Max Dry Accel	78
H-16 \dot{N}_G For Various F101 Accels	79
H-17 \dot{N}_G/P_{T2} For Various F101 Accels	80
I-1 Hydromechanical Backup Control Schematic	89
I-2 Transfer Valve for the Hydromechanical Approach	94
I-3 Schematic of the Electrical Portion of the Hydromechanical Approach	96
I-4 Partial Section Showing the Speed Sensor	97
I-5 Partial Section Showing the PLA Cam and Several Levers	98
I-6 Partial Section Showing the Metering Valve Servo	99
I-7 Partial Section Showing the $T_{2.5}$ Servo	100
I-8 Side View of Hydromechanical Backup Control With Integrated Fuel Valve	101
I-9 End View of Hydromechanical Backup Control	102
I-10 Components Included in the Hydromechanical Backup Control	103
I-11 Schematic of Metering Valve Servo	105
I-12 Functional Block Diagram of the Metering Valve Servo	107

LIST OF FIGURES (Continued)

<u>FIGURE</u>		<u>PAGE</u>
I-13	Revised Block Diagrams Showing Linearizations	110
I-14	Response While Flapper Is Fixed Open (Saturated)	111
I-15	Fuel Flow Response To a Step Torque Input Not Causing Flapper Saturation	113
I-16	Response While Flapper Is Closing - Simplified Case (Unsaturated)	115
I-17	Fuel Flow Transient Upon Transfer From FADEC to Hydromechanical Control	116
K-1	Schematic for the Combination Electrical/Hydromechanical Backup Control	121
K-2	Section View A	124
K-3	Section View B	125
K-4	Top View	126
K-5	End View	127
K-6	Components Included in the Combination Electrical/Hydromechanical Backup Control	128
K-7	W_f/P_{amb} vs. PLA From F101 PV Cycle Data	134
K-8	Backup Control β_c vs. W_f/P_{T2} Schedule	135
K-9	W_f/P_{amb} vs. β_c F101 PV Cycle Data, Steady-State Conditions	136
K-10	Backup Control Fuel Flow Demand Cam Definition	139
K-11	Hydromechanical Backup Control Model Block Diagram As Combined With An Existing Engine Main Control Model	140
K-12	Hydromechanical Backup Control Model Block Diagram As Run in Backup Mode	141
K-13	Backup Control Fuel Flow Rate vs. Fuel Flow Min To Max Dry Power	142
K-14	Backup Control Throttle Burst at $P_{T2} = 4.0$ PSIA	143
K-15	Backup Control Throttle Burst at $P_{T2} = 9.4$ PSIA	144
K-16	Backup Control Model Throttle Burst at SLS Standard Day	145
K-17	Backup Control Throttle Burst at $P_{T2} = 23$ PSIA	146
K-18	β_c vs. $N_G/\sqrt{\theta}$ 2.5 Steady-State and Throttle Burst at $P_{T2} = 4.0$ PSIA	147

LIST OF FIGURES (Concluded)

<u>FIGURE</u>	<u>PAGE</u>
K-19 β_c vs. $N_G/\sqrt{\theta}_{2.5}$ Steady-State and Throttle Burst at $P_{T2} = 9.37$ PSIA	148
K-20 β_c vs. $N_G/\sqrt{\theta}_{2.5}$ Steady-State and Throttle Burst at $P_{T2} = 14.7$ PSIA	149
K-21 β_c vs. $N_G/\sqrt{\theta}_{2.5}$ Steady-State and Throttle Burst at 23.0 PSIA	150
M-1 Tracking System	155
N-1 Block Diagram for the Electrical Approach	158
N-2 Transfer Valve for the Electrical Approach	159
N-3 Fuel Valve Interface for the Electrical Control	161
N-4 Core Stator Actuator Interface for the Electrical Approach	162
N-5 Electrical Backup Control Block Diagram	163
N-6 Electrical Backing Control Power Supply	165
N-7 Electrical Backup Control LVDT Sine Wave Generator	167
N-8 Electrical Backup Control $T_{2.5}$ and β_c Schedule Circuits	169
N-9 Electrical Backup Control PLA, P_{T2} , S/V Driver, N_G Circuits	171
N-10 Layout - Backup Control	175
N-11 FADEC Substrate Cross Section	178
N-12 Components Included In the Electrical Backup Control	181
N-13 Estimated Response of the Electrical Backup Control to a Throttle Burst at SLS ($\dot{N}_G = 30$ rpm/sec/PSIA)	183
N-14 Estimated Response of the Electrical Backup Control to a Throttle Burst at $P_{T2} = 10.1$ PSIA	184
N-15 Estimated response of the Electrical Backup Control to a Throttle Burst at $P_{T2} = 5.91$ PSIA	185
O-1 Fluidic Backup For Variable Cycle Engine	189
O-2 Amplifier Stackups	191

LIST OF TABLES

TABLE	PAGE
1. Comparison of Technologies	22-24
2. Summary of the Reliability Analyses	25
3. Reliability Summary of Parts Common to Primary and Backup Controls	28
4. Summary of Comparative Analysis	32
G-1 Estimated Engine Level Failure Effects	58
I-1 Hydromechanical Backup Control Reliability	104
J-1 Reliability Summary for the Backup Control Based Upon Present MFC Practice - Hydromechanical/Series/ N_G / W_f Scheduled	118
K-1 Combination Electrical/Hydromechanical Backup Control Element Failure Rates/ 10^6 Hours	130
K-2 Combination Backup Control Reliability Summary	131
K-3 Total Combination Backup Control Configuration Reliability	131
K-4 Hydromechanical Elements of the Combination Backup Control Approach Which Contribute to Get Home Power Loss	132
L-1 Reliability Summary for the Hydromechanical/Series/ W_f / \dot{W}_f Backup Control	153
M-1 Reliability Summary for the Hydromechanical/Parallel/ W_f / \dot{W}_f Backup Control	154
N-1 Electrical Backup Control Circuitry Parts Count and Reliability	180
N-2 Electrical Backup Control Reliability	182

LIST OF SYMBOLS

A_4	—	Turbine Nozzle Area, High Pressure
A_{54}	—	Turbine Nozzle Area, Low Pressure
A_8	—	Exhaust Nozzle Area
DAO	—	Discovered at Overhaul
FADEC	—	Full Authority Digital Electronic Control
FBTV	—	Forward Bypass Transition Valve
F_N	—	Thrust, Net
FR	—	Failure Rate
GHPL	—	Get Home Power Loss
JTDE	—	Joint Technology Demonstrator Engine
LVDT	—	Linear Voltage Differential Transformer
MFC	—	Main Fuel Control
M_o	—	Mach Number
MPL	—	Mission Power Loss
N_1	—	Fan RPM
N_G (or N_2)	—	Gas Generator RPM
\dot{N}_G	—	Gas Generator RPM Rate
P_1	—	Pump Discharge Pressure
P_{C1}	—	Metering Valve Servo Pressure, Closing
PDM	—	Pulse Duration Modulation
PL	—	Power Loss
PLA	—	Power Lever Angle
P_o	—	Case Pressure, Control
P_S	—	Servo Pressure
P_{S3}	—	Compressor Discharge Pressure, Static

LIST OF SYMBOLS (Concluded)

P_{T2}	—	Inlet Pressure, Total
P_x	—	Throttling Valve Servo Pressure, Opening
$T_{2.5}$	—	Compressor Inlet Temperature
T_{41}	—	Turbine Inlet Temperature
UCR	—	Unscheduled Component Removal
$VABI_A$	—	Variable Area Bypass Injectors, Aft
$VABI_F$	—	Variable Area Bypass Injectors, Forward
W_f	—	Fuel Flow
\dot{W}_f	—	Fuel Flow Rate
W_{FM}	—	Fuel Flow, Main
W_{FR}	—	Fuel Flow, Reheat (Augmentor)
β_c	—	Core Stator Angle
β_F	—	Fan Stator Angle
$\theta_{2.5}$	—	$T_{2.5}/518.7^\circ R$

SUMMARY

Phase I of the program, Backup Control for a Variable Cycle Engine, involved identifying trade study ground rules, a definition of the backup control requirements and the performance of hardware trade studies. The Joint Technology Demonstrator Engine (JTDE-23) was selected as the engine for the trade studies. The Full Authority Digital Electronic Control (FADEC), the selected primary control, is being designed for this engine. The aircraft used in the trade study was the YF17 modified to have a single GE JTDE-23 engine. The JTDE-23 airflow is directly compatible with the aircraft and drag polar data and other information were available to develop realistic backup control evaluations.

Minimum "get home" capability was defined, namely those functions which the aircraft/engine system should be capable of doing while transferring to and while operating on backup control. This capability included completing a takeoff, a minimum climb rate, deceleration from supersonic flight, windmill air start, minimum cruise range, wave-off, landing and safe runway roll. Operational constraints were determined including pilot action to adjust for tolerable but undesirable overspeed or overtemperature, for decelerating from supersonic speeds and for windmill air starting. There will be no PLA restrictions at subsonic conditions. The control environmental requirements are those of a Mach number 2.5 aircraft engine.

Then the backup control requirements were determined. The engine thrust requirements were taken from the available data on the YF17. Using the JTDE-23 computer model, it was found that satisfactory thrust and engine protection was provided by controlling only fuel flow and core stator angle. The remaining variables would be allowed to drift slowly toward and remain at fixed stops during transfer to and operation in the backup mode. Accel data on the F101 engine was used to establish transient requirements of the control. Three acceptable control modes were defined; one was based on fuel flow and inlet pressure (W_f/P_{T2}), and the second was based on core speed rate (\dot{N}_G) and the third was based on schedules determined by N_G and compressor inlet temperature ($T_{2.5}$).

Four backup control approaches, one hydromechanical, one fluidic, one electrical and one combination electrical/hydromechanical, were defined schematically. The three technologies (hydromechanical, electrical and fluidic) and the resulting schematics were compared. The fluidic approach was eliminated based on this comparison and a preliminary design study was conducted on the remaining three.

The hydromechanical backup control, which is of the parallel or standby type, demands N_G and schedules W_f for the transient limit. The W_f and β_c schedules are computed based on N_G , $T_{2.5}$, and compressor discharge pressure (P_{S3}). This computer is very similar to those used on many prior hydromechanical main fuel controls. A transfer valve is used to switch W_f and β_c servo pressures from the primary servovalves to those of the backup servovalves.

The electrical backup control, also of the parallel or standby type, demands N_G and uses speed rate (\dot{N}_G) as the transient limit. The speed rate is varied directly with P_{T2} . This approach also uses a transfer valve in the same manner as the hydromechanical approach.

The combination electrical/hydromechanical backup, which is of the series or summing type, demands W_f and uses fuel flow rate (\dot{W}_f) as the transient limit. The \dot{W}_f is varied as a function of fuel flow level and P_{T2} . With this approach, the primary and backup W_f and β_c demands are summed. In the primary mode, the backup W_f and β_c demands are higher during both steady-state and transient operation. The primary control subtracts from the backup limits to attain the desired W_f and β_c position.

The backup control is active in both the primary and backup modes. Transfer is initiated by a zero current signal to the primary W_f and β_c servovalves after which the primary W_f and β_c demands slowly drift toward the backup limits. This type of transfer is ideal since it essentially switches rates and no transfer valve is used.

The three above defined backup controls were analyzed in regards to reliability, volume, weight and cost. The significant result of the reliability analysis was that a parallel type of backup control provided better protection against loss of get home capability than the series type. The volume, weight and cost estimates indicated that the combination electrical/hydromechanical is larger, heavier and more costly than either electrical or hydromechanical types. Performance studies were also conducted. The combination control, which uses fuel flow rate as the accel parameter, was least familiar. The combination control model was superimposed on an F101 engine model and an estimate of its steady state and transient performance was obtained. F101 accel data were also used to estimate transient performance of the electrical control. The hydromechanical backup control uses a conventional accel/decel approach so only its transfer action was investigated analytically. In addition, the inherent advantages of each of the control approaches and the advantages of parallel and series backup/primary systems were compared.

Based on the results of the above analyses and comparisons, the parallel hydromechanical backup control, which demands N_G and schedules W_f , was recommended for design fabrication and test in Phase II of this program. This selection was made because it has the reduced unscheduled shutdown associated with parallel systems and because the analyses showed this to be a lightweight economical approach. It has the further advantage of representing a construction technology inherently different from the primary electronic control, thus assuring a reduction in common mode single cause failure.

SECTION I

INTRODUCTION

This program covers the design, fabrication, and testing of a Backup Control for a Variable Cycle Engine. This development effort is in support of the evolving full-authority digital electronic control technology. The backup control will provide the aircraft with at least a "get-home" capability in the event that the primary electronic control system is inoperative due to a failure or loss of electrical power.

The need for the electronic engine control relates fundamentally to the increased complexity, i.e., number of controlled engine variables, inherent cycle variability, inlet-engine-exhaust control integration, of the next generation of sophisticated variable cycle engines. This level of engine complexity and the expanding need for more complete aircraft/engine control integration forces a commensurate increase in the complexity and required capability of the control system. This increased control system capability is needed to provide stable, responsive, safe, and precise engine control.

Digital electronics represents the only viable means of meeting the significantly more sophisticated requirements of the variable cycle engine of the future. With its inherent ability to "time-share" in the computational section of the control, increasing requirement complexity yields a very much smaller increase in hardware when compared to present control system mechanizations. Digital electronics also lends itself to "hardening" to the aircraft engine environment through hybrid construction, packaging, and environmental conditioning techniques.

As good as digital electronics are today, significant improvements are being developed for application to gas turbine engine controls in order to achieve the higher levels of control reliability desired in 1985-1990. It is recognized that the full-authority digital electronic control for VCE is yet to be evaluated under field conditions and compared to the reliability record demonstrated by hydromechanical computer/controllers. This program was pursued in consideration of the significantly increased complexity of a VCE control system, and the current development status of the digital electronic approach. Since VCE propulsion systems are rapidly becoming a reality, conducting this program to develop VCE backup control technology is most timely.

The program consists of two primary phases. The Phase I objectives were to conduct comprehensive reliability, cost and performance evaluations on a variety of hydromechanical, electronic and fluidic backup control approaches for variable cycle engines having a primary electronic control system and then to select a single approach for subsequent design, fabrication and testing. The objectives of Phase II are to conduct the detailed design of the selected backup control, fabricate the control, and conduct bench testing in conjunction with a specifically designed backup control test console.

The trade studies begin with an examination of the various potential backup control techniques. Based on system concept, demand and transient limit parameters and alternative implementation technologies, theoretically many different backups could be considered. Seven of these were identified for various levels of study on this program. Parametric studies were conducted to identify satisfactory backup control parameters. Also, the steady-state cycle deck was used to determine overtemperature levels and constraining areas of the flight map. System concepts and transfer techniques were evaluated to establish requirements. Here the series vs parallel system configuration takes on fundamental importance. In a series system as used in this study, the backup and primary fuel flow demands are summed in the primary mode. This means that in a series system any reliability limits in the backup can influence the "get home" power loss rates. On the other hand, in a parallel system, the backup control is normally in a standby mode and comes into action only when backup is needed.

With these considerations in place, comparative reliability calculations have been performed for six investigated concepts. In the most promising approaches detailed study was performed. This involves preparing schematics which depict the implementation of each control function with the associated interfacing. From these schematics design studies were conducted yielding size, weight and other important tradeoff data.

This report is organized to provide a straightforward understanding of the tradeoff/selection work by covering possible approaches, approach selection, conclusions and recommendations in that order. Appendices follow which provide the complex and sometimes lengthy technical detail supporting these tradeoffs and through which the tradeoff numbers were obtained.

A brief description of each concept studied is given in Section II - Possible Approaches. A comparison of these alternatives with respect to reliability, size, weight and production cost together with advantages and disadvantages is given in Section III - Selection of Recommended Approach. Section IV - Conclusions identifies the selected approach with its anticipated performance capability. Recommendations for proceeding with the development of this one selected approach are given in Section V - Recommendations. Such development is planned as a Phase II activity.

The engines, aircraft and primary control system which interface with this backup control have been delineated in Appendices B, C and D, respectively. The requirements including get home capability, operational, engine steady state and transient as well as backup control requirements will be found in Appendices E through H inclusive. The detailed technical developments and conceptual designs which were prepared to support the trade studies will be found in the last seven appendices as follows:

- I. Hydromechanical Backup, N_G/W_f , Parallel
- J. Hydromechanical Backup, N_G/W_f , Series
- K. Hydromechanical/Electronic Backup, W_f/\dot{W}_f , Series
- L. Hydromechanical Backup, W_f/\dot{W}_f , Series
- M. Hydromechanical Backup, W_f/\dot{W}_f , Parallel
- N. Electronic Backup, N_G/\dot{N}_G , Parallel
- O. Fluidic Backup, W_f/\dot{W}_f , Series

Finally, note that the contract Statement of Work has been provided in Appendix A for reference.

SECTION II

POSSIBLE APPROACHES

1. BACKGROUND

The alternate possibilities for backup engine control are many because alternates exist in mechanization technologies, configuration relationship to the primary control, and demanded parameters and transient limits (i.e., control logic). For example the following mechanization technologies are available to the backup engine control designer:

- Hydromechanical - the proven technology of many primary engine controls today.
- Electrical - either analog or digital utilized in simplified form in the more complex prior engine controls.
- Fluidic - utilizing new technologies for freedom from mechanical moving part controls.
- Combination of technologies - which are often found in present engine controls.

The backup engine control may assume alternate configuration relations to the primary control:

- A series arrangement in which the backup control acts as an interface between the primary control and the engine is shown in Figure 1. Failure of the primary control permits continued operation of the engine without transfer action to the backup control which sets base values at all times. Production engines having electrical trim of hydromechanical controls use this approach.
- A parallel or standby arrangement in which a transfer valve can either manually or automatically select the backup control upon primary control failure as shown in Figure 2.

The backup control may demand alternate steady state engine parameters. Two fundamental alternates were considered in this study, namely:

- Pilot's PLA demands core rpm and then fuel flow is controlled to meet that demand (i.e., a speed governor approach).
- Pilot's PLA more directly demands the fuel flow to inlet pressure ratio (\dot{W}_f/P_{T2}).

The backup control, when in command of the engine, requires limits to permit unrestricted pilot's PLA movement without engine damage due to overtemperature, overpressure, or combustor blowout (identified as an operational requirement). The alternate engine limits considered in this study were the following:

- Limit fuel flow by limiting the rate of change of core rpm.
- Limit the rate of change of fuel flow or the ratio of fuel flow rate to inlet pressure (\dot{W}_f , \dot{W}_f/P_{T2} , \dot{W}_f/P_{T2}^2).
- Limit fuel flow as a scheduled limit which is a function of core rpm, inlet or compressor discharge pressure, and inlet temperature (conventional practice today).

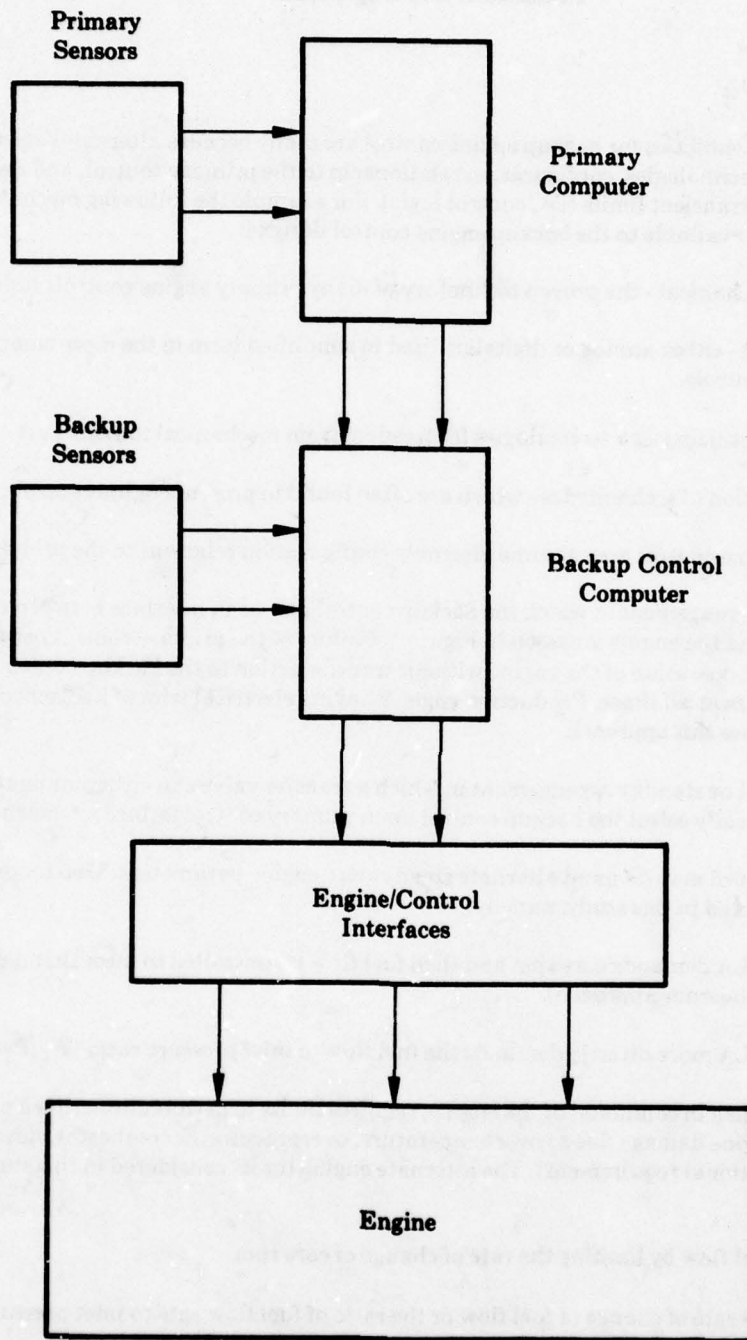


**Figure 1 - Series Arrangement
of Primary and Backup Controls.**

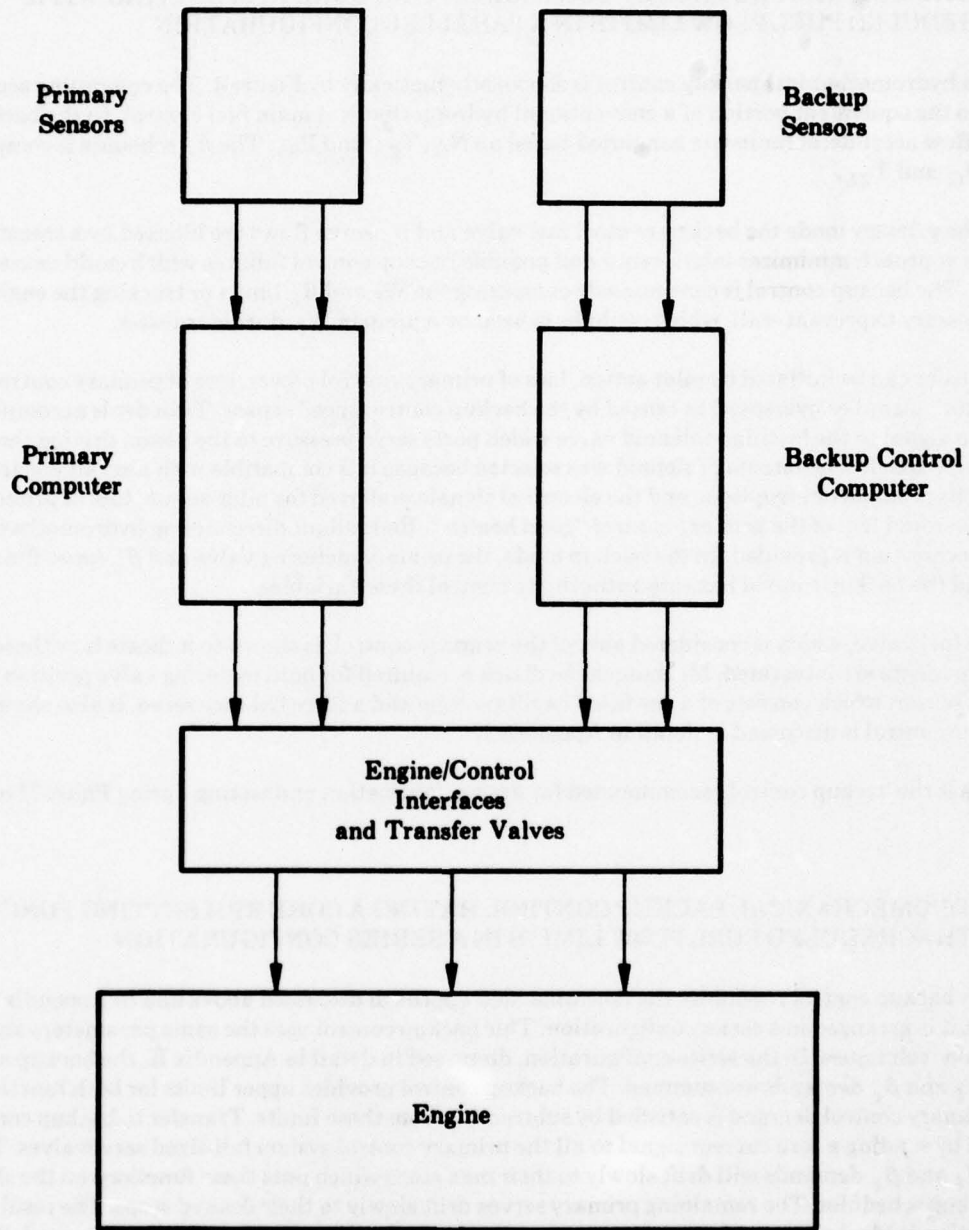


Figure 2 - Parallel or Standby Arrangement of Primary and Backup Controls.

When all of the combinations of these alternates are considered, 48 possibilities evolve as shown on Figure 3. Of these, seven were explored in this study as indicated. Each is briefly described below with design details included in the appendices. In addition to those discussed below, backup controls with no transient limits were considered. This type is not recommended based on unsatisfactory past experience and pilot work load considerations.

2. **HYDROMECHANICAL BACKUP CONTROL HAVING CORE RPM SETTING WITH SCHEDULED FUEL FLOW LIMITS IN A PARALLEL CONFIGURATION**

This hydromechanical backup control is shown schematically by Figure 4. The computing section is similar to the equivalent portion of a conventional hydromechanical main fuel control. In the backup mode fuel flow accel/decel limits are computed based on N_G , $T_{2.5}$ and P_{S3} . The β_c schedule is computed based on N_G and $T_{2.5}$.

In the primary mode the backup control fuel valve and β_c servo flows are blocked by a transfer valve. This approach minimizes interference and possible backup control failures which could cause power loss. The backup control is continuously computing the W_f and β_c limits or tracking the engine. This is necessary to prevent stall, which could be caused by a jump in W_f , during transfer.

Transfer can be initiated by pilot action, loss of primary control power, loss of primary control "good health" signal or overspeed as sensed by the backup control speed sensor. Transfer is accomplished by a current signal to the latching solenoid valve which ports servo pressure to the piston driving the transfer valve spool. The latching solenoid was selected because it is compatible with aircraft electrical power and its possible interruptions and the electrical signals preferred for pilot action, loss of primary control power and loss of the primary control "good health". Redundant direct acting hydromechanical overspeed protection is provided. In the backup mode, the primary metering valve and β_c servo flows are blocked and the backup control has sole authority to control these variables.

The fuel valve, which is considered part of the primary control, is shown to indicate how these two major components are integrated. Mechanical feedback is required for both metering valve position and β_c . A $T_{2.5}$ sensor, which consists of a gas filled capillary tube and a force balance servo, is also shown. This backup control is discussed in detail in Appendix I.

This is the backup control recommended for design, fabrication and testing during Phase II of this program.

3. **HYDROMECHANICAL BACKUP CONTROL HAVING A CORE RPM SETTING FUNCTION WITH SCHEDULED FUEL FLOW LIMITS IN A SERIES CONFIGURATION**

This backup control resembles the recommended approach discussed above and in Appendix I except that it is arranged in a series configuration. This backup control uses the same parameters and computation techniques. In the series configuration, discussed in detail in Appendix K, the backup and primary W_f and β_c demands are summed. The backup control provides upper limits for both functions and the primary control demand is satisfied by subtracting from these limits. Transfer to backup control is initiated by sending a zero current signal to all the primary control system fail-fixed servovalves. The primary W_f and β_c demands will drift slowly to their max stops which puts these functions on the slightly higher backup schedules. The remaining primary servos drift slowly to their desired stops. The resulting transfer action is ideal since no abrupt changes occur in any variable and no transfer valve is needed.

Additional information on this control is given in Appendix J.

Backup System	Demanded Parameter	Transient Limit	Alternate Mechanization			
			Hydromechanical	Combination	Electrical	Fluidic
Series	N_G	\dot{N}_G				
		\dot{W}_f				
		W_f	Reliability Estimate Reported in Appendix J			
	W_f	\dot{N}_G				
		\dot{W}_f	Reliability Estimate Reported in Appendix L	Design, Estimates Reported In Appendix K		Preliminary Design Investigation Reported in Appendix O
		W_f				
Parallel (Standby)	N_G	\dot{N}_G			Design, Estimates Reported In Appendix N	
		\dot{W}_f				
		W_f	Recommended-Reported in Appendix I			
	W_f	\dot{N}_G				
		\dot{W}_f	Reliability Estimate Reported in Appendix M			
		W_f				

Figure 3 - A Matrix Of Backup Control Alternate Approaches.

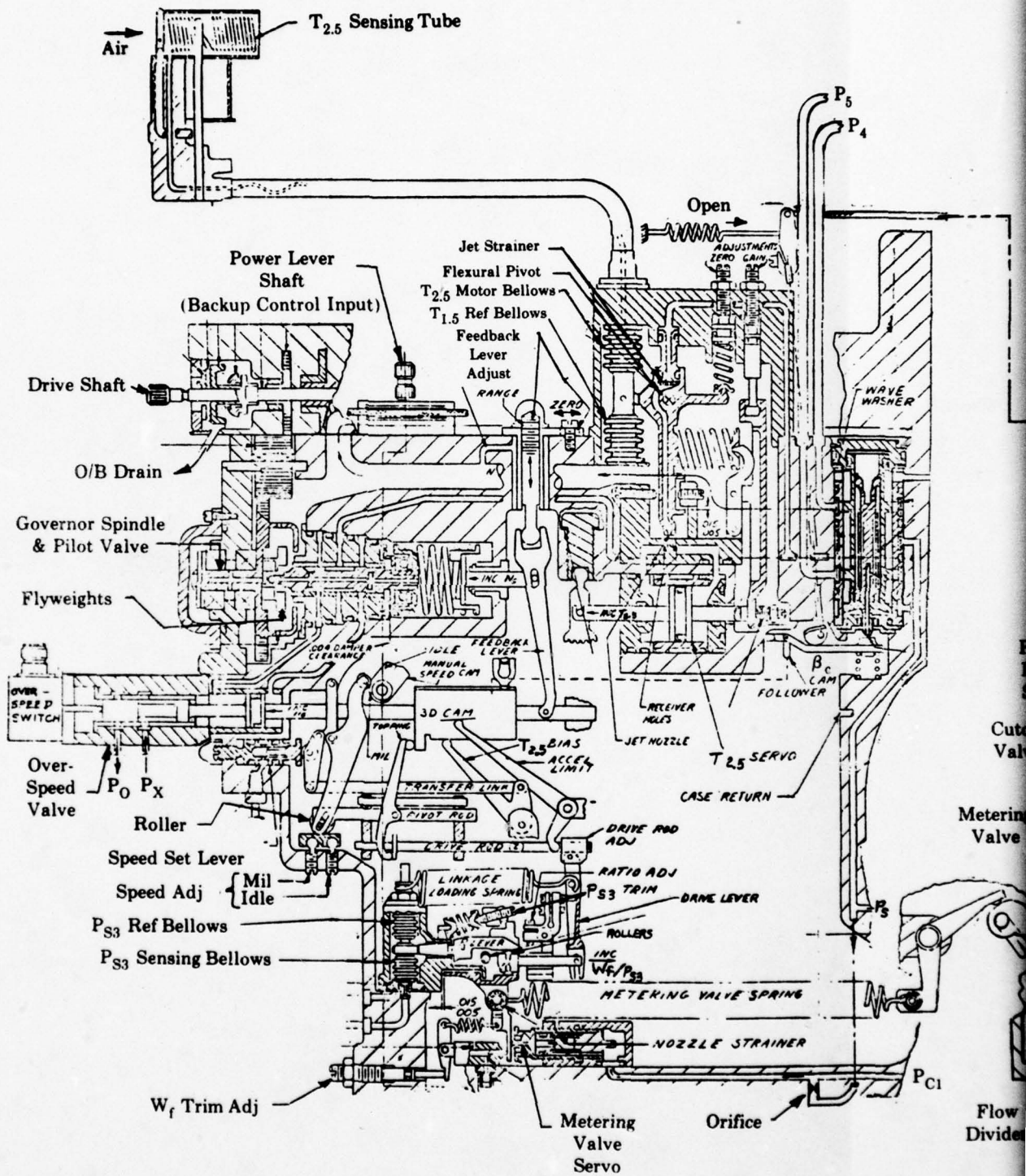
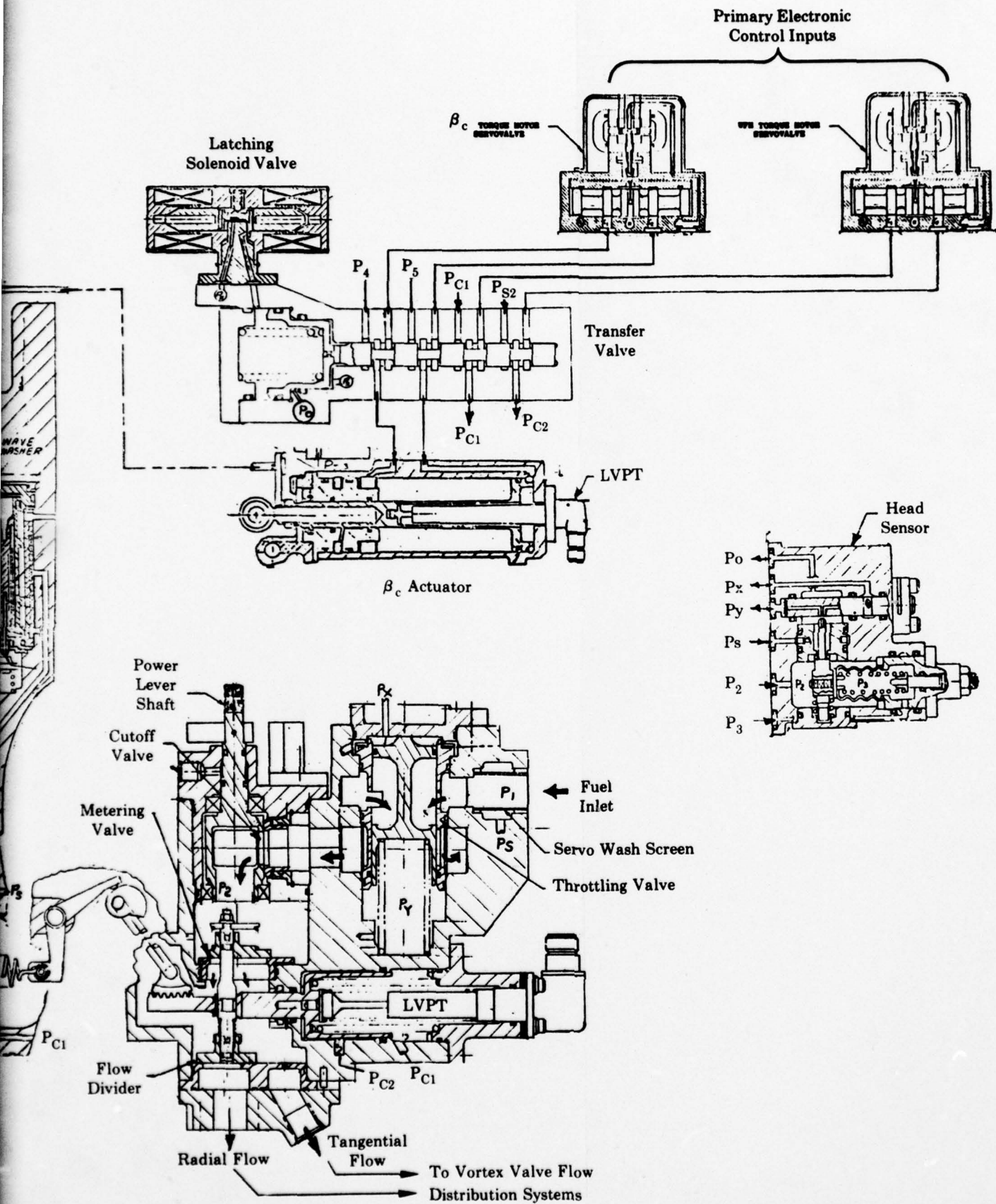


Figure 4 - Hydromechanical



Hydromechanical Backup Control Schematic.

4. COMBINATION ELECTRICAL/HYDROMECHANICAL APPROACH HAVING FUEL FLOW SETTING FUNCTION WITH FUEL RATE LIMITS IN SERIES CONFIGURATION

The combination approach is shown schematically by Figure 5. This approach is based on the W_f/P_{T2} parameter. The backup control acts only on W_f and β_c and its demands are continuously summed with those of the primary control. The operation of the backup control can be discussed in the various modes. During primary mode steady-state operation, W_f and β_c are controlled by the fail-fixed servovalves. These servovalves control the summing pistons. In this mode, the backup control outputs, W_f and β_c demand, are essentially fixed and at values above normal. The summing piston motions subtract from the limits set by the backup control and the results are the inputs into the flapper type metering valve servovalve, and the spool type β_c servovalve.

During primary mode accel, the PLA cam strokes the spool valve which ports servo pressure to the rate piston. The rate piston moves to the left at the rate determined by the needle valve slot (A_1) and the A_2 port in the primary W_f servovalve. The resulting piston velocity would cause an excessive acceleration and the primary control counteracts this by driving the summing piston in the decrease W_f direction. The same type of action occurs in the β_c control loop. In other words, the backup control stays ahead of the primary control so as to avoid interference.

During a primary mode decel, port A_2 is blocked by a land on the spool valve translated by the PLA cam. The rate piston moves slowly which demands a decel rate slower than any expected on primary control. The primary control decel is satisfied by driving the W_f and β_c summing pistons in the decrease direction. The backup control transiently demands more W_f and more open β_c and the primary control subtracts to achieve the desired response.

Transfer to the backup mode is initiated by applying zero current to the primary W_f and β_c fail-fixed servovalves. The servovalve output flows, with the aid of hydraulic locks, are essentially zero. Servo pressure, P_S , is ported to the summing pistons through small orifices causing the W_f and β_c summing pistons to stroke to their max stops in about 15 to 90 seconds. With the summing pistons on their stops, W_f is about 107% of normal and β_c is about 2 degrees more open than normal. Reset is provided, however. A lever driven by the W_f summing piston unseats a ball valve which ports P_S to a reset piston. The reset piston, linked to the rate piston feedback lever, strokes a predetermined amount having the effect of decreasing PLA. The new rate piston position demands normal W_f and β_c .

During backup mode operation, steady-state W_f is determined by PLA (representing W_f/P_{T2}) and P_{T2} while β_c is determined by PLA only. Desired steady-state W_f is the product of W_f/P_{T2} times P_{T2} so a multiplier is needed. A P_{T2} transducer is used to translate a 3D cam and the rate piston is used to rotate the cam. The cam rise is the desired product ($W_f/P_{T2} \times P_{T2} = W_f$). The rate piston also drives the β_c cam which has the backup schedule as a function of W_f/P_{T2} .

During transients in the backup mode, the desired fuel flow rate, \dot{W}_f , is proportional to the W_f level and P_{T2} ($\dot{W}_f = K W_f P_{T2}$). The rate piston velocity is determined by Port A_1 in the needle valve driven by the P_{T2} transducer. Port A_2 is blocked by the W_f servovalve in this mode. This results in a rate piston velocity proportional to P_{T2} . The 3D cam has a slope in the rotary direction which is proportional to W_f . The rate piston velocity combined with the cam slope yields the product ($W_f \times P_{T2}$).

A W_f/P_{T2} limit allows too much fuel flow at high Mach numbers. Overspeed protection is provided by an electrohydraulic servovalve shown and a related electrical circuit. The circuit is similar to that discussed under the electrical approach (Appendix N). The servovalve resets the rate piston so W_f/P_{T2} and β_c demands track. If overspeed increases further, an additional land modulates the throttling valve opening pressure to reduce W_f as required.

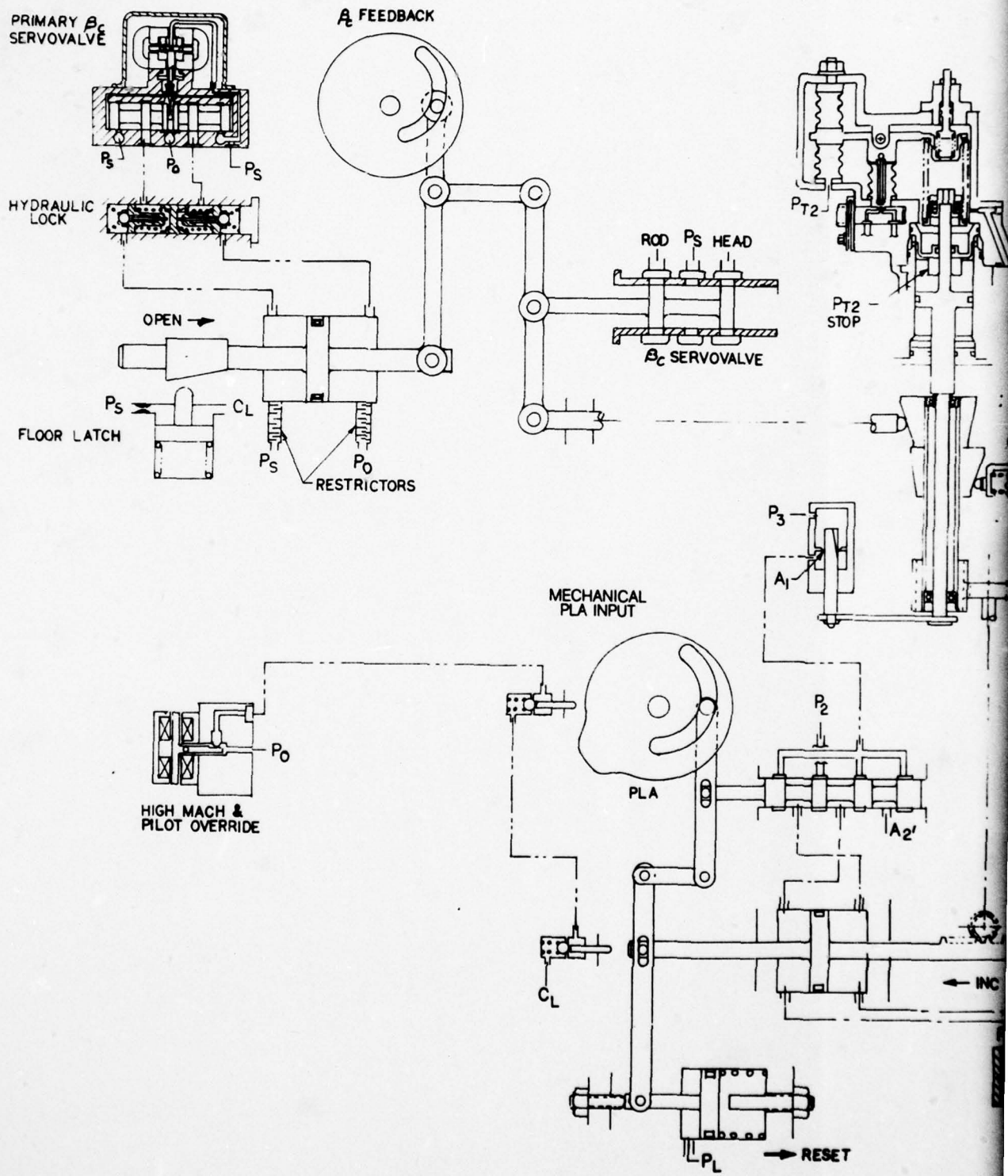
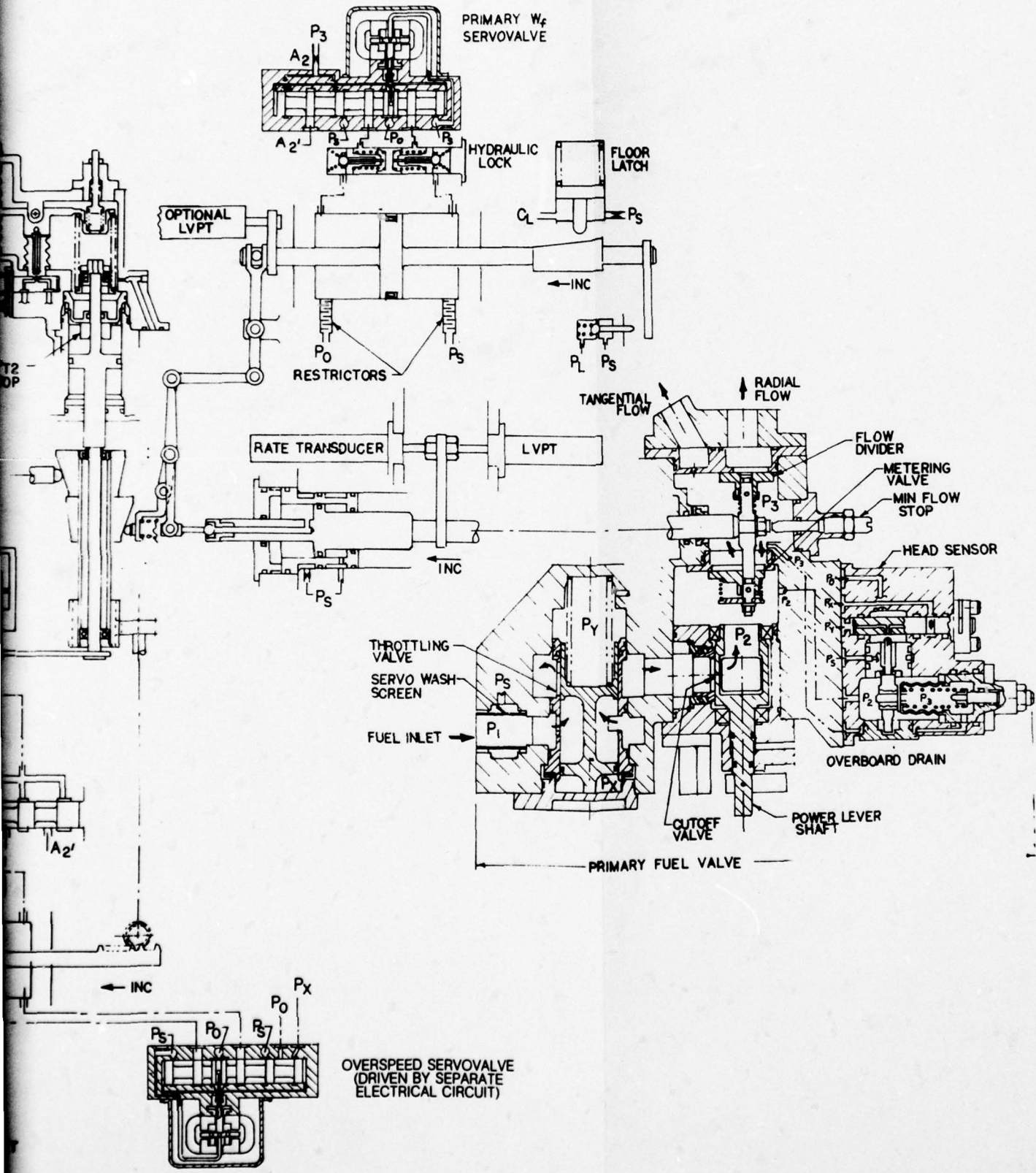


Figure 5 - Schematic for the Combination Elec



Combination Electrical/Hydronechanical Backup Control.

The W_f and β_c floors protect against inadvertent closing of the metering valve and stators due to the primary control failure during takeoff. The mechanization shown uses latches to limit summing piston stroke in the decrease direction. These floors would interfere with primary control accel and decel and also during high Mach number operation. Ball valves are used to keep the latch disengaged at PLA's less than 69° and rate piston positions representing PLA less than 69° . This eliminates interference for primary control accel and decel. A floor schedule override servovalve is used to allow removing the floor at high Mach number. The logic is that the two ball valves and the servovalve must be open to allow the latch to act. Pilot authority to remove the floor is also provided by the servovalve. It is intended that the signal to close the override servovalve is from the primary control because it has Mach number intelligence.

Control systems usually provide a compressor discharge pressure (P_{S3}) floor to prevent engine shutdown at high altitudes and part power settings. The summing scheme allows the pilot to decrease W_f in spite of a P_{S3} floor so a P_{T2} stop is used to prevent this. The drawing, Figure 5, also shows the fuel valve, which is considered a part of the primary control, to aid in defining the interface.

Additional information on this control is given in Appendix K.

5. HYDROMECHANICAL BACKUP CONTROL HAVING FUEL FLOW SETTING FUNCTION WITH FUEL RATE LIMITS IN A SERIES CONFIGURATION

This backup control resembles the combination electrical/hydromechanical approach discussed in the previous section and in Appendix K. The major difference is that a hydromechanical overspeed governor is substituted for the electrical speed function. The hydromechanical portion of the combination backup control is used without change.

Appendix L provides additional information on this backup control.

6. HYDROMECHANICAL BACKUP CONTROL HAVING FUEL FLOW SETTING FUNCTION WITH FUEL RATE LIMITS IN A PARALLEL CONFIGURATION

This backup control is based on the combination electrical/hydromechanical backup control described in Appendix K. The changes include:

- a. Substituting a hydromechanical overspeed governor for the electrical speed function.
- b. Removing the floor limits.
- c. Removing the N_G sensor and the summing piston position sensor.
- d. Removing the summers.
- e. Adding a high M_o servo.
- f. Adding a transfer valve and the related wiring, switches, etc.
- g. Adding a zero ΔP servo to provide precise tracking in the primary mode.

The major differences between this and the recommended approach described in Appendix I are

that fuel flow setting is used instead of speed setting for steady state operation and that fuel rate limits are used instead of fuel flow scheduling for transient operation.

Appendix M provides additional information on this backup control.

7. ELECTRICAL BACKUP CONTROL HAVING CORE RPM SETTING WITH SPEED RATE LIMITS IN A PARALLEL CONFIGURATION

The block diagram of the electrical backup control is shown by Figure 6. The operation of this control in the various modes is as follows:

a. Primary Mode - In this mode the backup control provides only N_G overspeed protection. The objective is to minimize the amount of electronics in use during primary mode operation and, thus, minimize the power loss failures due to the backup control. If overspeed occurs, the overspeed detector and latch cause automatic transfer to the backup mode. The backup control integrator tracks N_G actual so its output (N_{GR}) is essentially N_G actual. A speed error amplifier speeds up the integrator only in this mode. This is necessary so that transfer to backup can occur at steady state or during a transient without a jump in speed error. The output of the backup W_f servovalve is blocked by a transfer valve so that the primary W_f servovalve alone controls the metering valve. The transfer valve is spring and pressure loaded toward the primary mode operation stop. A torque motor operated single acting flapper is intended for the transfer valve. A continuous power supply is needed to hold the transfer valve in the backup mode and for operation of the electrical backup control.

The electronics are functioning and computing a rate limited speed request signal (N'_{GR}). A standby β_c schedule as a function of $N_G / \sqrt{\theta_{2.5}}$ is also being computed. A transfer valve, mechanically coupled to the one causing switching of W_f servovalve output, blocks the backup β_c servovalve and allows only the primary control β_c servovalve to control the actuator.

b. Transfer to Backup Mode - Transfer is initiated by either pilot action, loss of electrical power to the primary control, overspeed or by action of the primary control when it senses faulty operation. After initiation, the following occurs:

(1) A switch is closed and an 80 ma signal is transmitted to the electrohydraulic transfer valve. The valve strokes to the backup mode stop at which it ports only backup W_f and β_c servovalve flow to the actuators.

(2) A switch is opened between the speed error amplifier and the summer. This allows only the signal determined by the function of P_{T2} to be transmitted to the variable saturation limit device.

(3) The third switch changes the upstream speed request signal (N_{GR}) from N_G actual to PLA.

(4) The fourth switch is shown in the line to the transfer valve and allows the pilot to prevent transfer to the backup control or to transfer back to primary control at his discretion.

Since essentially N_G actual is at the output of the integrator and the β_c schedule is determined by N_G actual and $T_{2.5}$ actual, transfer occurs without a jump or dip in thrust. If the PLA speed setting is different than N_G actual, the difference is also rate limited thus preventing stall.

c. Backup Control Mode - The speed request signal, N_{GR} , is set by PLA. The speed signal is rate limited as a function of P_{T2} by the action of the pressure transducer, function generator, variable saturation limit and integrator. The maximum speed is rated, not 4% overspeed, so pilot action is not needed to avoid overtemperature and overspeed. Core stators, β_c , follow N_G and $T_{2.5}$ so there should be

no tracking problems during the slower backup control accels and decels. Corrected speed ($N_G / \sqrt{\theta_{2.5}}$) limiting is also provided.

Closed loop N_G and β_c control result from this approach. A rate transducer is used at the metering valve to help stabilize the N_G loop. If N_G overspeed occurs due to an inoperable open metering valve, the backup W_f servovalve has a land which can vary the throttling valve opening servo pressure (P_x). The throttling valve will be modulated to hold speed at approximately 104%.

Additional information on the electrical backup control is given in Appendix N.

8. FLUIDIC BACKUP CONTROL HAVING FUEL FLOW SETTING WITH FUEL RATE LIMITS IN A SERIES CONFIGURATION

The fluidic backup control approach is similar to the combination electrical/hydraulic control described in Appendix K. A schematic of the fluidic approach is shown in Figure 7. The operation of this control is as follows:

Throttle position is converted to a push-pull pressure differential by a cam linked to the throttle. The cam varies the skirt area of two nozzles. The nozzles in conjunction with two upstream orifices produce a pressure differential linearly related to cam rotation. This pressure signal is applied through a summing junction to the input of a 3-stage proportional amplifier (G_1). The nozzle supply for the last stage is generated by the P_{T2} sensor, hence the saturated output of G_1 is proportional to P_{T2} . For rapid changes of throttle angle, a large error will be present at the summing junction and the three stage amplifier will saturate. The integrator, consisting of G_2 and associated resistors and capacitors, has a steady state input proportional to P_{T2} . The output of the integrator is fed back to the summing junction through resistor R_2 . When the error signal at the summing junction becomes sufficiently small, G comes out of saturation and operates on a proportional gain characteristic of the amplifiers. At this point steady state operation is achieved and the output of the integrator is the pressure signal at the cam multiplied by R_2/R_1 .

Resistance R_3 and capacitance C_1 generate a lag time-constant to cancel a lead time-constant resulting from the specific method used to mechanize the integrator.

The output of the integrator is summed with the output of the overspeed governor by a 3 stage summing amplifier (G_3). The overspeed governor is assumed to be an electrical governor with a flapper nozzle or jet pipe to generate a proportional push-pull signal in the overspeed range. The governor scale factor and the ratio of R_5 to R_4 are selected to permit the governor to override the integrator output in an overspeed condition.

The output of G_3 is applied to one channel of the multiplier. The multiplier is a conventional PDM configuration, consisting of a triangular wave oscillator, a summing amplifier to sum the triangular wave and the analog input signal plus digital elements to convert the summed signals to a pulse width directly proportional to signal input. The height of the pulse is determined by the supply pressure to the digital output amplifier. This supply (P_{T2}) is the second input to the multiplier.

The output of the multiplier is filtered by R_7 and C_3 and applied as an input to G_4 where it is summed with the output of a feedback cam on the primary fuel valve. The output of G_4 positions a pilot actuator which can effect control of the primary fuel metering valve if the primary control fails. A bias is

also applied to the summing junction through R_{10} and C_4 . The bias holds the actuator "hardover" and essentially deactivates the backup control. This bias is removed by closing S_3 if the primary control fails. The bias slowly decays to zero through the R_{10} and C_4 time constant to smooth the transition from primary to backup control.

Operation of the β_c control circuit is the same as the fuel control with the exception that the input to the G_5 amplifier is taken off before the multiplier.

The P_{T2} sensor consists of an evacuated bellows with P_{T2} applied to the outside of the bellows. The torque generated by P_{T2} , the effective area of the bellows and its moment arm, is applied to a pivoted beam. Motion of the beam varies the skirt area of a flapper nozzle and produces a pressure which is applied to a control bellows. The pressure in the control bellows acting through its effective area and moment arm produces a torque equal and opposite to that produced by P_{T2} . In steady-state the differential pressure between the control bellows and the ambient surrounding the control bellows is directly proportional to P_{T2} . This torque summation does have droop; consequently, the pivot beam has finite motion and maximum and minimum pressure stops can be applied to the beam.

The control bellows pressure is applied to one channel of the multiplier and also to the rate limiter through R_{11} and R_{12} . R_{11} and R_{12} are linear resistances scaled relative to the nozzle of the output amplifier in G_1 , to obtain the required temperature compensation on the rate limit.

The pneumatic switches (S_1 and S_2) are actuated by the primary fuel valve spool and function to maintain the backup control transient schedule higher than the primary control schedule. When operating on primary control and accelerating, S_2 is open and S_1 is closed. This increases the P_{T2} pressure applied to the G_1 limiter and increases the rate schedule. On decel, S_2 is closed and S_1 opens which decreases the P_{T2} pressure and consequently reduces the rate limit. On backup control both S_1 and S_2 are closed.

Additional information on the fluidic backup control is given in Appendix O.

SECTION III

SELECTION OF RECOMMENDED APPROACH

1. GENERAL

The design results and reliability estimates were prepared for the several possible backup control approaches.

2. COMPARISON OF TECHNOLOGIES

A comparison was made summarizing the advantages and disadvantages of the three possible technologies—hydromechanical, electrical, and fluidic. This summary is shown in Table 1. On the basis of this summary and the design details shown in the appendices, the fluidic approach was eliminated and further tradeoffs were conducted for the electrical and hydromechanical possibilities.

3. COMPARISON OF ESTIMATED RELIABILITY

Reliability estimates and comparisons were then prepared for the six remaining backup control approaches. Unscheduled Component Removal (UCR), Mission Power Loss (MPL), and Get Home Power Loss (GHPL) probabilities were computed for each approach for both the FADEC controller and the overall control system. UCR includes all unscheduled removals for failures found at any time. MPL includes events causing loss of power of more than 10% of that selected by the power lever. This is limited to events found after the initiation of a mission. GHPL includes only those events that cause power loss to the extent that "get home" capability is lost. This is limited to events that occur after takeoff speed disallows abort and until a safe landing is accomplished. The results are shown on Table 2. Data other than those for the FADEC controller, fuel valve and backup control are for the F101 control system.

The goal of this program is to provide a backup control which, when combined with the FADEC controller, would result in an acceptable GHPL rate. An objective of the backup control is to provide protection until the predicted FADEC failure rates are proven true by field experience. Referring to Table 2, the GHPL rate for the FADEC controller is 40.2 events per 10^6 hours after 640,000 cumulative engine flight hours. This GHPL rate is reduced significantly when the FADEC controller is combined with any parallel type backup control. This presumes that the reliability goals for FADEC will be met at maturity. If the actual failures rates of FADEC prove to be higher, the impact of adding a backup control will be even more beneficial. The failure rate of two controls in parallel when there is no common cause is, theoretically, the product of the individual failure rates which is a number much less than one (1). The GHPL rate resulting when the FADEC controller is combined with the hydromechanical, N_G/W_f , parallel type backup control is 3.0 events per 10^6 hours. The two contributors to this rate are the transfer valve (1.5 events) and the hydromechanical overspeed components (1.5 events). This low GHPL rate shows the primary goal of the program was met very successfully.

The overall control system impact was also investigated. The system GHPL rate was 87.0 events per 10^6 hours when no backup control is used. The data show that the FADEC controller is the major contributor of this rate. When the hydromechanical, N_G/W_f , parallel backup control is added, the GHPL rate is reduced to 37.5 events. It should be noted that GHPL rates for the alternator, fuel valve, harnesses and servos are reduced in addition to that of the FADEC controller. The hydromechanical backup controls do not depend on the alternator and they protect against primary system harness and servovalve failures. This may still be unsatisfactory for a single engine aircraft. The results show that actuator and pump GHPL rates are now significant when compared to the GHPL rate of the FADEC controller

TABLE 1
COMPARISON OF TECHNOLOGIES

TECHNOLOGY	ADVANTAGES	DISADVANTAGES
Hydromechanical	<ol style="list-style-type: none"> 1. Very mature technology. 2. Proven reliability - readily applied without redundancy. 3. Interfaces readily with the hydromechanical fuel valve. 4. Servo pressure available over wide engine speed range. 5. Good environmental resistance since it is inherently fuel cooled and fuel provides some vibrational damping of parts. 6. Necessary accuracy readily achieved. 7. Free from some of the environmentally caused failures of the primary control. 	<ol style="list-style-type: none"> 1. Some control functions more difficult to mechanize. 2. Sensing temperature is difficult especially if fast response is required. 3. A 20 second integrator is a relatively large device. 4. Mechanical feedback can cause problems in some applications. 5. Servo flow may increase fuel pump size. 6. Cost is relatively high. 7. Weight is relatively high. 8. Harder to make changes in the development phase. 9. Sensing speed requires a mechanical input but sensor could be remote from fuel valve.

TABLE 1 (Cont'd)

TECHNOLOGY	ADVANTAGES	DISADVANTAGES
Electrical	<ol style="list-style-type: none"> 1. Flexible - various control functions readily available. 2. Can draw upon extensive proven on-engine experience. 3. Temperature sensing has been successfully accomplished. 4. Necessary accuracy readily achieved. 5. Speed sensing does not require a drive pad. 6. Relatively easy to make changes in the development phase. 7. Cost and weight expected to be less than hydromechanical. 8. Electronics is the most rapidly advancing technology. 	<ol style="list-style-type: none"> 1. Requires a separate alternator, separate alternator winding or other power source. 2. Is subject to some of the same environmentally caused failures as the primary control. 3. Does not have the proven reliability of the hydromechanical control. 4. Requires cooling because reliability decreases rapidly as temperature approaches 250°F. 5. Requires electrohydraulic servovalves and position transducers to interface with the fuel valve. 6. Desired low electrical power level requires hydraulic force amplification.

TABLE 1 (Concluded)

TECHNOLOGY	ADVANTAGES	DISADVANTAGES
Fluidics (Air)	<ol style="list-style-type: none"> 1. High temperature capability. 2. Air supply is available. 3. Has good environmental resistance. 4. Necessary control functions can be provided. 5. Not subject to some of the environmentally caused failures of the primary system. 	<ol style="list-style-type: none"> 1. Less mature technology. 2. Air supply pressure varies so regulator probably required. 3. Fine filtration is probably required. 4. Experience indicates that accuracy is more difficult to achieve. 5. Requires air flow for computation functions. 6. Pressure is low at low speed so hydraulic force amplification will probably be required. 7. Limited research effort in progress. 8. Limited on-engine experience. 9. Subject to icing problems.

TABLE 2
SUMMARY OF THE RELIABILITY
(EVENTS PER 10⁶ HOURS AFTER 640,000 EN

Component	No Backup Control			Hydromechanical, N_G/W_f , Parallel (Appendix I)			Hydromechanical, N_G/W_f , Series (Appendix J)			Combination, N_G/W_f , (Appendix K)	
	UCR	MPL	GHPL	UCR	MPL	GHPL	UCR	MPL	GHPL	UCR	MPL
FADEC Controller	118.4	44.7	40.2	118.4	4.2	—	118.4	16.5	2.0	118.4	19.5
Fuel Valve	30.0	6.8	3.4	30.0	4.0	2.0	30.0	6.0	3.4	30.0	6.0
Alternator & Ignition	34	12.1	6.1	34.0	1.5	1.0	34.0	1.5	1.0	34.0	7.2
Harnesses	59.2	11.5	5.8	59.2	9.2	1.2	59.2	9.2	1.2	59.2	11.5
Sensors	120.4	0.1	0.1	120.4	0.1	0.1	120.4	0.1	0.1	120.4	0.1
Actuators	94.9	30.4	16.8	94.9	30.4	16.8	94.9	30.4	16.8	94.9	30.4
Servos	159.2	11.6	5.4	159.2	11.0	4.2	159.2	11.0	4.2	159.2	11.0
Pumps	78.0	18.3	9.2	78.0	18.3	9.2	78.0	18.3	9.2	78.0	18.3
Augmentor Fuel Control	70	—	—	70.0	—	—	70.0	—	—	70.0	—
Backup Control	—	—	—	68.2	—	3.0	69.1	—	14.9	63.0	—
FADEC System	764.1	135.5	87.0	832.3	78.7	37.5	833.2	93.0	52.8	827.1	104.5
Impact				+68.2	-56.8	-49.5	+69.1	-42.5	-34.2	+63.0	-30.0

TABLE 2
RELIABILITY ANALYSES
(AFTER 640,000 ENGINE FLIGHT HOURS)

Combination W_f/\dot{W}_f , Series (Appendix K)			Hydromechanical W_f/\dot{W}_f , Series (Appendix L)			Hydromechanical W_f/\dot{W}_f , Parallel (Appendix M)			Electrical N_G/\dot{N}_G , Parallel (Appendix N)		
UCR	MPL	GHPL	UCR	MPL	GHPL	UCR	MPL	GHPL	UCR	MPL	GHPL
118.4	19.5	2.0	118.4	20.5	2.0	118.4	5.2	—	118.4	4.9	—
30.0	6.0	3.4	30.0	6.0	3.4	30.0	4.0	2.0	30.0	4.0	2.0
34.0	7.2	3.6	34.0	1.5	1.0	34.0	1.5	1.0	34.0	12.1	5.0
59.2	11.5	5.8	59.2	9.2	1.2	59.2	9.2	1.2	59.2	9.8	1.4
120.4	0.1	0.1	120.4	0.1	0.1	120.4	0.1	0.1	120.4	0.1	0.1
94.9	30.4	16.8	94.9	30.4	16.8	94.9	30.4	16.8	94.9	30.4	16.8
159.2	11.6	5.4	159.2	11.0	4.2	159.2	11.0	4.2	159.2	11.0	4.8
78.0	18.3	9.2	78.0	18.3	9.2	78.0	18.3	9.2	78.0	18.3	9.2
70.0	—	—	70.0	—	—	70.0	—	—	70	—	—
63.0	—	15.9	60.1	—	16.0	74.6	—	3.0	63.7	—	4.4
827.1	104.6	63.9	824.2	97.0	51.9	838.2	79.7	37.5	827.8	90.6	43.7
+63.0	-30.9	23.1	+60.1	-38.5	-34.1	+74.6	-55.8	-49.5	+63.7	-44.9	-43.3

combined with a parallel type backup control and that these components should be targets for future design and development efforts.

The results of the reliability analysis indicate that the three parallel type backup controls all have satisfactorily low GHPL rates. However, the hydromechanical, W_f/\bar{W}_f , parallel backup control has the highest UCR rate.

The reliability analyses on the two parallel type hydromechanical controls were based on past controls or similar components. This type of hardware is highly developed and has proven failure rates so no significant improvement with further development is expected. The electrical parallel backup control reliability analysis was based on an advanced hybrid packaging approach intended specifically for on-engine use. The reliability predictions are based on the assumption that this packaging approach will be fully developed. Further, rapid advancements are being made in electronic technology so reliability improvements due to more integration, better chips, etc., are possible.

4. RELIABILITY OF COMMON PARTS

Hydromechanical components have proven reliability and are usually used without backup. For example, during 1977 the CF6-50 engine accumulated 1,429,749 flight hours and there was only one hydromechanical main fuel control UCR. All backup controls investigated used the same metering, throttling and cutoff valves and the same head sensor for the primary and backup modes. Table 3 shows a reliability summary of these components. The throttling valve and head sensor data are based on F101 Augmentor Control reliability data. The metering valve and cutoff valve rates are based on estimates of similar devices. These UCR and GHPL rates are included as a portion of the fuel valve failure rates in Table 2. These low failure rates are one reason common parts are used.

The second reason that common hydromechanical parts are used is the large increase in complexity with redundancy. Figure 8 shows the major components for a fully redundant fuel metering approach. The vortex valves, which provide enhanced gum and contamination resistance plus a significant cost reduction, add to the complexity because metered flow is divided into tangential and radial flows. Increased complexity causes an increase in UCR and cost for the additional hardware including the second head sensor and metering and throttling valves plus the special transfer valve. The transfer valve will require development to achieve the desirable transfer characteristics resulting from integrating the common metering valve to the new position using the backup servovalve (see Appendix I).

TABLE 3
RELIABILITY SUMMARY OF PARTS COMMON TO PRIMARY AND BACKUP CONTROLS*

	<u>Throttling Valve</u>	<u>Head Sensor</u>	<u>Metering Valve</u>	<u>Cutoff Valve</u>	<u>Total</u>
<u>System Effects</u>					
No Effect	2.334	13.69	7.977	3.96	27.96
Increases Fuel Flow	1.836	6.786	0	0	8.62
Maximum Fuel Flow	0.05	0.39	0.168	0	0.61
Decreases Fuel Flow	1.608	4.442	0.461	0.02	6.53
No Flow	2.136	0.812	0	0	2.95
External Leak	1.950	1.668	0.708	0.320	4.65
Leak to Boost Pressure	—	0.109	—	—	0.11
Incorrect flow split	—	—	0.268	—	0.27
<u>Engine Effects</u>					
No Effect	6.151	19.207	9.146	4.28	38.78
F_N Loss > 10%	2.456	3.134	0.268	0.02	5.88
Excess F_N	1.073	5.438	0	—	6.51
Loss Stall Margin	0.019	0.117	0.168	—	0.30
DAO	4.781	20.977	7.977	3.96	37.70
UCR	4.915	6.919	1.605	0.34	13.78
GHPL	1.112	1.493	0.216	0.02	2.83

*Events per 10^6 hours after 640,000 cumulative engine flight hours.

5. SUMMARY OF ESTIMATED PERFORMANCE

The hydromechanical, N_G/W_f , parallel backup control is based on existing main fuel controls. The performance of these devices is well known and it is expected that W_f and β_c scheduling can be comparable to that of the primary control. Also this backup control will have the capability to schedule W_f from minimum to idle flow thus providing automatic windmill starting.

Also, the expected performance of the electrical, N_G/\dot{N}_G , parallel backup control is very satisfactory. The β_c scheduling is based on N_G actual and $T_{2.5}$ which is the same as in the hydromechanical backup control. The accel W_f is scheduled so as to provide a speed rate (\dot{N}_G) as a function of P_{T2} . Speed rate type fuel controls have been and are being used as primary controls but schedule type fuel controls have won wider acceptance in this application. The speed rate approach is considered more acceptable for backup controls since longer accel times are allowed. The electrical backup control does not provide an ideal windmill starting means. A manual procedure is suggested during which the pilot sets PLA at minimum flow, watches for ignition, and then slowly advances the PLA as RPM increases.

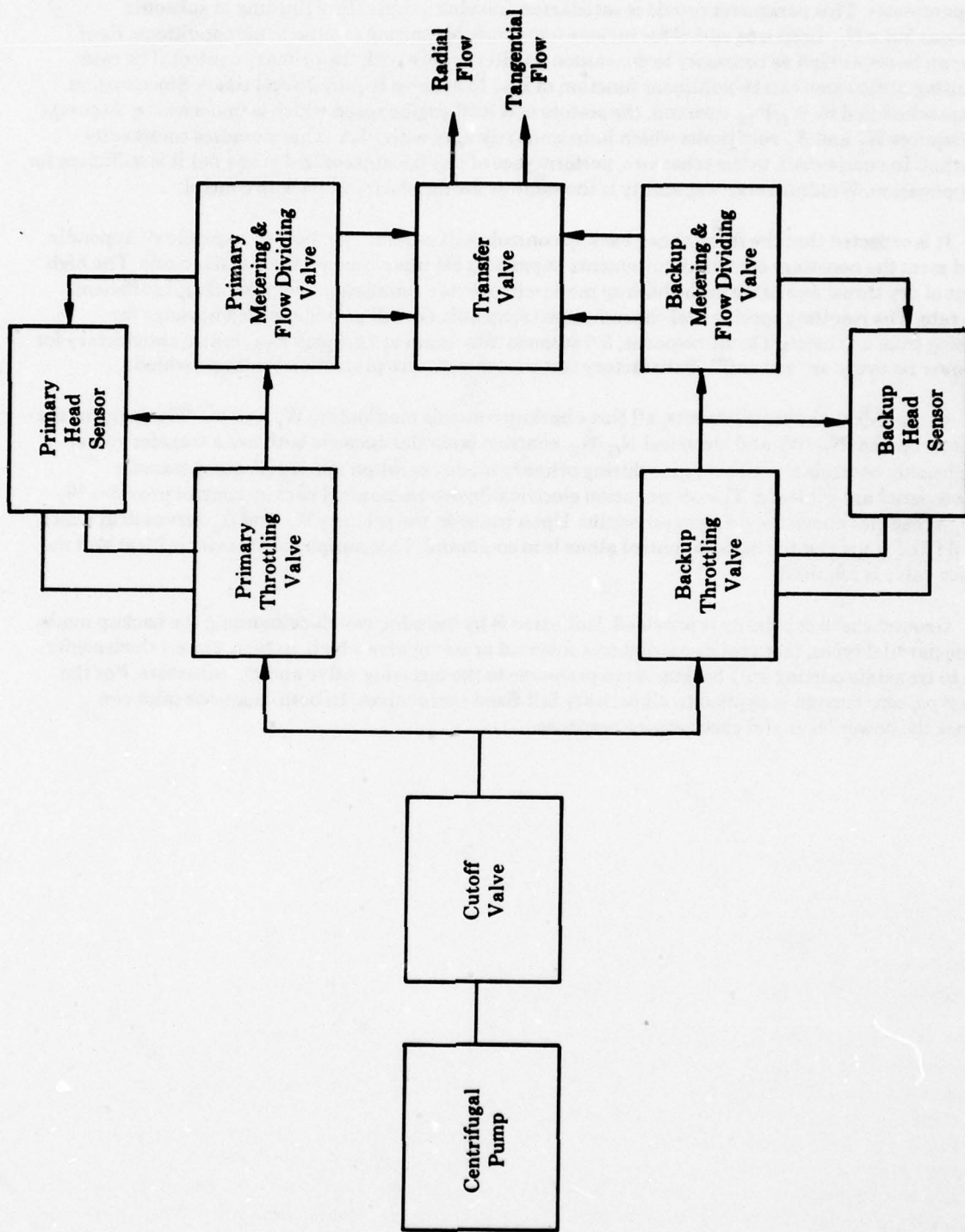


Figure 8 - Components Required for a Parallel Redundant Fuel Metering Approach.

The combination electrical/hydromechanical, W_f/\dot{W}_f , series backup control uses W_f/P_{T2} as the accel parameter. This parameter provides satisfactory turbine temperature limiting at subsonic conditions but a N_G limit was added for turbine temperature limiting at supersonic conditions. Roof limits can be set as high as necessary to guarantee no interference with the primary control. The rate controlling orifice area can be nonlinear function of P_{T2} to achieve required accel times. Since stators (β_c) are scheduled by W_f/P_{T2} demand, the stators will lead engine speed which is undesirable. Accurate reset requires W_f and β_c roof limits which independently vary with PLA. This increases complexity somewhat. In comparison to the other two, performance of this backup control is less but it is sufficient for this application. Windmill start capability is the same as for the electrical backup control.

It is expected that the three above backup controls will provide "get home" capability (Appendix E) and meet the necessary control requirements (Appendix H) when used on the JTDE engine. The high percent of dry thrust available in the backup mode will provide completion of a takeoff and sufficient climb rate. The resulting specific fuel consumption (Appendix G) will provide sufficient range for returning from a mission. Thrust response, 8.0 seconds maximum at 14.7 psia P_{T2} , is also satisfactory for maneuver recovery or "waveoff". Satisfactory turbine temperature protection is also provided.

In regards to the requirements, all three backup controls manipulate W_f and β_c . The logic for the hydromechanical N_G/W_f and electrical N_G/\dot{N}_G controls is similar because both use a transfer valve. These backup controls track the engine during primary mode operation and satisfactory transfer characteristics are achieved. The combination electrical/hydromechanical backup control provides W_f and β_c schedules above the primary schedules. Upon transfer, the primary W_f and β_c servos drift slowly toward fixed stops and the backup control alone is in command. This automatic transfer is ideal and no transfer valve is required.

Ground check capability is provided. Initiation is by the pilot switch demanding the backup mode. For the parallel types, this applies current to a solenoid or servovalve which, in turn, causes the transfer valve to translate porting only backup servo pressures to the metering valve and β_c actuators. For the series type, zero current is applied to all primary fail-fixed servovalves. In both cases, the pilot can advance the power lever and check engine response.

6. DESIGN COMPARISON

Comparative analyses regarding volume, weight and cost were performed for the three approaches for which detail design results were available. The identification of the three approaches and a summary of the results are given in Table 4. The combination electrical/hydromechanical backup control approach proved inferior to either the hydromechanical or electrical so it was not considered further. There is very little difference in cost, weight and volume between the electrical and hydromechanical approach.

The hydromechanical and electrical designs each have inherent advantages which must also be considered in the selection. The advantages of the hydromechanical, N_G/W_f , parallel backup control are:

- a. The hydromechanical backup control is not subject to some types of failures which could cause malfunctioning simultaneously in both the primary and backup controls if both are electrical.
- b. The hydromechanical mechanization interfaces well with the fuel valve.
- c. The reliability of hydromechanical controls is well proven as noted in Paragraph 3 above.

The advantages of the electrical, N_G/N_G , parallel backup control are:

- a. Both core and fan speed can be sensed without the necessity of a drive pad.
- b. The electrical mechanization interfaces well with both the FADEC and the cockpit.
- c. Electronic technology is advancing at a rapid pace.

7. SUMMARY

The technology comparison, the estimated performance, the reliability volume, weight and cost analyses and the list of inherent advantages were used to select the backup control to be designed in Phase II of this program. The fluidic approach was eliminated based on the technology comparison. The reliability analyses indicated that the parallel approach yields a lower GHPL rate than the series approach. The reliability analyses also indicated that the hydromechanical, W_f/W_f , parallel backup control has the highest UCR rate and, together with its higher inherent complexity, this indicates that only the hydromechanical, N_G/W_f , parallel and the electrical, N_G/N_G , parallel should be considered further. The cost, weight and volume comparison indicated little difference between the remaining hydromechanical control and the electrical control. The hydromechanical, N_G/W_f , parallel backup control was selected over the electrical, N_G/N_G , parallel type based on the better GHPL rate, the better estimated performance, and the significant inherent advantage that it is not subject to some types of failures which could cause simultaneous malfunction in both the primary and backup control if both are electrical.

TABLE 4
SUMMARY OF COMPARATIVE ANALYSES

CRITERIA	FADEC SYSTEM	IMPACT		
		Hydromechanical, N_G/W_f , Parallel	Electrical, N_G/N_G , Parallel	Combination, W_f/W_f , Series
Volume	3751 cu. in.	+ 259 cu. in.	+ 228 cu. in.	+ 597 cu. in.
Weight	250.5 lbs.	+ 20.2 lbs.	+ 19.7 lbs.	+ 39.8 lbs.
Cost, Production	\$158,082	+\$11,800	+\$11,100	+\$14,615

SECTION IV

CONCLUSIONS

The stated objective for Phase I of the Backup Control for a Variable Cycle Engine Program was to select a simple, reliable backup (or emergency) control to function with primary digital electronic controls until the electronics have demonstrated the needed reliability to "go it alone"; specifically in a single engine airplane. Implicit in the objective was a desire to keep the hardware impact of the backup control to a minimum.

Reliability, cost, weight, volume and estimated performance studies were conducted and these studies provided a major part of the basis for the backup control selection. Based on these studies, the following conclusions can be reached:

1. The reliability analyses indicated that parallel type primary/backup systems provide a lower Get Home Power Loss (GHPL) rate, because backup control mechanizations are in standby and do not contribute to primary failure rates.
2. Although series type primary/backup systems provide ideal transfer action and better limit protection, the advantages of minimum interference during primary mode operation and significantly lower GHPL make the parallel types more preferred.
3. Both scheduled limits and rate backup controls were considered. For mechanization and performance reasons scheduled types were preferred.
4. The comparative analyses indicate that the hydromechanical and electrical backup controls are lower in volume, weight and production cost than the combination electrical/hydromechanical versions.
5. Fluidic backup controls using air were considered. However, these were found to be less advantageous than either hydromechanical or electrical because of functional, maturity, accuracy, force level and icing limitations.
6. Since the primary control is electrical, the hydromechanical backup control is preferred because some of the specification environments could induce common cause malfunction in both the primary and backup when both are electrical.
7. Hydromechanical main fuel controls have demonstrated high levels of reliability as primary controls, and similar mechanizations can be used for backup control.
8. The hydromechanical, N_G/W_f , parallel backup control is superior and is, therefore, selected for this application.

The hardware impact of the selected control is very acceptable. A 9% increase in UCR and a 7% increase in cost have been identified, together with an 8% increase in weight and a 7% increase in volume for adding the selected backup control to the FADEC System. Paving this price, a reduction in GHPL rate for the electronic controller from 40.2 to 3.0 events per 10^6 hours was achieved. In addition, the whole system GHPL rate due to all causes was more than halved. With the selected design, the objectives have been achieved.

SECTION V

RECOMMENDATIONS

As indicated in the preceding conclusions, the hydromechanical approach in a parallel (standby) relationship to the primary offers superior reliability, performance, and get home capability. Therefore, this approach is recommended for selection for further development. It should be designed, fabricated and tested in Phase II of this program. The recommended version is described in detail in Appendix I.

The objectives of this further development should be to conduct a detail design of the recommended backup control, fabricate the control, and conduct bench testing in conjunction with a specifically designed test console. This program would provide hardware and bench test confirmation of the design approach. This is the specific effort that is identified in Phase II of the Statement of Work (Appendix A).

Looking beyond the current contract and this immediate development phase, it is further recommended that the backup control be systems tested in combination with the full authority digital electronic primary control. Such systems tests should include simulated failures to demonstrate transfer action and subsequent uninterrupted performance in the backup mode. Following this systems test the backup control should be engine tested again in combination with the primary full authority digital control.

APPENDIX A - STATEMENT OF WORK

The AFAPL Statement of Work lists the tasks, in chronological order, performed during the program. The Statement of Work is included in this report because it provides a background or outline for the subsequent sections.

4.2 PHASE I — BACKUP CONTROL TRADE STUDIES

4.2.1 Trade Study Ground Rules

4.2.1.1 The contractor shall identify the specific variable cycle engine (VCE) concept to be used in the trade studies. The complexity of the selected VCE concept will have a direct impact on the nature and extent of the backup control requirements. Consideration shall be given to the availability of a digital simulation for the selected VCE concept.

4.2.1.2 The contractor shall identify an appropriate single engine aircraft application for the selected VCE concept. Aircraft flight envelope and probable missions shall also be identified.

4.2.1.3 The contractor shall define a minimum "get-home" capability for the aircraft/engine concept selected in 4.2.1.1 and 4.2.1.2. This definition shall include but not be limited to a discussion of such items as takeoff, cruise, and landing requirements, engine airstart capability and impact on pilot workload.

4.2.1.4 The contractor shall provide a description of the primary (digital electronic) control system for the VCE engine. Of particular concern are areas of possible interface with the backup control. In the event of primary control system failure, the required position/condition of all controlled variables shall be identified.

4.2.1.5 The contractor shall identify pertinent operational constraints for the backup control. These constraints shall include but not be limited to such items as number and types of inputs allowed, unique restrictions due to primary-to-backup control system transfer, sharing hardware items with the primary control, and control system environment.

4.2.1.6 The ground rules identified in 4.2.1.1 through 4.2.1.5 will be documented and submitted to the government for approval. Approval/disapproval shall be given by the Procuring Contracting Officer within 15 days after receipt.

4.2.2 Definition of the Backup Control Requirements

4.2.2.1 Based on the aircraft and engine selections of 4.2.1.1 and 4.2.1.2 and a "get-home" capability as identified in 4.2.1.3, the contractor shall determine steady state and transient engine performance requirements. Utilizing an appropriate engine simulation, the contractor shall identify the minimum number of control output variables that must be incorporated in a backup control to satisfy those performance requirements.

4.2.2.2 The contractor shall prepare a detailed list of backup control requirements to include backup control input and output variables, detailed backup control logic, desired primary-to-backup transfer characteristics, and a steady state and transient performance specification. Where possible, these backup control requirements will be simplified to permit a maximum number of possible solutions.

NOTE: The paragraph numbers of this section retain the Government established numbering given in the contract Statement of Work.

4.2.3 Hardware Trade Studies

4.2.3.1 Based on the control requirements identified in 4.2.2.2 the contractor shall identify possible backup control approaches. These approaches shall consider hydromechanical, electronics, and fluidics technology. All approaches will be screened as to strengths and weakness and a minimum of two (2) approaches selected for further study.

4.2.3.2 The contractor shall conduct preliminary designs of the selected backup control approaches. These designs will be for production version controls and of sufficient detail to permit production cost, size and weight estimates. The component/system technology incorporated in these designs must be suitable for production aircraft incorporation prior to 1985.

4.2.3.3 The contractor shall conduct a reliability and maintainability (R&M) analysis for the selected control approaches. R&M studies will be based upon sound, practical engineering judgment, experience and available test data. Since reliability is of utmost concern in a backup control system, those areas where reliability predictions are difficult or areas that lack suitable foundation/experience for proper analysis shall be highlighted. A prediction of the degree of reliability and maintainability inherent in the backup control approaches, and that which may be achieved through further development, will be included with an explanation in the Phase I final report.

4.2.3.4 The contractor shall conduct a failure mode and effect analysis (FMEA) for the selected control approaches. Of particular concern are areas such as the transfer system, where a single failure can disable both the primary and backup control functions.

4.2.3.5 The contractor shall estimate the steady state and transient performance capabilities of the selected approaches and shall evaluate these estimates against the backup control requirements of 4.2.2.2.

4.2.3.6 The contractor shall conduct a comparative analysis of the selected backup control approaches and detail the advantages and disadvantages of each approach. One approach shall be recommended for the Phase II detailed design, fabrication and test effort, and the rationale for this recommendation documented and submitted to the government.

4.2.3.7 The contractor shall prepare, for publication, a comprehensive technical report summarizing the results of items 4.2.1, 4.2.2 and 4.2.3.

4.3 PHASE II — HARDWARE DEVELOPMENT AND EVALUATION

4.3.1 Hardware Design

4.3.1.1 The contractor will conduct a detailed design of the backup control approach selected in 4.2.3.6. Although the design should incorporate those features identified in Phase I, the specific application will be a test (or slave) engine selected by the contractor and approved by the government. The backup control design shall be capable of interfacing with the primary (electronic) control system developed for this test engine. The design will include control logic elements, fuel metering and actuator servo hardware, primary-to-backup transfer hardware, sensors and interfaces, and any additional items required to provide a functional demonstration of the backup control. Primary and/or backup fuel pumping schemes will be specifically excluded from the design activity unless they are an integral part of the backup control concept. The detailed design will be for a prototype, flight-type backup control for the

selected slave engine; consequently, some differences may exist between this flight-type system and the production configuration identified in 4.2.3.2. Such differences may include machined "hog-outs" instead of castings for the hydromechanical hardware or discrete components rather than custom LSI chips for the electronics hardware. In all cases, the contractor shall identify the similarities and identify/justify the differences between the flight-type and production configurations.

4.3.1.2 The contractor shall develop specific control logic suitable for implementation in the backup control hardware/software for control of the slave engine.

4.3.1.3 The contractor shall design a backup control test console to be used during bench testing of the backup control. This console, when operating in conjunction with a test (flow) bench, should be capable of evaluating all backup control functions. If necessary, this test console will function as the primary (electronic) control system prior to transfer to the backup control.

4.3.1.4 During the detailed design of 4.3.1.1, the contractor shall perform a system safety analysis in accordance with paragraph 5.8.2.1 of MIL-STD-882 dated 15 July 1969. The technical effort associated with this analysis should not exceed one (1) man-week. The documentation resulting from this analysis shall be provided to the government as part of the design report of 4.3.1.5.

4.3.1.5 The contractor shall prepare a design report summarizing the results of 4.3.1.1 through 4.3.1.4 and submit this report to the government. This report will be published as part of the Phase II final report (Item 4.3.4.1).

4.3.2 Hardware fabrication and assembly

4.3.2.1 The contractor shall fabricate and assemble one set of those backup control items identified in 4.3.1.1.

4.3.2.2 The contractor shall fabricate, assemble, and functionally checkout the backup control test console of 4.3.1.3.

4.3.3 Bench testing and evaluation

4.3.3.1 The contractor shall develop a digital, analog, or hybrid real-time simulation of the slave engine. This simulation will be used in conjunction with a flow bench to evaluate the steady state, transient, and transfer performance characteristics of the backup control hardware over a representative engine flight envelope.

4.3.3.2 Using an appropriate flow bench, the real-time simulation of the slave engine, and the backup control test console, the contractor shall conduct a steady state calibration of the backup control system. If there exist hardware common to both the backup and primary system (e.g., fuel metering valve) which is fabricated in 4.3.2.1, calibration of this hardware for both primary and backup operation is required.

4.3.3.3 Using the test set-up of 4.3.3.2, the contractor shall conduct transient performance and backup control transfer tests.

4.3.3.4 The contractor shall conduct those additional bench assurance tests needed to qualify the backup control hardware for subsequent slave engine testing.

4.3.3.5 The contractor shall refurbish, if necessary, the control hardware fabricated in 4.3.2.1 and 4.3.2.2 and deliver this hardware to the government.

4.3.4 Final Report

The contractor shall prepare, for publication, a comprehensive report which includes the hardware design report of 4.3.1.5 and which summarizes the test and evaluation results of 4.3.3.

APPENDIX B - DESCRIPTION OF THE VARIABLE CYCLE ENGINE

The Joint Technology Demonstrator Engine (JTDE-23) was selected as the engine for the trade studies. The reasons were as follows:

1. The JTDE-23 is the engine selected by the General Electric Company for the joint technology engine program. The JTDE-23 cycle and engine configuration were based on extensive mission optimization trade studies conducted under that program.
2. The Full Authority Digital Electronic Control (FADEC) will be designed for this engine. The FADEC program is a multimillion dollar, 40-month US Navy-funded effort aimed at the design, fabrication, and test of an engine-mounted, flight-type full authority digital electronic control. The FADEC program runs concurrent with the JTDE program.
3. The engine test dates are compatible with a possible follow-on program for demonstrating the backup control.
4. A steady-state and dynamic simulation of the engine was available from the JTDE and FADEC programs. This allowed investigating alternate backup control approaches and disclosing any restrictions imposed on the engine while on backup control.
5. The complexity of the engine provides a suitable challenge for the backup control program.

An engine cross section is shown in Figure B-1. The engine requires manipulation of two variable fuel flows (W_{FM} and W_{FR}) and eight variable geometries while on primary control. It is a double-bypass, single-nozzle (A_8), mixed-flow, augmented variable-cycle turbofan with forward and aft variable-bypass injectors ($VABI_F$ and $VABI_A$). Both fan blocks and both turbines are single stage with variable inlet guide vanes and stators (β_F) on the second stage and variable-area nozzles (A_4 and A_{54}). The first stage has no inlet guide vanes or variable stators. Variable bypass of the second stage fan is provided by the forward VABI which incorporates a forward bypass transition valve (FBTV) operating on the outer stream and the injector valve to set bypass flow conditions.

The JTDE's variable geometry gives it the ability to operate over a range of power settings without varying airflow and in so doing vary cycle pressure and temperature ratio. Conventional turbojets or turbofans modulate thrust by reducing airflow along with pressure and temperature ratio.

At intermediate power setting the JTDE operates as a low bypass ratio mixed flow augmented turbofan. The forward bypass transfer valve is closed, the forward VABI is open and the cycle is operating at its maximum pressure ratio. All airflow is compressed by both blocks of the fan. As power is reduced, cycle pressure ratio cannot only be lowered by opening the nozzle but also by bypassing air around the second block of the fan. By control of the FBTV, $VABI_F$, and the β_F the second fan block can be unloaded without changing engine airflow or the operating conditions of the front block of the fan. Fan turbine nozzle area can be increased to reduce its power to match the reduced power required to drive the fan in the double-bypass mode. Engine operation is thereby transformed into that of a higher bypass ratio turbofan for subsonic cruise power conditions. $VABI_A$ adjusts to accommodate the increased ratio of bypass air-to-core air. It still retains the ability to operate at high specific thrust where high power operation is necessary, i.e., during takeoff and high Mach number operation.

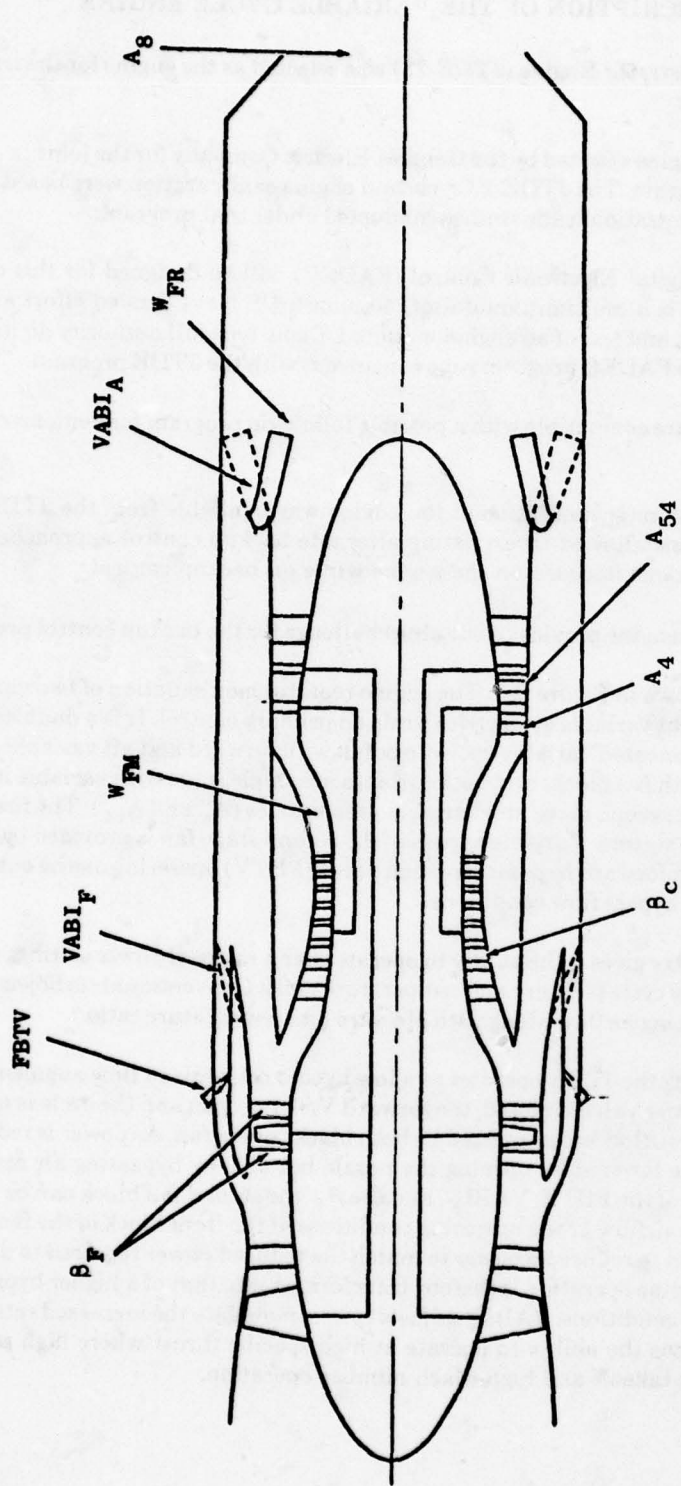


Figure B-1 - JTDE-23 Engine.

APPENDIX C - SELECTION OF THE AIRCRAFT

The aircraft selected for the backup control trade studies was the YF17 modified to have a single GE JTDE-23 engine. The reasons for this selection were:

1. The JTDE-23 airflow was directly compatible with the aircraft.
2. The aircraft is in 1980-1985 operational time frame.
3. Drag polar data were available and the General Electric Company had background technology in place to address this application.
4. A computer installation program was available. This was needed to determine steady-state and transient engine performance requirements.
5. Data from earlier flight tests were available and useful.
6. Flight envelope and probable mission data were available.
7. Single engine versus two engine installation effects were small from the viewpoint of the backup control trade study.

This aircraft has M_o 2.0 and 65,000 feet altitude capabilities which affect the control environment and engine thrust requirements. Aircrafts of this type usually have more than sufficient dry thrust for completing takeoffs, satisfactory climb rates, maneuver recovery, subsonic cruise and "waveoffs". Even a small loss (10%) in dry thrust is allowable which, in turn, permits control simplifications.

APPENDIX D - DESCRIPTION OF THE PRIMARY ELECTRONIC CONTROL SYSTEM

The primary electronic control system selected for the JTDE, the variable cycle engine selected for this program, includes the Full Authority Digital Electronic Control (FADEC). The FADEC system is shown in Figure D-1.

The heart of the control system is a special purpose digital computer (on-engine mounted) uniquely designed to provide the computational requirements. The computer design will be based on the capacity to control 10 manipulated variables, process 32 input parameters, receive up to 20 digital command inputs from the aircraft interface, and transmit up to 64 channels of monitor data to the aircraft. The digital electronic control functions include:

- Computation
- Memory
- Data Processing, Timing, and Signal Conditioning
- Actuator Interface

The remainder of the control system includes the fuel handling components, the actuators, and sensors. It is anticipated that the main fuel metering functions will be provided by the backup control. The unitized pump, being developed under the U.S. Navy Lightweight Fuel Delivery System program, is the intended fuel pressure source. Fluidic vortex valves, which have no close fitting gum and contamination sensitive moving parts, will be used for main fuel distribution. Most of the actuators will be hydraulic cylinders. The hydraulic actuators will be controlled by the fail-fixed servovalves developed under a USAF program.

Another part of this task was to identify possible interfaces between the primary control system and the backup control. The interfaces are dependent on the type of backup control hardware or approach selected (hydromechanical, electrical or fluidic). Possible interface approaches between the primary control system and the backup control in regards to fuel metering are:

1. Hydromechanical
 - a. The backup and primary control inputs into a common metering valve (See Figure D-2).
 - b. A backup metering valve in parallel to the primary metering valve.
 - c. A backup metering valve in series with the primary metering valve.
 - d. A mechanical override in the primary fail-fixed servovalve controlling the metering valve.
 - e. Hydraulically sum the servo flows from the fail-fixed servovalve and a servovalve driven by the power level gain cam (Figure D-2) to drive a common metering valve.
2. Electrical
 - a. The backup and primary control signals can be combined upstream of the primary servovalve driver amplifier.

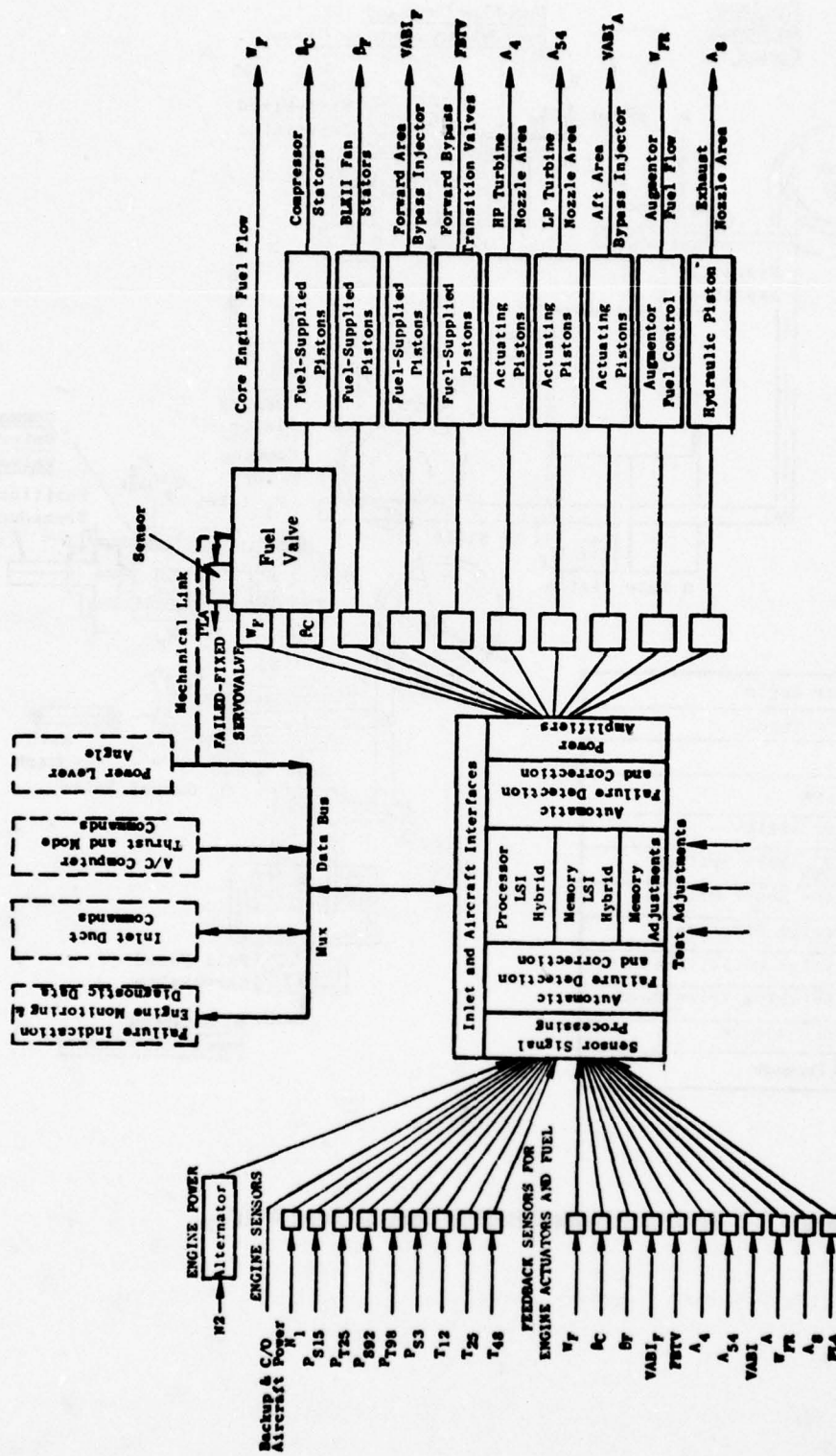
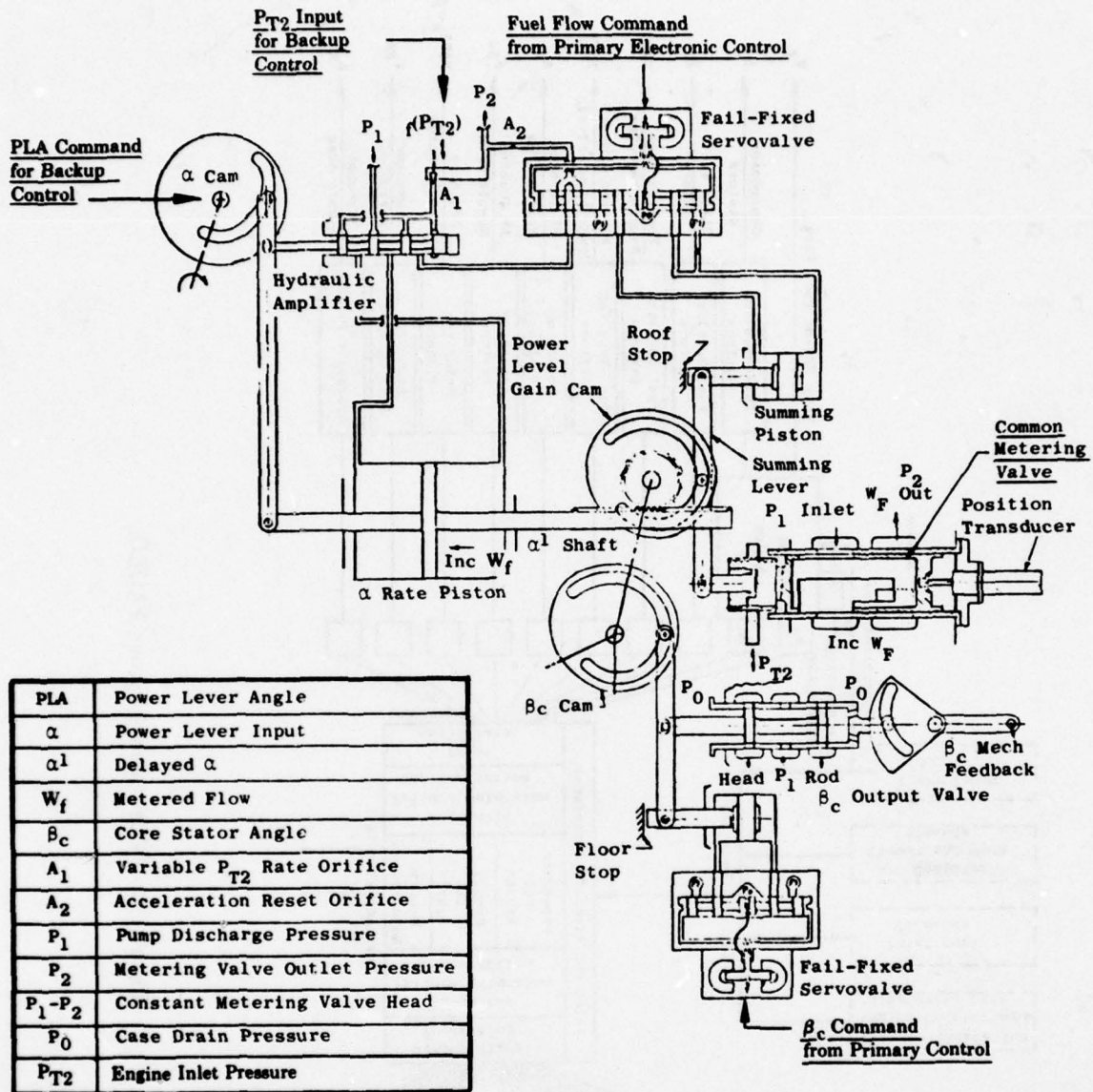


Figure D-1 - JTDE Control System FADEC.



PLA	Power Lever Angle
α	Power Lever Input
α^1	Delayed α
W_f	Metered Flow
β_c	Core Stator Angle
A_1	Variable P_{T2} Rate Orifice
A_2	Acceleration Reset Orifice
P_1	Pump Discharge Pressure
P_2	Metering Valve Outlet Pressure
$P_1 - P_2$	Constant Metering Valve Head
P_0	Case Drain Pressure
P_{T2}	Engine Inlet Pressure

Figure D-2 - Hydromechanical Backup Control Using W_f/P_{T2} .

- b. A separate fail-fixed servovalve/servo piston combination can be used to provide a second mechanical input equivalent to the input provided by the power level gain cam shown in Figure D-2.
- c. A separate fail-fixed servovalve could drive a separate metering valve either in parallel or series with the primary metering valve.

3. Fluidic

- a. A fluidic override of the primary fail-fixed servovalve controlling the metering valve (See Figure D-3).
- b. A fluidic servovalve (see Figure D-4) and servo piston combination whose output is summed with the primary electrohydraulic fail-fixed servovalve and servo piston combination output to drive a common metering valve (similar to hydromechanical scheme shown in Figure D-2).
- c. A fluidic servovalve driving a separate metering valve in series or parallel with primary metering valve.

Possible interface approaches between the primary control system and the backup control in regards to variable geometry are:

1. Hydromechanical

- a. The primary fail-fixed servovalve/servo piston combination mechanical position is summed with a mechanical position generated by the backup control to provide an input into a servovalve (see β_c output valve and related hardware in Figure D-2).
- b. The backup control could provide a mechanical override for the primary fail-fixed servovalve.
- c. The backup control could provide a servovalve output which operates in parallel or series with the primary fail-fixed servovalve.

2. Electrical

- a. The backup control signals can be combined with the prime control signals upstream of the torque motor amplifier.
- b. A separate servovalve/servo piston combination can provide a mechanical output equivalent to the β_c cam output shown in Figure D-2.
- c. A separate servovalve could be used in parallel or series with the primary servovalve.

3. Fluidic

- a. A fluidic override mechanism could be added to the primary fail-fixed servovalve (see Figure D-3).
- b. A separate fluidic servovalve/servo piston combination can provide a mechanical output to the β_c cam output shown in Figure D-2.

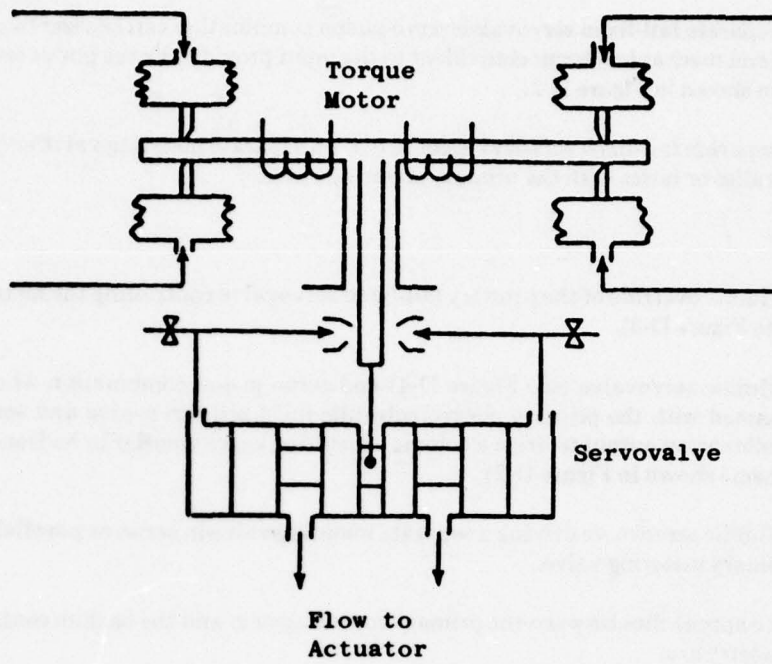


Figure D-3 - Servovalve with Fluidic Override.

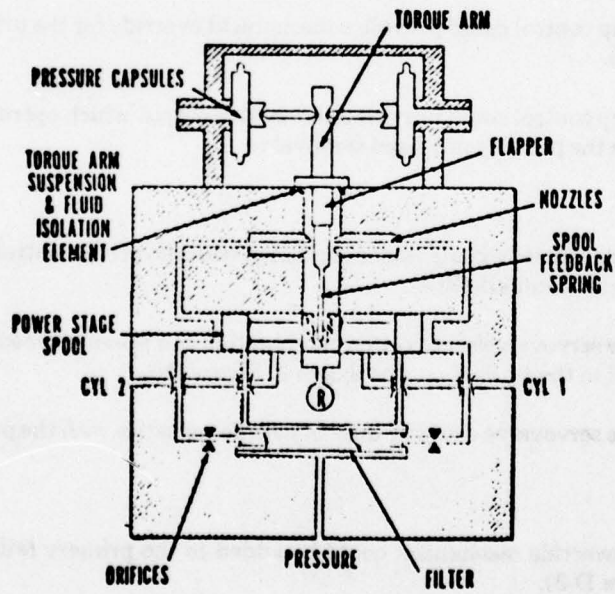


Figure D-4 - Fluidic Servovalve.

- c. A separate fluidic servovalve could be used in parallel or series with the primary electrohydraulic servovalve.

The required position/conditions of all the controlled variables during backup control operation were selected as follows:

<u>Variable</u>	<u>Symbol</u>	<u>Position/Condition</u>
Core Fuel Flow	W_{FM}	Manipulated
Compressor Stators	β_c	Manipulated
Fan Stators	β_F	Open
Fwd. Variable Bypass Injector	$VABI_F$	Closed
Fwd. Bypass Transition Valves	FBTV	Closed
HP Turbine Inlet Area	A_4	Open
LP Turbine Inlet Area	A_{54}	Open
Aft Variable Bypass Injector	$VABI_A$	Open
Augmentor Fuel Flow	W_{FR}	Off
Jet Nozzle Area	A_8	Closed

APPENDIX E - DEFINITION OF MINIMUM "GET HOME" CAPABILITY

In this case, minimum get home capability is what the aircraft/engine system should be capable of doing while transferring to and while operating on backup control. Unless otherwise specified, all functionally related aircraft subsystems, e.g., the inlet subsystem and the engine itself, are assumed to be operating normally. As envisioned, the get home capability includes:

1. If a primary control failure occurs during takeoff, and after reaching an aircraft speed which rules out an aborted takeoff, the aircraft shall be able to complete the takeoff with maximum gross weight at standard sea level conditions, while requiring no more than an additional 2000 feet of runway length over that required for takeoff under primary control.
2. If a primary control failure occurs during climb, the minimum climb rate shall be 2000 feet/minute with maximum gross weight at standard day sea level conditions or 500 ft/minute with maximum gross weight at hot day conditions at 6000 feet altitude.
3. If a primary control failure occurs during supersonic flight, the aircraft shall be able to decelerate to a subsonic speed without encountering engine "flameout", stall or physical damage to the engine or aircraft.
4. If "flameout" occurs while on either primary or backup control, a windmill or "spool down" air start shall be attainable, provided that the cause of the "flameout" has been eliminated, in either the primary or backup mode. The air start envelope will not be compromised except for the reduced flight envelope while on backup control.
5. If a primary control failure occurs during a mission, the aircraft shall be able to return subsonically at altitudes up to 50,000 feet with no more than 10% reduction in cruise range when compared to cruise range attainable under primary control mode operation.
6. If a primary control failure occurs during a combat, maneuver or landing, the engine shall be able (on backup control) to conduct a stall-free acceleration from backup idle to maximum backup thrust within 20 seconds at 23,000 feet and within 8 seconds at sea level for maneuver recovery or "waveoff" capability.
7. If a primary control failure occurs, the resulting additional pilot workload must be acceptable. Pilot attention will probably be required during backup control air starts and at maximum backup thrust to watch cockpit gages and trim the PLA to prevent small overspeed or overtemperature occurrences.
8. If a primary control failure occurs, the engine shall be suitably protected from intolerable overspeed, overtemperature or over pressure operation even if the pilot takes no corrective action or in spite of any pilot PLA action.
9. If a primary control failure occurs after "touch down", the aircraft must be capable of attaining a safe runway roll and stop. The maximum ground idle thrust shall be 9% of dry rated (normal is 5%).

APPENDIX F - OPERATIONAL OBJECTIVES AND CONSTRAINTS

In regards to operational objectives and constraints, the backup control must function as part of the overall control system under three conditions. These conditions are:

1. When the primary control is functioning properly and it has full authority.
2. Upon a primary control system failure and during the transfer from primary to backup control mode.
3. When the backup control has authority.

When the primary control system is functioning properly, the backup control must:

1. Not interfere with the steady-state and transient performance of the primary control.
2. Have its primary failure mode in the direction of "loss of protection".
3. Not restrict pilot action in regards to power lever.
4. Not add any operational constraint or restriction to the engine/control system.

Upon primary control system failure and during transfer to the backup control mode, the combined control system must:

1. Allow automatic transfer to the backup control when the primary control system self-test operations indicate a failure.
2. Allow automatic transfer to backup control upon loss of electrical power to the primary control.
3. Allow transfer to the backup control by pilot action.
4. Maintain thrust for a short time (15 to 90 seconds) at essentially existing levels or transfer to thrust determined by backup control without causing engine stall if no pilot action is taken and allow the pilot to make thrust changes by PLA action.
5. Allow all nonmanipulated variables to drift toward and attain their preselected fixed positions.
6. Provide cockpit indication that the control system is functioning in the backup mode.

After the transfer to backup control is complete and all nonmanipulated variables are at their desired fixed positions, the backup control must:

1. Provide aircraft get home capability which includes sufficient thrust level and thrust response for takeoff, climb, cruise, loiter, and landing.
2. Allow the pilot to trim power level angle (PLA) to reduce possible slight overspeed or over-temperature conditions.

3. Not impose undue pilot workload.

The operational constraints are dependent on the selected backup control mechanization. As initially envisioned, the constraints during transferring to the backup control included:

1. The fuel flows and variable geometries are moving toward their desired fixed positions so the thrust may be less or more than after transfer is complete.
2. There will be no PLA restrictions when the aircraft is flying subsonically other than limiting operation to the dry regime. At augmented supersonic flight conditions, a reduction in power demand to intermediate will be required. Additional constraints on PLA demands significantly below intermediate will depend on the nature of the inlet control and its signals to the engine control. If airflow (minimum) limiting is required, it may be necessary to delay any retard to low power setting until the aircraft decelerates below Mach 1.5.

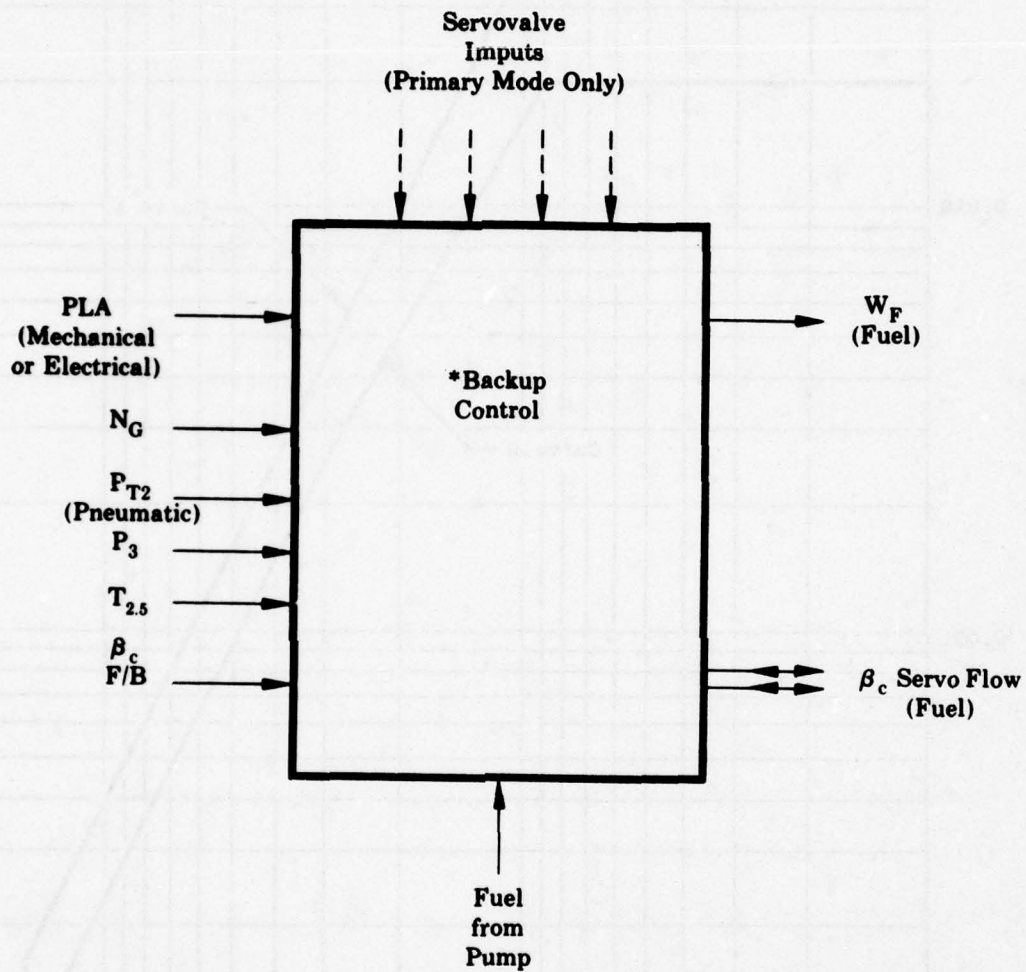
The operational constraints while on backup control included:

1. Thrust response will be reduced because a simple accel/decel control is intended.
2. Slight overspeed (about 4% above nominal) and slight overtemperature (about 150° F) may occur especially at maximum backup thrust. These possible overspeed and overtemperature conditions will not cause serious engine damage but could shorten engine life; therefore, the pilot should adjust the PLA per the engine indicators.
3. The pilot will not have to limit PLA rate in order to prevent stall or serious engine damage.
4. Pilot action may be required during an air start. It is expected the pilot will be required to set the power lever at a specific angle and advance the power lever after lightoff is detected.

The number and types of possible inputs and outputs and the control system environment were identified. The possible inputs and outputs to and from the backup control are shown by Figure F-1. For this study, it was assumed that main fuel flow (W_{FM}) and compressor stators (β_c) will be manipulated in the backup mode. Also, it was assumed that both electrical and mechanical PLA were available. Previous studies indicated that engine inlet pressure (P_{T2}) and PLA are suitable parameters for the backup control. Core speed, N_G , compressor discharge pressure, P_{S3} , and compressor inlet temperature, $T_{2.5}$ were also considered as input parameters. The signals to the primary fail-fixed servovalves will be zero current during backup mode operation.

The environmental requirements are:

Ambient Air Temperature	-54° F to 470° F
Fuel Temperatures	-65° F to 210° F (at fuel pump inlet)
Aircraft Mach No.	2.0 max.
Vibration Level	See Figure F-2
Acoustic Environment	150 dB max at 100 to 10,000 Hz



***Includes Backup and Primary Fuel Metering and Core Stator Servovalves**

Figure F-1 - Possible Backup Control Inputs and Outputs.

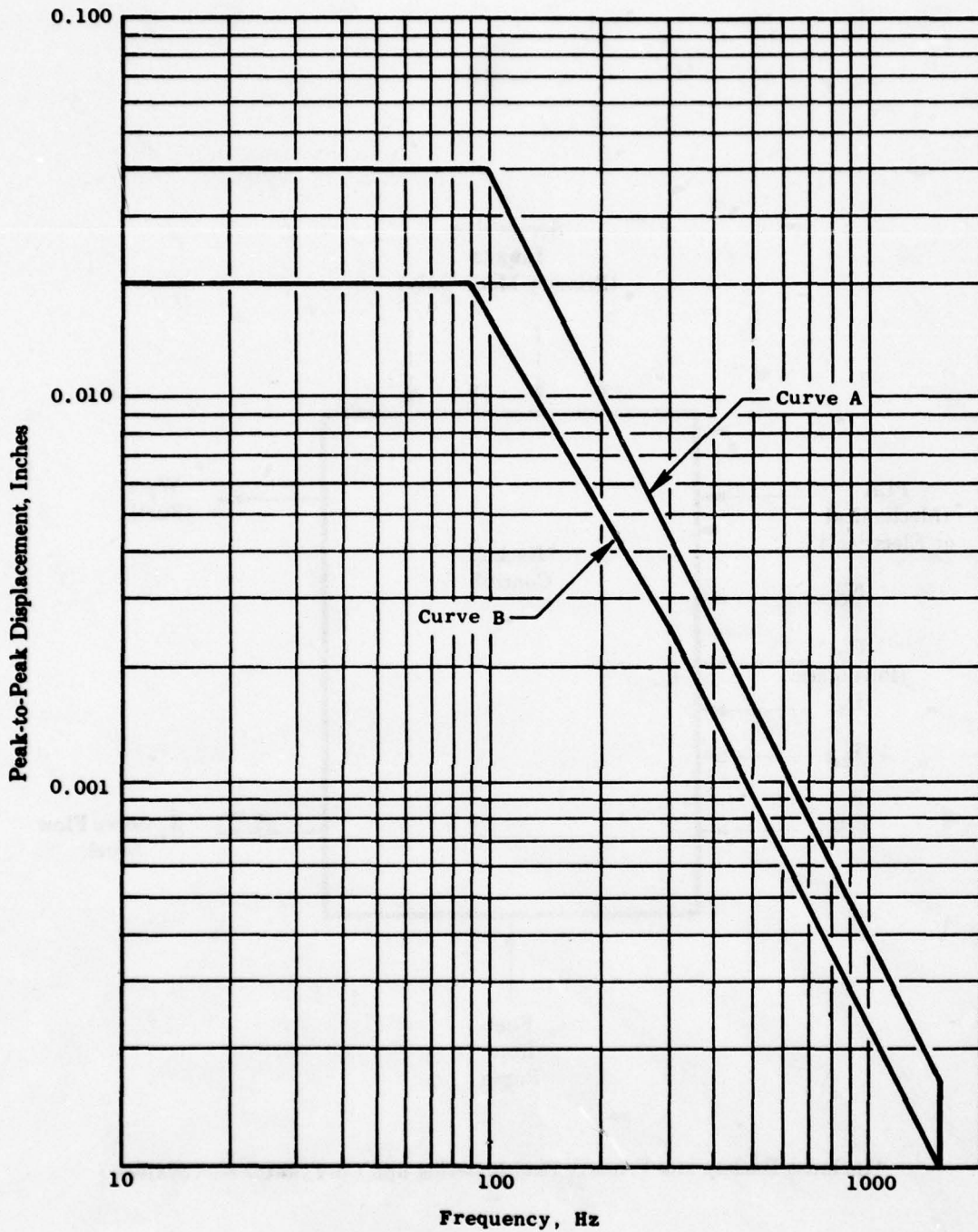


Figure F-2 - Vibration Requirements for Gearbox Mounted Components.

The air temperatures and Mach number shown are for primary mode operation; steady-state operation on the backup control will be at reduced temperatures and Mach number. However, the backup control must not have deleterious effects on normal operation of the primary control at these conditions and must be capable of proper operation if transfer to backup control is initiated at these conditions. The vibration requirements are per MIL-E-5007D for gearbox mounted components. Curve B is used to find the resonant frequencies and Curve A is used for running at the resonant frequencies.

APPENDIX G — STEADY STATE AND TRANSIENT ENGINE PERFORMANCE REQUIREMENTS

1. ENGINE THRUST REQUIREMENTS

The first step was to determine thrust requirements for an aircraft with drag polars of the YF17. Sufficient data were available and the following plotted data were reviewed in detail:

- a. Takeoff performance which shows the thrust required for various takeoff distances with different aircraft weights for a given takeoff velocity.
- b. Takeoff performance which shows the takeoff distance for various aircraft weights and takeoff velocities for two given thrust levels.
- c. Actual versus predicted takeoff performance for two given thrust levels and one aircraft weight.
- d. Thrust required for various rates-of-climb and aircraft weights for one velocity at sea level.
- e. Thrust required for various rates-of-climb and Mach numbers at three aircraft weights at sea level.
- f. Actual and predicted thrust required at two altitudes with one aircraft weight for a range of rates-of-climb.
- g. Cruise performance showing thrust required for three aircraft weights at one Mach number for a range of altitudes.
- h. Cruise performance showing thrust required with various aircraft weights at various Mach numbers at sea level.
- i. Cruise thrust required at 36,089 feet and one aircraft weight for a range of Mach numbers.
- j. Thrust required for approach at sea level for a range of aircraft weights and glide slope angles at one Mach number.
- k. Change in "waveoff" decision height per second delay in backup control system response for a range of approach glide slope angles.
- l. Landing distance for a range of aircraft weights and thrust levels for one landing velocity and a clean, dry runway.
- m. Landing distance for one aircraft weight and a range of thrust levels and friction coefficients for one landing velocity.

The above data provided ample information for establishing backup control requirements. The data were from a report titled, "YF17 - Performance and Flying Qualities Evaluation" (AFFTC-TR-75-18). The classified curves were not included in this unrestricted report.

2. INPUT AND OUTPUT VARIABLES

Determination of the minimum number of input and output variables began with a failure effects analysis in terms of the manipulated variables used for primary control. This analysis yielded the desirable dominant failure modes of all manipulated variables to allow safe engine operation after failure of the primary control for each particular variable. It also yielded the particular variables that have no safe dominant failure mode that provides adequate thrust. Table G-1 is a tabulation of the estimates made for the JTDE. It can be seen that dominant failure modes can be selected for all but two manipulated variables to provide not only safe operation but also low thrust loss.

Main fuel flow, (W_{FM}) and core compressor variable stators (β_c) remain the variables for which no dominant failure mode can be obtained that will provide safe operation and adequate thrust. Failing to high fuel flow will yield catastrophic engine reaction; overspeed or overtemperature, while failure to a low value will not provide thrust. It is clear that main fuel flow is one of the manipulated variables that will have to be controlled by the backup control.

Core compressor variable stators also have no dominant failure mode that can be selected that will permit acceptable operation. Their complete closure will cause stalls at high speed while failure to the full open position will not allow stall free operation at low speeds.

The operation of the backup control with only fuel flow and compressor stators was simulated on a steady-state basis using the variable cycle engine (JTDE) model. The preliminary backup control scheme was selected based on the selected failure directions of the manipulated variables shown in Table G-1. If the designated failure effects can be achieved for the balance of the manipulated variables, sufficient control can be provided by backing up main fuel flow and core stators.

It was assumed that for a fixed inlet pressure, the backup control will schedule fuel flow directly as a function of power setting. Based on this assumption, a simulation was conducted by scheduling fuel flow as a function of power setting while scheduling core stator vane angle (β_c) to the same schedule as that used for primary control. Figure G-1 is a plot of the resultant thrust, percent increase of specific fuel consumption and fan speed versus power lever angle. The results show that essentially linear thrust variation with power lever angle (PLA) is obtained and that the backup mode thrust is about 97% of the primary mode thrust at intermediate power. The specific fuel consumption increase in the worse case is slightly above 10% which indicates that cruise range loss will be in the same order. Figure G-2 is a plot of the critical engine parameters as a function of PLA.

TABLE G-1
ESTIMATED ENGINE LEVEL FAILURE EFFECTS

Dry Operation				
Manipulated Variable	Failure Direction	Failure Effect	Desired Dominant Failure Mode	Backup Control Function Req'd
β_F	Open Closed	SFC Deterioration Stall Potential	Open	No
β_C	Open Closed	Stall Low F_n	<u>None</u>	<u>Yes</u>
A_4	Open Closed	Small F_n Loss Small F_n Loss	Open	No
A_{54}	Open Closed	Small F_n Loss High N_f	Open	No
A_8	Open Closed	Large F_n Loss Small Stall Margin Loss	Closed	No
VABI Fwd	Open Closed	No Effect Small F_n Loss	Closed	No
Front Bypass Transfer Valve	Open Closed	Stall No Effect	Closed	No
VABI Aft	Open Closed	Small F_n Loss Small F_n Loss	Open	No
W_f	High Low	Overtemp - Overspeed Low F_n	<u>None</u>	<u>Yes</u>

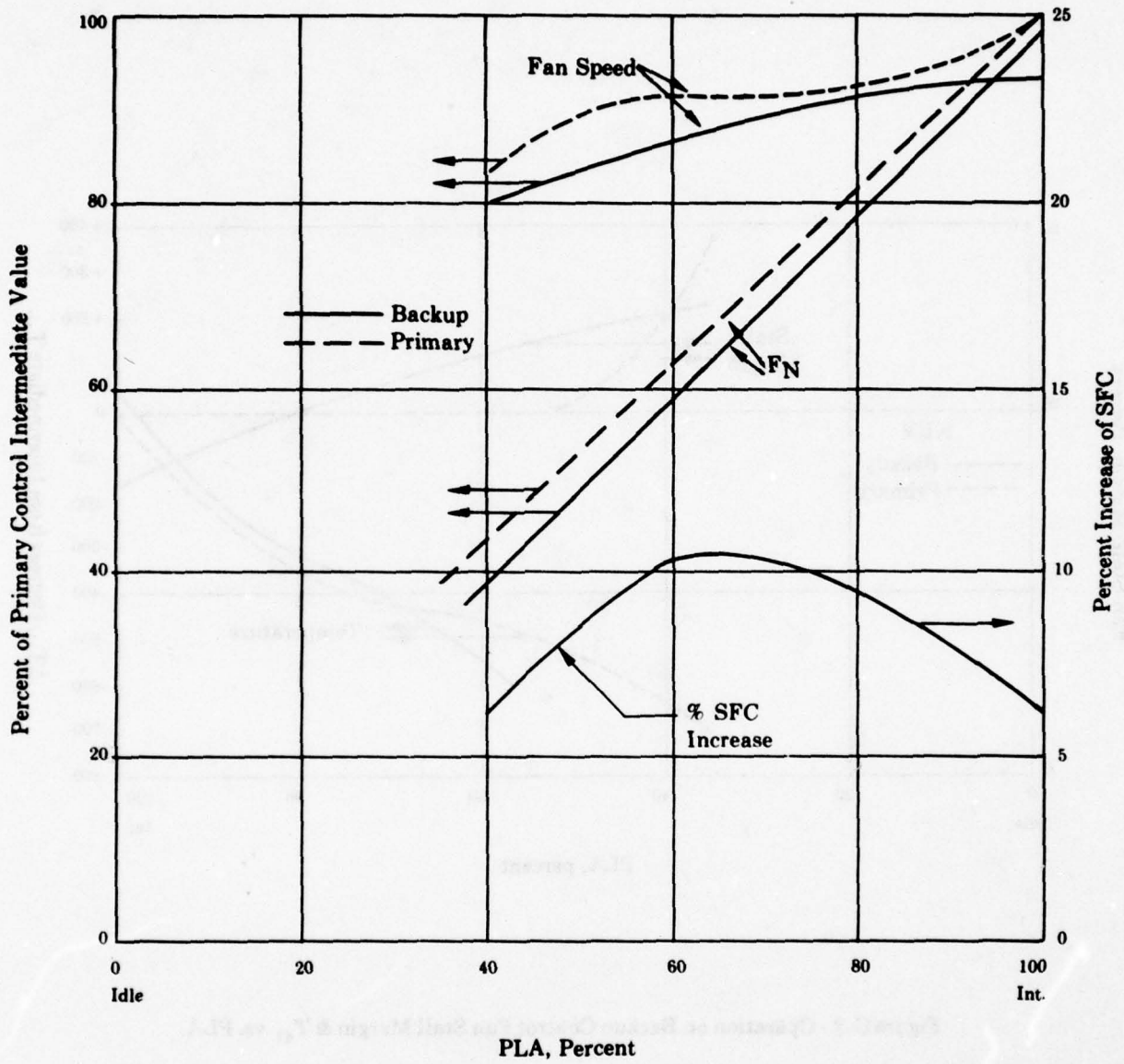


Figure G-1 - Estimated Performance on Backup Control Operation Showing Fan Speed, Percent Increase of Specific Fuel Consumption (SFC) and F_N versus PLA.

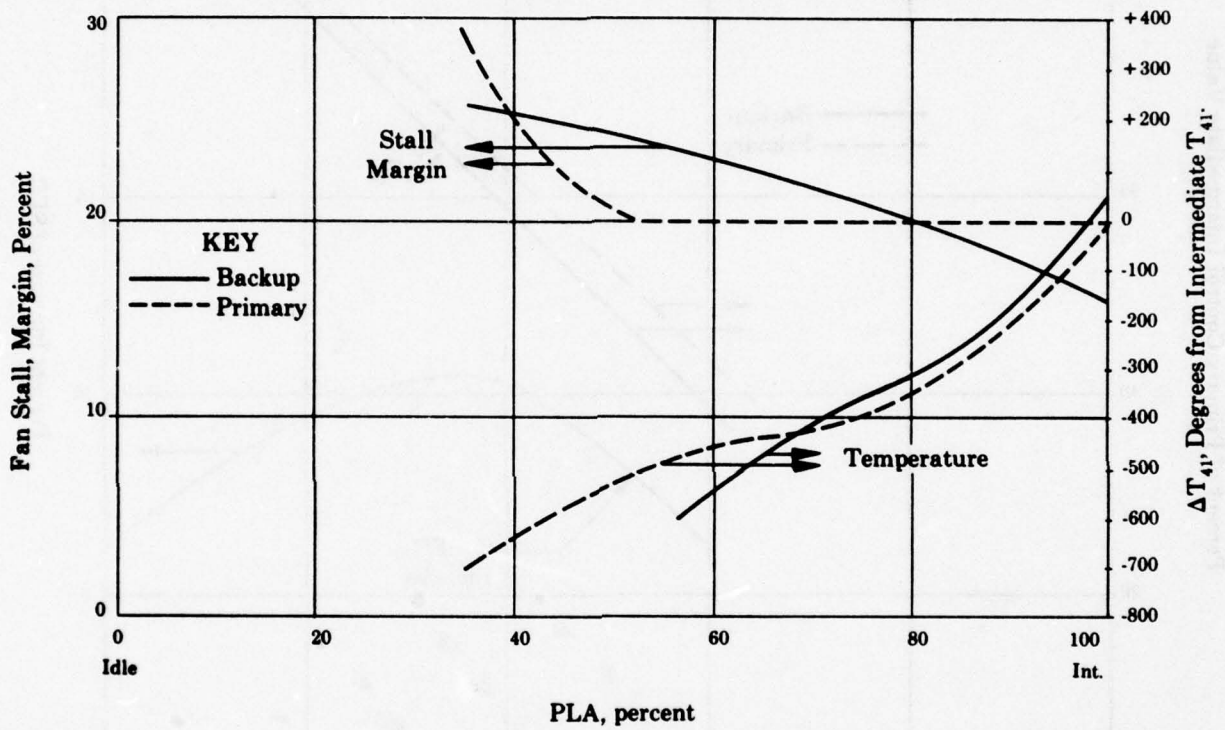


Figure G-2 - Operation on Backup Control Fan Stall Margin & T_{41} vs. PLA.

APPENDIX H - BACKUP CONTROL REQUIREMENTS

1. BACKUP CONTROL LOGIC

All of the backup controls considered provide full time upper or roof limits on W_f or N_G . Upper limits on W_f or N_G provide overspeed and overtemperature protection which is considered more critical than providing a lower limit. Loss of fuel flow during takeoff is critical so a W_f lower limit or floor was considered.

The backup control can be combined with the primary control either in series or in parallel (standby). Both techniques were applied. With the series technique as used in this study, the backup control computer output is added to that of the primary. In the primary mode, the backup control provides upper limits on W_f and β_c and the primary control subtracts from the limits to satisfy its demands. During transients in the primary mode, the backup control W_f and β_c demands must always be greater than the primary control demands so that interference is avoided.

With the parallel technique, the backup control is on standby. During primary mode operation, the backup control computer output is blocked by a transfer valve. This technique avoids interference between the two controls.

2. TRANSFER CHARACTERISTICS

The series technique, which sums the primary and backup W_f and β_c demands, used in this study provides ideal transfer characteristics. Transfer involves changing from the primary steady-state schedules and accel/decel rates to the backup steady-state schedules and slower accel/decel rates. Transfer action is initiated by applying zero current to all 10 fail-fixed servovalves used in the FADEC system. The 8 nonmanipulated variable actuators slowly drift to their desired stops. The metering valve and the β_c actuators slowly drift to the upper limits set by the backup control. There is no abrupt change in fuel flow or any other parameter. PLA modulations are allowed without restrictions when the aircraft is flying subsonically (see Appendix F - Operational Objectives and Constraints).

The parallel or standby technique can also provide satisfactory transfer characteristics. To provide smooth transfer, the backup control tracks the primary control. This causes the backup W_f or N_G demand, and the backup β_c demand to be equal to or almost equal to the primary demands at the instant of transfer. Transfer is initiated by applying zero current to the 10 fail-fixed servovalves used in the FADEC system and by sending a current signal, approximately 80 milliamps, to the transfer valve. The 8 nonmanipulated variable actuators slowly drift toward their desired stops. The transfer valve strokes to its other stop and at this position only the backup servovalve output flows control the metering valve and the β_c actuators. If any difference in backup PLA requested N_G and actual N_G exists at the initiation of transfer, for example, the difference is integrated per the rates allowed by the backup control. PLA modulation is allowed during transfer as it is in the series technique.

3. PARAMETRIC STUDIES

Preliminary studies indicated that W_f/P_{T2} was a satisfactory backup control parameter or mode especially in the subsonic region. To establish feasibility of the control mode, the JTDE-23 engine steady state cycle was run at various flight conditions and max dry power level with turbine temperature T_{41} limited to a constant value. This yielded data for the required values of W_f/P_{T2} to maintain the desired T_{41} limit. Figure H-1 shows a series of points run at a constant altitude of 30,000 at Mach numbers up to 2.0 and another series of points run at a constant Mach number of 1.2 with altitude up to 50,000. The data

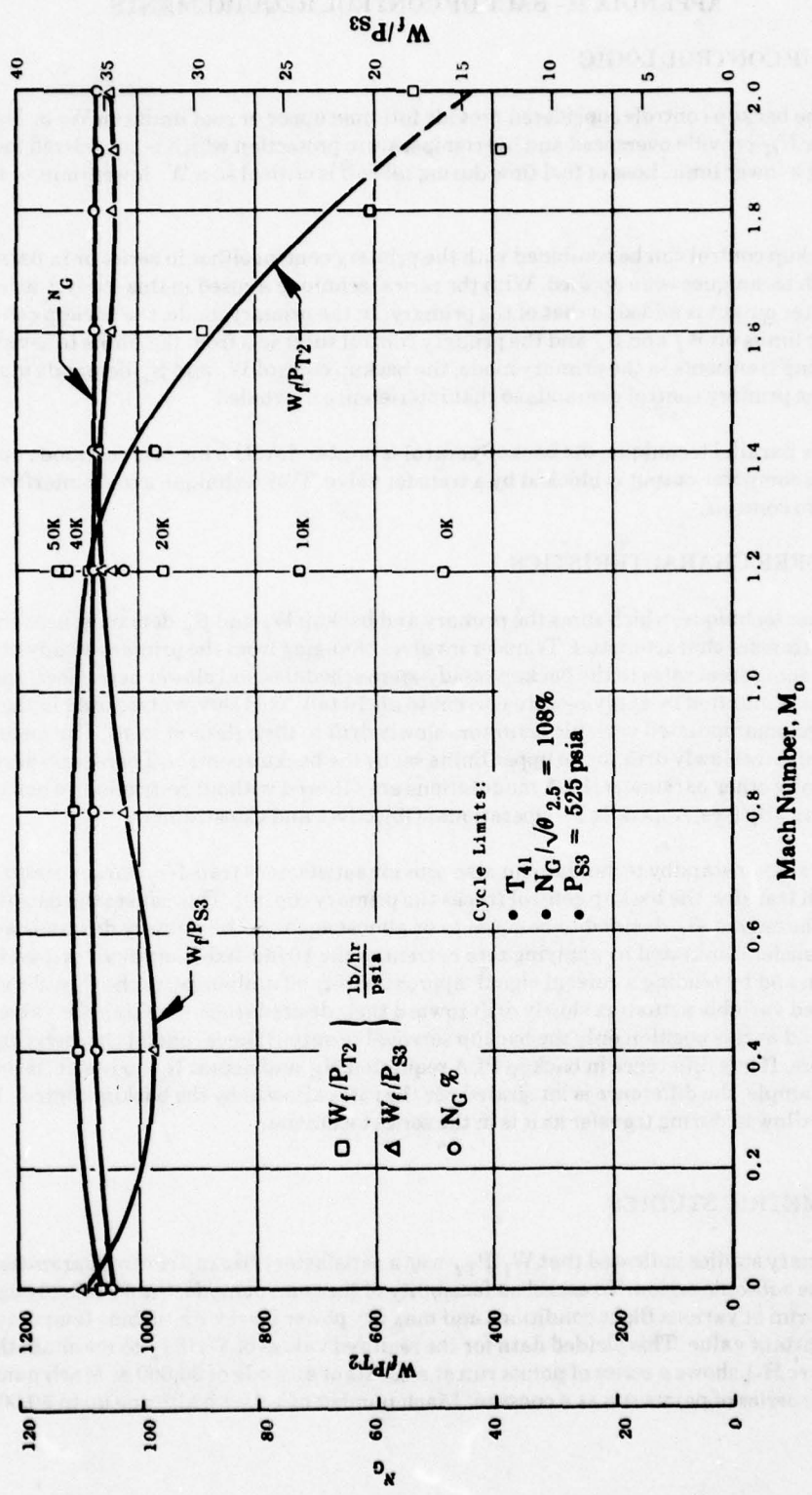


Figure H-1 - Backup Control Parameters Vs. Mach Number, JTDE-23 Cycle Operating on Limits.

show, that at subsonic speeds, a $W_f/P_{T2} = 1100$ pph/psia schedule, at power settings of intermediate and above, would provide a satisfactory limit. In order to not restrict or interfere with primary control operation at normal conditions, the backup control should be at a higher limit. A margin of 7% was added resulting in a backup control schedule of $W_f/P_{T2} = 1184$ pph/psia. At a flight Mach number of 1.2, low altitudes and at higher M_o , high altitudes, however, the data show that a much lower W_f/P_{T2} ratio is needed to limit T_{41} and pressure to the desired values. Figure H-2 shows how T_{41} varies with $T_{2.5}$ at SLS when a constant $W_f/P_{T2} = 1184$ pph/psia schedule at intermediate is used.

Other control parameters, such as W_f/P_{S3} and gas generator speed (N_G) were studied as possible additions or alternates. The results are also shown in Figure H-1. The ratio W_f/P_{S3} appears to provide satisfactory T_{41} protection but, alone, it is not satisfactory for scheduling part power. The combination of W_f/P_{S3} and W_f/P_{T2} may be feasible with W_f/P_{T2} limiting at low Mach numbers and W_f/P_{S3} at Mach numbers above 1.2. The parameter N_G also appears promising. It can be seen from Figure H-1 that holding a core physical speed limit will limit T_{41} within narrow limits even at the higher Mach numbers.

To determine overtemperature levels and the flight map areas where overtemperature occurs, the steady state cycle deck was again run at various flight conditions, this time without observing the engine temperature, speed, and pressure limits but running on the potential backup control limit schedule of $W_f/P_{T2} = 1184$ pph/psia. The non-manipulated variables were fixed at the sea level standard (SLS) positions as an overall base condition. The SLS positions were used because at the time of this study, the steady state values of all the JTDE manipulated variables over the entire flight map were not yet determined. The use of SLS positions was justified by running the cycle deck at one of the most severe temperature/flight conditions using both SLS variable positions and an assumed set of fail-fixed positions. Results showed an insignificant difference in T_{41} penalty. In addition, a W_f limit was imposed. The W_f limit value (17,181 pph) was based on the maximum required flow at $M_o = 1.2$ at sea level to put the engine on one of its limits (pressure). The results of operating the cycle deck in this mode are shown on Figure H-3. They show that the addition of W_f limiting improved the temperature problem at the low altitude, high M_o portion of the flight map but the predicted overtemperature at high M_o remains.

As previously indicated, W_f/P_{S3} appeared to provide satisfactory T_{41} limiting at high M_o . The value selected for W_f/P_{S3} was 38.9 pph/psia which is again 7% above primary control normal operation, high enough to prevent interference with normal primary control operation, but low enough to provide tolerable overspeed and overtemperature. The engine cycle deck runs were repeated at the overtemperature flight conditions with this W_f/P_{S3} limit imposed in addition to the previous W_f/P_{T2} and W_f limits. The results are shown in Figure H-4. There was a significant improvement in the resulting T_{41} overtemperature at high flight Mach number. The overtemperature is still significant at $M_o = 1.6$. Figures H-5 and H-6 show how T_{41} varies with $T_{2.5}$ and M_o respectively with W_f/P_{T2} , W_f and W_f/P_{S3} limits imposed.

In addition to the above, the engine cycle deck was used to determine if T_{41} overtemperature occurred due to hot day conditions. At a max dry power setting and at sea level hot day takeoff condition, the results showed that T_{41} overtemperature will occur with the control at $W_f/P_{S3} = 38.9$ pph/psia.

Because of its potential T_{41} limiting capability seen in previous studies, a physical core speed (N_G) limit was imposed, replacing the W_f/P_{S3} limit. A value of $N_G = 104\%$, corresponding to a max $\Delta T_{41} = 250^\circ\text{F}$ (see Figure H-7) was selected. Figure H-8 shows the results of this W_f/P_{T2} , W_f , and N_G control mode. It appears that satisfactory T_{41} limiting at all high altitude, high Mach number portions of the flight map is provided. Figures H-9 and H-10 show how ΔT_{41} varies with $T_{2.5}$ and M_o in this imposed mode compared to the other modes analyzed.

Analyses were also done with the nonmanipulated variables in their failed positions to simulate conditions after primary failure when the fail-fixed servos had time to creep to their preferred failure

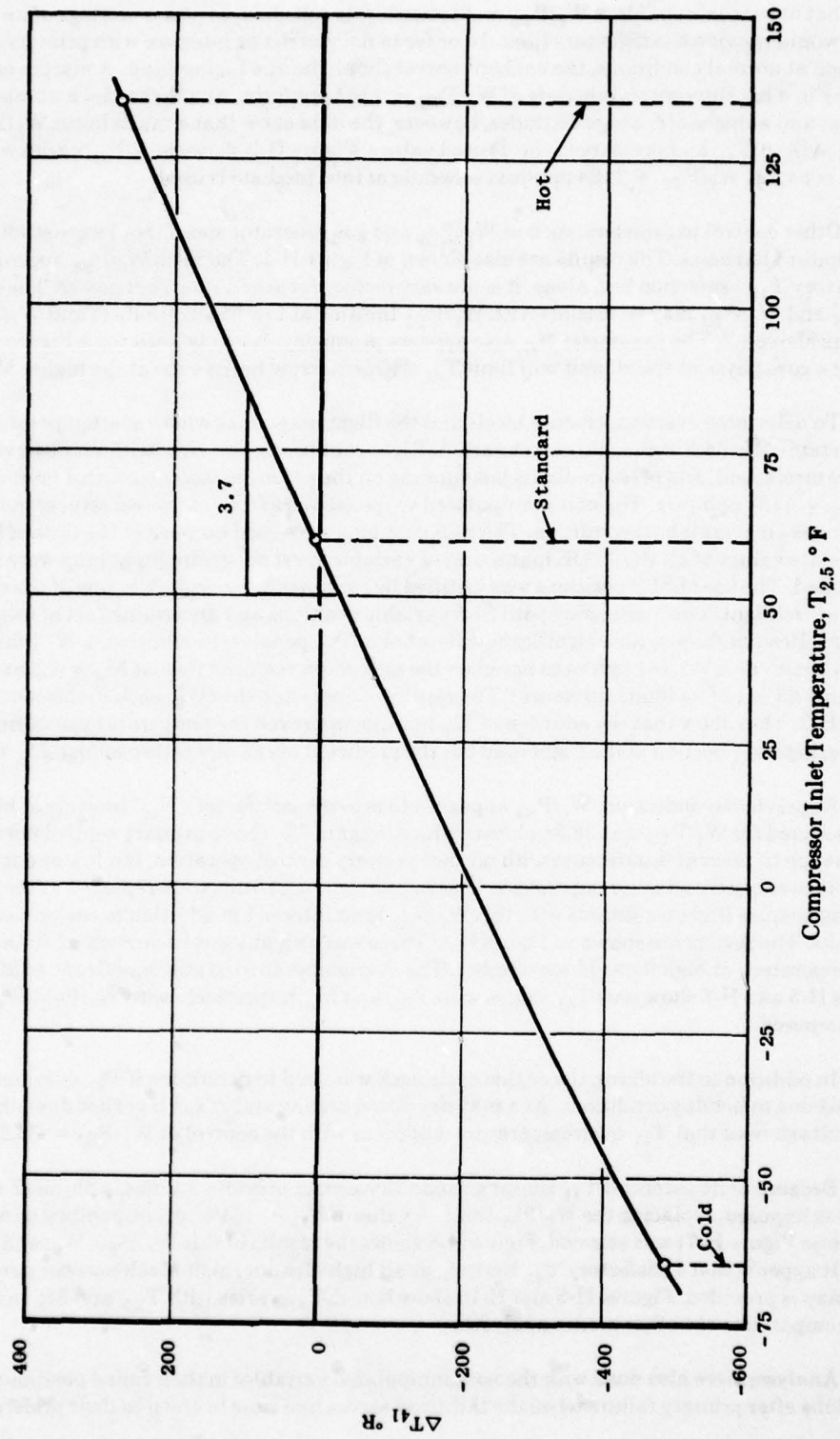


Figure H-2 - Variation in T_{41} for Hot and Cold Day.

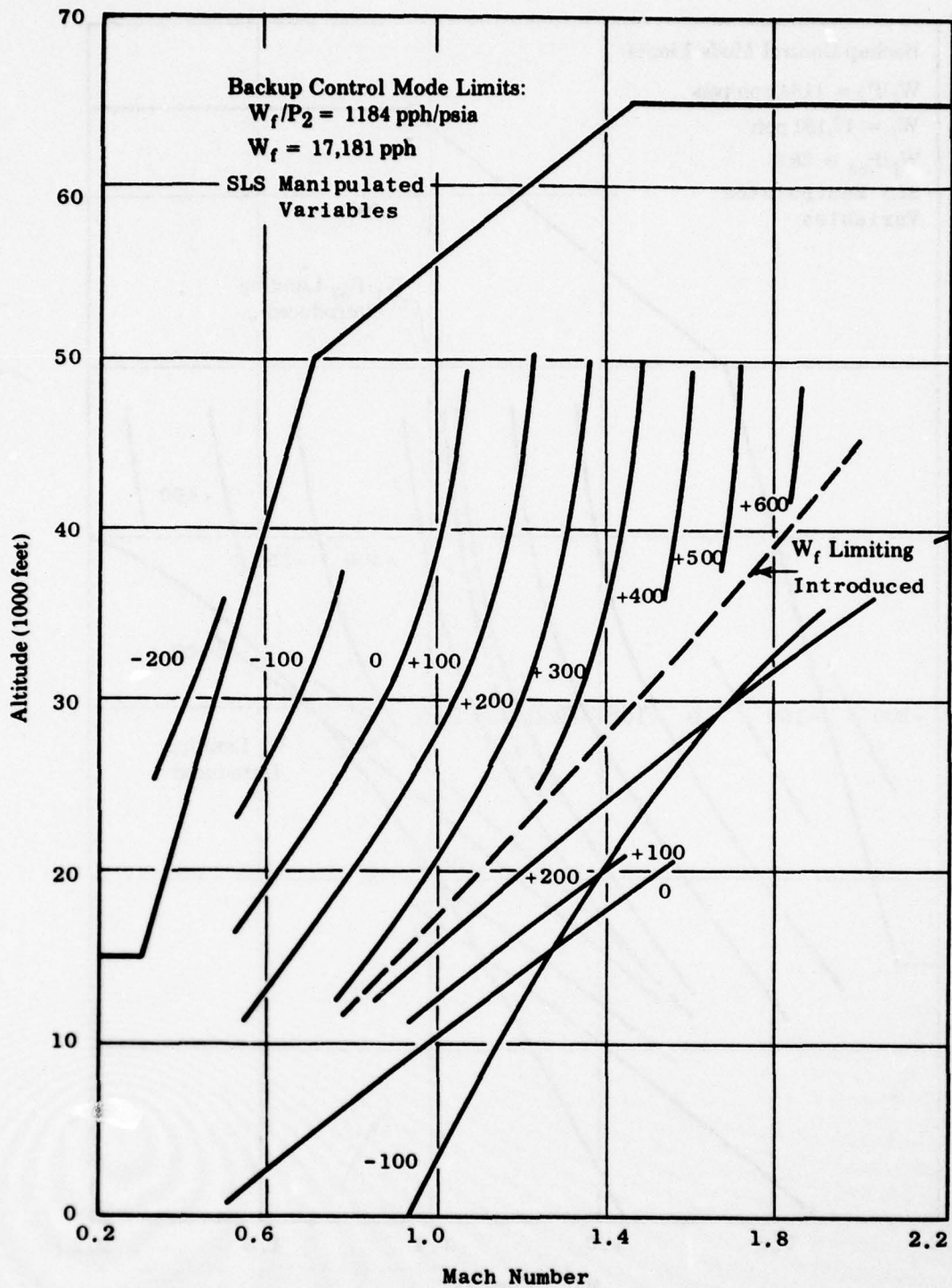


Figure H-3 - Temperature Limiting on W_f and W_f/P_{T2} Backup Control.

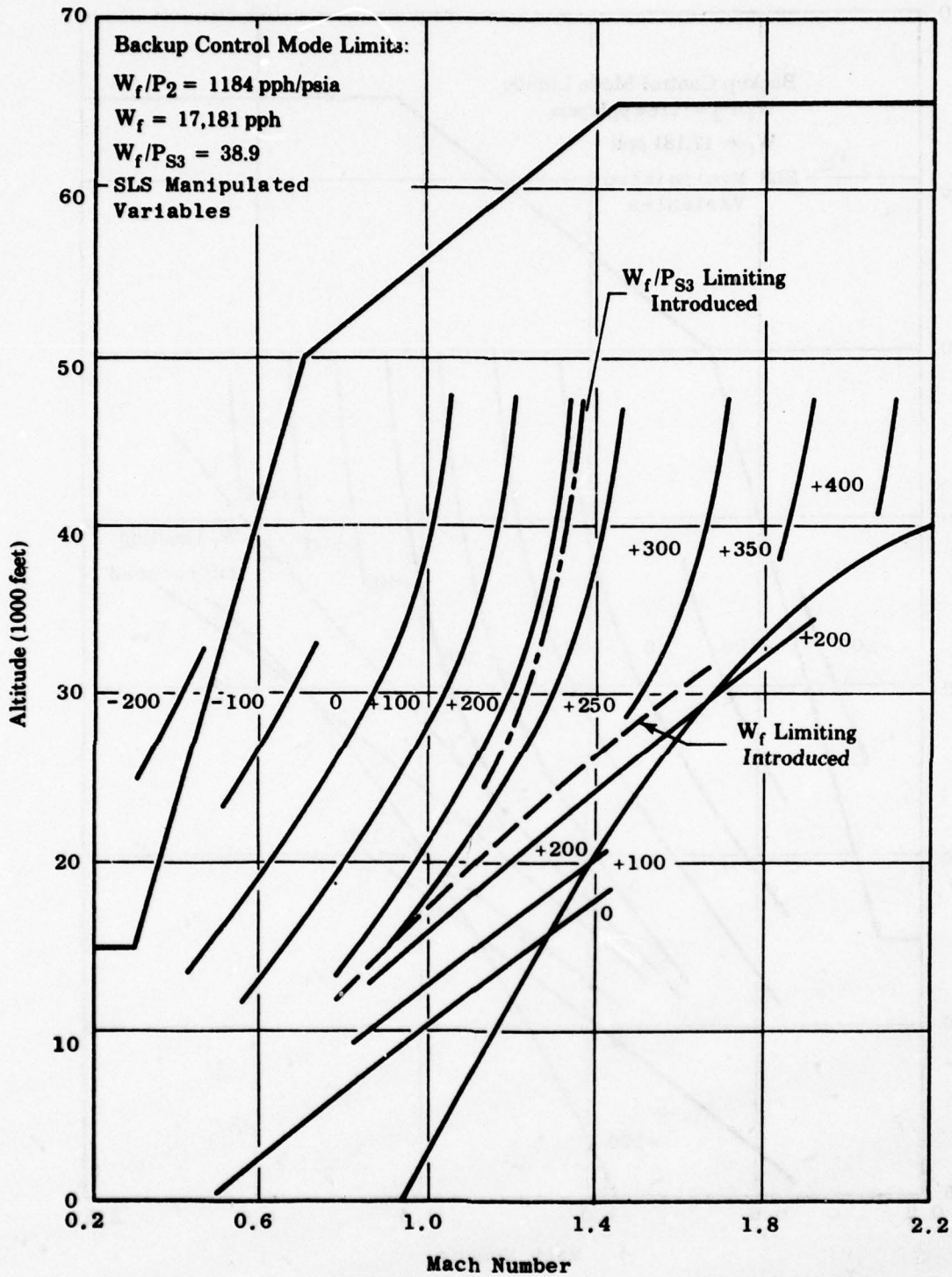


Figure H-4 - Temperature Limiting on W_f , W_f/P_{T2} and W_f/P_{S3} Backup Control.

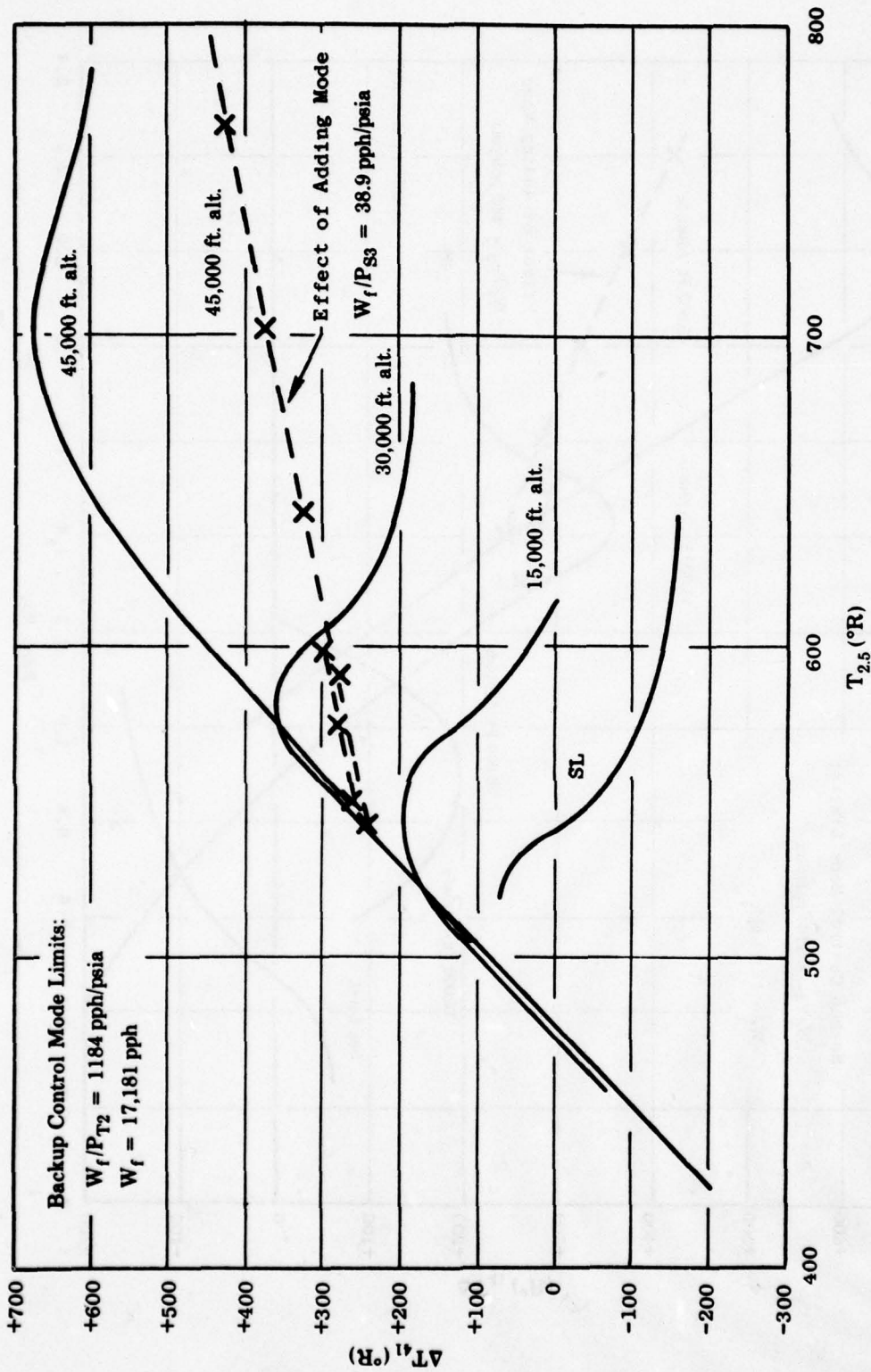


Figure H-5 - Effect on Turbine Temperature Variation of Adding W_f/P_{S3} Backup Control Mode - T_{41} Vs. $T_{2.5}$.

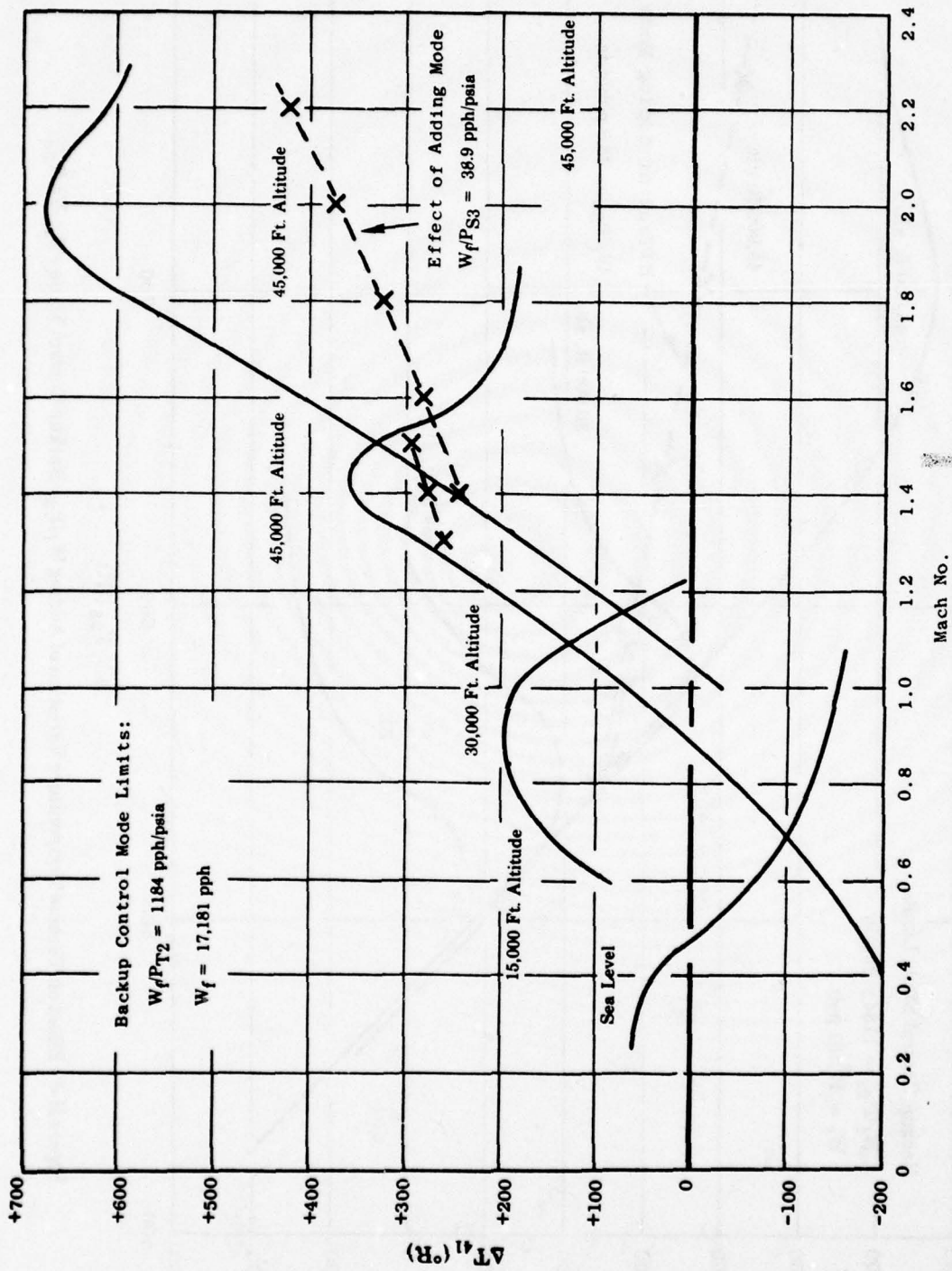


Figure H-6 - Effect On Turbine Temperature Variation of Adding W_f/P_{S3} Backup Control Mode ΔT_{41} Vs Mach Number.

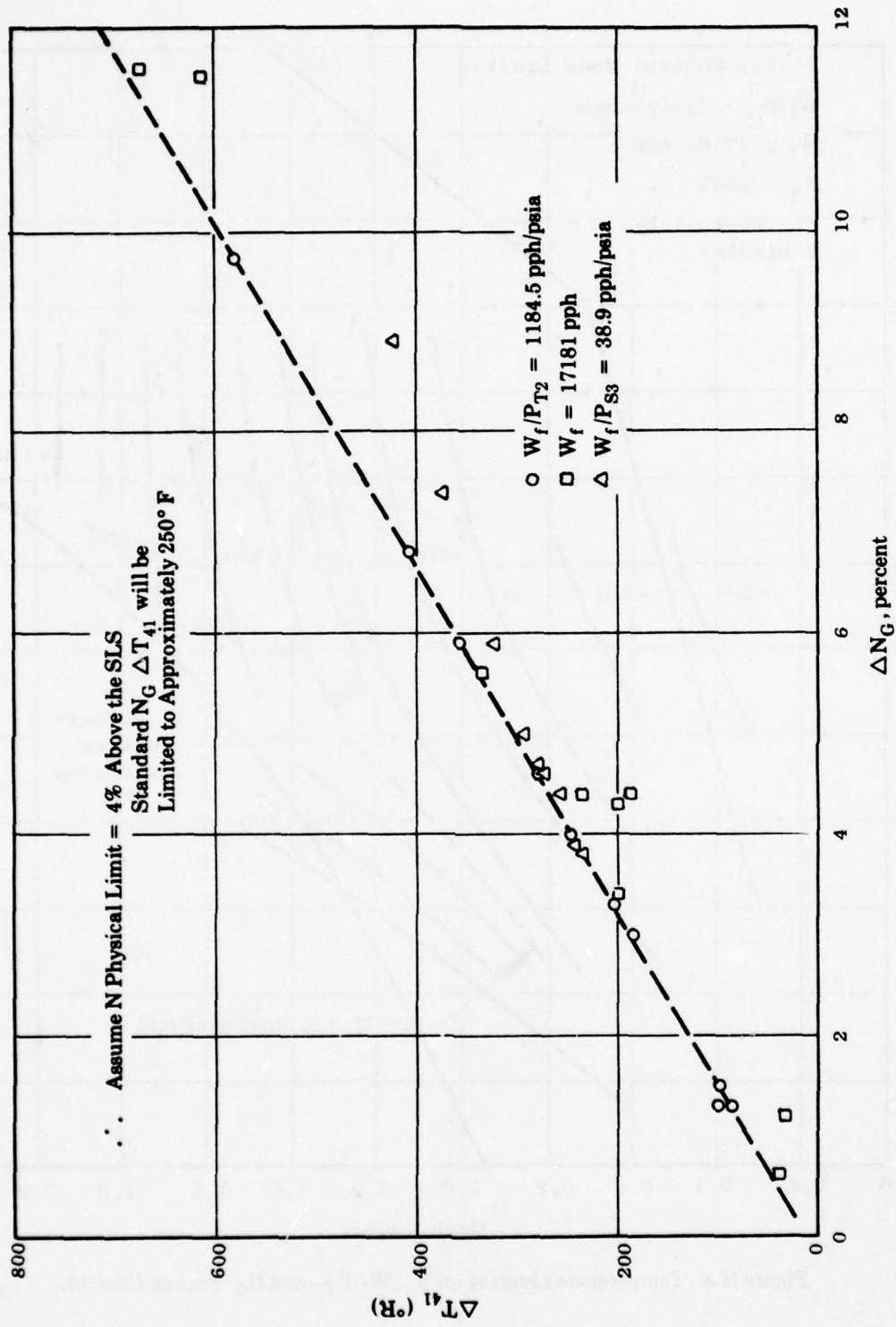


Figure H-7 - Overspeed Limit Selection.

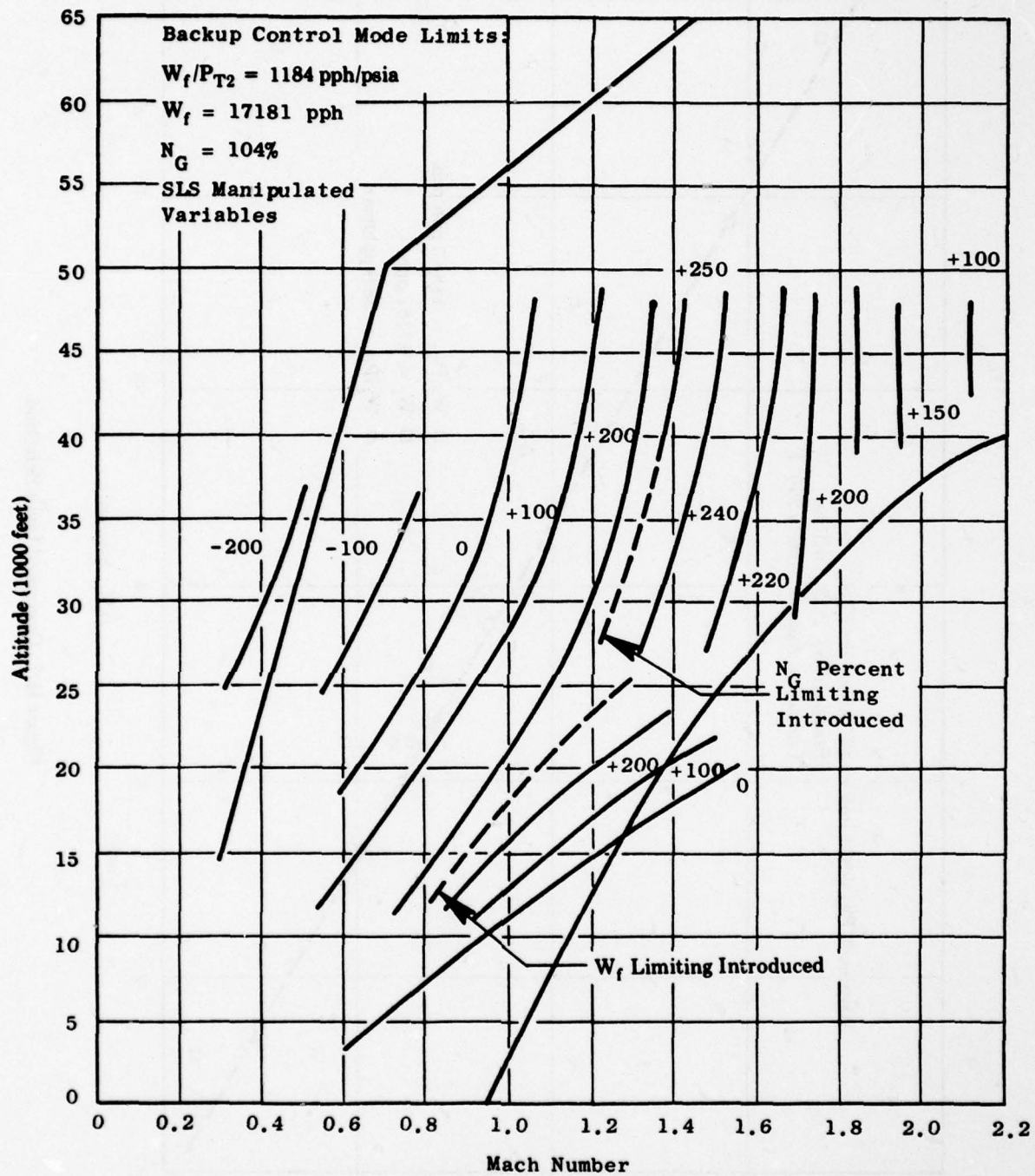


Figure H-8 - Temperature Limiting on W_f , W_f/P_{T2} and N_G Backup Control.

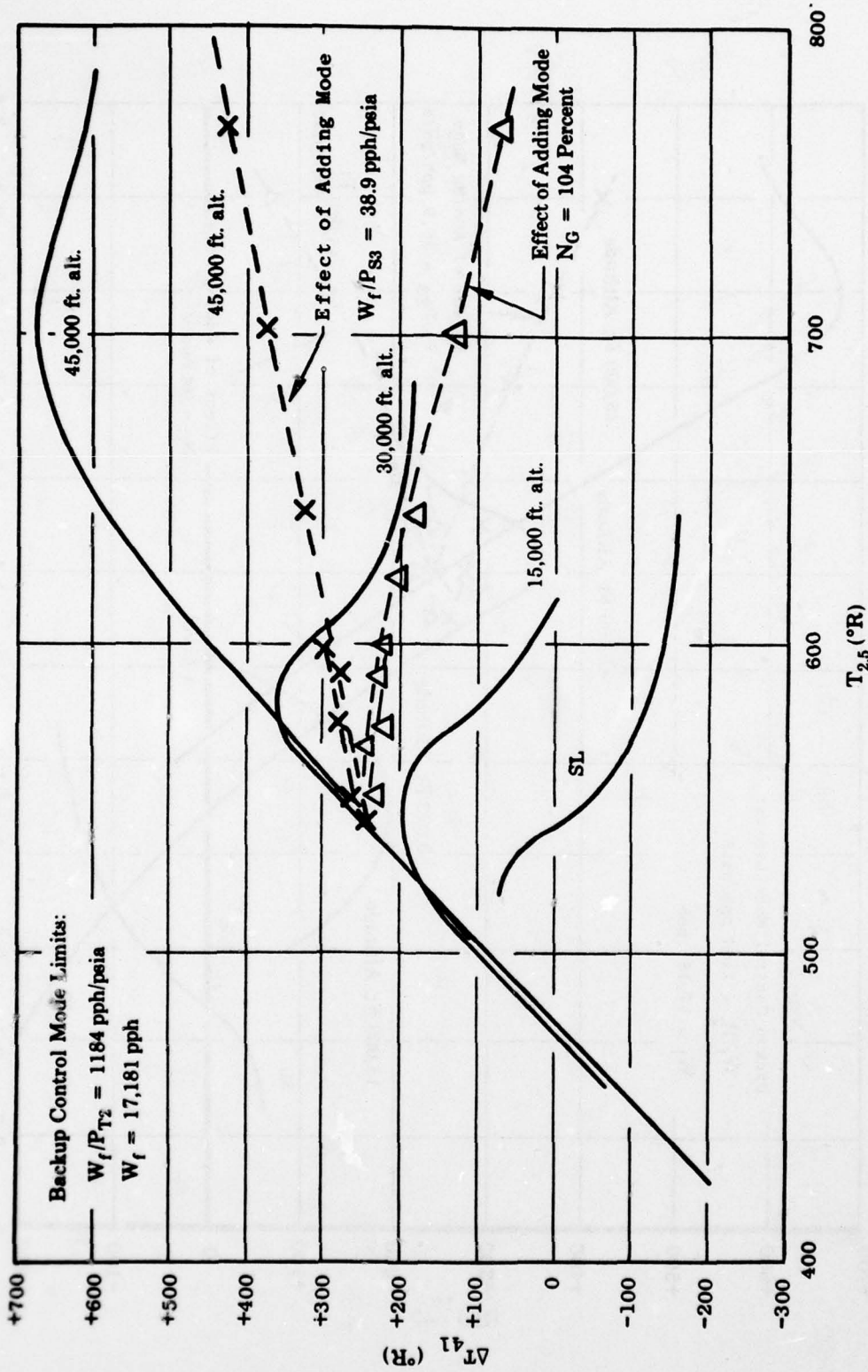


Figure H-9 - Backup Control Mode Investigation with Variation in T_{41} as a Function of $T_{2.5}$.

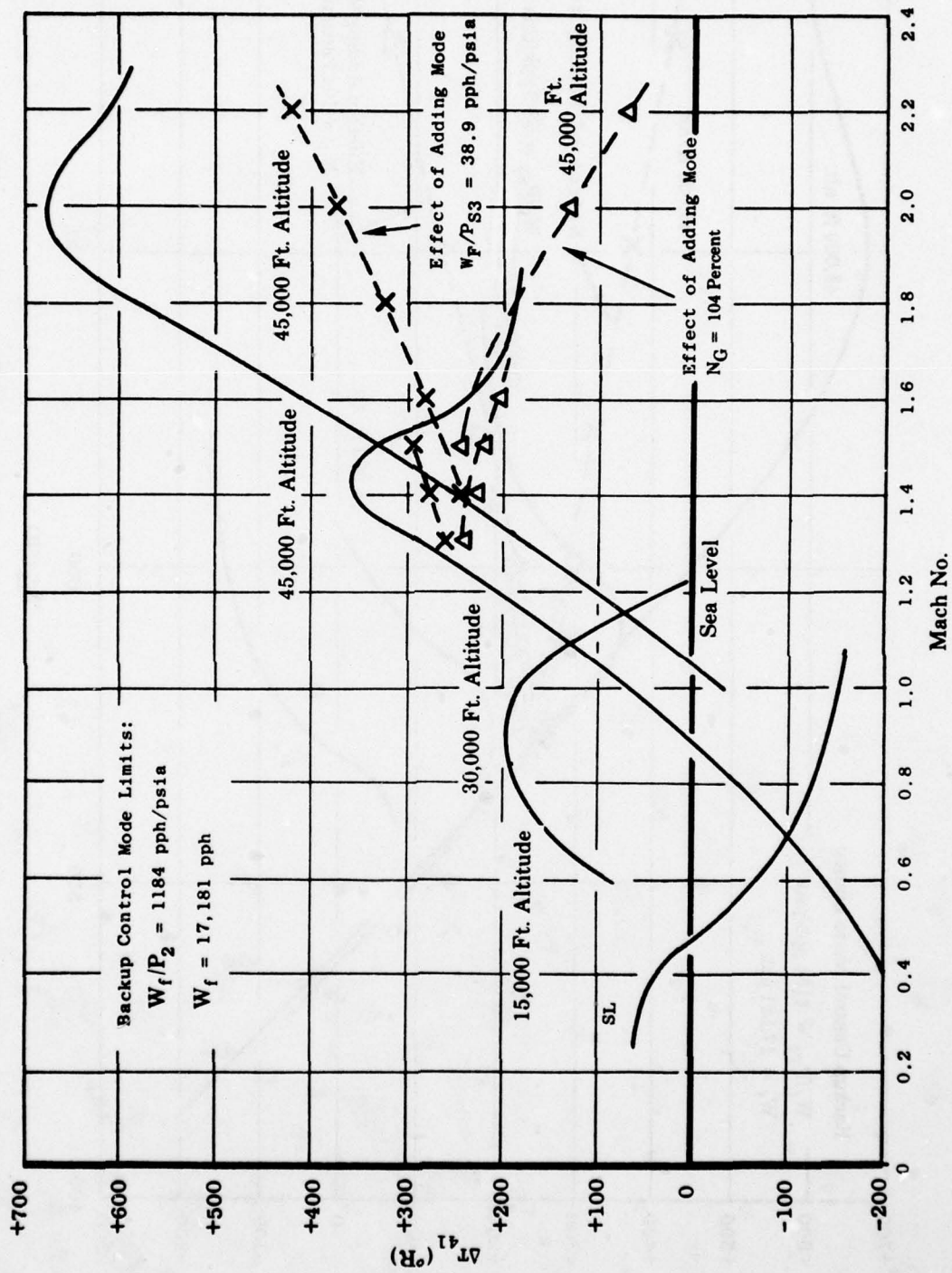


Figure H-10 - Backup Control Mode Investigation with Variation in T_{41} as a Function of Mach Number.

positions. The results of imposing only the W_f/P_{T2} and W_f limits under these conditions are shown in Figures H-11 and H-12. Compared to where the nonmanipulated variables are at SLS positions (Figure H-13), the portion of the flight map in which T_{41} overtemperature occurred is greatly reduced. An N_G limit of 108.5% was also imposed at these conditions and the results are shown in Figure H-13. The negative temperatures (T_{41} computed minus T_{41} maximum) show that N_G limiting significantly decreases the overtemperature at all speeds and altitudes and provides satisfactory T_{41} limiting.

Shown in Figure H-14 is a plot of corrected core speed $N_G/\sqrt{\theta}_{2.5}$ which correlates fairly well with W_f/P_{T2} . This indicates W_f/P_{T2} is satisfactory for β_c scheduling.

Parametric analyses indicated that, for transients, fuel flow rate should be proportional to fuel flow times inlet pressure ($\dot{W}_f = K \times W_f \times P_{T2}$). This could be achieved by having fuel flow rate as a function of fuel level and by varying acceleration rate directly with P_{T2} . Verification was needed, however. Because JTDE transient simulation data were not available, F101 engine data were obtained at various flight conditions having widely different engine inlet temperatures (T_2), yet approximately the same engine inlet pressures (P_{T2}) for various accelerations. The data are shown in Figure H-15. The data do show that \dot{W}_f versus W_f does correlate well at different P_{T2} levels thus verifying that $\dot{W}_f = K W_f P_{T2}$ is a suitable accel parameter. The table shown on Figure H-15 also shows that percent rpm change per second varies almost directly with P_{T2} . This indicates that the accel time does increase as P_{T2} decreases. This is as expected since inertia is fixed and torque available for acceleration of the engine is less at low P_{T2} 's. The accel requirement was selected as 7.5 ± 0.5 second at P_{T2} of 14.7 psia or higher and it increases linearly as P_{T2} decreases so that at P_{T2} of 4.0 psia, the time is 20 ± 3 seconds.

Speed rate was also investigated as an accel/decel parameter. Figure H-16 shows how speed rate, \dot{N}_G versus N_G , varied at different flight conditions. The curves have similar shapes with the minimum \dot{N}_G occurring between 11,000 and 12,000 rpm. The range of \dot{N}_G at SLS is 660 to 490 rpm per second or 575 ± 85 rpm/sec ($\pm 15\%$). $\dot{N}_G/\sqrt{\theta}_{2.5}$ versus N_G was also investigated. The curve had a decreasing trend with N_G and the spread was from 560 rpm per second to 240 rpm per second. This indicated that, if it were used as a parameter, it would be necessary to make it a function of speed.

Since \dot{N}_G appeared more independent of N_G , it was investigated further. Figure H-17 shows the results a plot of \dot{N}_G/P_{T2} versus N_G actual. The plot shows good correlation for P_{T2} pressures of 14.7, 10.1 and 22.41 psia. The plot for 5.91 psia is above the remaining plots which is acceptable. In other words, if the F101 engine were accelerated at a rate of 30 rpm/sec/psia, no problem should be encountered.

The F101 engine accel time at SLS is 7.4 seconds from 69% to 97.3% rated rpm. A fighter engine would probably be designed to accel that rpm range in about 4.5 seconds so curves shown in Figure H-17 would be about 50% higher. The backup control should be designed to schedule from backup flight idle to rated speed in $7.5 \pm .5$ seconds at SLS. Assuming backup flight idle is 10,000 rpm and rated speed is 14,700 rpm, the required \dot{N}_G/P_{T2} at SLS is 42.5 rpm/sec/psia. Based on the above data and assumptions, this speed rate appears feasible.

4. REQUIREMENTS FOR A SERIES TYPE W_f/P_{T2} BACKUP CONTROL

- a. Input Variables - The input variables and their ranges are as follows:

Power Lever Angle, PLA	0 to 135 degrees
Ground Idle	18 degrees
Flight Idle, Backup	To be defined
Max Intermediate	75 degrees
Inlet Pressure, Total P_{T2}	2.2 to 35.3 psia

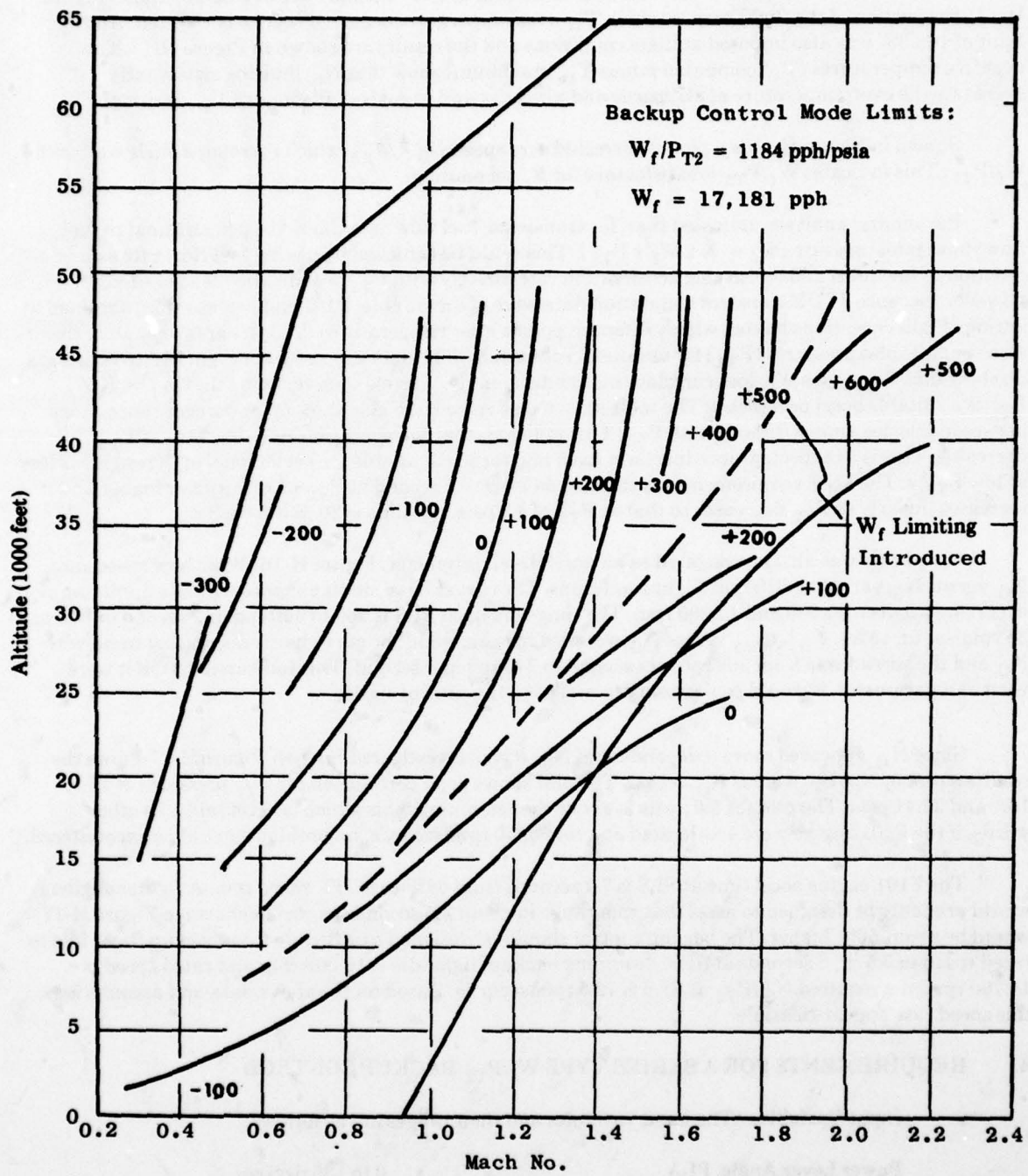


Figure H-11 - Temperature Limiting on W_f and W_f/P_{T2} Backup Control, all Other Variables Failed on Stops.

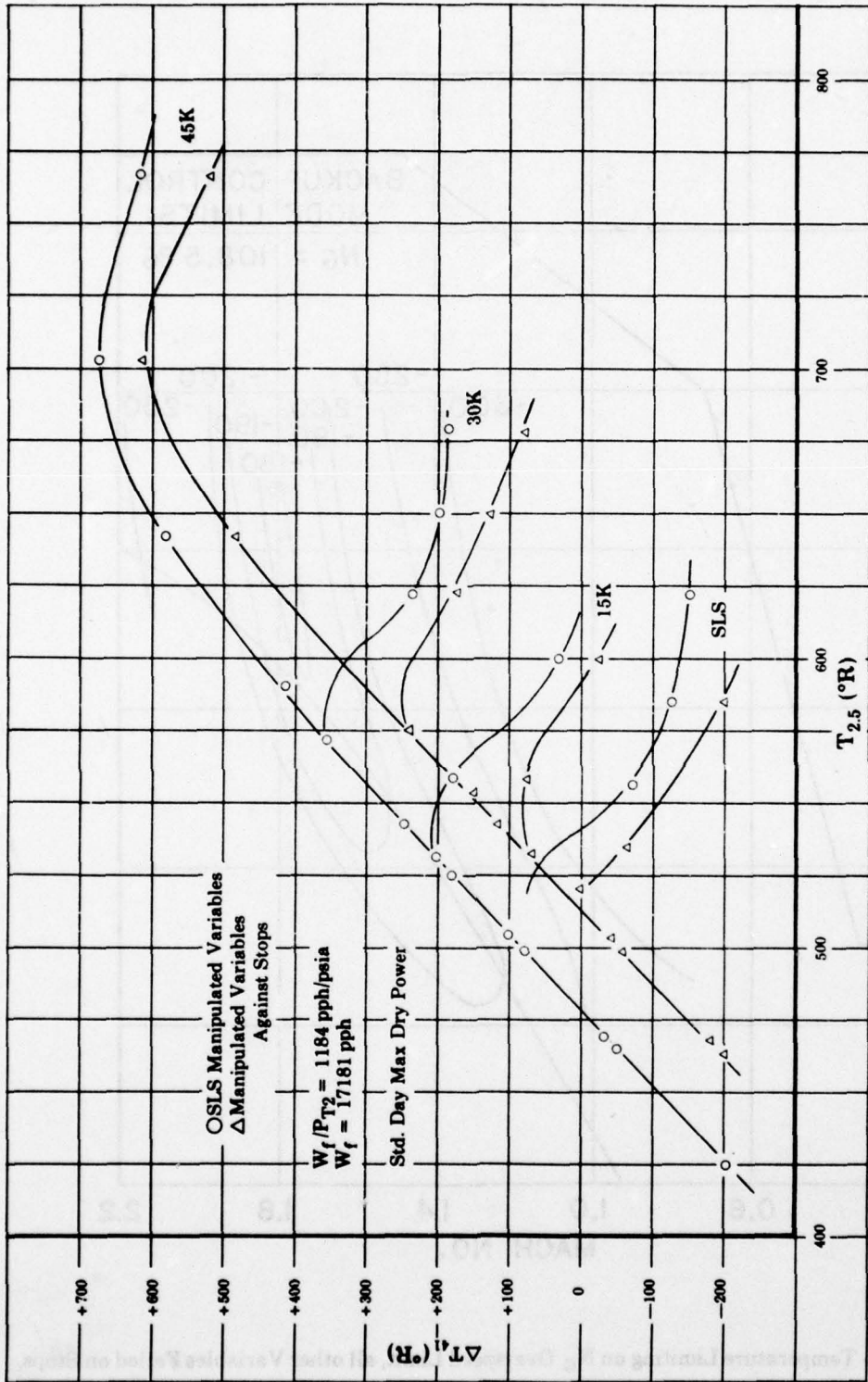


Figure H-12 - Turbine Temperature Variation Comparison: Nonmanipulated Variables At SLS & Against Stops W_f/P_{T2} & W_f Backup Mode.

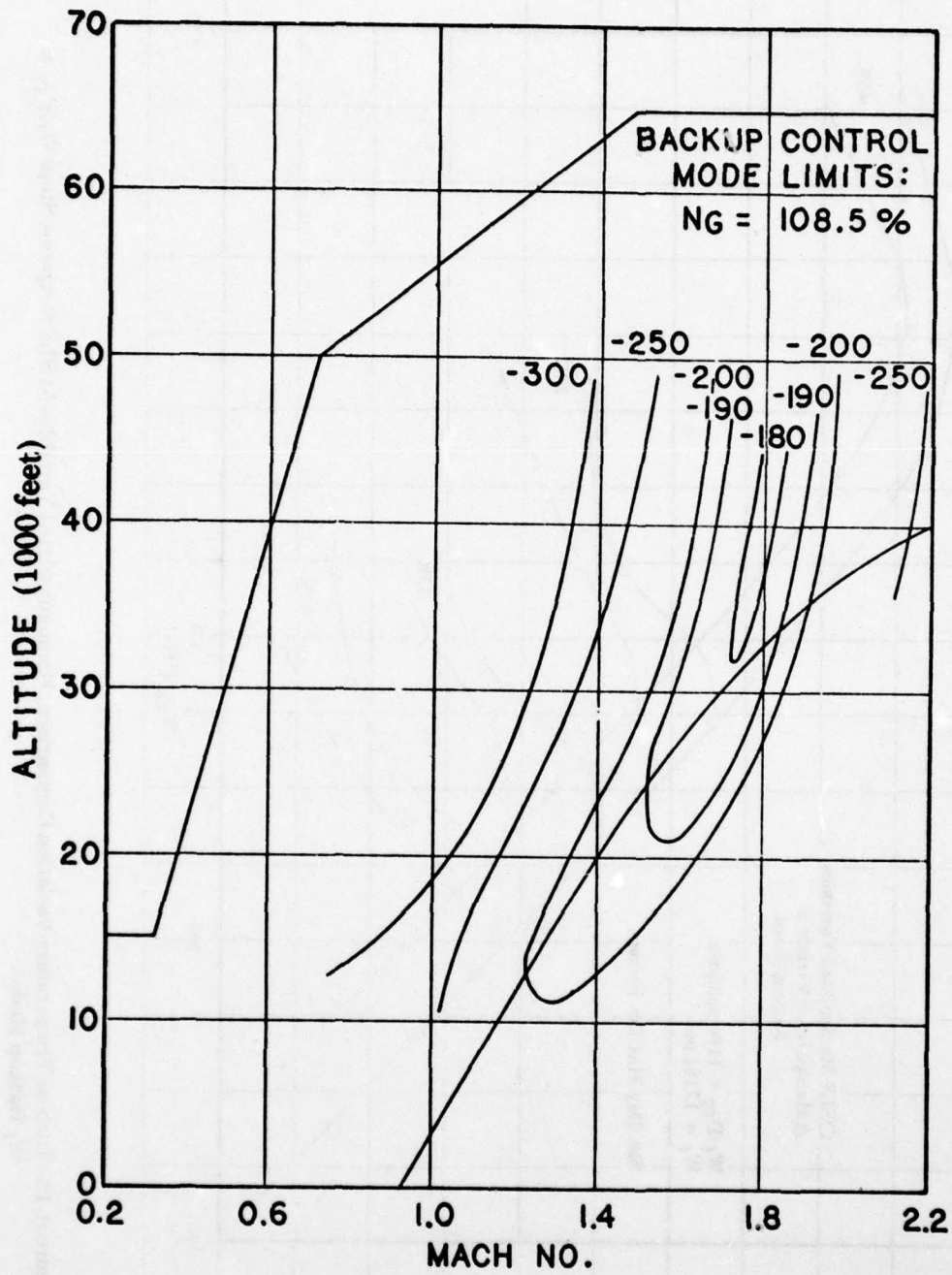


Figure H-13 - Temperature Limiting on N_G Overspeed Limit, all other Variables Failed on Stops.

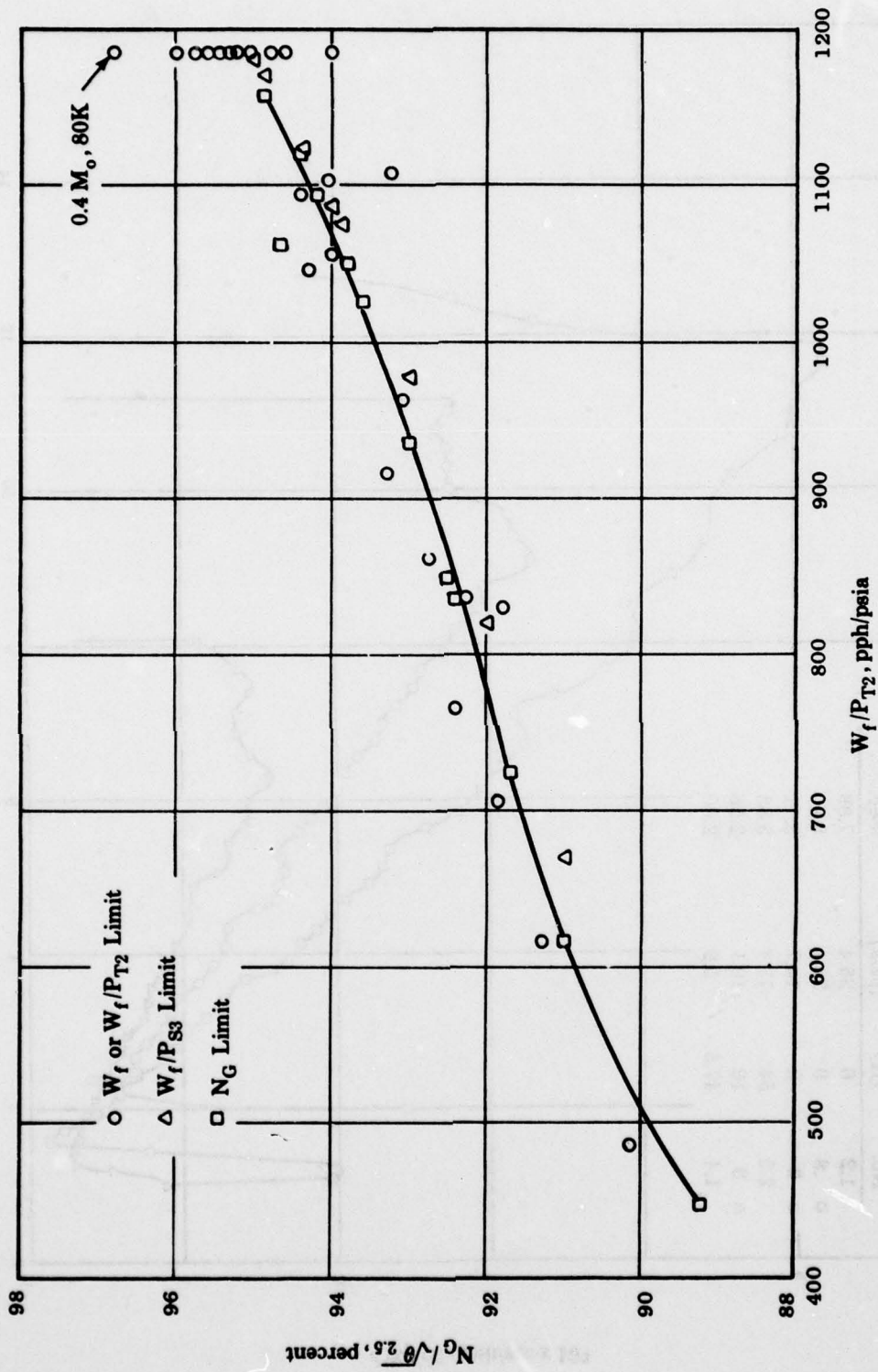


Figure H-14 - Corrected Core Speed Vs. W_f / P_{T2} .

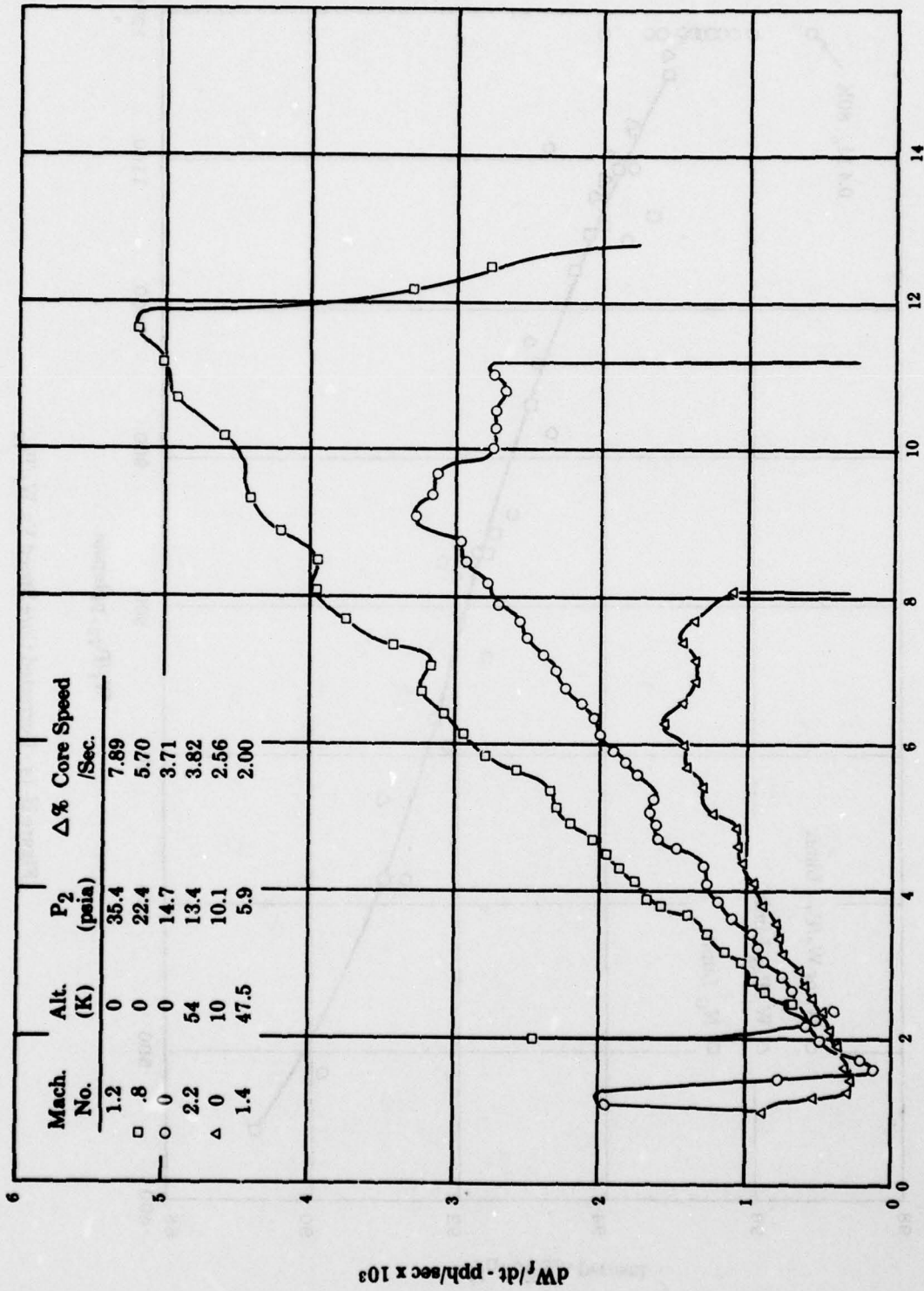


Figure H-15 - F101 \dot{W}_f Vs. W_f , Min Dry to Max Dry Accel.

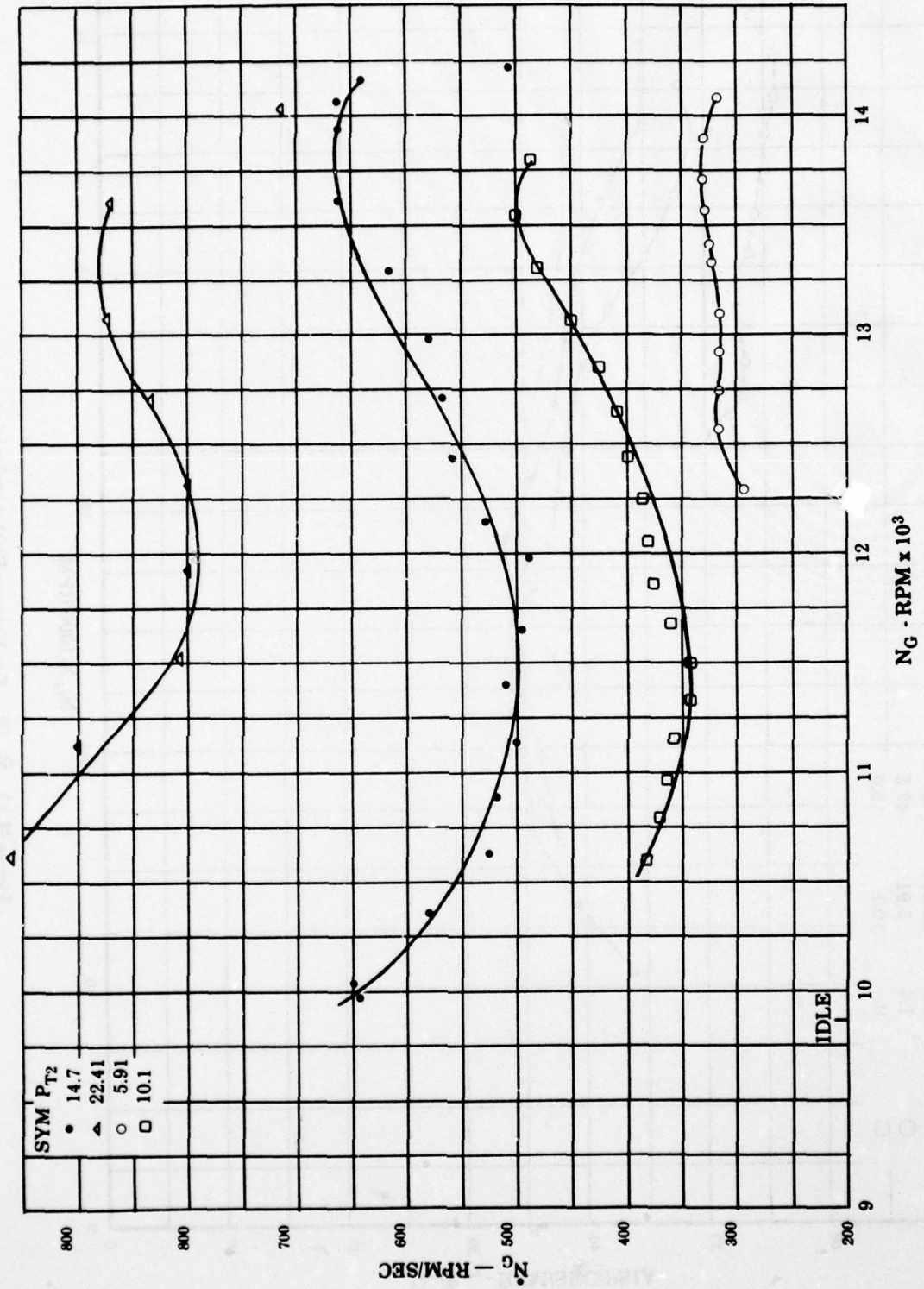


Figure H-16 - \dot{N}_G For Various F101 Accels.

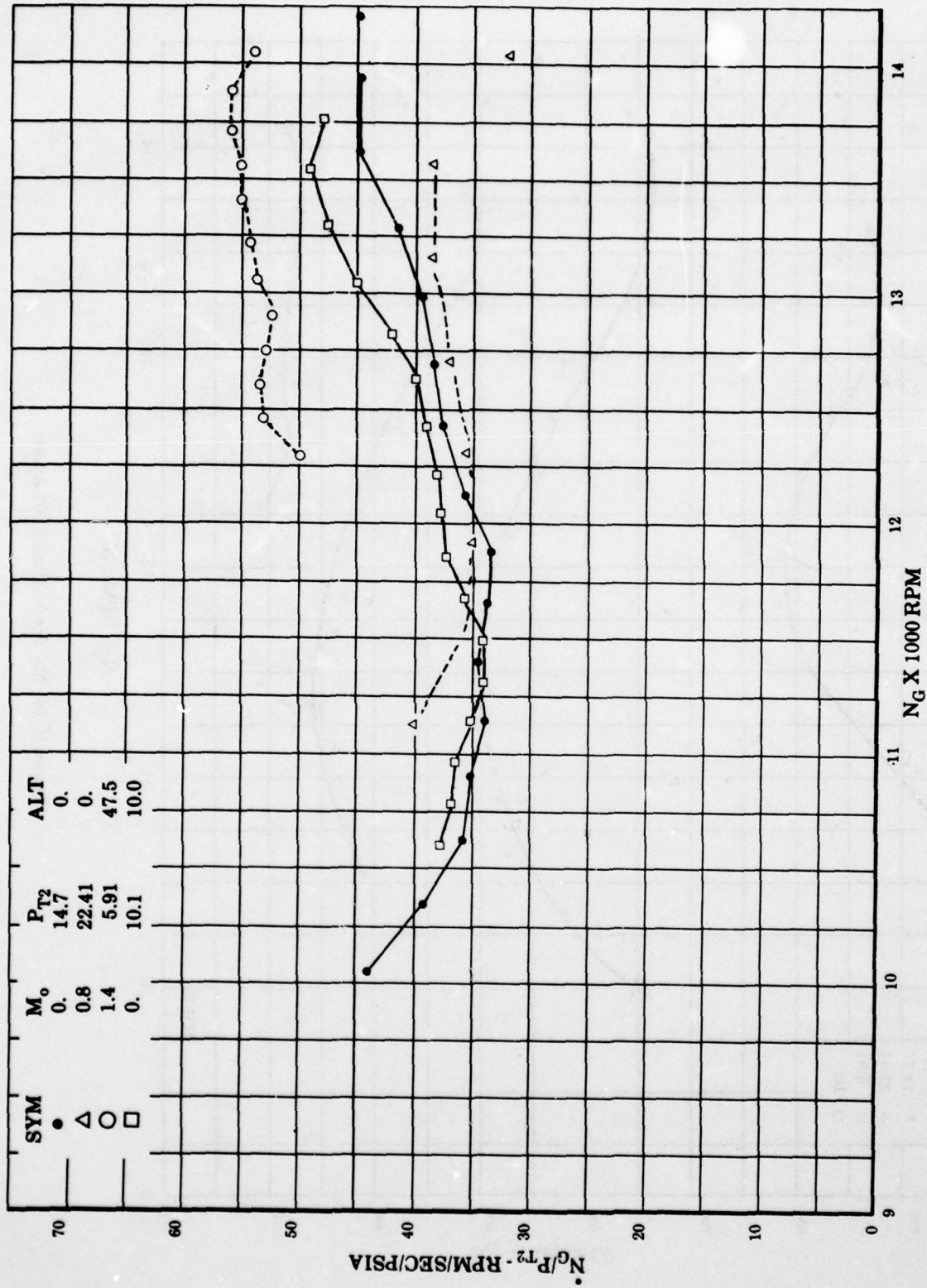


Figure H-17 - \dot{N}_G/P_{T2} For Various F101 Accelerations.

Core Speed, Rated, N_G	14,700 rpm
Inlet Temperature, Total, T_{T2}	-30 to 400°F
Compressor Discharge Pressure, Max, P_{S3}	500 psia
Compressor Inlet Temperature, Max, $T_{2.5}$	625°F

- b. **Manipulated Output Variables** - The backup control outputs will be as follows:

Fuel Flow, Main (W_f)	
Minimum, nominal	300 pph
Minimum Adjustable Range	250 to 500 pph
Maximum, nominal	17,181 pph
Maximum Adjustable Range	± 1000 pph

Core Stator Position (β_c)	
Stroke	3.1 inches
Load, max	1000 lbs.
Slew Rate	2.3 in/sec

- c. **Fixed Variables** - The JTDE engine has eight manipulated variables in addition to fuel flow and core stators. All the variables and the failure direction, failure effect, desired dominant failure mode and whether backup control function is required is shown in Table G-I.

- d. **Environmental Requirements** - The environmental requirements for the control while on primary mode are:

Ambient Air Temperature	-54°F to 470°F
Fuel Temperature (at pump inlet)	-65°F to 210°F
Aircraft Mach No.	2.0 max
Vibration Level	See Figure F-2
Acoustic Environment	150 db max at 100 to 10,000 Hz

- e. **Backup Control Logic** - The backup control logic is discussed below for the various modes of operation.

- (1) **Primary Mode** - The design objective is that the backup control not compromise primary control operation. During steady state operation, the backup control will schedule W_f at 7% above normal and β_c at 2 degrees more open than normal. The primary control will override by subtracting from the backup control and schedule W_f and β_c at the normal values.

During accel, the backup control will increase its W_f schedule at a rate greater than the maximum rate expected from the primary control. The core stators (β_c) will also be opened at a rate greater than the maximum rate expected from the primary control. The primary control will override the backup control by subtracting from the backup W_f and β_c schedules to attain the normal values during accel.

During decel, the backup control will decrease its W_f and β_c schedules at rates less than the minimum rate expected from the primary control. The primary control will override the backup control by subtracting from the backup schedules to attain the normal values.

- (2) **Transfer to Backup Control** - The backup control will have a means for transferring to the backup mode by pilot action, by loss of electrical power to the primary control, or by action of the primary control when it senses a malfunction. The combined control system shall cause all actuation loops to fail-fixed and then slowly stroke the actuators to their desired fixed position. Fuel flow (W_f) and core stators (β_c), which are the two manipulated variables, will drift toward the max or roof limits set by the backup schedules.
- (3) **Backup Mode** - The eight variables not manipulated will be held at their desired fixed position. W_f/P_{T2} and β_c will be scheduled as a function of power lever angle during steady state operation. During transients, the PLA input signal to the scheduling device will be rated limited. The rate limiting device will be between the PLA input and the W_f/P_{T2} and β_c scheduling devices. The rate limit will vary directly with P_{T2} . Since the rate limit affects the W_f and β_c schedules simultaneously, the W_f/P_{T2} demand and β_c demand will track.

During supersonic operation, high $T_{2.5}$ causes the W_f/P_{T2} scheduling parameter, when operating alone, to schedule too much fuel flow resulting in overspeed. An overspeed governor will be used to reset the W_f/P_{T2} and β_c demands at this flight condition. This will also provide additional overspeed protection at subsonic speeds.

f. Primary-To-Backup Transfer Characteristics

- (1) Transfer to backup control will be initiated by a zero current signal to all the primary system fail-fixed servovalves.
- (2) The backup control will be of the type which allows drifting toward the backup schedules at a rate so that it takes at least 15 seconds to make a 7% fuel flow or a 2 degree β_c change.
- (3) The remaining variables, not manipulated in the backup mode, will stroke to their desired fixed positions in 15 to 90 seconds. This action will occur independently of possible PLA modulation.
- (4) If transfer to the backup control occurs at max dry thrust setting, the backup control must limit overspeed to 4% without pilot action.
- (5) There will be no PLA restrictions when the aircraft is flying subsonically, other than limiting operation to the dry regime.
- (6) If transfer to the backup mode occurs during augmented supersonic flight conditions, a reduction in power demand to a value just below intermediate will be required of the pilot.

g. Steady-State Performance in Backup Mode

- (1) The W_f/P_{T2} demand schedule versus PLA shall be linear. At 18° PLA, W_f/P_{T2} shall be 65 pph/psia and at 75° PLA, W_f/P_{T2} shall be 1184 pph/psia.
- (2) An overspeed governor shall limit N_G to 104%.

- (3) The backup core stator (β_c) versus PLA schedule shall be 2 degrees more open than the primary schedule.
- (4) If the primary and backup control use a common metering valve, the backup control must provide overspeed protection if the common metering valve fails in the open position. In other words, no single failure in the backup or primary control shall allow a catastrophic overspeed, pressure or temperature failure of the engine.

h. Transient Performance in the Backup Mode

- (1) The W_f/P_{T2} demand schedule shall change from backup control flight idle to max intermediate in $7.5 \pm .5$ seconds at P_{T2} of 14.7 psia or higher. This PLA rate shall decrease directly with P_{T2} so that at P_{T2} of 4.0 psia, the time is 20 ± 3 seconds.
- (2) The fuel flow rate (\dot{W}_f) shall be proportional to P_{T2} and fuel flow level ($\dot{W}_f = K W_f P_{T2}$). If a parameter other than W_f/P_{T2} is used, the resulting \dot{W}_f shall be equivalent.
- (3) The rate device that schedules W_f/P_{T2} versus time shall also schedule the β_c rate.
- (4) The overspeed governor dynamics will be similar to those of the primary governor.
- (5) The backup control will not cause discontinuities in its demanded value of W_f or β_c that require abrupt or large changes in override action of the primary control.

i. Miscellaneous Requirements

- (1) The primary/backup control system shall provide cockpit indication when transfer to backup control occurs.
- (2) The backup control must have a ground check capability.
- (3) Air start capability will be provided on backup control of P_{T2} of 10 psia or higher. The procedure will be to set the PLA to 10 degrees which sets minimum flow. After lightoff is detected, the pilot must advance the throttle slowly, about one degree every two seconds, toward flight idle while he observes N_G . The throttle motion must follow the increase in N_G .
- (4) The backup control shall provide fuel flow and β_c floors at PLA's from 79 to 135 degrees. Means shall be provided which allow the pilot to remove the floors thus decreasing the possibility of interference during primary mode operation.
- (5) It is very desirable that the backup control have the capability to automatically reset from the 107% W_f and the 2 degree more open β_c to nominal values after transfer is complete.
- (6) The backup control shall not require periodic trimming.

5. REQUIREMENTS FOR A PARALLEL TYPE, SPEED RATE BACKUP CONTROL

- a. Similarity - The first part of this list is the same as Paragraph 4, a. through c. above.

b. **Backup Control Logic** - The backup control logic is discussed below for the various modes of operation.

- (1) **Primary Mode** - The design objective is that the backup control not compromise primary control operation. During primary mode steady state, accel and decel operation, the backup control servovalve outputs will be blocked by a transfer valve. However, if N_G overspeed occurs, an overspeed detector action will cause transfer to the backup control. In this mode the backup control will also provide a standby β_c schedule.
- (2) **Transfer to Backup Control** - The backup/primary control system will have means for transferring to the backup mode by pilot action, by loss of power to the primary control, by action of the primary control when it senses a malfunction or by N_G overspeed. A transfer valve will be used to switch from the primary W_f and β_c servovalve output to the backup W_f and β_c servovalve output. The combined control system shall cause all the remaining actuator loops to fail fixed and then slowly stroke the actuators to their desired stops.
- (3) **Backup Mode** - Core speed (N_G) will be scheduled as a function of PLA during steady state operation. During transients, the PLA input signal to the scheduling device will be rate limited. The rate limiting device will be between the PLA input and the N_G scheduling device. The rate limit will vary directly with P_{T2} . Core stators (β_c) will be scheduled as a function of N_G actual and $T_{2.5}$. The remaining variables not manipulated will be held at their desired stop.

c. **Primary-To-Backup Transfer Characteristics**

- (1) Once transfer to the backup control is initiated by any of the four means mentioned in Paragraph 4.e.(2) above, a signal is sent to the transfer valve which causes it to stroke to the second stop. In this position the transfer valve ports backup servovalve pressures to the fuel valve and β_c pistons and blocks the flow from the primary W_f and β_c servovalves.
- (2) If a large speed error exists upon transfer, the slew rate will be limited to that used in the backup mode.
- (3) The remaining variables, not manipulated in the backup mode, will stroke to their desired stops in 15 to 90 seconds.
- (4) If transfer to the backup control occurs at max dry thrust setting, the backup control must limit overspeed to 4% without pilot action.
- (5) There will be no PLA restrictions when the aircraft is flying subsonically other than limiting operation to the dry regime.
- (6) If transfer to the backup mode occurs at augmented supersonic flight conditions, a reduction in power demand to a value just below intermediate will be required.

AD-A055 658

GENERAL ELECTRIC CO CINCINNATI OHIO AIRCRAFT ENGINE GROUP F/G 21/5
BACKUP CONTROL FOR A VARIABLE CYCLE ENGINE.(U)
DEC 77 H B KAST, G L POPPEL, J E HURTLE F33615-76-C-2086
77AEG-633 AFAPL-TR-77-92 NL

UNCLASSIFIED

2 OF 3
ADA
055658



d. **Steady-State Performance in Backup Mode**

- (1) The N_G versus PLA schedule shall result in thrust varying linearly, or approximately so, with PLA. The backup control will provide corrected speed ($N/\sqrt{\theta_{2.5}}$) limiting.
- (2) At max PLA, the N_G speed request shall be $100\% \pm 0.5\%$. The backup PLA at all other settings will be equivalent to the primary control.
- (3) The overspeed reference speed setting will be $104\% \pm 0.5\%$.
- (4) The β_c schedule shall be set the same as the primary control for the JTDE engine.
- (5) If the primary and backup control use a common metering valve, protection against a failed open metering valve is needed. The backup control must manipulate the throttling valve if speed exceeds 104%.

e. **Transient Performance in the Backup Mode**

- (1) The N_G demand schedule shall change from backup control flight idle to max intermediate in $7.5 \pm .5$ seconds at P_{T2} of 14.7 psia or greater. The N_G demand time, shall increase inversely to P_{T2} so that at P_{T2} of 4.0 psia, the time is 28 ± 3 seconds.
- (2) The speed rate (\dot{N}_G) shall be 625 ± 50 rpm per second at P_{T2} of 14.7 psia or higher. The speed rate shall decrease proportional to P_{T2} so that at P_{T2} of 6.0 psia, or less, the rate shall be 250 ± 40 rpm per second. Speed rate (\dot{N}_G) shall be adjustable from 700 to 500 rpm/second at 14.7 psia.
- (3) Core stators, β_c , shall track a schedule which is a function of N_G actual and $T_{2.5}$. An alternate is to have β_c track a schedule which is a function of W_f and P_{T2} .
- (4) The overspeed governor dynamics will be the same as the FADEC requirements.
- (5) The backup control will not cause discontinuities in its demanded values of N_G or β_c that require abrupt or large changes in override action of the primary control.

f. **Miscellaneous Requirements**

- (1) The primary/backup control system shall provide cockpit indication when transfer to backup control occurs.
- (2) The backup control must have a ground check capability.
- (3) Air start capability will be provided on backup control at P_{T2} of 10 psia or higher. The procedure will be to set the PLA to 10 degrees which sets minimum flow. After lightoff is detected, the pilot must advance the throttle slowly, about one degree every two seconds, toward flight idle while he observes N_G . The throttle motion must follow the increase in N_G .
- (4) The pilot shall be able to block automatic transferring to the backup control. He shall also be able to transfer back to primary control operation.

(5) The backup control shall not require periodic trimming.

6. REQUIREMENTS FOR A PARALLEL TYPE, LIMIT SCHEDULING BACKUP CONTROL

- a. **Similarity** - The first part of this list is the same as Paragraphs 4, a. through d. above.
- b. **Backup Control Logic** - The backup control logic is discussed below for the various modes of operation.

- (1) **Primary Mode** - The design objective is that the backup control not compromise primary control operation. During primary mode steady state, accel and decel operation, the backup control servovalve outputs will be blocked by a transfer valve. However, if N_G overspeed occurs an overspeed detector action will cause transfer to the backup control. In this mode the backup control will also provide a standby β_c schedule.
- (2) **Transfer to Backup Control** - The backup/primary control system will have means for transferring to the backup mode by pilot action, by loss of power to the primary control, by action of the primary control when it senses a malfunction or by N_G overspeed. A transfer valve will be used to switch from the primary W_f and β_c servovalve output to backup W_f and β_c servovalve output. The combined control system shall cause all the remaining actuator loops to fail fixed and then slowly stroke the actuators to their desired stops.
- (3) **Backup Mode** - Core speed (N_G) will be scheduled as a function of PLA during steady state operation. During transients, accel and decel W_f will be scheduled as a function of N_G , $T_{2.5}$ and P_{S3} . Core stators (β_c) will be scheduled as a function of N_G and $T_{2.5}$ during both transient and steady-state operation. The remaining nonmanipulated variables will be held at their desired stops.

c. **Primary-To-Backup Transfer Characteristics**

- (1) Once transfer to the backup control is initiated by any of the four means mentioned in Paragraph 4.e.(2) above, a signal is sent to the transfer valve which causes it to stroke to the second stop. In this position the transfer valve ports backup servovalve pressures to the fuel valve and β_c pistons and blocks the flow from the primary W_f and β_c servo valves.
- (2) If a large speed error exists upon transfer, the slew rate will be limited to that used in the backup mode.
- (3) The remaining variables not manipulated in the backup mode will stroke to their desired stops in 15 to 90 seconds.
- (4) If transfer to the backup control occurs at max dry thrust setting, the backup control must limit overspeed to 4% without pilot action.
- (5) There will be no PLA restrictions when the aircraft is flying subsonically other than limiting operation to the dry regime.

- (6) If transfer to the backup mode occurs at augmented supersonic flight conditions, a reduction in power demand to a value just below intermediate will be required of the pilot.

d. Steady-State Performance in Backup Mode

- (1) The N_G versus PLA schedule shall result in thrust varying linearly, or approximately so, with PLA. The backup control will provide corrected speed ($N/\sqrt{\theta_{2.5}}$) limiting.
- (2) At max PLA, the N_G speed request shall be $100\% \pm 0.5\%$. The backup PLA at all other settings will be equivalent to the primary control.
- (3) The overspeed reference speed setting will be $104\% \pm .5\%$.
- (4) The β_c schedule shall be set the same as the primary control for the JTDE engine.
- (5) If the primary and backup control use a common metering valve, protection against a failed open metering valve is needed. The backup control must manipulate the throttling valve if speed exceeds 104%.

e. Transient Performance in the Backup Mode.

- (1) Accel and decel fuel flow will be scheduled as a function of N_G , $T_{2.5}$ and P_{S3} typical of existing hydromechanical fuel controls. The core stators (β_c) will be scheduled as a function of N_G and $T_{2.5}$. These schedules will be the same as those in FADEC.
- (2) The overspeed governor dynamics will be the same as those in the FADEC.

f. Miscellaneous Requirements

- (1) The primary/backup control system shall provide cockpit indication when transfer to backup control occurs.
- (2) The backup control must have a ground check capability.
- (3) Air start capability will be provided on backup control of P_{T3} of 10 psia or higher. The procedure will be to set the PLA to 10 degrees which sets minimum flow. After lightoff is detected, the pilot advances the throttle to "Idle".
- (4) The pilot shall be able to block automatic transferring to the backup control. He shall also be able to transfer back to primary control operation.
- (5) The backup control shall not require periodic trimming.

APPENDIX I — HYDROMECHANICAL BACKUP CONTROL HAVING CORE SPEED SETTING FUNCTION WITH SCHEDULED FUEL FLOW LIMITS IN A PARALLEL CONFIGURATION

1. APPROACH

The hydromechanical approach is shown schematically by Figure I-1. This approach is the recommended backup control resulting from this study. The computing section of this backup control is similar to the equivalent portion of a conventional hydromechanical fuel control. In the backup mode, this control computes a metering valve position for each engine operating condition. Steady state conditions are maintained in conjunction with limiting and biasing functions such as core maximum rpm, accel/decel limits, minimum W_f and $T_{2.5}$ bias. Engine operating parameters, such as power lever angle, core rpm, compressor discharge pressure (P_{S3}) and $T_{2.5}$ are integrated and a single output signal representing W_f demand is generated.

The W_f lever movement can be considered a true fuel flow signal. Motion of the W_f lever occurs whenever an unbalance exists in the moments of force acting on it. The position of the rollers represents the proper value of W_f/P_{S3} , as determined by the integration of three engine operating parameters, N_G , PLA and $T_{2.5}$. A multiplying force acts on the rollers through a lever and is a function of P_{S3} absolute. The lever system is arranged as a multiplier such that the load, P_{S3} , times the point of load application, W_f/P_{S3} , equals fuel flow. In equation form, it is:

$$P_{S3} \times W_f/P_{S3} = W_f$$

P_{S3} is sensed by a bellows. The pressure times the bellows area produces a force. The multiplying force is transmitted to the rollers by a lever attached to the sensing bellows. An evacuated bellows of equal effective area is mounted opposite the sensing bellows to serve as a reference. This second bellows also provides compensation for undesired sensing bellows movement due to changes of temperature and pressure in the bellows chamber. The bellows chamber is sealed off from the control casing and vented to atmosphere through a small orifice. A ruptured sensing bellows would fill the chamber with compressor discharge air, the seal and orifice maintaining a level of P_{S3} . P_{S3} acting on the outside of the reference bellows generates a force on the P_{S3} lever to prevent complete loss of the P_{S3} signal if the sensing bellows fails.

The speed sensing system is composed of an engine-driven fly-weight governor, pilot valve, feedback spring and lever, 3D cam, and power piston. During engine steady state operation, governor fly-weight centrifugal force is balanced by feedback spring force. Under these conditions, the pilot valve is held in null position. Assume an increase in fuel flow in response to a control lever advance. Additional fuel flow produces increased engine speed in response to which the governor flyweights move outward, displacing the pilot valve to the right. High-pressure fuel, ported to the right end of the power piston, moves it to the left. By virtue of its mechanical connection, the 3D cam follows this motion. Movement of the power piston to the left rotates the feedback lever clockwise and around its pivot point. This action compresses the spring until the spring force overcomes the centrifugal force of the flyweights. The pilot valve moves back toward the null position and the flyweights move toward their steady state position. When spring force is balanced by flyweight centrifugal force, the pilot valve is in a null position. The speed sensing system responds to changes in engine speed and schedules fuel flow to the engine in accordance with prescribed limiting functions to provide safe engine operation.

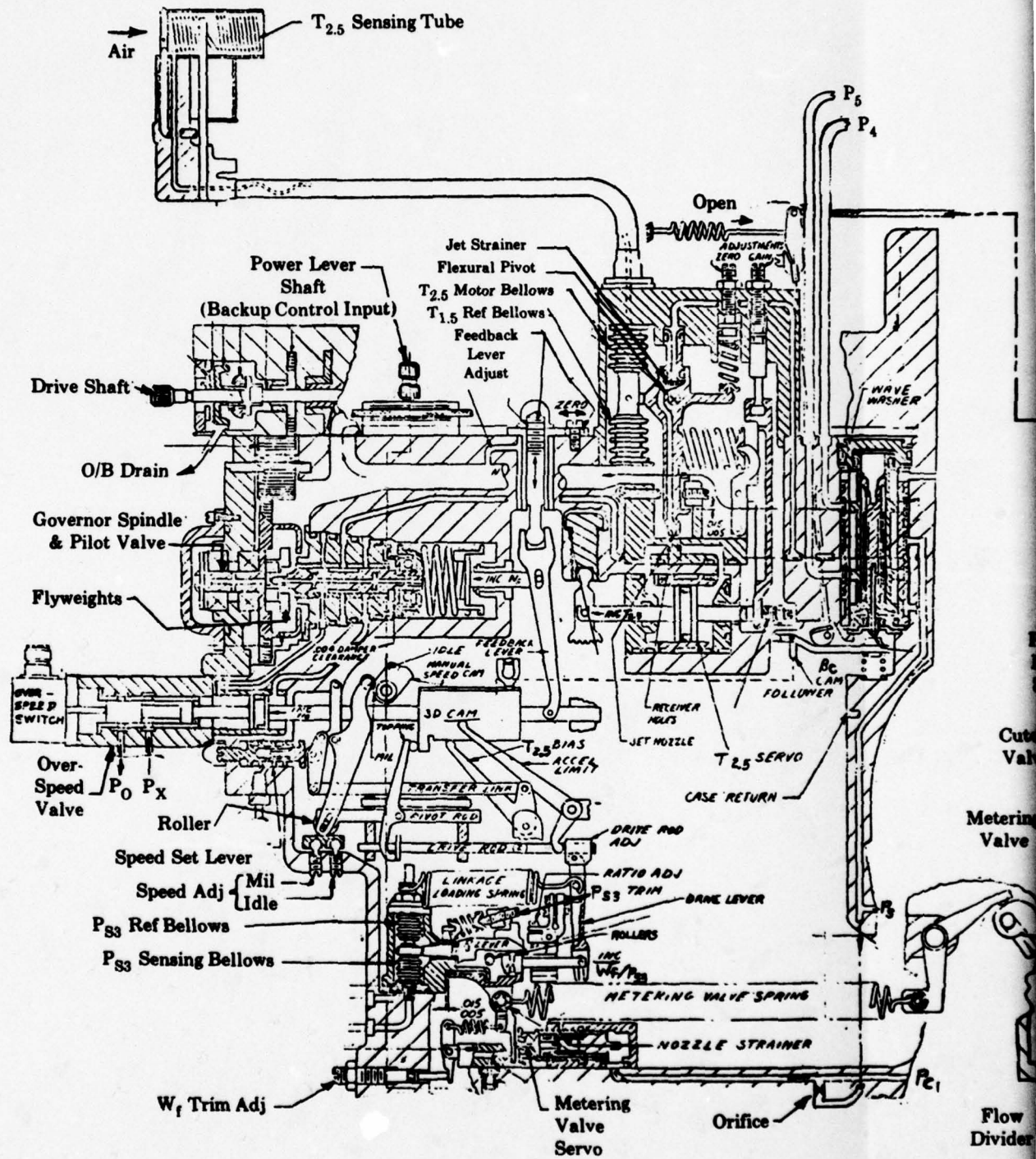


Figure 1-1 - Hydromechanical E

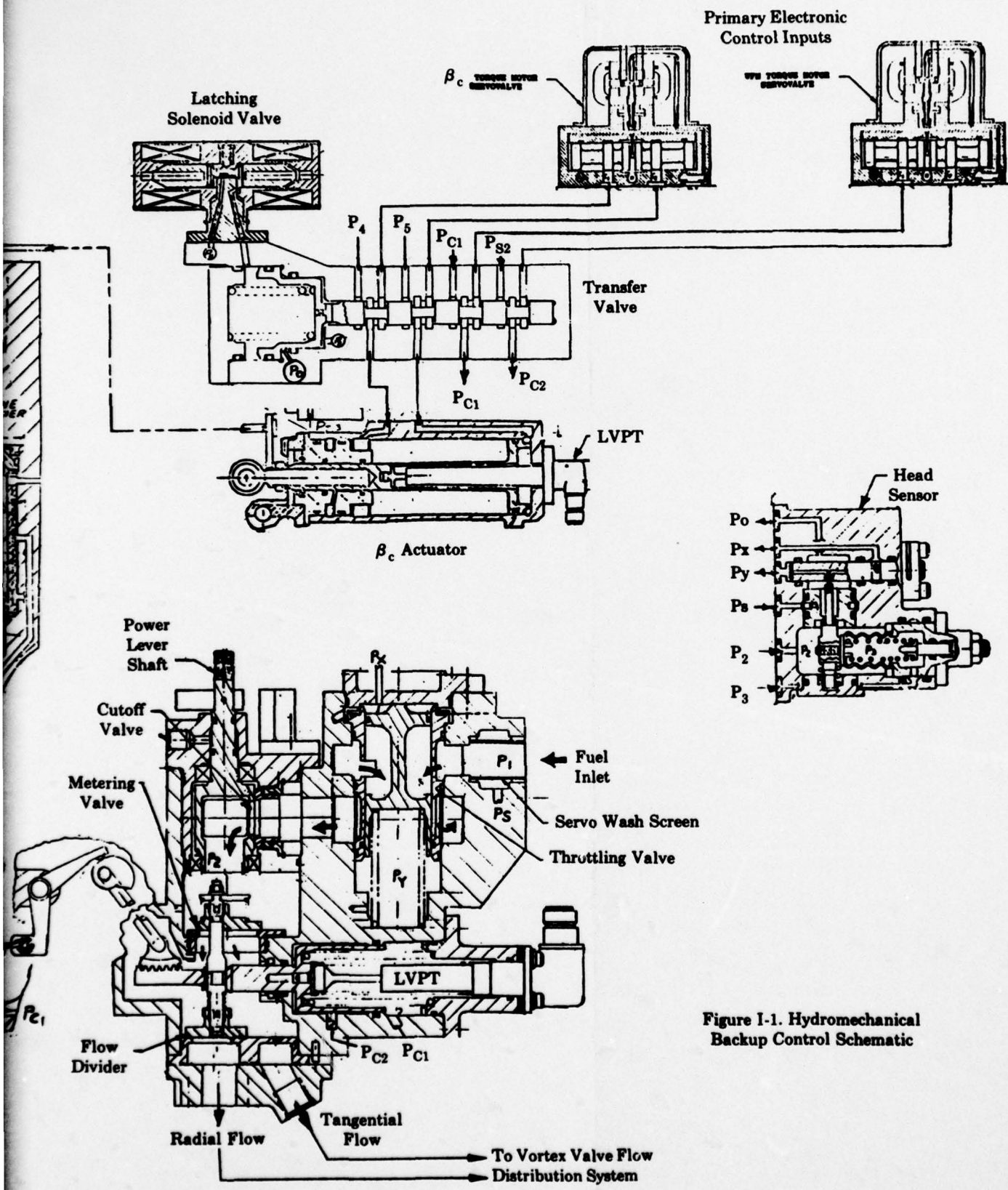


Figure I-1. Hydromechanical Backup Control Schematic

Hydromechanical Backup Control Schematic.

2

The incorporation of a 3D cam minimizes control size and weight by employing a single cam to perform a number of functions. Translation of the cam, a function of engine speed, is provided by the speed sensing system. Rotation of the cam, a function of compressor inlet temperature, is provided by the $T_{2.5}$ servo system. During steady-state operation, governor flyweight force is balanced against feedback spring force. For each steady state operating point, the 3D cam has a corresponding equilibrium position. The contoured surface of the 3D cam provides for signals to initiate the limiting and scheduling functions of the control. Four contours are used. The topping contour provides a top speed setting as well as a constant idle speed regardless of $T_{2.5}$ droop operation. The acceleration contour provides a W_f/P_{S3} versus RPM schedule to protect against stall and overtemperature. The $T_{2.5}$ bias and topping contour provides for resetting engine speed at high RPM and low $T_{2.5}$'s to ensure optimum engine performance. The variable geometry contour provides for scheduling the position of the variable stator vanes as a function of compressor inlet temperature and engine rotor speed.

Compressor inlet temperature controls rotation of the 3D cam. The $T_{2.5}$ sensing tube is filled with nitrogen. The spiral tubes in the inlet are shrouded for protection. The gas is very sensitive to minute changes in temperature which causes a motor bellows located within the control to expand or contract with changes in compressor inlet temperature. A reference bellows, also filled with gas but at a lower pressure, is located opposite the motor bellows. The reference bellows compensates for changes in fuel temperature within the control. The $T_{2.5}$ servo nozzle, connected to the bellows assembly, pivots with expansion and contraction of the bellows thereby directing servo fuel to the right or left side of the servo piston which moves axially within the chamber. The piston is mounted on a shaft with one end of the shaft attached to a gear sector which in turn mates with a similar gear sector on the 3D cam. The other end of the shaft is attached to a control arm which works, along with a feedback spring, to establish a force-balance system within the servo. In a null or steady-state position, a force-balance positions the servo nozzle, so that servo fuel discharging through the nozzle impinges upon a spike at the entrance to the servo piston, dividing the flow to create equal or balanced pressure on both sides of the piston. Assume that an increase in $T_{2.5}$ causes the bellows to expand. The servo nozzle, attached to the bellows, will pivot in a counterclockwise direction directing high pressure servo fuel to the right side of the spike and to the right side of the servo piston. Because the greater portion of servo fuel is directed to the right side of the servo piston, a pressure differential now exists creating a force unbalance across the piston. With this force unbalance, the servo piston now moves to the left rotating the 3D cam counterclockwise. The servo piston is moving to the left, moves the feedback arm in a counterclockwise direction compressing the servo nozzle spring. As the spring force increases, with the piston moving to the left, it moves the nozzle servo counterclockwise gradually directing more flow to the left side of the servo piston. A steady-state or null position is reached when a force balance is reached, i.e., forces generated by the bellows expanding are balanced by counteracting spring force. At this point, the servo nozzle is located so that servo fuel flow is directed equally to the right and left-hand sides of the servo piston maintaining equal pressure on both sides of the servo piston.

The metering valve positioning servo is the link between the computing section and the metering valve. Hydraulic force on the metering valve piston, shown as part of the fuel valve in Figure I-1, provides the motion necessary for changing the flow area. The magnitude and direction of the force is provided by a hydraulic servo which consists of the metering valve piston, a fixed supply orifice, a flapper valve with a pressure balancing piston, a metering valve feedback spring and the W_f lever. Servo supply pressure (P_S), essentially pump discharge, is taken from the back side of a wash screen in the fuel valve. In the backup mode, one side of the servo piston sees a fraction of servo pressure, while the spring side sees the variable pressure (P_{C1}) generated by the fixed orifice and the flapper valve. During steady-state, hydraulic forces on the metering valve servo piston are balanced and the flapper valve gap is constant. If a signal to the W_f lever "requests" an increase, the flapper gap increases which causes the pressure on the spring side (P_{C1}) of the servo piston to decrease, and the metering valve moves in the more open direction. The fuel valve, which is considered part of the primary control, is shown here to clarify the interface with the various other components.

Operation of the variable compressor stator vanes, β_c , is scheduled as a function of engine speed and $T_{2.5}$ by a contour on the 3D cam. A hydraulic force amplifier controls high pressure fuel flow to the variable geometry actuators. High pressure servo fuel is ported to the β_c servo entering the servo piston from the side. After filling the passages in the piston, the fuel passes through an orifice to a chamber on the underside of the piston. The fuel discharges through another orifice into the fuel control casing. The rate of flow is controlled by the size of a gap between the servo discharge orifice and a beam. During steady-state conditions, the gap size as determined by beam position, is such that hydraulic forces on both sides of the servo piston are balanced. Assume that the right end of the beam moves downward in response to 3D cam movement. The gap increases, allowing more fuel to be discharged to the case. Pressure on the underside of the piston decreases, upsetting the force balance and the piston moves downward. The piston lands uncover the bottom port, allowing high pressure fuel to flow to one side of the β_c actuator pistons to open the stator vanes. Fuel from the other side of the β_c actuator pistons returns through the upper port and exits into the bypass flow area. Movement of the β_c actuators is fed back to the feedback cam which rotates presenting a shorter radius to the beam, so that the right end of the beam moves upward. The gap decreases, allowing a pressure buildup on the underside of the piston, moving it upward. Motion stops when the actuators have reached the scheduled position and the steady state gap is reestablished, providing balanced hydraulic forces on the piston.

A discussion of the operation of the backup control during a backup mode acceleration follows. The most severe change in throttle setting is a rapid advance from idle to military involving, of course, an engine acceleration of considerable magnitude. The following discussion will be primarily concerned with an acceleration of this type but will also cover variations in control operation where they differ in less severe throttle angle changes.

Rotation of the control power lever causes rotation of the manual speed cam inside the control because they are mechanically connected. When the manual speed cam is rotated from idle to military, it presents a shorter radius to the top end of the speed set lever. The speed set lever rotates clockwise about its pivot point moving the pivot rod to the left. Since the topping lever is pinned to the pivot rod and therefore pivots about this point, it will also move to the left with the pivot rod leaving both the 3D cam and the Z-rod. The linkage loading spring is constantly exerting a force on the Z-rod to the left. When the topping lever shifts to the left, the Z-rod will therefore attempt to follow it. The drive lever pivots counterclockwise moving the rollers to the right. This increases the moment arm on top of the W_f lever and hence increases the force downward, rotating the W_f lever clockwise. An increase in the gap between the W_f lever and the metering valve servo orifice causes increased flow and a decay in pressure behind the metering valve. The force balance on the metering valve piston is upset and the piston moves the metering valve more open causing an increase in fuel flow to the engine. Since the power lever advance was considerable, the resultant movement of the linkage is proportional. The Z-rod movement to the left towards the bottom end of the topping lever continues until the Z-rod contacts the acceleration limit lever. The acceleration limit lever pivots clockwise until its upper end contacts the 3D cam, at which point movement of the Z-rod is restricted. The result is that roller movement ceases and further increase in fuel flow is prevented until the 3D cam moves. The fuel flow now scheduled by the control exceeds the engine steady state requirements causing an increase in engine speed. The centrifugal force of the governor flyweights overcomes the spring force and the flyweights extend outward moving the pilot valve to the right. High pressure servo fuel, flowing to the right-hand side of the power piston, moves the piston and the 3D cam to the left. Now, the acceleration limit lever further rotates clockwise in response to the changing acceleration schedule cut on the cam. This allows the Z-rod to move to the left and the rollers to the right scheduling fuel flow as dictated by the acceleration schedule on the 3D cam. Meanwhile, as engine speed increases as a result of increased fuel flow, compressor discharge pressure also rises. This expands the P_{S3} sensing bellows tending to rotate the P_{S3} lever clockwise and increasing the force downward on the W_f lever. The cumulative effect of increased engine rpm and P_{S3} is an acceleration based on the fuel flow scheduled by the cam and P_{S3} .

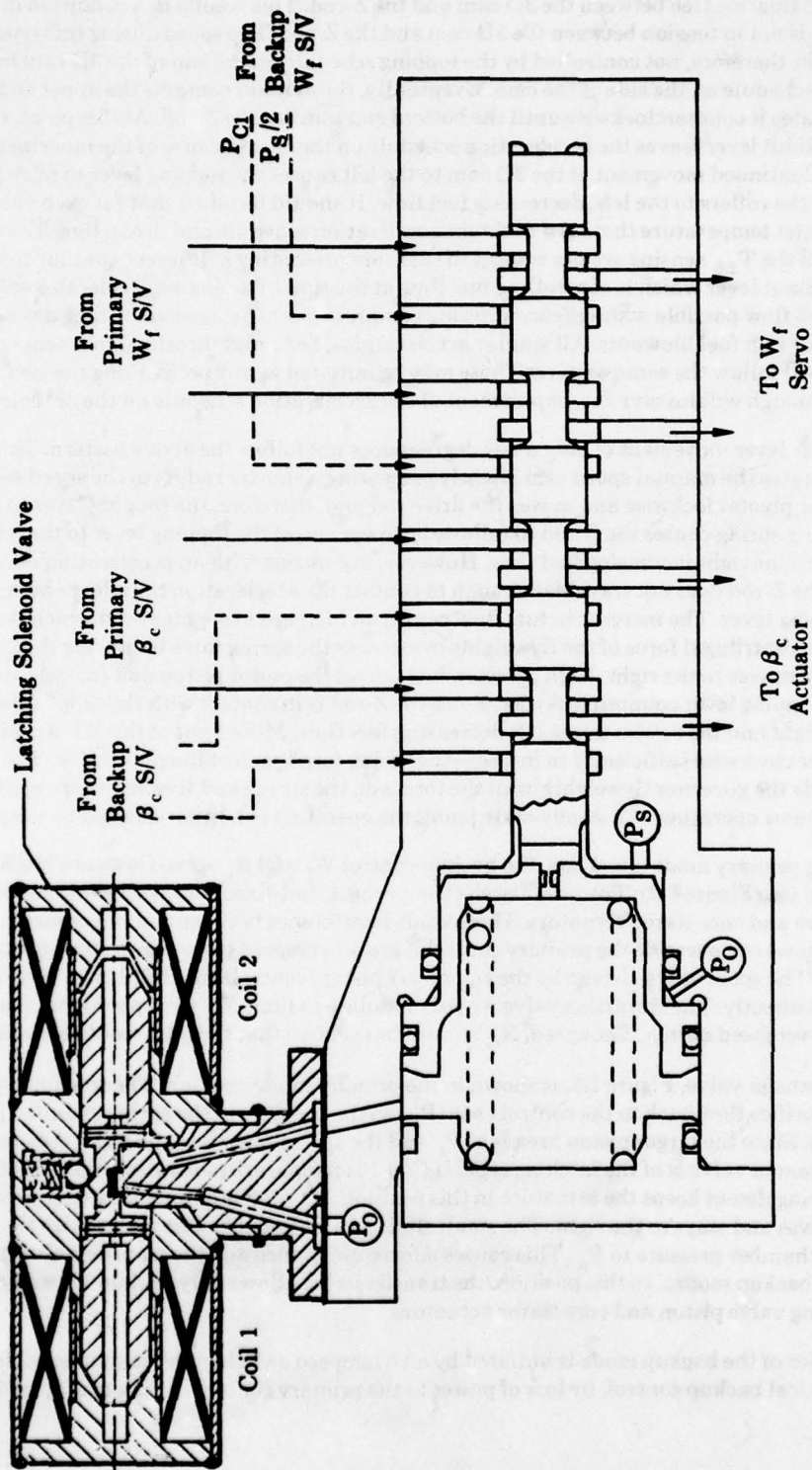
During the acceleration the 3D cam and the Z-rod are moving toward the topping lever, which is unloaded and floating free between the 3D cam and the Z-rod. This results in a condition in which the topping lever is not in tension between the 3D cam and the Z-rod. Top speed during this type of acceleration is, therefore, not controlled by the topping schedule on the end of the 3D cam but by the acceleration schedule on the side of the cam. Eventually, the 3D cam contacts the upper end of the topping lever and rotates it counterclockwise until the bottom end touches the Z-rod. At this point, the acceleration limit lever leaves the acceleration schedule on the cam because of the movement of the Z-rod to the right. Continued movement of the 3D cam to the left causes the topping lever to push the Z-rod to the right and the rollers to the left, decreasing fuel flow. It should be noted that for each value of compressor inlet temperature there is a different acceleration schedule and droop line. The schedule is changed when the $T_{2.5}$ sensing system rotates the 3D cam presenting a different contour to the acceleration limit lever which is controlling fuel flow at the time. The engine accelerates with the maximum fuel flow possible without encountering compressor stall, excessive turbine discharge temperature or rich fuel blowouts. All similar accelerations, i.e., rapid throttle movements of considerable magnitude, will follow the same pattern. These may be initiated at any point along the steady state line and if great enough will involve the employment of the acceleration schedule on the 3D cam.

A power lever movement of only a few degrees does not follow the above pattern. This slight movement rotates the manual speed cam slightly presenting a shorter radius to the speed set lever. The speed set lever pivots clockwise and moves the drive rod and, therefore, the topping lever to the left. The linkage loading spring causes the Z-rod to follow the lower end of the topping lever to the left and the rollers move to the right increasing fuel flow. However, in contrast with an acceleration of considerable magnitude, the Z-rod does not travel far enough to contact the acceleration limit lever before it catches up with the topping lever. The increase in fuel flow causes an increase in engine speed which is sensed in the governor. The centrifugal force of the flyweights overcomes the spring force balancing the pilot valve and the pilot valve moves to the right. High pressure fuel moves the power piston and the 3D cam to the left rotating the topping lever counterclockwise. Since the Z-rod is in contact with the topping lever, it will move to the right and the rollers to the left decreasing fuel flow. Movement of the 3D cam pivots the feedback lever clockwise sufficiently to increase the spring force against the pilot valve. The pilot valve moves towards the governor flyweights until the forces on the spring and flyweights are again in balance. The engine is now operating at a steady-state point, the operating condition selected by the power lever.

During primary mode operation, the backup control W_f and β_c servo flows are blocked by a transfer valve (see Figure I-2). The primary electrohydraulic fail-fixed servovalves alone control the metering valve and core stator actuators. This avoids interference between the two controls. The backup control can, however, override the primary control if gross overspeed caused by a stuck open metering valve occurs. The spool valve, driven by the N_G power piston, controls the throttling valve opening pressure (P_x) directly. The throttling valve would modulate to limit N_G to a rpm higher than that tripping the overspeed switch. The speed, N_G , would be cyclic so that the pilot would sense a problem.

The transfer valve, Figure I-2, is shown in the primary mode position. The solenoid valve is blocking the orifice flow back to the control case (P_o) so the pressure in the spring chamber is servo supply pressure (P_s). Since the larger piston area is at P_s and the spring force is to the right, the net force is to the right. The solenoid valve is of the latching type. If Coil 1 is temporarily energized, the armature moves to the left. A spring detent keeps the armature in this position. If Coil 2 is temporarily energized, the armature moves and stays to the right. The small sliding valve member also moves with the armature and ports spring chamber pressure to P_o . This causes a force unbalance and the transfer valve spool strokes to the left stop (backup mode). In this position, the transfer valve allows only backup W_f and β_c servo flows to the metering valve piston and core stator actuators.

Transfer of the backup mode is initiated by an overspeed switch in the computer portion of the hydromechanical backup control, by loss of power to the primary control, by loss of a "good health"



Scale ≈ 2:1

Figure I-2 - Transfer Valve For The Hydromechanical Approach.

signal from the primary control and by pilot action. The intended logic is shown in Figure I-3. Any of the above switch actions allow a 28 volt (aircraft power) signal to reach Coil 2 of the latching solenoid. The pilot also has an arm/disarm switch which allows or blocks automatic transferring and a primary switch which allows transferring back to primary operation by temporarily energizing Coil 1.

2. PRELIMINARY DESIGN

This backup control computation section will be similar to those in existing hydromechanical fuel controls. Figure I-4 is a partial section showing the speed (N_G) sensor. The input gear is driven by the engine and the flyweight force is proportional to N_G^2 . If speed increases, the increased flyweight force moves the pilot valve up porting flow to the upper side of the power piston. The piston, along with the 3-D cam and the right end of the feedback lever, moves downward. Motion stops when the spring force balances the flyweight force.

Figure I-5 shows some of the levers and the PLA cam. The centerline of the $T_{2.5}$ servo piston is indicated and the piston motion rotates the 3-D cam. Figure I-6 shows the metering valve servo. The multiplying mechanism is hidden by the support member. The flapper valve controls the variable metering valve servo piston pressure (P_{C1}).

The $T_{2.5}$ servo and β_c servovalve are shown by the partial view of Figure I-7. The $T_{2.5}$ servo piston position is a function of $T_{2.5}$. As temperature increases, the pressure $T_{2.5}$ motor bellows (not shown) increases and the force moves the jet pipe downward increasing flow to the lower side of the piston. The piston strokes upward increasing the feedback spring force which, in turn, moves the jet pipe upward. Piston motion ceases when the forces are balanced and the jet pipe applies equal pressures to both sides of the piston.

Figure I-8 shows a side view of the hydromechanical backup control with the fuel valve included in the same assembly. The primary W_f and β_c servovalves are also shown. The fuel valve and the two servovalves are not included in the subsequent comparative analysis but are shown here to depict a production version of the integrated assembly. This backup control requires a mechanical N_G input so it will be mounted to a gearbox pad. Figure I-9 shows an end view. The centerlines of the transfer, throttling and metering valves are indicated.

3. RELIABILITY ANALYSES

a. Procedure

The computer portion of the hydromechanical backup control is very similar to those of existing main fuel controls. This allows using actual failure rates for this component. The same is true for the $T_{2.5}$ sensor and β_c feedback cable. The other major component is the transfer valve. This transfer valve uses two latching solenoids. Figure I-10 shows the major components.

b. Results

The results of the reliability analysis are shown in Table I-1. The failure rates are based on CF6-50 main fuel control experience after 500,000 cumulative flight hours. The hydromechanical backup control computer is similar to that in the CF6-50 main fuel control. The computer is estimated to be equivalent to 60% of the complexity of a main fuel control. This factor was used to determine the failure rates of the backup control computer. The failure rates of the $T_{2.5}$ sensor and the β_c feedback cable are also based on CF6-50 experience.

The transfer valve uses two solenoids so the failure rate will be higher than the rate used for a servovalve. The electrical power for momentarily energizing the solenoids is from the aircraft. For this

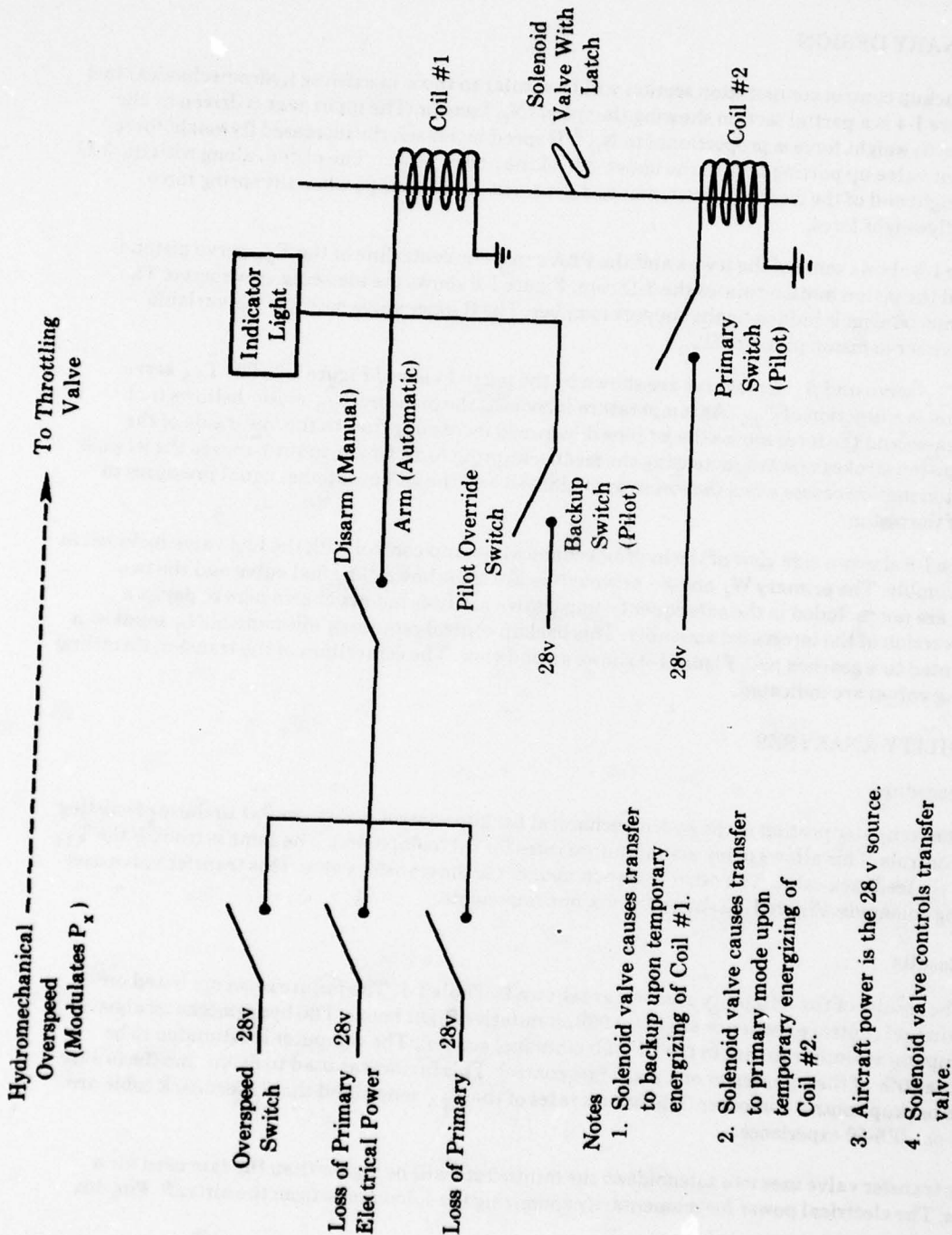


Figure I-3 - Schematic of the Electrical Portion of the Hydromechanical Approach.

THIS PAGE IS BEST QUALITY PRACTICABLE
FROM COPY FURNISHED TO DDC

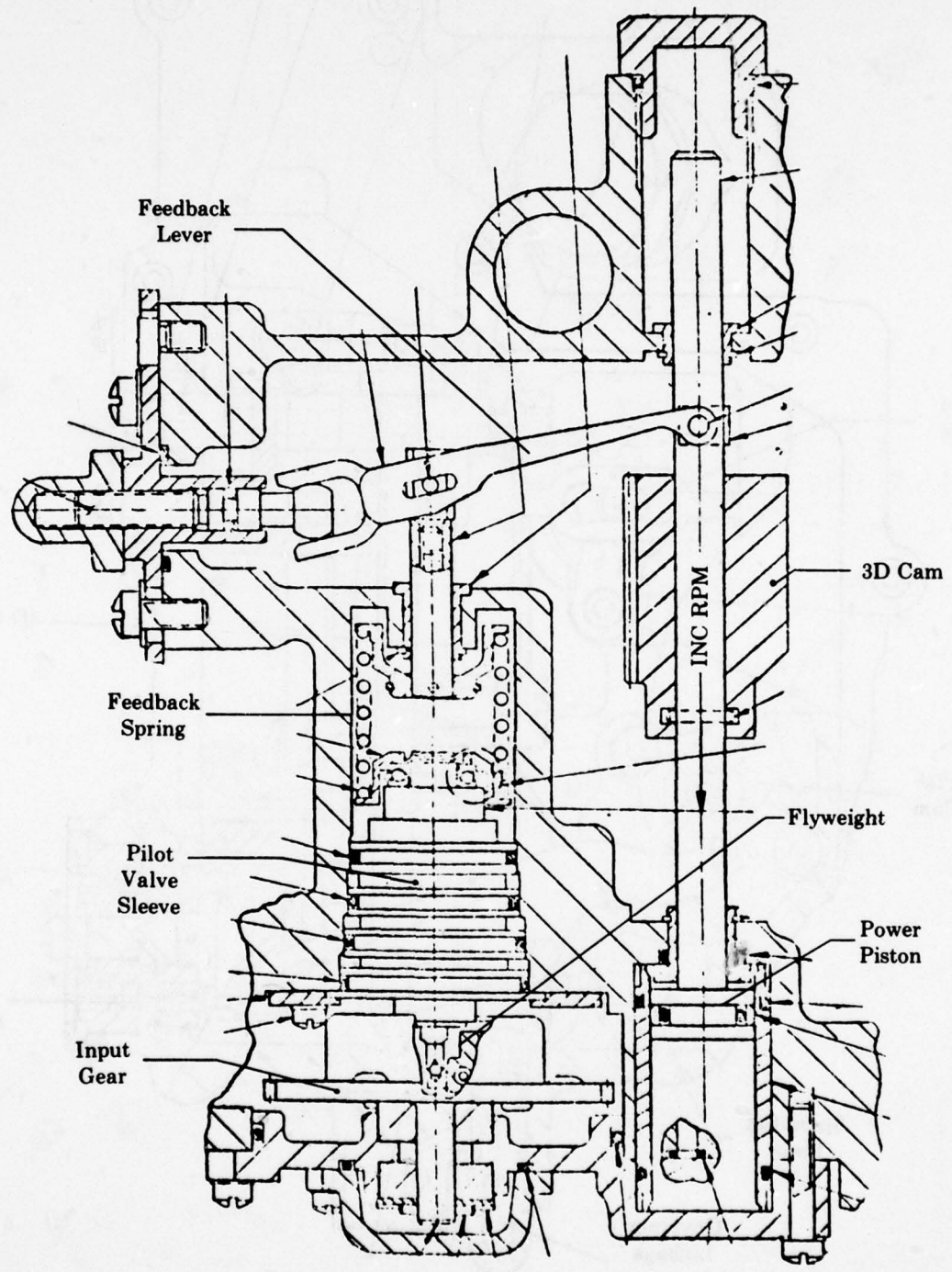


Figure I-4 - Partial Section Showing the Speed Sensor.

THIS PAGE IS BEST QUALITY PRACTICABLE
FROM COPY FURNISHED TO DDG

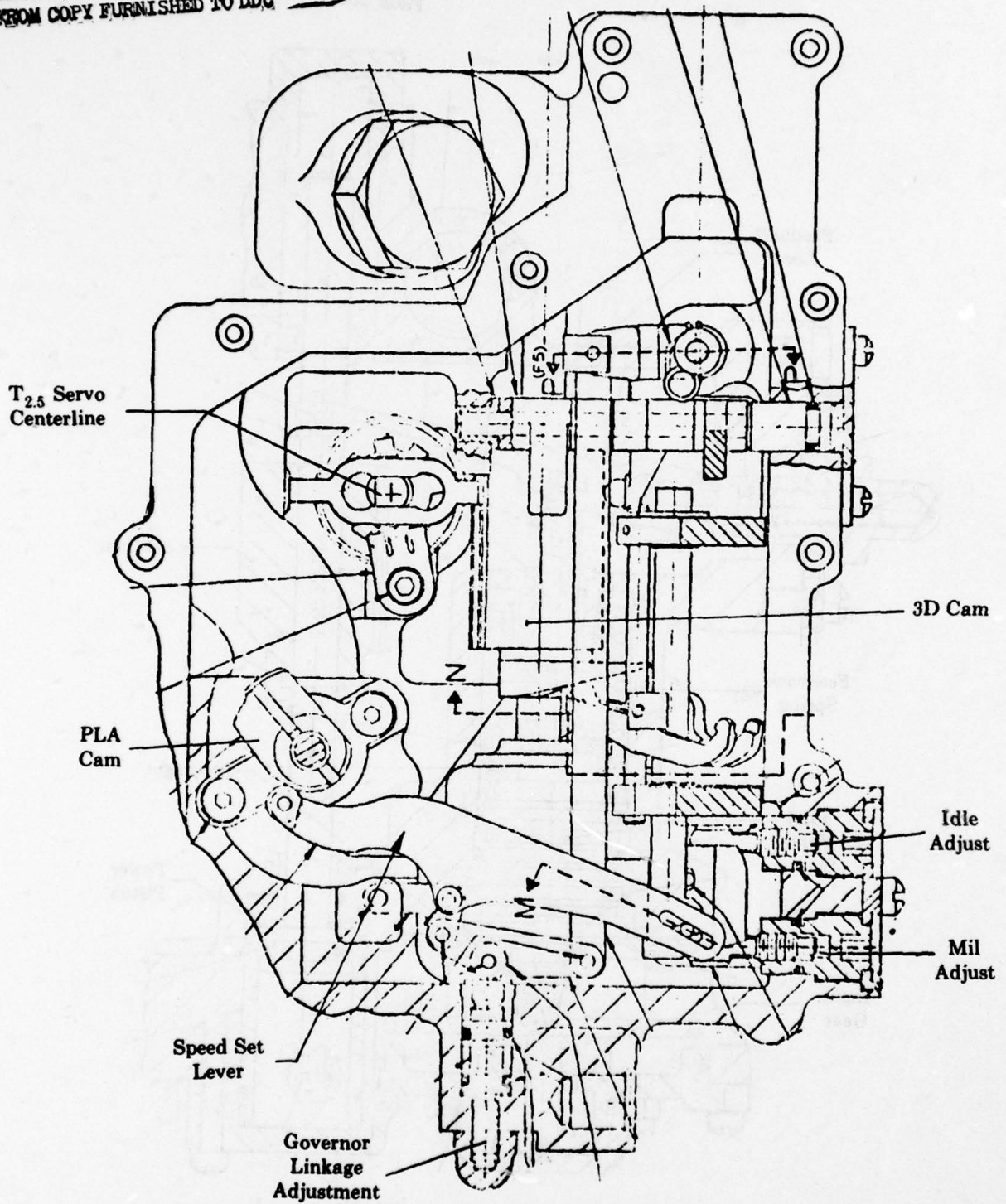


Figure I-5 - Partial Section Showing the PLA Cam and Several Levers.

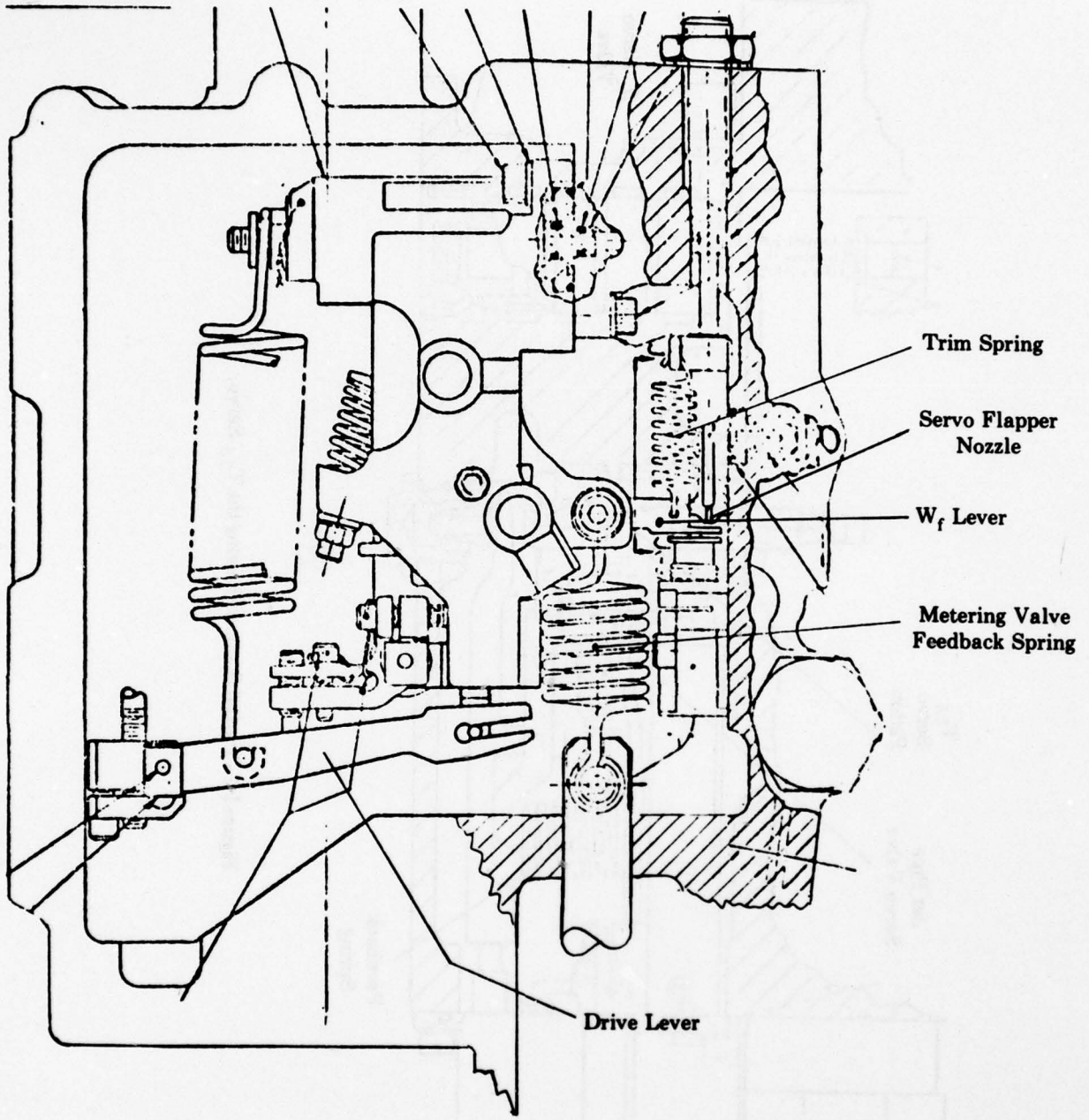


Figure I-6 - Partial Section Showing the Metering Valve Servo.

THIS PAGE IS BEST QUALITY PRACTICABLE
FROM COPY FURNISHED TO DDC

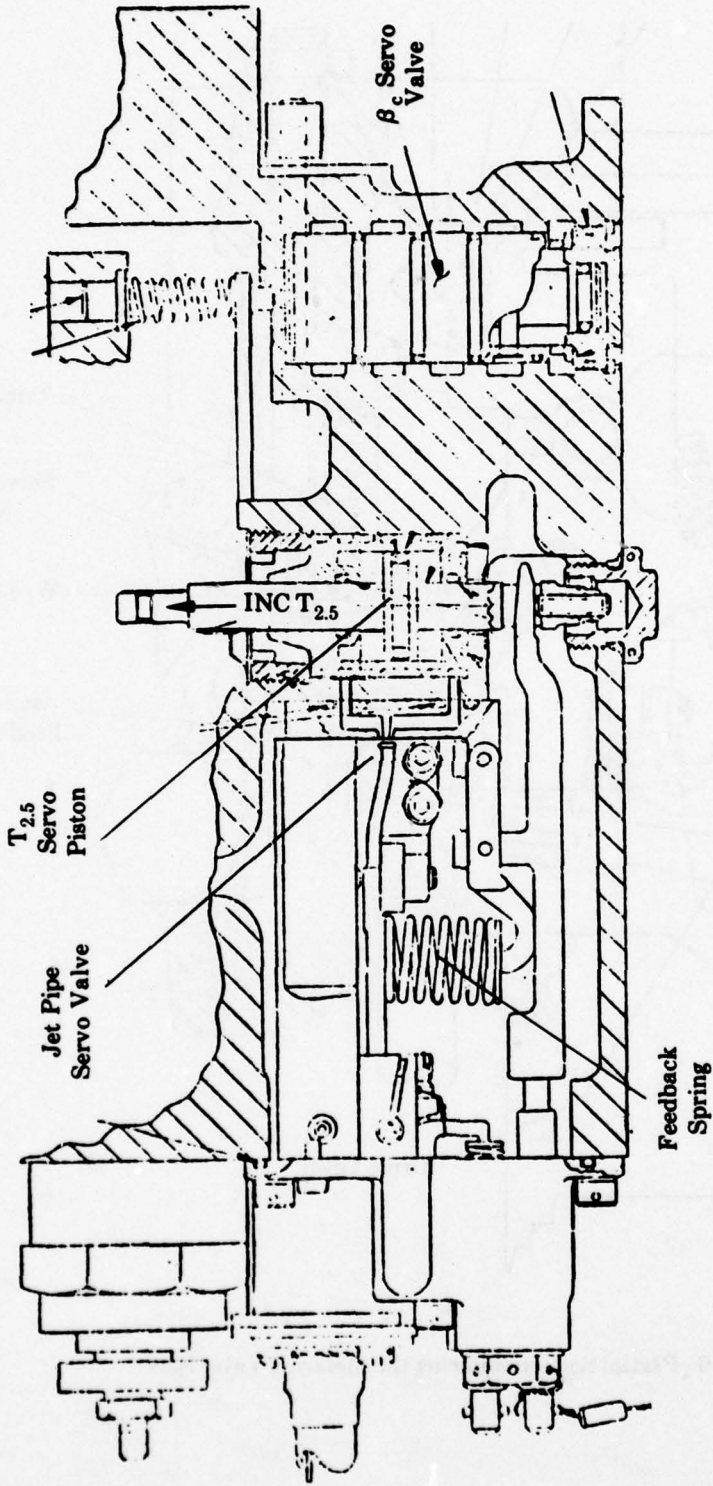


Figure I-7 - Partial Section Showing the T_{2.5} Servo.

THIS PAGE IS BEST QUALITY PRACTICABLE
FROM COPY FURNISHED TO DDG

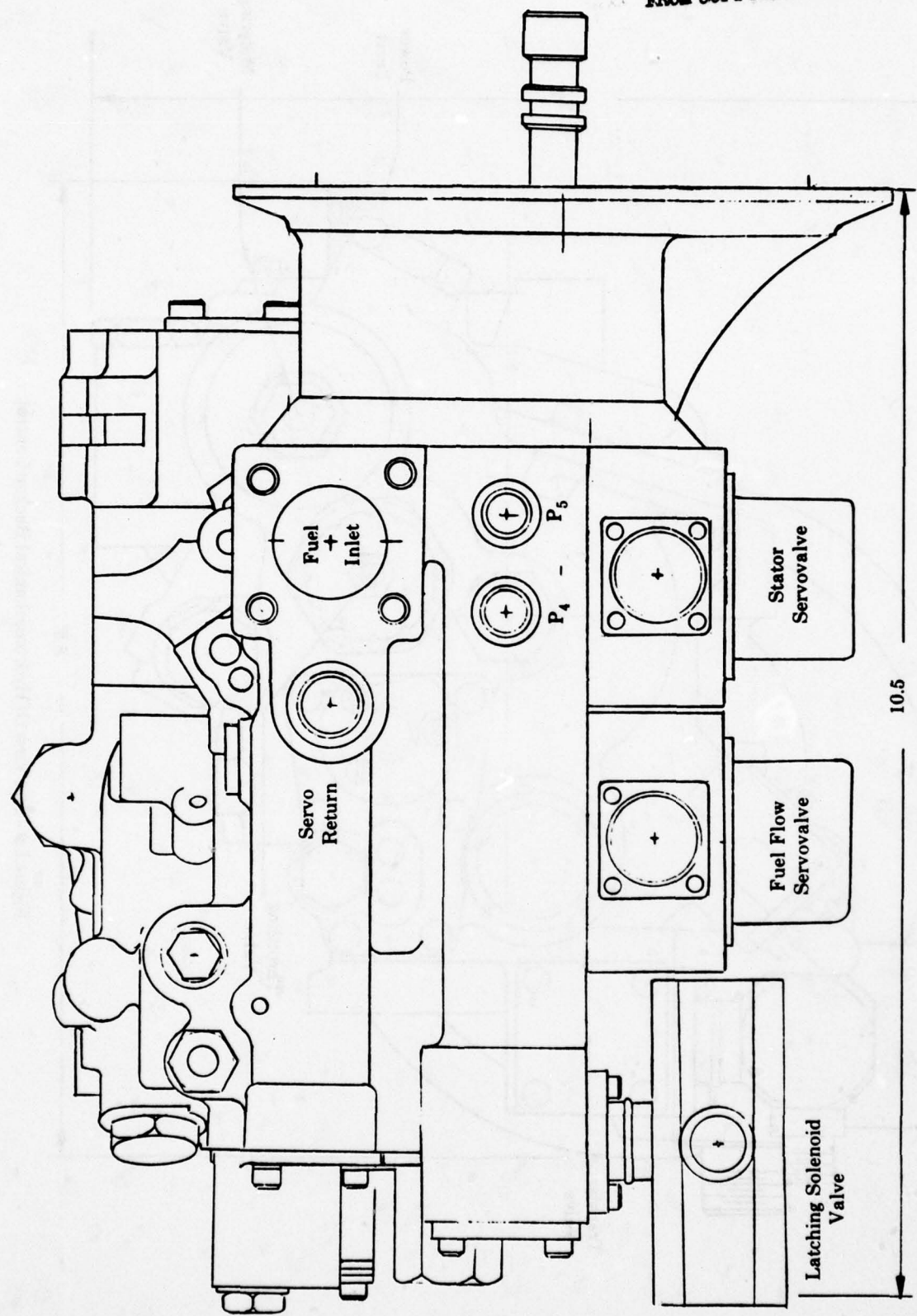


Figure I-8 - Side View of Hydromechanical Backup Control with Integrated Fuel Valve.

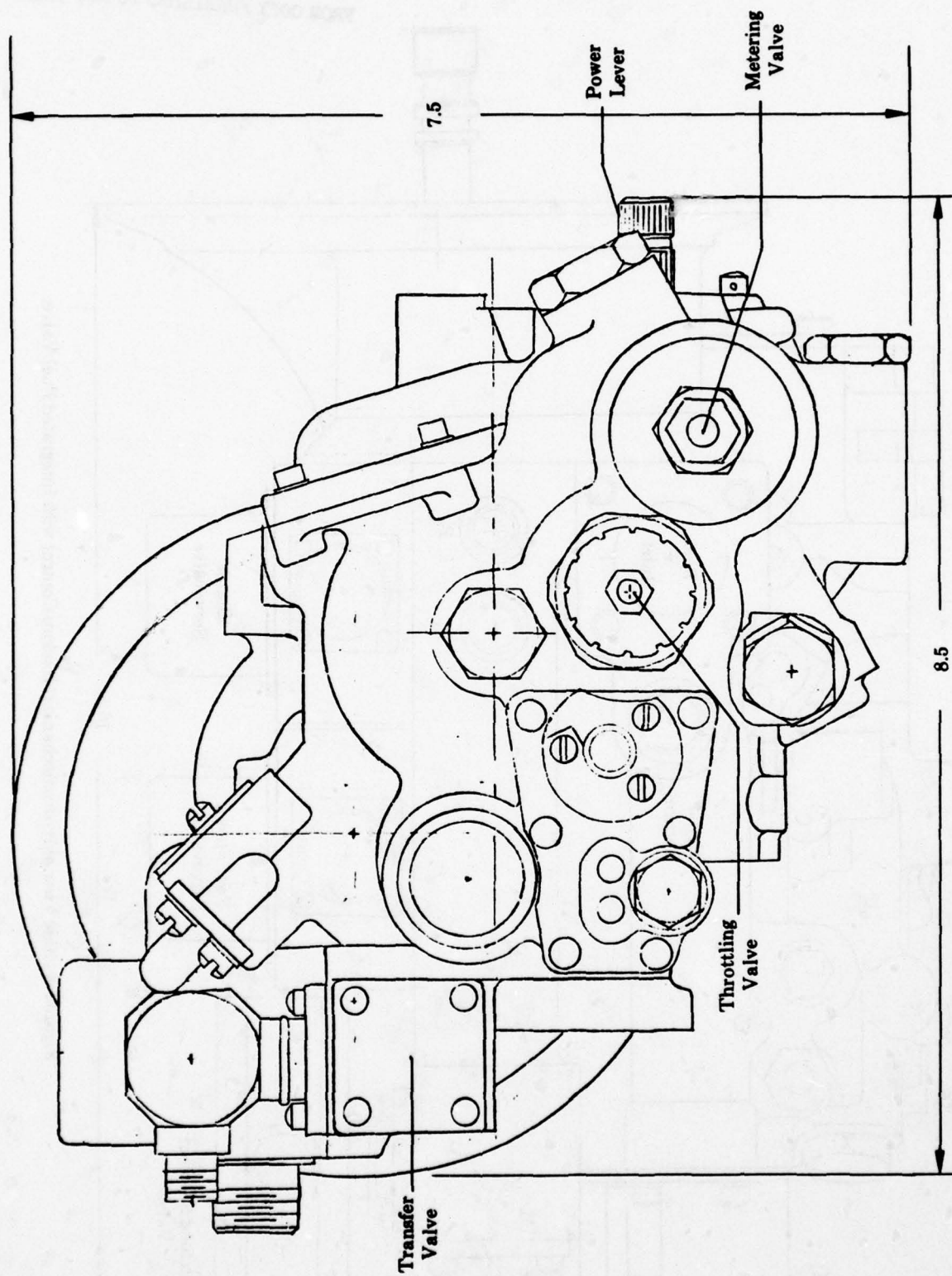


Figure I-9 - End View Of Hydromechanical Backup Control.

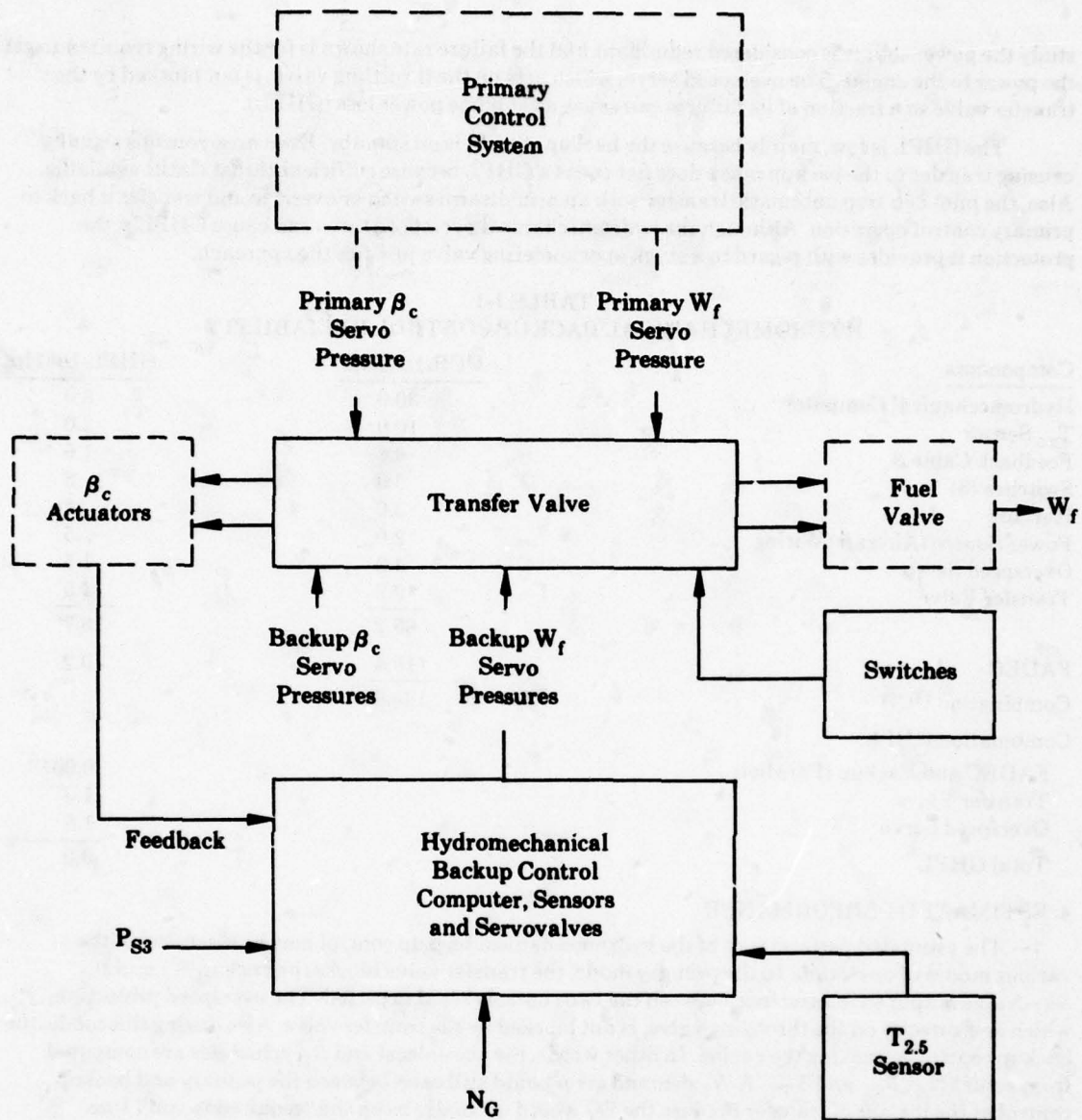


Figure I-10 - Components Included in the Hydromechanical Backup Control.

study the power source is considered redundant and the failure rate shown is for the wiring required to get the power to the engine. The overspeed servo, which acts on the throttling valve, is not blocked by the transfer valve so a fraction of its failures can cause a get home power loss (GHPL).

The GHPL is low, mainly because the backup control is on standby. Even an erroneous signal causing transfer to the backup mode does not cause a GHPL because sufficient thrust is still available. Also, the pilot can stop automatic transfer with an arm/disarm switch or override and transfer it back to primary control operation. Although the hydromechanical overspeed servo can cause GHPL's, the protection it provides with regard to a stuck open metering valve justifies the approach.

TABLE I-1
HYDROMECHANICAL BACKUP CONTROL RELIABILITY

Components	UCR/10 ⁶ Hrs.	GHPL/10 ⁶ Hrs.
Hydromechanical Computer	30.0	8.0
T _{2.5} Sensor	10.0	2.0
Feedback Cable β_c	6.8	1.6
Switches (6)	3.0	.8
Harness	3.0	.8
Power Source (Aircraft) Wiring	2.0	.5
Overspeed Servo	4.2	1.5
Transfer Valve	9.2	1.5
	<hr/> 68.2	<hr/> 16.7
FADEC	118.4	40.2
Combination UCR	186.6	
Combination GHPL:		
FADEC and Backup (Parallel)		0.0013
Transfer Valve		1.5
Overspeed Servo		1.5
Total GHPL		<hr/> 3.0

4. ESTIMATED PERFORMANCE

The estimated performance of the hydromechanical backup control may be discussed in the various modes of operation. In the primary mode, the transfer valve blocks the backup W_f and β_C servovalve output so interference between the two controls is not expected. The overspeed protection, which acts directly on the throttling valve, is not blocked by the transfer valve. Also during this mode, the backup control is tracking the engine. In other words, the accel/decel and β_C schedules are computed from actual N_G , P_{S3} and T_{T2} . A W_f demand error could still exist between the primary and backup control at the instant of transfer because the W_f would normally be on the "required to run" line.

An estimate of the W_f response during primary to backup transfer, assuming a difference in primary and backup demands existed, was conducted. The first step was to determine component sizes for the hydromechanical backup control. The selected dimensions and some assumptions on pressures are shown by Figure I-11. Conditions selected were sea level standard day (SLS) takeoff fuel flow. At this condition, metering valve discharge is approximately 690 psig and pump discharge pressure is approximately 1000 psig. The pressure at the right end of the metering valve piston is set by the orifices in series and the resulting pressure is selected as 0.69 P_g . The lever at the left sums the torques applied by the computer ($F \times a$), the feedback spring (24 lb/in \times 0.5 in \times cam rise) and the trim spring (4 lb/in \times 1.0 in \times X_p). The flapper spring rate was not included because the pressure change is very small during normal operation. The sketch represents conditions after the transfer valve has stroked to the backup mode stop.

The metering valve velocity is determined by the flow through the 0.021 inch diameter orifice less the flow through the flapper valve. The servo pressure is pump discharge pressure less case pressure since

no servo pressure regulator is used. The metering valve port is triangular in shape so W_f is not proportional to stroke. A cam is used to convert metering valve stroke to a feedback spring stroke which is proportional to fuel flow.

Figure I-12 shows a functional block diagram. W_f increases when the metering valve piston motion (X) is to the left. Increasing flapper gap, X_p , is considered positive and the trim spring torque decreases as X_p increases. Again, the gains and throttling valve time constant are based on a 1000 psig servo pressure.

The transfer function for the inner loop, from torque in to flapper travel (X_p) out, was then determined. The transfer function of this type of loop can be found by using the following equation:

$$G' = \frac{G}{1+GH} \quad \text{where}$$

$$G' = \text{loop gain}$$

$$G = \text{forward gain}$$

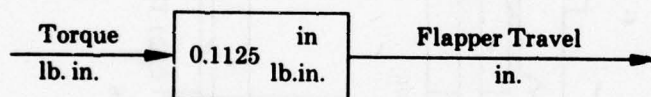
$$H = \text{feedback gain}$$

Substituting in values from Figure I-12, we get:

$$G' = \frac{(1.5)(1/24)(2.25)}{1 + (1.5)(1/24)(2.25)(1.000/1.125)(4)(1.0)}$$

$$G' = 0.1125$$

This can be shown as:



Next, the flapper flow characteristics were determined at the given condition. Using the flow equation, we get:

$$Q_F = C_C A C \sqrt{P_{C1} - P_O} \quad \text{where}$$

$$Q_F = \text{flow in in}^3/\text{sec.}$$

$$C_C = \text{area coefficient}$$

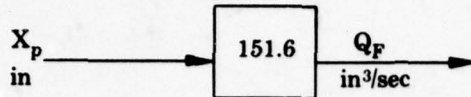
$$A = \text{flapper flow area}$$

$$C = \text{constant (109.3)}$$

Substituting in values, we get:

$$\begin{aligned} Q_F &= (0.6) (\pi D_n X_p) (109.3 \sqrt{690}) \\ &= (0.6) (\pi .028) X_p (109.3) (26.27) \\ &= 151.6 X_p \end{aligned}$$

The transfer function for this flapper valve is:



The flow of the fixed orifice at the given condition was determined. Using the above flow equation we get:

$$\begin{aligned} Q_O &= C_C A C \sqrt{P_S - P_{C1}} \\ &= 0.75 (\pi/4) (.021)^2 (109.3) \sqrt{1000 - 690} \\ &= 0.50 \text{ in}^3/\text{sec}. \end{aligned}$$

At null, flapper flow equals orifice flow ($Q_O = Q_F$). The null gap is determined by dividing Q_O by the flapper valve transfer function or gain. Dividing, we get:

$$\begin{aligned} \text{Null Gap} &= \frac{0.50 \text{ in}^3/\text{sec}}{151.6 \text{ in}^3/\text{sec}/\text{in}} \\ &= 0.0033 \text{ in}. \end{aligned}$$

For this study, the piston area acted on by $0.69 P_S$ is 1.03 in^2 . The piston area acted on by P_{C1} is 1.23 in^2 . The rod area (0.196 in^2) is acted on by P_3 which is metering valve downstream pressure and for this study it was assumed to be 690 psi above P_o . This results in P_{C1} of 690 psi above P_o . The pressure, $0.69 P_S$, is determined by the area ratio of the orifices.

The gain of the metering valve is $41,500X^2$. This can be linearized as follows:

$$\begin{aligned} W_f &= 41,500X^2 \\ \Delta W_f &= 2(41,500) X \Delta X \\ \text{or} \\ \frac{\Delta W_f}{\Delta X} &= 83,000 X \end{aligned}$$

At SLS takeoff, the stroke, X , is .613 inches (15,600 pph) so

$$\frac{\Delta W_f}{\Delta X} = 50,900 \text{ pph}/\text{in}.$$

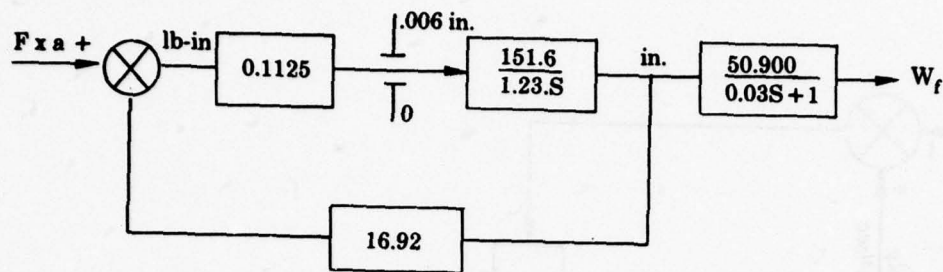
The gain of the feedback cam is:

$$X' = 1.152 X^2$$

This can be linearized as follows:

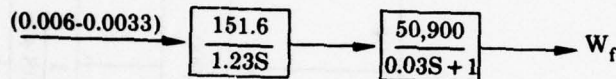
$$\begin{aligned} \Delta X' &= (2)(1.152)X \Delta X \\ \text{or} \\ \frac{\Delta X'}{\Delta X} &= 2.304 X \\ \frac{\Delta X'}{\Delta X} &= 1.41 \text{ at } X = .613 \text{ in}. \end{aligned}$$

Figure I-13 shows a revised block diagram showing the above derived transfer functions and linearizations. This block diagram can be consolidated to that shown below:

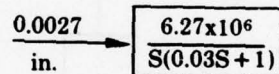


Flapper valve gap is 0.0033 inches at null and the flapper valve is linear to about 0.006 inch in the opening direction. Further opening causes little change in flow so 0.006 inch gap is considered saturation.

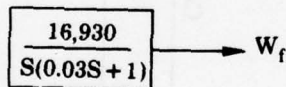
It was assumed that a W_f error existed in the backup control at the instant of transfer. For the initial time period, a constant flapper gap of 0.006 inch (0.0027 inch from null) was used. The transfer function from flapper travel to W_f is:



Combining, this becomes:



For the .0027 flapper travel, this becomes:



which is a LaPlace transform. The inverse of the LaPlace transform is:

$$W_f = 16930 [t - 0.03(1 - e^{-t/0.03})]$$

A plot (see Figure I-14) of this function shows what happens to W_f versus time if the flapper is at 0.006 inch gap upon transfer and then stays at this gap.

For the following period, the flapper travels from 0.006 inch toward null (0.0033 inch). Going back to the block diagram shown by Figure I-13, a second LaPlace transform can be derived. Using the equation for a feedback loop we get:

$$G'' = \frac{(.1125)(151.6/1.23S)}{1 + (.1125)(151.6/1.23S)(16.92)}$$

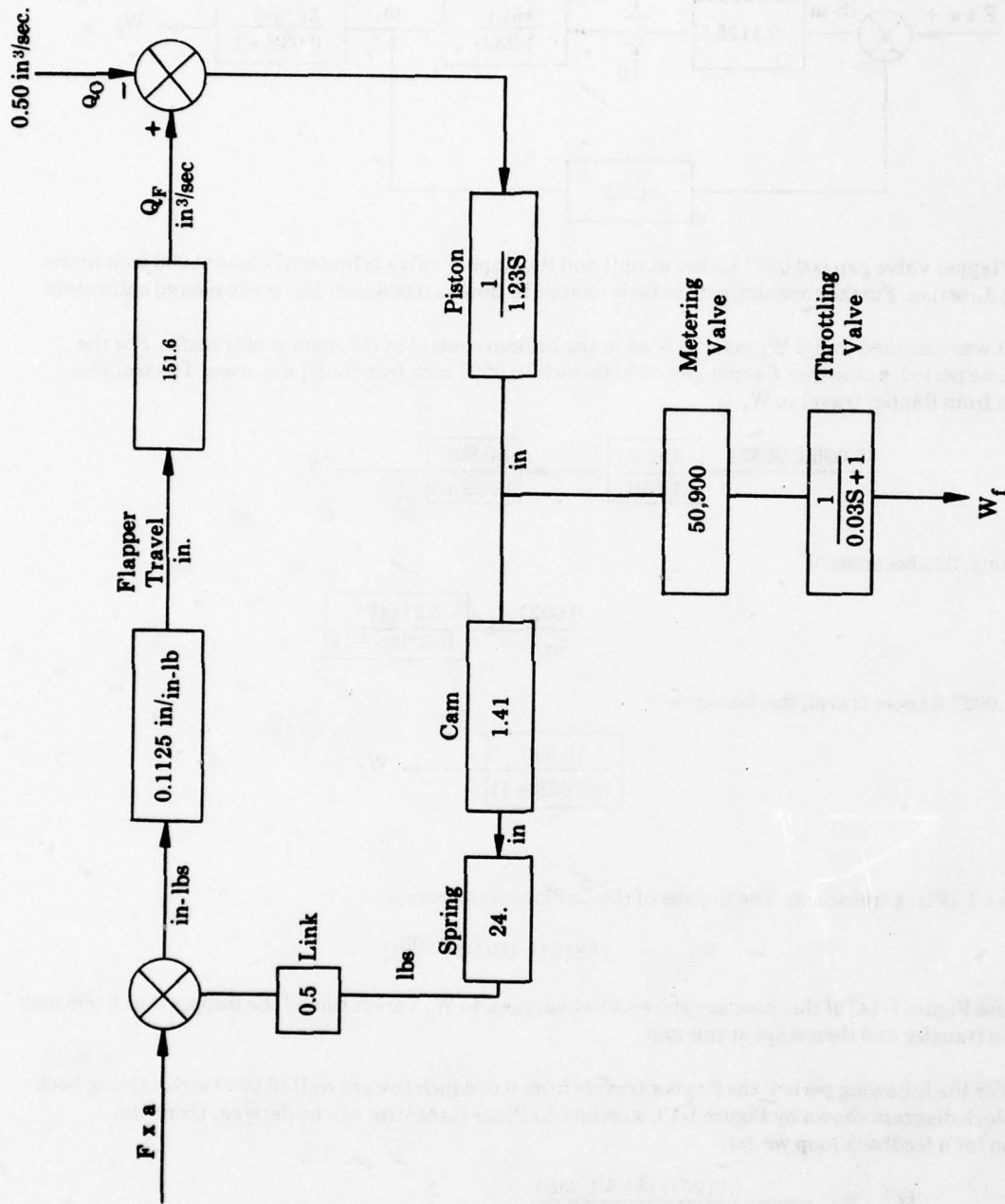


Figure I-13 - Revised Block Diagram Showing Linearizations.

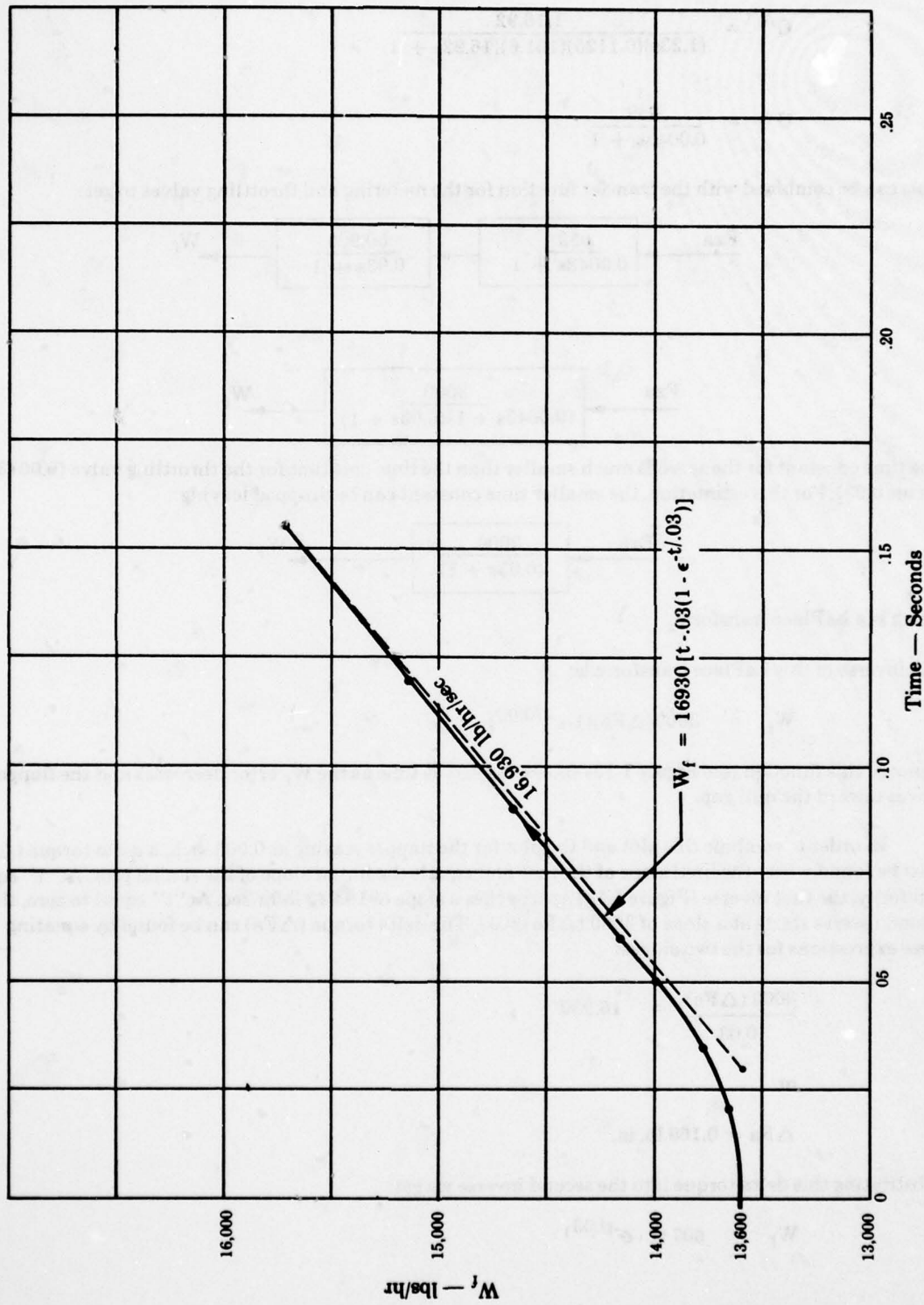


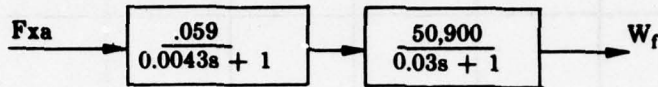
Figure I-14 - Response While Flapper Is Fixed Open (Saturated).

$$G'' = \frac{(.1125)(151.6)}{1.23s + (0.1125)(151.6)(16.92)}$$

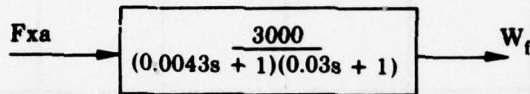
$$G'' = \frac{1/16.92}{(1.23s)(0.1125)(151.6)(16.92) + 1}$$

$$G'' = \frac{.059}{0.0043s + 1}$$

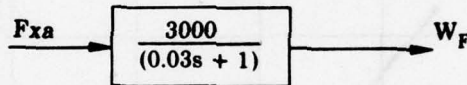
This can be combined with the transfer function for the metering and throttling valves to get:



or



The time constant for the servo is much smaller than the time constant for the throttling valve (0.0043 versus 0.03). For this estimation, the smaller time constant can be dropped leaving:



which is a LaPlace transform.

The inverse of this LaPlace transform is:

$$W_f = 3000(\Delta Fa)(1 - e^{-t/0.03})$$

A plot of this function (see Figure I-15) shows W_f versus time as the W_f error decreases and the flapper moves toward the null gap.

In order to combine this plot and the plot for the flapper staying at 0.006 inch, a delta torque (ΔFa) must be found where the final slope of the first plot equals the initial slope of the second plot. At "t" equal to infinity, the first inverse (Figure I-14) approaches a slope of 16,930 lb/hr/sec. At "t" equal to zero, the second inverse starts at a slope of $3000(\Delta Fa)/0.03$. The delta torque (ΔFa) can be found by equating these expressions for the two slopes:

$$\frac{3000(\Delta Fa)}{0.03} = 16,930$$

or

$$\Delta Fa = 0.169 \text{ lb. in.}$$

Substituting this delta torque into the second inverse we get:

$$W_f = 507(1 - e^{-t/0.03})$$

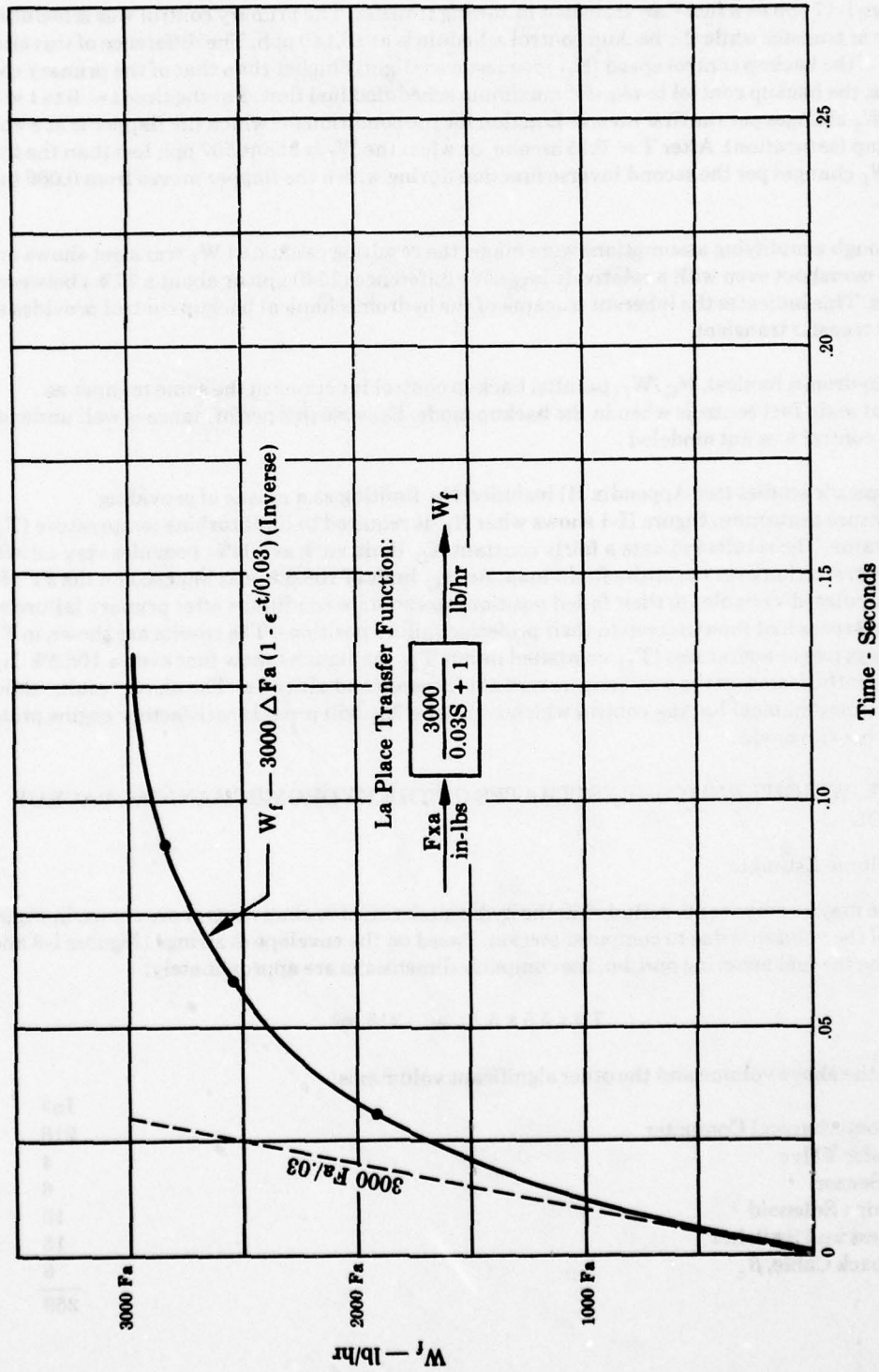


Figure I-15 - Fuel Flow Response To A Step Torque Input Not Causing Flapper Saturation.

Figure I-16 is a plot of this inverse. This shows that a W_f error of 507 lb/hr at SLS takeoff conditions would cause the flapper to be 0.006 inch open.

Figure I-17 shows a fuel flow transient following transfer. The primary control was scheduling 13,600 lb/hr at transfer while the backup control schedule is at 16,140 pph. The difference of this size could occur if the backup control speed (N_G) request was slightly higher than that of the primary control which causes the backup control to request maximum scheduled fuel flow. For the time $t = 0$ to $t = 0.15$ second the W_f changes per the first inverse function for the condition for which the flapper is at a constant 0.006 inch gap (saturation). After $T = 0.15$ second, or when the W_f is about 507 pph less than the final value, the W_f changes per the second inverse function during which the flapper moves from 0.006 inch to 0.0033 inch.

Although simplifying assumptions were made, the resulting estimated W_f transient shows no tendency to overshoot even with a relatively large W_f difference (2540 pph or about a 17%) between the two controls. This indicates the inherent tracking of the hydromechanical backup control provides a satisfactory transfer transient.

The hydromechanical, N_G/W_f , parallel backup control functions in the same manner as conventional main fuel controls when in the backup mode. Because this performance is well understood, this backup control was not modeled.

Parametric studies (see Appendix H) included N_G limiting as a means of providing overtemperature protection. Figure H-1 shows what N_G is required to limit turbine temperature (T_{41}) to a constant value. The results indicate a fairly constant N_G limit, such as 104%, provides very satisfactory temperature protection over the entire flight map. An N_G limit of 108.5% was imposed on the JTDE with the nonmanipulated variables in their failed positions to simulate conditions after primary failure when the fail-fixed servos had time to creep to their preferred failure positions. The results are shown in Figure H-13. The negative temperatures (T_{41} computed minus T_{41} maximum) show that even a 108.5% N_G limit significantly decreases the overtemperature at all speeds and altitudes. The above results indicate that this hydromechanical backup control which schedules N_G will provide satisfactory engine protection while in the backup mode.

5. VOLUME, WEIGHT AND COST ESTIMATES OF THE HYDROMECHANICAL BACKUP CONTROL

a. Volume Estimate

The major components included in the hydromechanical backup control are shown in Figure I-10. Most of the volume is due to computer section. Based on the envelope drawings (Figures I-8 and I-9) which include the fuel metering portion, the computer dimensions are approximately:

$$7.6 \times 5.5 \times 5.2 = 218 \text{ in}^3$$

The total of the above volume and the other significant volumes is:

	In ³
Hydromechanical Computer	218
Transfer Valve	4
T _{2.5} Sensor	6
Latching Solenoid	10
Harness and Switches	15
Feedback Cable, β_c	6
	259

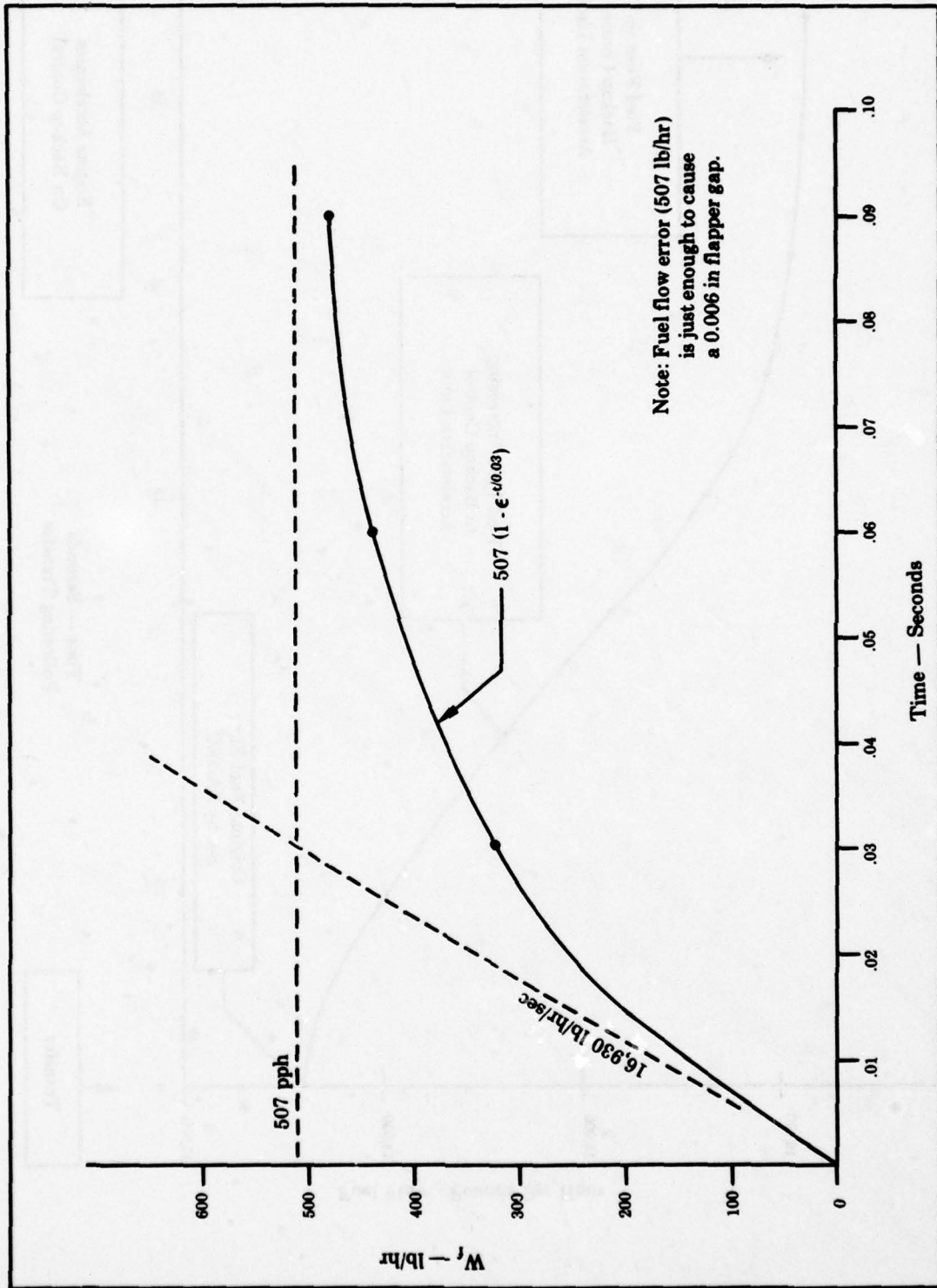


Figure I-16 - Response While Flapper Is Closing — Simplified Case (Unsatuated).

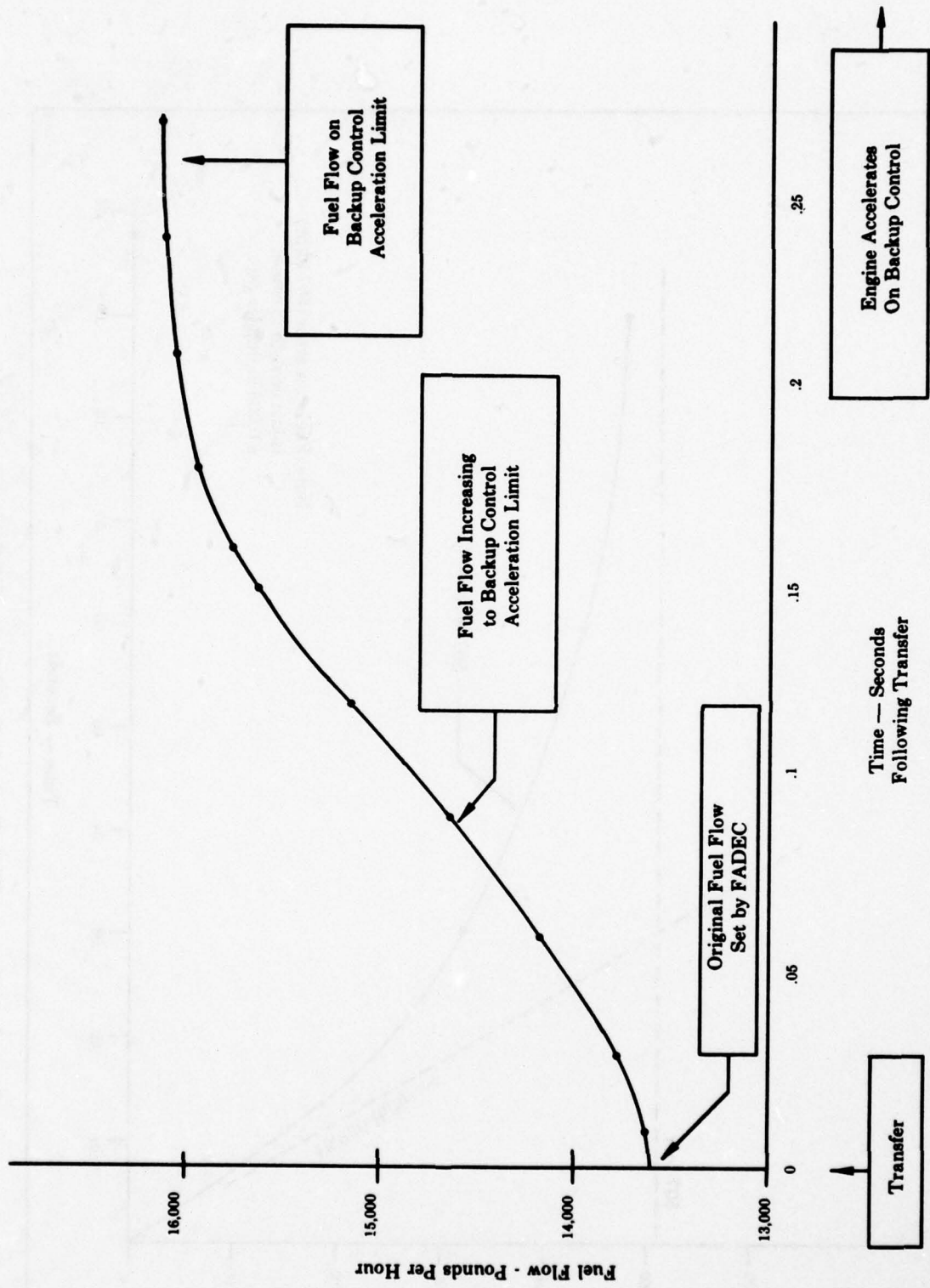


Figure I-17 - Fuel Flow Transient Upon Transfer From FADEC to Hydromechanical Control.

b. Weight

The computer weight estimate was based on the J85-21 main fuel control. The present weight is 15.5 lbs. From this was subtracted the weight of the metering, bypass, and shutoff valves and required housing. To this was added the weight for the overspeed valve and switch and the mounting flange. The result is:

	Lbs.
Present Weight of J85-21 MFC	13.9
Less Weight of Valves and Related Casting	-2.5
Plus Weight of Overspeed Switch, Overspeed Valve, and Mounting Flange	+ 1.0
Computer Weight	<u>12.4</u>

The total of the computer weight and the weight of the other significant components is:

	Lbs.
Hydromechanical Computer	12.4
Transfer Valve	.8
T _{2.5} Sensor, Hydromechanical	1.6
Latching Solenoid	.9
Harness and Switches	2.0
Feedback Cable, β_c	1.5
Miscellaneous Fasteners, Brackets, etc.	1.0
	<u>20.2</u>

c. Cost Estimate

The computer cost was based on the J85-21 main fuel control. The cost was estimated by taking the present cost less the cost of metering, bypass and shutoff valves and related housing plus the cost of the overspeed switch and valve and the mounting flange and input drive. The result, including assembly and test, is:

Present J85-21 MFC Cost	\$10,500
Less Cost of Metering, Bypass and Shutoff Valve Portion	-\$1,550
Plus Cost of Overspeed Switch, Overspeed Valve and Mounting	+ \$250
Computer Cost	<u>\$ 9,200</u>

The total cost is the cost of the computer and the cost of other significant components which is:

Computer Cost	\$9,200
Transfer Valve	700
T _{2.5} Sensor	500
Latching Solenoid	500
Harness and Switches	700
Feedback Cable, β_c	200
	<u>\$11,800</u>

APPENDIX J - HYDROMECHANICAL BACKUP CONTROL HAVING A CORE SPEED SETTING FUNCTION WITH SCHEDULED FUEL FLOW LIMITS IN A SERIES CONFIGURATION

This approach resembles the recommended approach in Appendix I except that it is arranged in a series configuration with the primary control acting as a bias upon the backup control which is in operation at all times. UCR and GHPL estimates were made for this approach as shown on Table J-1. Established main fuel control reliability experience was used as a base value to which was added failure rate estimates for the summing piston and lever assemblies which permit primary control to subtract from the base values set by the backup control. This practice is also shown in Appendix K but for W_f/W_f rather than this N_G/W_f approach. Floor limits upon fuel flow and stator position were also added.

The resulting estimated UCR is similar to the UCR of the recommended approach described in Appendix I. However, there is a significant increase in the estimated GHPL rate because a backup mechanization is used in series with the primary. Therefore, this system was neither recommended nor pursued further.

**TABLE J-1
RELIABILITY SUMMARY FOR THE
BACKUP CONTROL BASED UPON PRESENT MFC PRACTICE —
HYDROMECHANICAL/SERIES/ N_G/W_f SCHEDULED**

	UCR Per 10^6 Hrs.	Get Home Power Loss (GHPL) Per 10^6 Hrs.
Base Reliability (MFC less fuel & β_c valves)	30.0	8.0
Add Summers	8.0	2.00
Sensors, F/B Cable, etc.	19.8	2.0
Add Floor: Servo valve & circuit Cams/ball valves (2) Latches (2)	11.3	2.9
Backup Control Alone	<hr/> 69.1	<hr/> 14.9
FADEC	118.4	40.2
Combination UCR	<hr/> 187.5	
Combination GHPL:		
Backup		14.9
Unprotected Primary Valve Signals		2.0
Total GHPL		<hr/> 16.9

APPENDIX K - COMBINATION ELECTRICAL/HYDROMECHANICAL APPROACH HAVING FUEL FLOW SETTING FUNCTION WITH FUEL RATE LIMITS IN SERIES CONFIGURATION

1. APPROACH

The combination approach is shown schematically by Figure K-1. This approach is based on the W_f/P_{T2} parameter. The backup control acts only on W_f and β_c and its demands are continuously summed with those of the primary control. The operation of the backup control can be discussed in the various modes. During primary mode steady state operation, W_f and β_c are controlled by the fail-fixed servovalves. These servovalves control the summing pistons. In this mode, the backup control outputs, W_f and β_c demand, are essentially fixed and at values above normal. The summing piston motions subtract from the limits set by the backup control and the results are the inputs into the flapper type metering valve servovalve and the spool type β_c servovalve.

During primary mode accel, the PLA cam strokes the spool valve which ports servo pressure to the rate piston. The rate piston moves to the left at a rate determined by the needle valve slot (A_1) and the A_2 port in the primary W_f servovalve. The resulting piston velocity would cause an excessive acceleration and the primary control counteracts this by driving the summing piston in the decrease W_f direction. The same type of action occurs in the β_c control loop. In other words, the backup control stays ahead of the primary control so as to avoid interference.

During a primary mode decel, port A_2 is blocked by a land on the spool valve translated by the PLA cam. The rate piston moves slowly which demands a decel rate slower than any expected on primary control. The primary control decel is satisfied by driving the W_f and β_c summing pistons in the decrease direction. The backup control transiently demands more W_f and more open β_c and the primary control subtracts to achieve the desired response.

Transfer to the backup mode is initiated by applying zero current to the primary W_f and β_c fail-fixed servovalves. The servovalve output flows, with the aid of hydraulic locks, are essentially zero. Servo pressure, P_S , is ported to the summing pistons through small orifices causing the W_f and β_c summing pistons to stroke to their max stops in about 15 to 90 seconds. With the summing pistons on their stops, W_f is about 107% of normal and β_c is about 2 degrees more open than normal. Reset is provided, however. A lever driven by the W_f summing piston unseats a ball valve which ports P_S to a reset piston. The reset piston, linked to the rate piston feedback lever, strokes a predetermined amount having the effect of decreasing PLA. The new rate piston position demands normal W_f and β_c .

During backup mode operation, steady-state W_f is determined by PLA (representing W_f/P_{T2}) and P_{T2} while β_c is determined by PLA only. Desired steady-state W_f is the product of W_f/P_{T2} times P_{T2} so a multiplier is needed. A P_{T2} transducer is used to translate a 3D cam and the rate piston is used to rotate the cam. The cam rise is the desired product ($W_f/P_{T2} \times P_{T2} = W_f$). The rate piston also drives the β_c cam which has the backup schedule as a function of W_f/P_{T2} .

During transients in the backup mode, the desired fuel flow rate, \dot{W}_f , is proportional to W_f level and P_{T2} ($\dot{W}_f = K W_f P_{T2}$). The rate piston velocity is determined by port A_1 in the needle valve driven by the P_{T2} transducer. Port A_2 is blocked by the W_f servovalve in this mode. This results in a rate piston velocity proportional to P_{T2} . The 3D cam has a slope in the rotary direction which is proportional to W_f . The rate piston velocity combined with the cam slope yield the product ($W_f \times P_{T2}$).

A W_f/P_{T2} limit allows too much fuel flow at high Mach number. Overspeed protection is provided by an electrohydraulic servovalve shown and a related electrical circuit. The circuit is similar to that

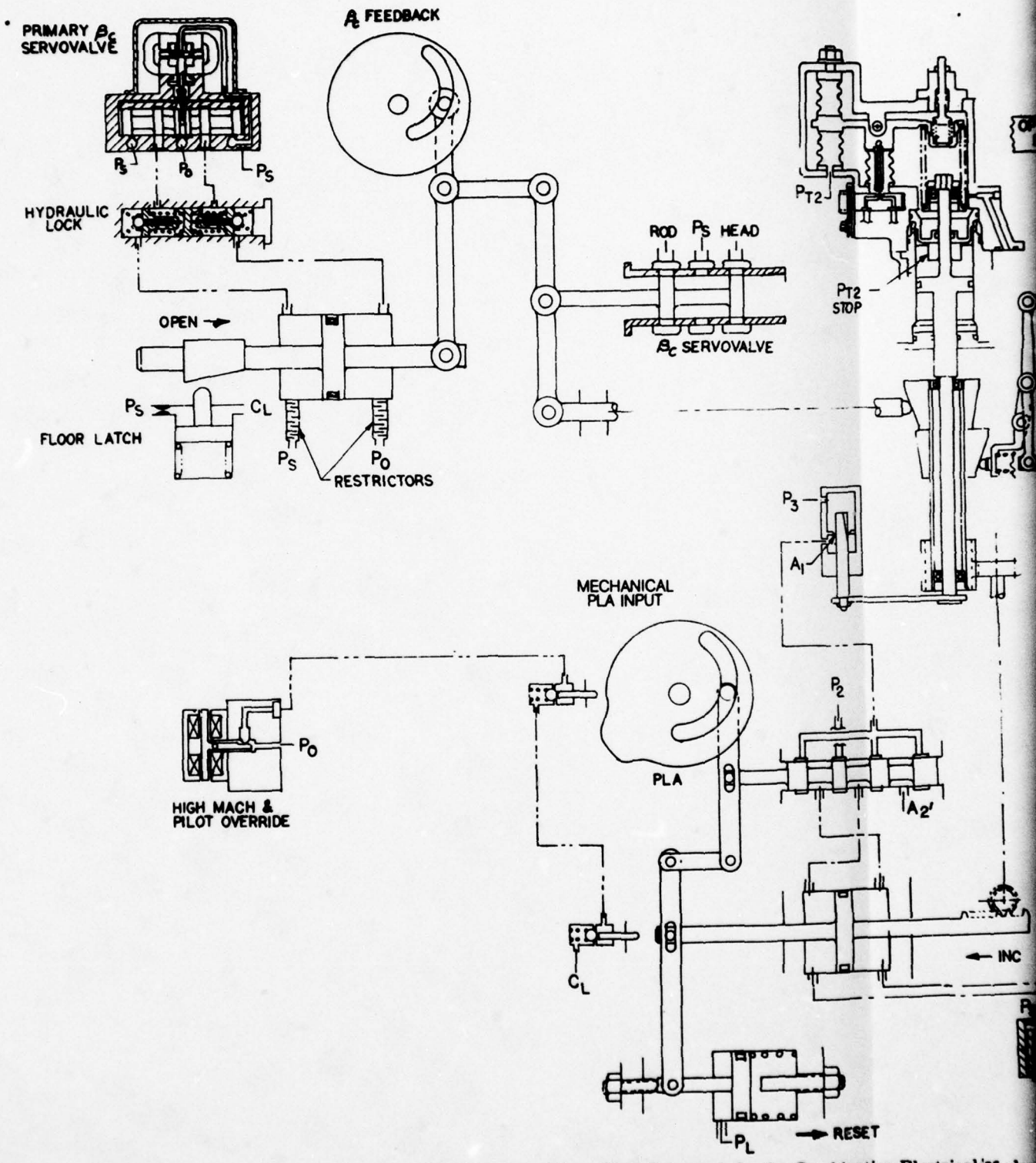
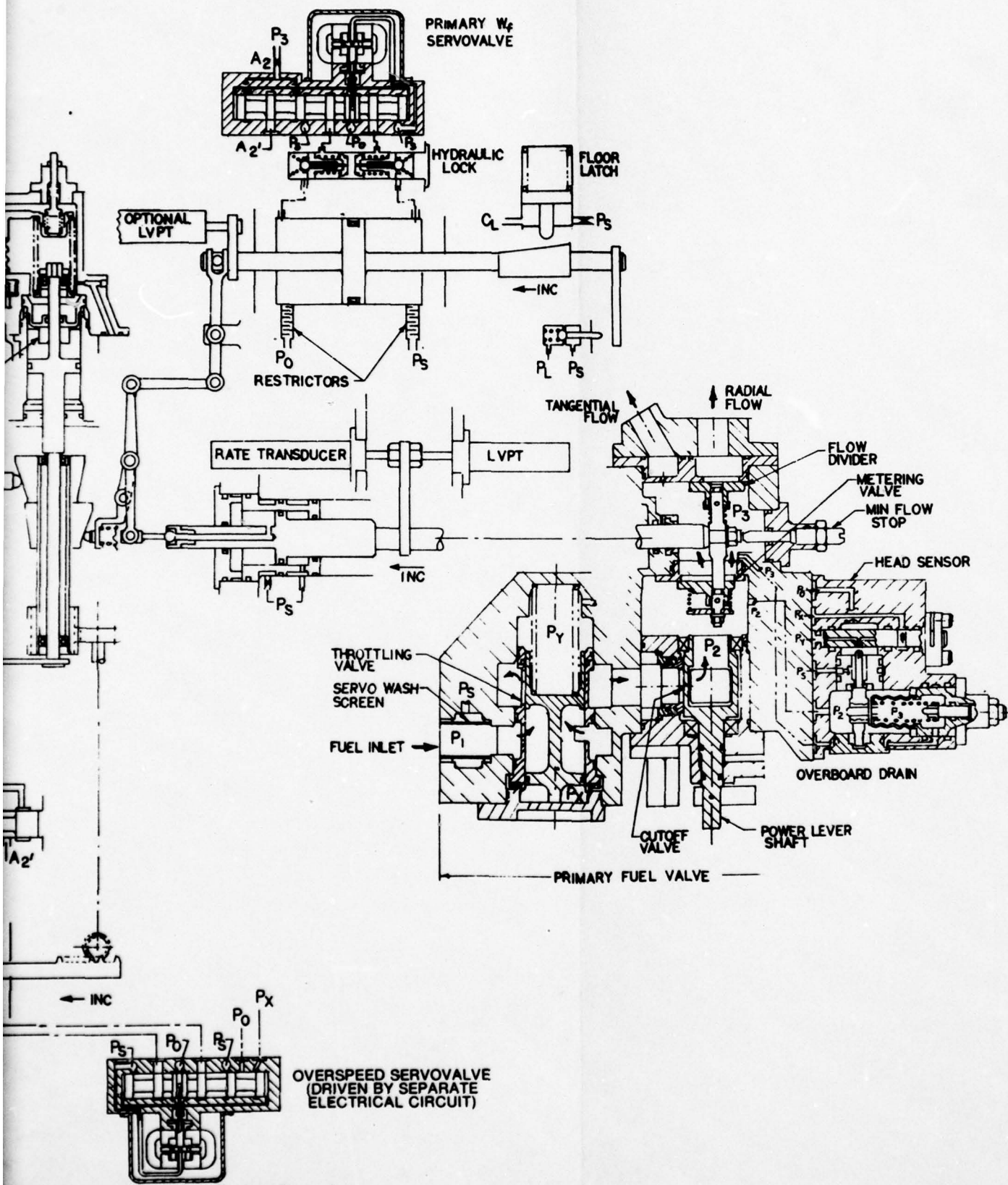


Figure K-1 - Schematic for the Combination Electrical/Hydraulic



Electrical/Hydromechanical Backup Control.

discussed under the electrical approach (Appendix N). The servovalve resets the rate piston so W_f/P_{T2} and β_c demands track. If overspeed increases further, an additional land modulates the throttling valve opening pressure to reduce W_f as required.

The W_f and β_c floors protect against inadvertent closing of the metering valve and stators due to the primary control failure during takeoff. The mechanization shown uses latches to limit summing piston stroke in the decrease direction. These floors would interfere with primary control during accel and decel and also during high Mach number operation. Ball valves are used to keep the latch disengaged at PLA less than 69° and rate piston positions representing PLA less than 69° . This eliminates interference for primary control accel and decel. A floor schedule override servovalve is used to allow removing the floor at high Mach number. The logic is that the two ball valves and the servovalve must be open to allow the latch to act. Pilot authority to remove the floor is also provided by the servovalve. It is intended that the signal to close the override servovalve be from the primary control because it has Mach number intelligence.

Control systems usually provide a compressor discharge pressure (P_{S3}) floor to prevent engine shutdown at high altitudes and part power settings. The summing scheme allows the pilot to decrease W_f in spite of a P_{S3} floor so a P_{T2} stop is used to prevent this. The drawing, Figure K-1, also shows the fuel valve, which is considered a part of the primary control, to aid in defining the interface.

2. PRELIMINARY DESIGN

The preliminary design of the combination backup control is shown by Figures K-2 through K-5. Figure K-2 shows section views of the P_{T2} transducer, the W_f and β_c cams, the W_f summing link, the throttle servo or rate piston, the metering valve servo, the metering valve and the shutoff valve. Figure K-3 shows the relative locations of the P_{T2} transducer, β_c or variable guide vane feedback shaft, the W_f and β_c summing pistons, the PLA or throttle shaft and the β_c and PLA amplifier valves. Figures K-4 and K-5 are external views giving some of the overall dimensions. The intent is to integrate the backup control and the primary fuel valve. This means the metering valve, throttling valve, cutoff valve, etc., are common to both primary and backup controls. In the subsequent comparative analyses, however, the fuel valve is not considered part of the backup control.

3. RELIABILITY ANALYSES

a. Analytical Procedure and Tools

To aid in the process of determining reliability and failure effects, a Reliability Analysis Program (RAP) was used. RAP is an automated method of reliability analysis at General Electric used to check or predict a component's inherent reliability before actual hardware is available for test. To use this method, all basic elements of the component are identified and certain design parameters are calculated for each element. In addition each element failure process is traced to its component failure effects. Normally, this information is inputted to a computer program which calculates modifiers for standard failure rates and categorizes the failure effects. In order to shorten the procedure involving computer inputs, the computer program modifier equations were used directly to hand-calculate failure rates. System and engine failure effects and reliability indices were traced for each element.

To aid in defining the hydromechanical RAP elements, the system was divided into basic subassemblies as shown in Figure K-6. In all, the analysis included some 415 hydromechanical elements. The P_{T2} transducer, being similar to that used on the F101 Augmentor Fuel Control, had already been analyzed and could be altered simply with respect to its failure effects; it included some 54 elements. In order to determine failure rate modifiers where sufficient material, dimensional, or loading information

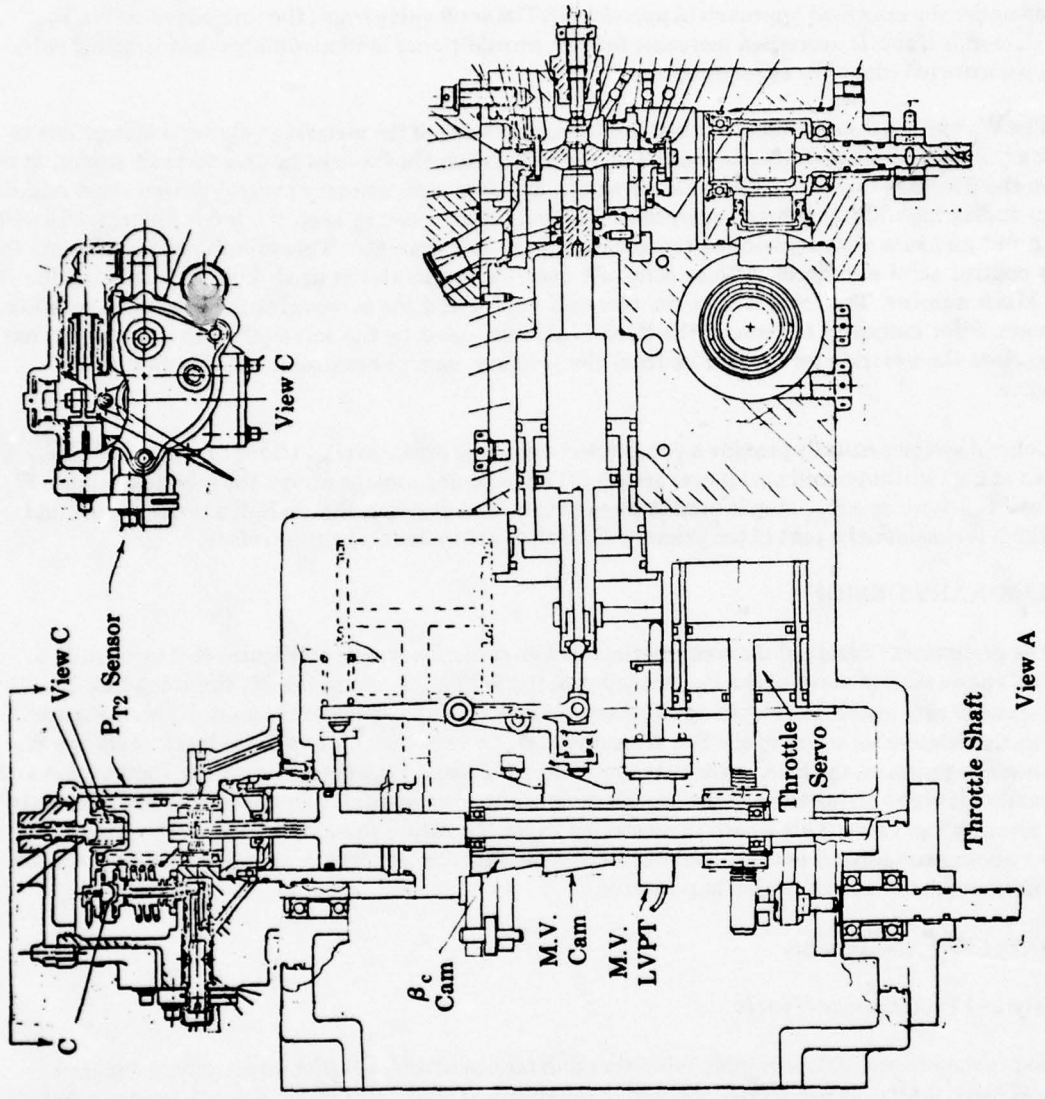
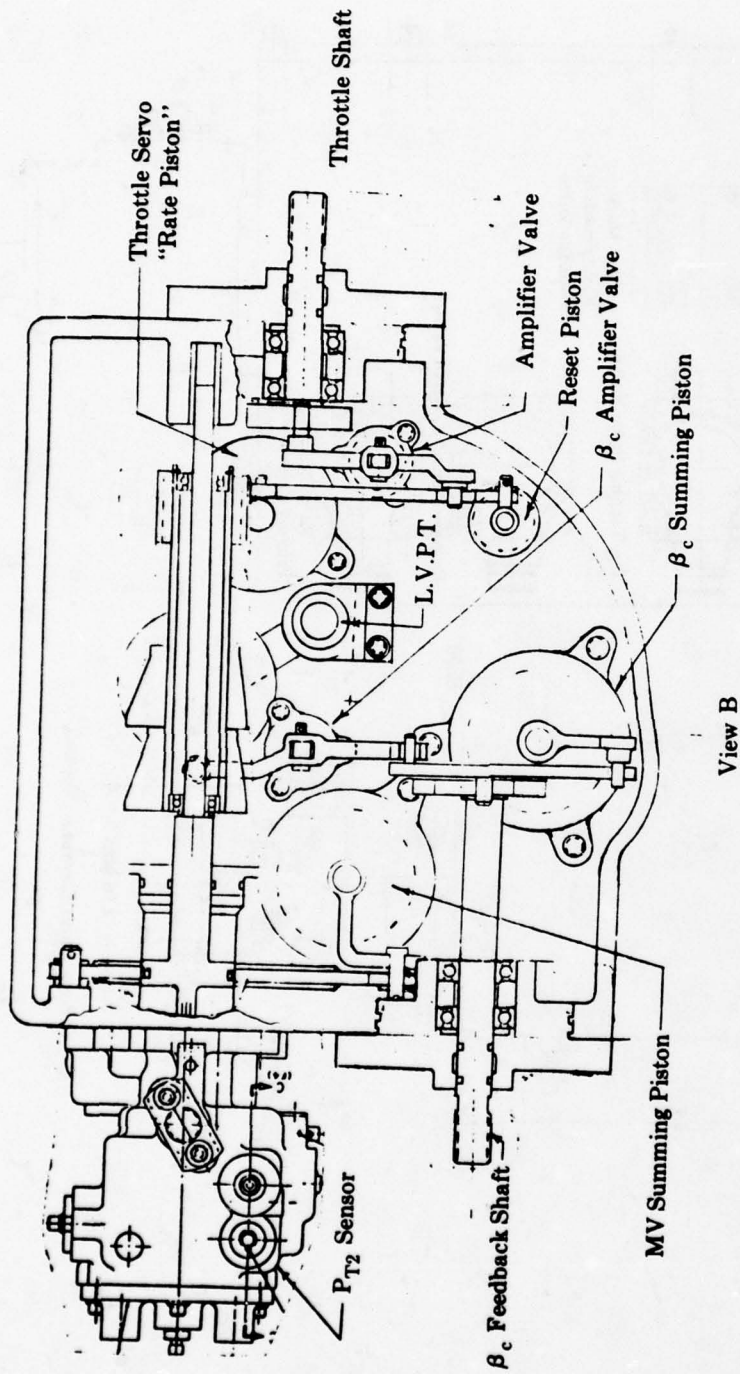
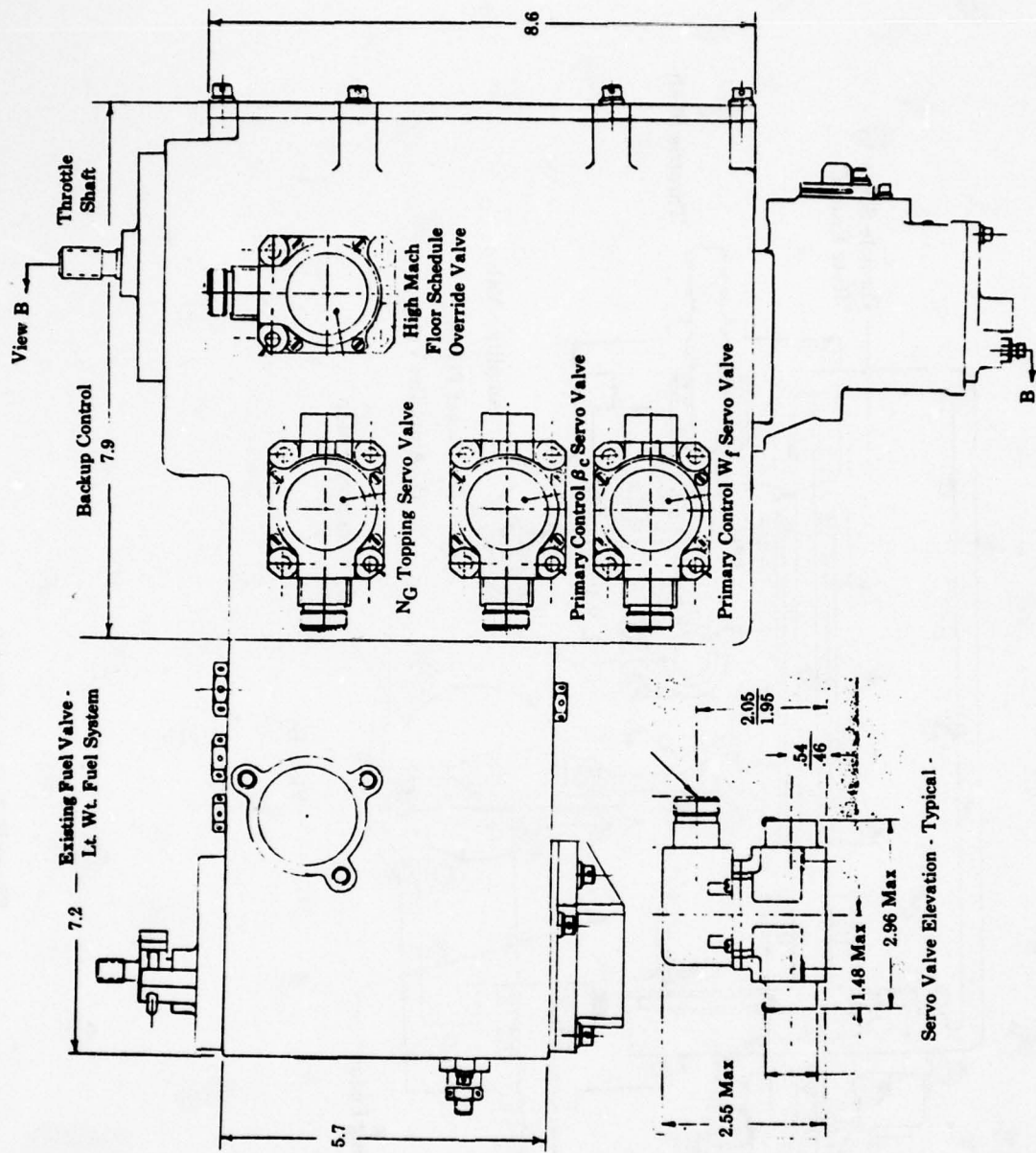


Figure K-2 - Section View A.



View B

Figure K-3 - Section View B.



Servo Valve Elevation - Typical -

Figure K-4 - Top View.

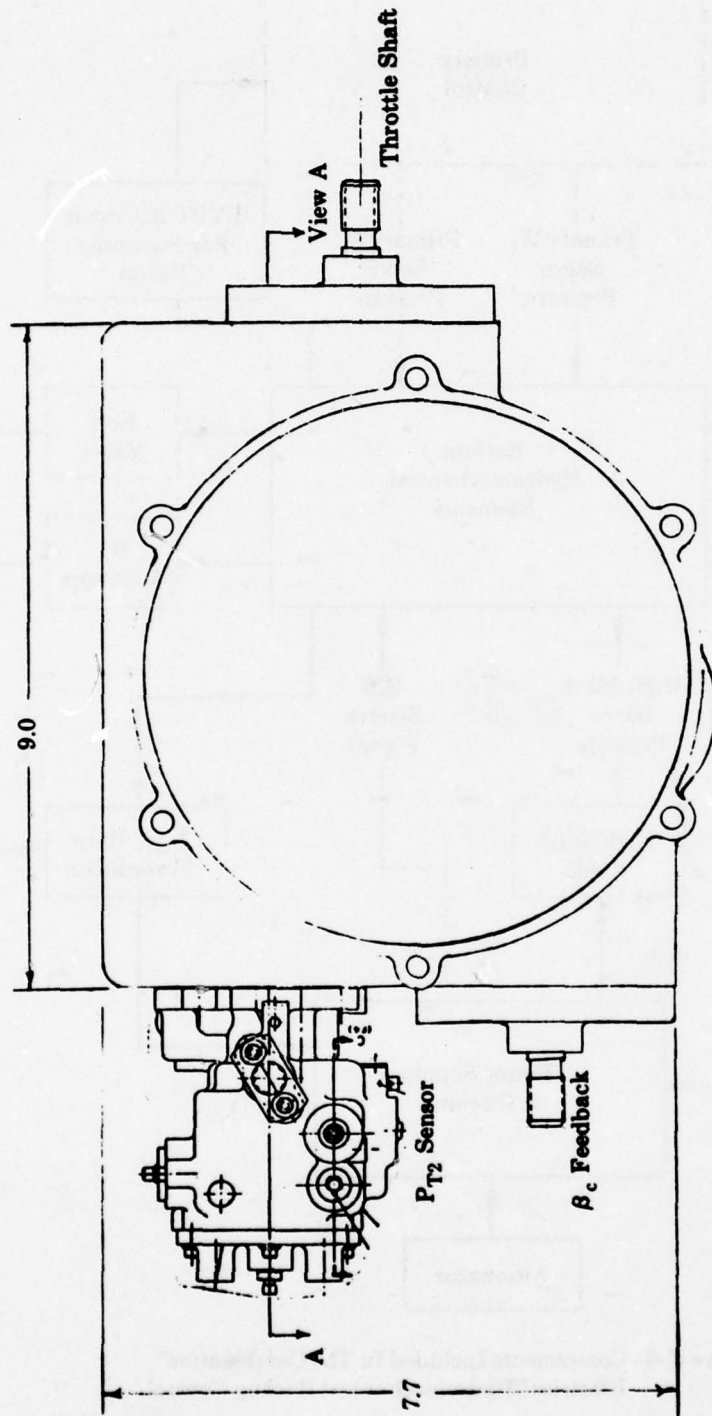


Figure K-5 - End View.

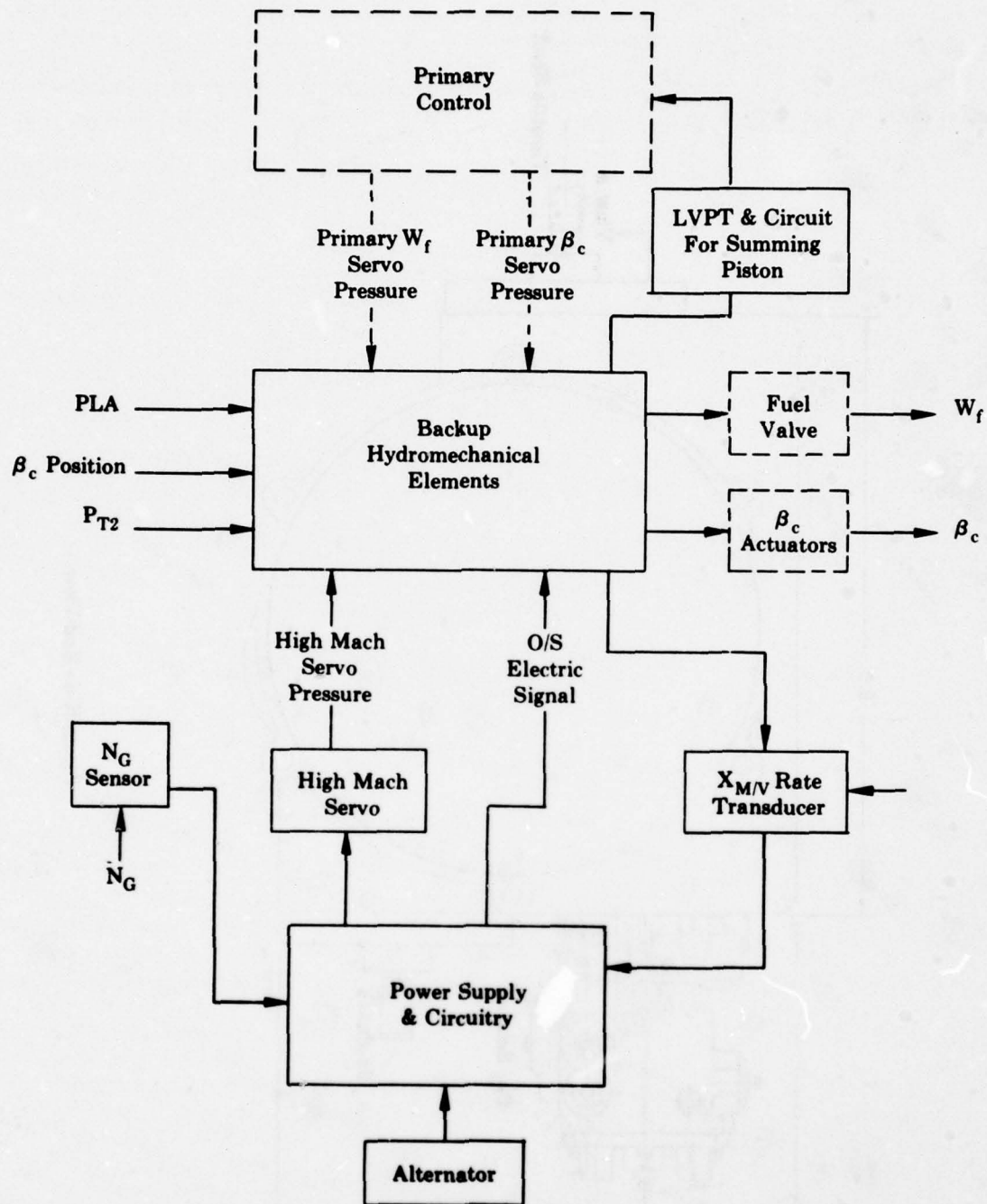


Figure K-6 - Components Included In The Combination Electrical/Hydromechanical Backup Control.

was lacking, comparable elements' modifiers from CF6 or F101 engine control RAP analyses were assumed. Thus a significant level of built-in design reliability experience is incorporated in this analysis. Resulting special features assumed are discussed under analysis results.

Electrical components in the hydromechanical approach were treated in a manner similar to that used for the primary engine electronic control system, envisioned for the JTDE program variable cycle engine. This consists primarily of utilizing MIL-HDBK-217B, "Military Standardization Handbook Reliability Prediction of Electronic Equipment". In addition, reference was made to failure rates of several electrical components included in the items capable of being analyzed by the RAP method such as the linear variable differential transformers (LVDT's).

In order to reason through the path from an elements failure process to system and engine failure effects and finally to reliability indices such as Unscheduled Component Removal (UCR) and Get Home Power Loss (GHPL), certain assumptions were made. The resulting failure rates were to be applicable to the unfailed case, where the primary control is in normal operation. A UCR could thus result from two instances: as a result of a preflight ground check of the backup control alone or as result of what the pilot observes during normal flight. Assumptions used in UCR determination were as follows:

- (1) If any failure causes the fuel flow summing piston to hit its max stop, a UCR occurs.
- (2) If a reduction in power could occur only during an accel or a decel, it is the same as happening at any time.
- (3) If a floor latch engages at the wrong conditions, a UCR occurs.
- (4) If the primary control must compensate for a backup control failure, e.g. a leak, with a steady state error signal, a UCR occurs.
- (5) If the primary control is prevented from subtracting from the backup control demand, no power loss occurs.
- (6) Floor latch springs are designed such that a seal leak will not reduce pressure enough to let the spring engage the latch.

b. Analysis Results

Table K-1 shows a list of the majority of the hydromechanical and electrical elements' failure rates which comprise the combination approach. They are listed beginning with those types of components which as a group contribute the most to the total failure rate. The single part column shows the average failure rate for say a single link, unmodified by possible improvements or inadequacies that may exist in the design. The total part column shows the total failure rate results for say all the links used, after their rates have been modified by each part's specific design or environment. It should not be assumed that all of a certain type of element have the same failure rate. Where information was available, elements were individually analyzed. Also shown are some typical failure rates of similar elements in the CF6-6 main engine fuel control.

Table K-2 shows a list of resulting engine effects and total reliability indices for those hydromechanical elements in the hydromechanical backup approach, which were analyzed together as a unit. Table K-3 shows a UCR and GHPL reliability list of all components associated with the hydromechanical approach of the backup control.

Key to the comparatively low failure rate for the hydromechanical backup control is the planned use of a 10 micron (μ) system servo filter. Also contributing to low failure rate modifiers are the following features assumed because of their appearance in the CF6 control:

- (1) All spool valves pulsate. (3) Cable telescopes cannot coke.
 (2) Cams use rolling contact. (4) Bearing inner race fit is non-interference.

TABLE K-1
 COMBINATION ELECTRICAL/HYDROMECHANICAL BACKUP
 CONTROL ELEMENT FAILURE RATES PER 10⁶ HOURS

Element or Component	Qty.	Single Part Unmodified Failure Rate	Total Part Modified Failure Rate	Single Part Failure Rate For Typical CF6 Element
P _{T2} Transducer	1	-	30.655	-
Threaded Joints	39	0.5	14.017	0.1 to 0.2
O-Ring, Static	49	0.55	10.686	0.225
Piston and Cylinder	9	1.92	8.689	1.2
*Electric Harness	1	-	8.0	-
O-Ring, Reciprocating	16	1.0	7.726	-
Cam and Follower	4	4.0	6.842	1.5
*Electric Power Source	1	-	5.0	-
*N _G Sensor	1	-	5.0	-
Bearing, Ball, Oscill.	7	2.6	3.892	0.1 to 0.5
*LVDT & Circuit	1	-	2.219	-
*LVPT & Circuit	1	-	2.10	-
*High Mach Servo	1	-	2.072	-
Gear, Light Load	2	2.0	1.985	0.7
Pin, Pivot	9	0.4	1.959	0.2
Threaded Inserts	39	0.15	1.886	0.05
Valve and Seat	7	0.3	1.750	-
O-Ring, Oscillating	4	1.0	1.624	0.33
O/S Servo Circuit	1	-	1.52	-
Spline	1	0.5	1.203	0.3 to 3.0
Link	12	0.4	0.905	0. to 0.15
Valve, Spool and Sleeve	3	6.3	0.654	0.1 to 0.2
Cable	1	1.1	0.55	0.55
Ball	3	0.4	0.480	0.16
Jet Pipe and Receiver	1	7.1	0.418	-
Bushing	1	0.4	0.40	0.4
Uniballs	2	0.5	0.376	0.5
Housing	1	0.5	0.320	0.3
Orifice	12	5.0	0.303	0.1-up
Rod & Guide	1	0.9	0.288	-
Pin & Slot	2	1.0	0.236	-
Braze Joints	3	0.1	0.21	-
Cover/Cap	8	0.09	0.20	0. to 0.04
Flapper/Orifice	1	5.7	0.194	-
Shaft	6	0.4	0.122	0.003 to 0.125
Spring, Seat	13	0.2	0.104	0.002
Telescopic Tube	2	1.0	0.098	-
Ratchet	2	0.8	0.086	-
Screen	18	0.7	0.002	-
Drilled Passage	43	0.1	0.	-

*Considered electrical elements

**TABLE K-2
COMBINATION BACKUP CONTROL RELIABILITY SUMMARY***

<u>Engine Effect</u>	<u>Accompanying Indices</u>	<u>Failure Rate/10⁶ Hours</u>
No Effect	DAO	58.68
No Effect	UCR	12.99
Slow Accel & Decel	DAO	1.72
Slow Accel & Decel	UCR	2.26
Slow Accel & Decel	UCR & GHPL	0.12
N _G Unstable	UCR	0.36
Excess W _f	UCR	8.78
β _c Off Schedule	UCR	2.82
β _c Off Schedule	UCR & GHPL	3.40
Reduced Power	UCR	0.88
Get Home Power Loss	UCR & GHPL	6.11
Totals: Discover at Overhaul (DAO)		60.4
Unscheduled Component Removal (UCR)		37.7
Get Home Power Loss (GHPL)		9.7

*Includes only hydromechanical elements

**TABLE K-3
TOTAL COMBINATION BACKUP CONTROL CONFIGURATION RELIABILITY**

<u>Components</u>	<u>UCR/10⁶ Hrs.</u>	<u>GHPL/10⁶ Hrs.</u>
Hydromechanical Components	37.7	9.7
Power Source	5.0	2.0
N _G Sensor	5.0	2.0
Power Supply (ACE 338)	0.27	0.045
Rate Transducer for Metering Valve	1.85	0.46
Rate Circuit	0.37	0.09
Overspeed Servo Driver & Processor	0.66	0.11
LVPT for Summing Piston	1.9	0.48
LVPT Circuit	0.30	0.05
Harness (24 wires, 10 connectors)	8.0	1.5
High Mach Servo	1.75	1.1
High Mach Servo Circuit	0.48	0.08
Total	62.96	17.62
FADEC	118.4	40.2
Combination UCR	181.4	
Combination GHPL:		
Backup Control		17.62
Unprotected Primary Valve Signals		2.0
Total GHPL		19.62

Failures pertinent to power loss are those which cause backup fuel flow or stator angle demand to be so low that the primary control cannot compensate, thus losing get home capability. The primary control can usually compensate for an extra large backup demand by subtracting, but it cannot add much when the backup demand is low. There was considerable judgement involved. Table K-4 shows a list of

most of the hydromechanical elements which contribute to backup control power loss, in order of failure rate contribution. Listed below are examples of the reasoning that produced this table:

- (1) P_{T2} transducer: A constant erroneous P_{T2} signal results in low fuel flow demand at higher P_{T2} levels. Possible causes are bellows rupture, spring failures, etc.
- (2) P_{T2} piston and cylinder: Modified failure rate, $1.87/10^6$ hours at null to low P_{T2} positions. Modifiers were high, primarily due to a poor force ratio. This piston may stick in a low P_{T2} position due to silting, fouling, coking or cocking.
- (3) Link pivot pins between amplifier valve and rate piston: Modified failure rate, $0.351/10^6$ hours for wear, with a modifier of 0.067. Modified failure rate, $0.225/10^6$ hours for change of position failure; modifier 0.75. Failure of any of these pins causes loss of feedback communication from the rate piston and eventually an erroneous min backup W_f demand.
- (4) β_c feedback cam and follower:
 - Wear adhesion nominal FR, $0.3/10^6$ hours; modifier 1.0
 - Wear abrasion nominal FR, $2.7/10^6$ hours; modifier 0.337
 - Foul nominal FR, $0.5/10^6$ hours; modifier 0.002
 - Change position nominal FR, $0.5/10^6$ hours; modifier 1.0

Assume 25% of wear cases, 50% of change position cases cause excessively closed β_c .
- (5) β_c feedback cable: Binding failure rate $0.090/10^6$ hours. Fracture failure rate $0.35/10^6$ hours. Both failures cause loss of β_c feedback eventually resulting in excessively low backup β_c demand.
- (6) A_1 orifice: Only failure mode is by fouling. Nominal FR is $5.0/10^6$ hours, modifier, 0.0212. Fouling of A_1 orifice would cause sluggish accel in backup demand. Assume 50% of cases are not severe.

The total hydromechanical approach backup control GHPL estimate is considered low because not all primary control GHPL failures are protected against. For example, the primary control fuel flow servo-valve may stick in the low flow position without backup compensation. On-schedule performance of the backup control alone requires the primary control to be in its desired failed position.

TABLE K-4
HYDROMECHANICAL ELEMENTS OF THE COMBINATION BACKUP CONTROL APPROACH
WHICH CONTRIBUTE TO GET HOME POWER LOSS

Element	GHPL/ 10^6 Hrs.	Element	GHPL/ 10^6 Hrs.
P_{T2} Transducer	3.40	PLA Input Gear	0.2
P_{T2} Piston & Cylinder	1.87	Rate Piston Rack & Pinion	0.2
Amplifier Valve to Rate Piston		β_c Feedback Link	0.2
Links Pivot Pins	0.58	A_1 Orifice Rod & Guide	0.2
β_c Feedback Cam & Follower	0.55	Amplifier Valve to Rate Piston Links	0.15
β_c Feedback Cable	0.44	Flapper Orifice	0.15
PLA Cam & Follower	0.43	β_c Valve, Spool & Sleeve	0.12
W_f Cam & Follower	0.43	Amplifier Valve, Spool & Sleeve	0.09
W_f Summing Links	0.24	A_1 Orifice	0.05
W_f Summing Links Pivot Pins	0.24		
Rate Piston & Cylinder	0.22		
		Total	9.76

4. ESTIMATED PERFORMANCE

a. Background

Since a complete JTDE hybrid model was not available at the time of this study, the F101 engine model was used to evaluate and estimate the combination backup control performance. Both steady-state and transient F101 cycle data were readily available to facilitate fashioning the backup W_f and β_c schedules. In addition, the backup control model could be combined easily with an existing hybrid model of the F101 engine and control in order to determine its control capabilities.

b. Steady-State Performance

The backup control model PLA versus W_f/P_{T2} linear schedule was based on some 42 steady-state F101 Product Verification engine subsonic cycle data points. Figure K-7 shows that the selection backup limit will schedule fuel flow higher than the primary control at almost all plotted flight conditions which represent Mach number ranges from 0 to 0.85 at ground levels and altitudes up to 55,000 feet with speeds to Mach 0.95. Not all PLA settings are represented at each flight condition. Selection of this schedule for this study was made as a compromise of steady-state fuel flow magnitude and transient accel times. It will be seen that the selected range of W_f/P_{T2} settings does affect accel times if the fuel flow rate is proportional to P_{T2} and fuel flow level ($W_f = K \times P_{T2} \times W_f$) mode is used since the W_f can be changed by altering the solution constants.

Using the same F101 data, a backup control β_c schedule as a function of W_f/P_{T2} was prepared. Figure K-8 shows that the β_c schedule would be more accurate if it is varied as a function of P_{T2} . Figure K-9 shows the resulting backup schedule found using a polynomial fit procedure. During primary mode operation, this schedule would need to be shifted 2 degrees open to avoid interference.

The accuracy of W_f/P_{T2} and β_c reset using the rate piston will have a large effect on steady-state performance in the backup mode. However, it can be shown that this form of reset is limited in accuracy, i.e. how close to nominal scheduling can be achieved. This will be demonstrated by an example. In order to satisfy transient requirements (details will be described in a following section), the following equation was derived:

$$W_f/P_{T2} = [9.22e^{-.3626} X_{RP}]^2$$

The typical equation used to describe the backup stator schedule was:

$$\beta_c = C_3 (W_f/P_{T2})^3 + C_2 (W_f/P_{T2})^2 + C_1 (W_f/P_{T2}) + C_0$$

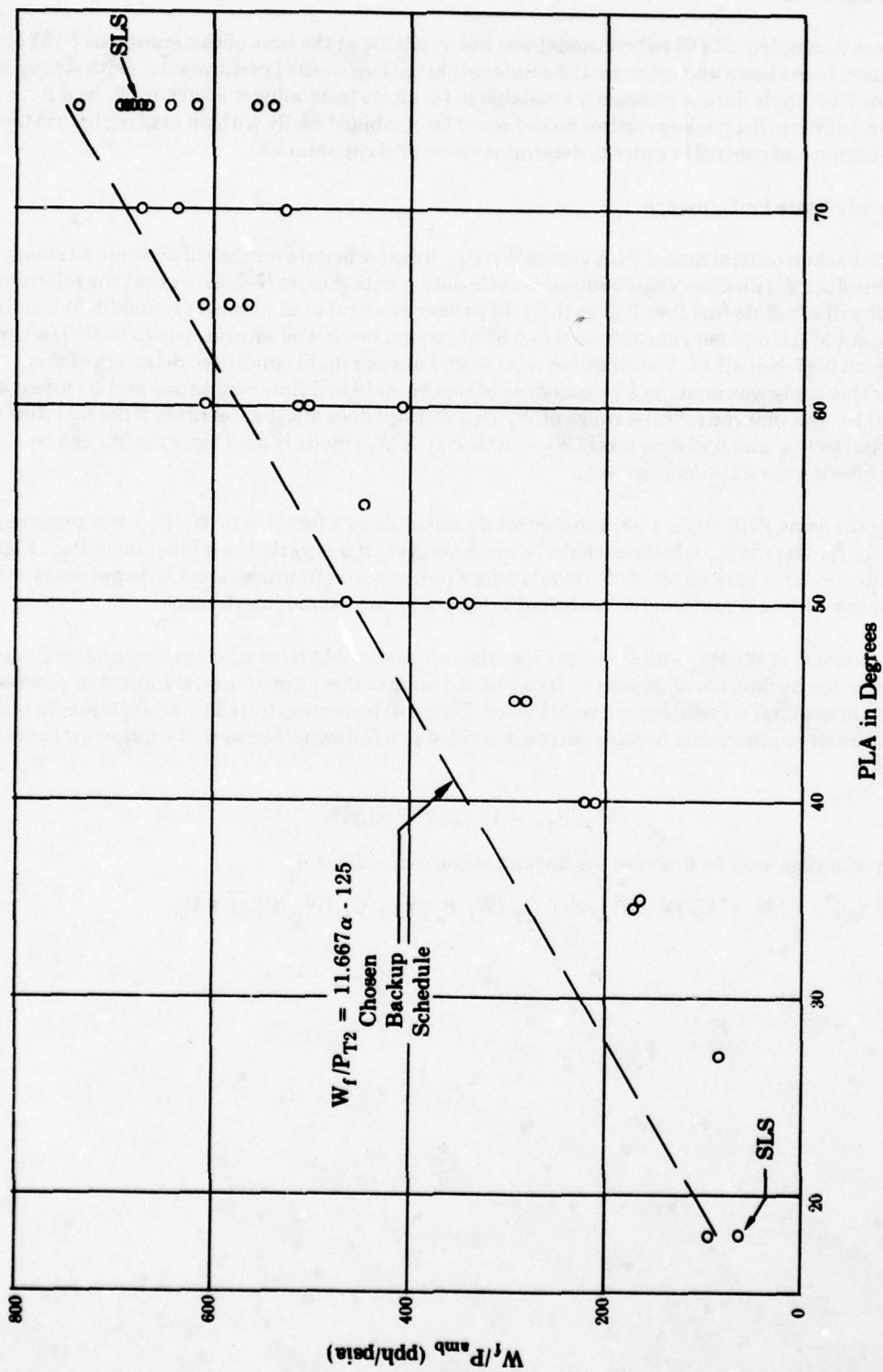


Figure K-7 - W_f/P_{amb} Vs PLA From F101 PV Cycle Data.

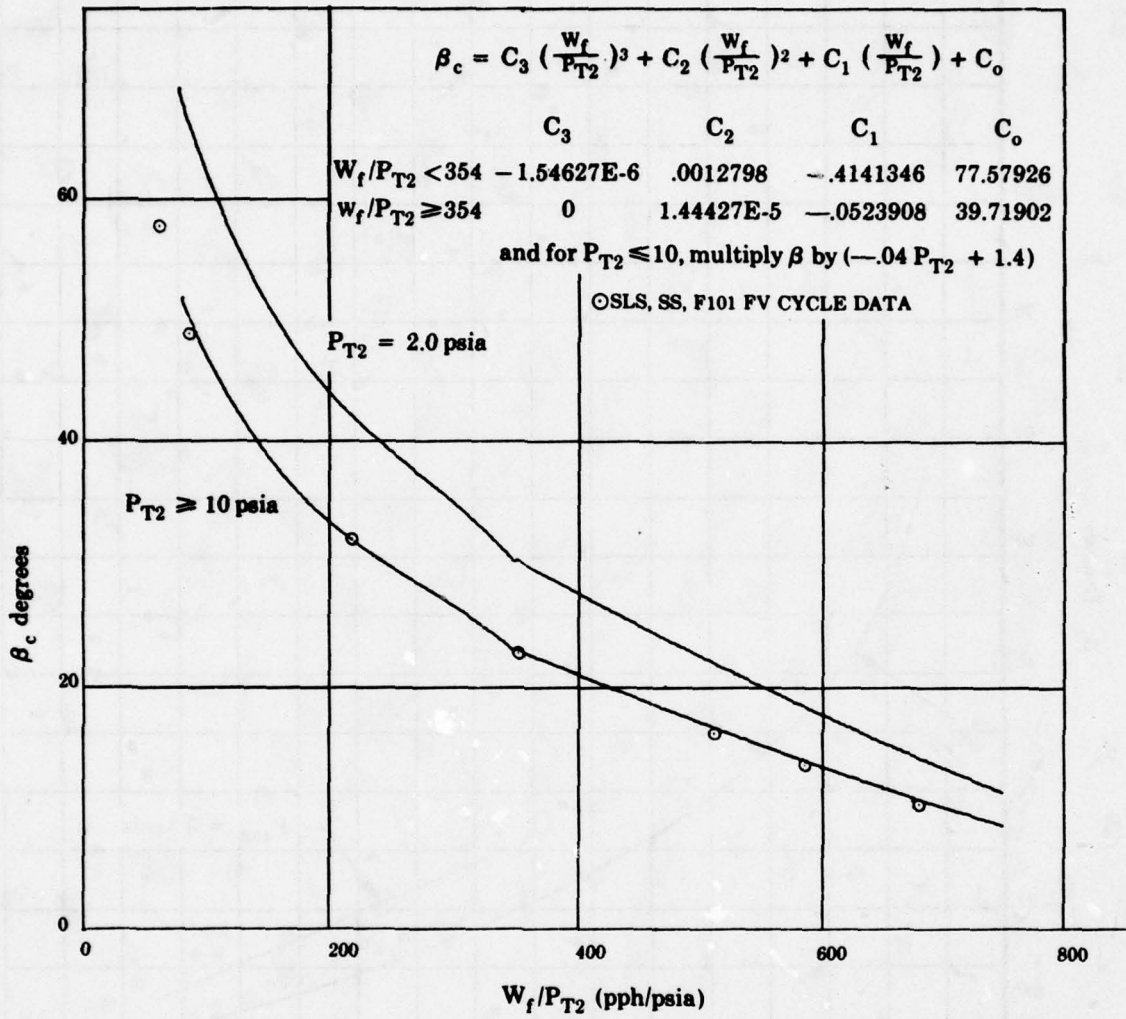


Figure K-8 - Backup Control β_c Vs. W_f/P_{T2} Schedule.

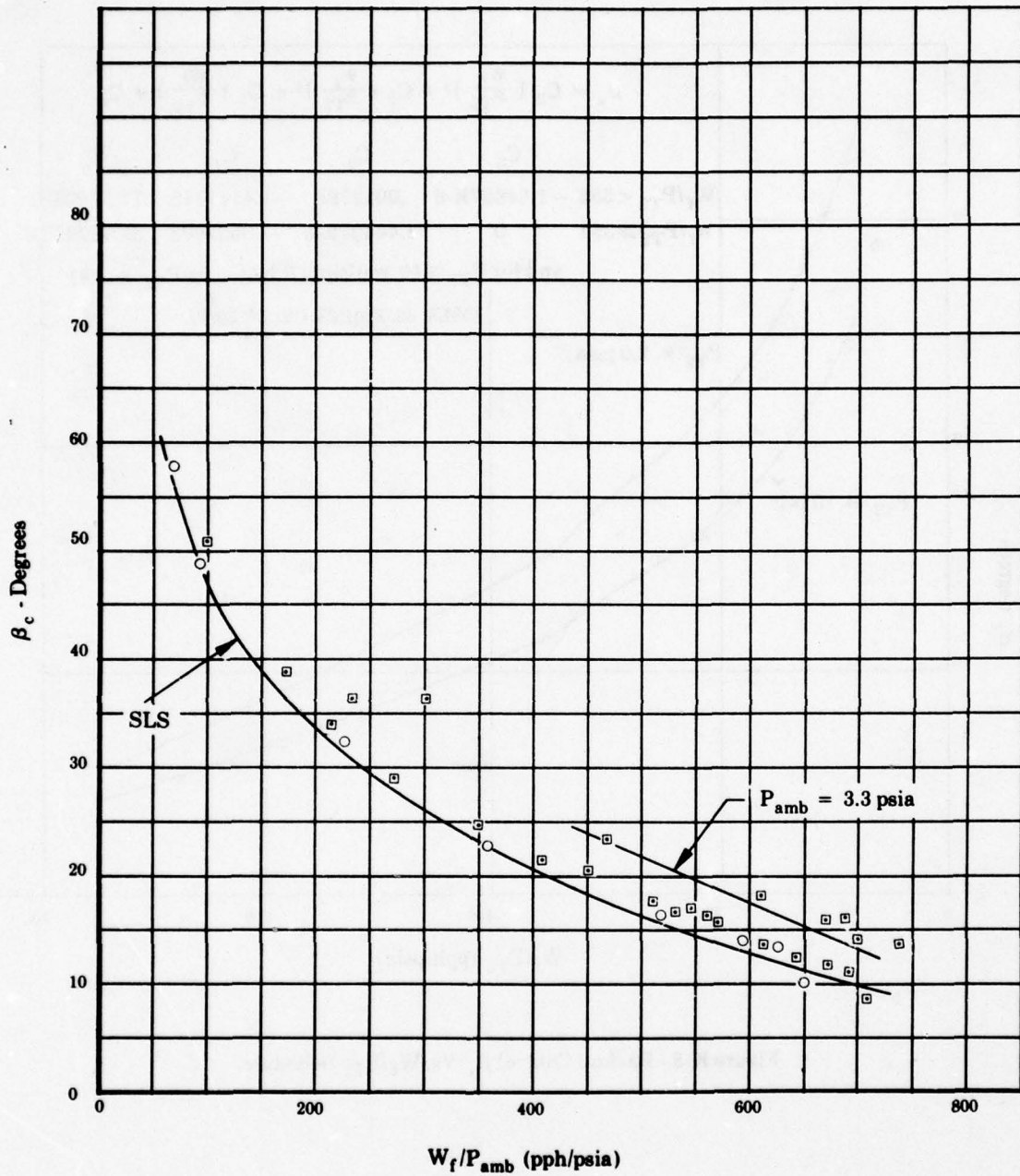


Figure K-9 - W_f/P_{amb} Vs. β_c F101 PV Cycle Data, Steady-State Conditions.

Derivatives of these equations are:

$$\frac{d(W_f/P_{T2})}{d(X_{RP})} = 61.648 \epsilon^{.7252} X_{RP}$$

$$\frac{d(\beta_c)}{d(X_{RP})} = \frac{d(\beta_c)}{d(W_f/P_{T2})} \times \frac{d(W_f/P_{T2})}{d(X_{RP})}$$

$$= [3C_3 (W_f/P_{T2})^2 + 2C_2 (W_f/P_{T2}) + C_1] \times 61.648 \epsilon^{.7252} X_{RP}$$

Using the positions at $X_{RP} = 0, 3$, the following values are calculated:

	$X_{RP} = 0$	$X_{RP} = 3$
$d(W_f/P_{T2})/d(X_{RP})$	61.648	542.96
$d(\beta_c)/d(X_{RP})$	-14.184	-16.68

It can be seen that a given X_{RP} reset will change W_f/P_2 and β_c different amounts depending on the X_{RP} position. In the above chosen backup schedules, for example, a reset of 0.129 inch is required to decrease demanded W_f/P_{T2} at $X_{RP} = 3$ from 750 to the desired F101 value of 680 at SLS. Consequently, this amount of reset would decrease demanded W_f/P_{T2} at $X_{RP} = 0$ from 85 to 77, whereas the desired F101 value at SLS is 61. The point is that the selection of the steady-state schedules must be based on a need to both schedule fuel flow high and stators more open than the primary control at all PLA's and applicable flight conditions in the primary mode, compromised with a knowledge of how a given reset modified the schedules for good backup mode accuracy. Thus, the requirements of the backup control strictly scheduling W_f at 107% above normal and β_c at 2 degrees more open than normal, may not necessarily yield the most accurate results.

c. Transient Performance

(1) Mathematic Description of Rate Relationships

It has been shown that for modelling of backup control rate relationships to describe the F101 accels, the fuel flow rate (\dot{W}_f) should be proportional to P_{T2} and fuel flow level ($\dot{W}_f = K X P_{T2} X W_f$). From examining F101 accels at several values of P_{T2} , the numerical expression necessary to describe it was found to be:

$$\frac{\dot{W}_f}{W_f} = \frac{P_{T2}}{37.5} \quad \text{or} \quad \frac{\dot{X}_{BU}}{X_{BU}} = \frac{P_{T2}}{75}$$

The solution of this differential equation is, $X_{BU} = C \epsilon^{(P_{T2} t/75)}$

Using the steady-state equations, $W_f = 17400 (2X_{BU})^2$

$$W_f/P_{T2} = 11.667 \alpha - 125$$

and the initial conditions, $\alpha = 18$ at $t = 0$,
the constant C becomes,

$$C = 0.03494 \sqrt{P_{T2}}$$

Since the rate piston stroke rate \dot{X}_{RP} is to be proportional to P_{T2} , ie. $X_{RP} = K P_{T2}$ or $X_{RP} = K P_{T2} t$, the fuel flow cam is thus defined as,

$$X_{BU} = 0.034943 \sqrt{P_{T2}} \epsilon^{.3626} X_{RP} \quad (\text{see Figure K-10})$$

and the X_{RP} versus the W_F/P_{T2} relationship is, $W_F/P_F/P_{T2} = (9.22 \epsilon^{.3626} X_{RP})^2$

It can be seen from the above results that accel times are not arbitrary. The rate piston versus P_{T2} relationship has become, $X_{RP} = 0.03677 P_{T2}$. If accel times are to be independently set, as will be done later, this relationship must become nonlinear.

Figure K-11 shows the hydromechanical backup control model block diagram as combined with the F101 engine main control model.

(2) Backup Control Computer Model

Since the most important problems of concern in the backup control performance were associated with the backup mode of operation, the model actually computerized to run with the F101 engine hybrid model was one simulating only the backup mode. Figure K-12 shows the model block diagram. The primary control was entirely disconnected. The W_f and β_c schedules were those associated with operation in the primary mode; thus, a reset of 0.133 inch was used to make backup mode fuel flow demand equal to normal at max dry SLS. Engine exhaust nozzle area was fixed at 700 square inches. Fan stators were fixed at full open.

(3) General Results

Throttle burst accels were made at four flight conditions representing a subsonic P_{T2} range from 4.0 to 23.0 psia. Accel times were set by the area rate factor (K) at 7.5 seconds at all values of P_{T2} at 14.7 psia or above, 12 seconds at P_{T2} of 9.37 psia, and 20 seconds at P_{T2} of 4.0 psia measured to where fuel flow rate (\dot{W}_f) peaks out. Figure K-13 shows plots of fuel flow rate versus fuel flow for three of these runs.

Figures K-14 thru K-17 show copies of the strip chart recordings of typical backup control computer model throttle burst runs. It may be noted that core speed exceeds its 104% limit of 15,038 rpm. Even though the overspeed governor was not included in the model, overspeed should not normally occur at this flight condition. It was found that the F101 engine cycle hybrid model somewhat predates the Product Verification engine data used to fashion this model's schedules, resulting in higher core speeds for the same fuel flow. Consequently, the $\Delta\beta_c$ stator error used to shift the cycle compressor map was disconnected so that while stators were positioned according to the PV schedule, there would be no stator error effect on the engine cycle. This made stall margin calculations from the engine model irrelevant, but it does not effect our study of backup control stator lead.

(4) Core Stator Lead and Accel Times

Figures K-18 through K-21 show comparisons of steady-state core stator angle with transient core stator angles set by the W_f/P_{T2} backup control, plotted versus percent corrected core speed in the above four accels. Positions where the overspeed governor would normally hold physical core speed to 104% of 14,460 rpm are shown. Maximum stator angle transient lead at SLS is about 5 degrees, but this represents a 5 second accel time imposed on an engine (F101) which has 7.3 seconds on primary control. The intended fighter engine is expected to have a normal primary control accel time of 5 seconds, so the expected β_c lead will be much less because a backup accel time of 7.5 seconds is actually longer than normal at SLS. At SLS, the response is expected to look similar to that shown in Figure K-21, where P_{T2} was 23.0 psia. Figure K-18, where P_{T2} was 4.0 psia, shows a maximum of 5.5 degrees of β_c lead. This can be improved by making the backup control accel time 27.5 seconds, which is more inversely proportional to P_{T2} .

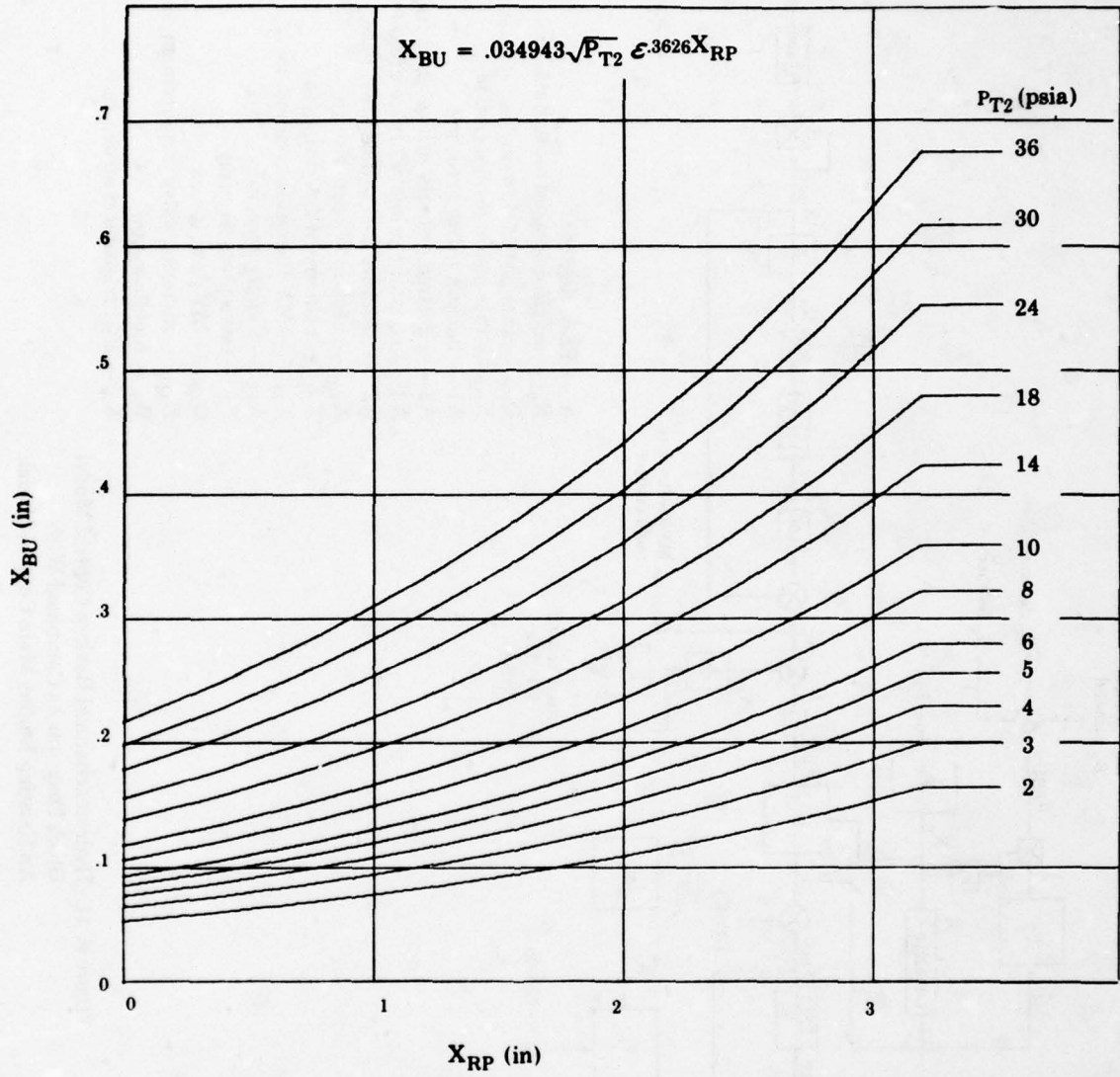
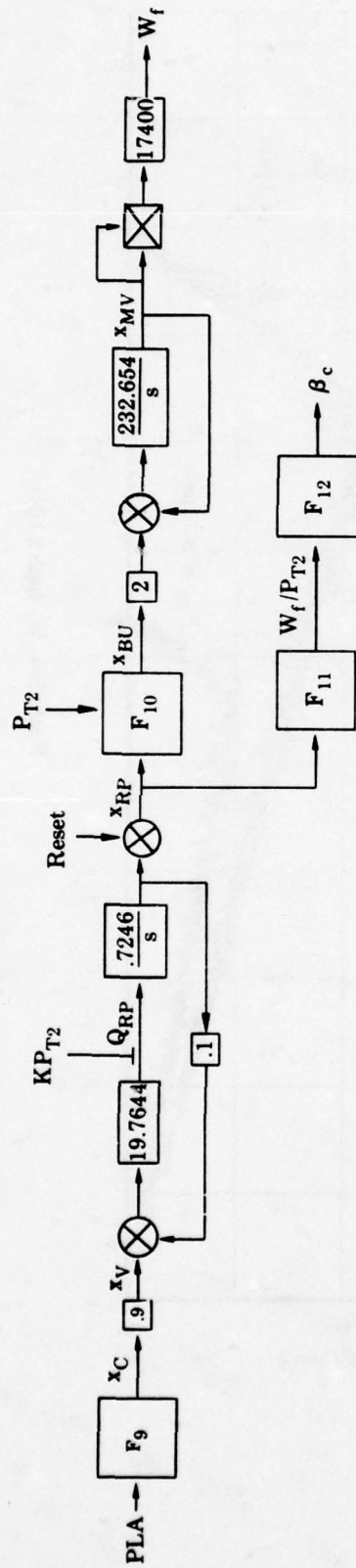


Figure K-10 - Backup Control Fuel Flow Demand Cam Definition.



- PLA — α , degrees
- x_C — α cam rise, in.
- x_V — amplitude, spool movement, in.
- Q_{RP} — rate piston flow, in³/sec
- K - rate factor
- x_{RP} — rate piston displacement, in.
- x_{BU} — backup W_f cam rise, in.
- x_{MV} — metering valve displacement, in.
- W_f — fuel flow, pph

Figure K-12 - Hydromechanical Backup Control Model Block Diagram As Run In Backup Mode.

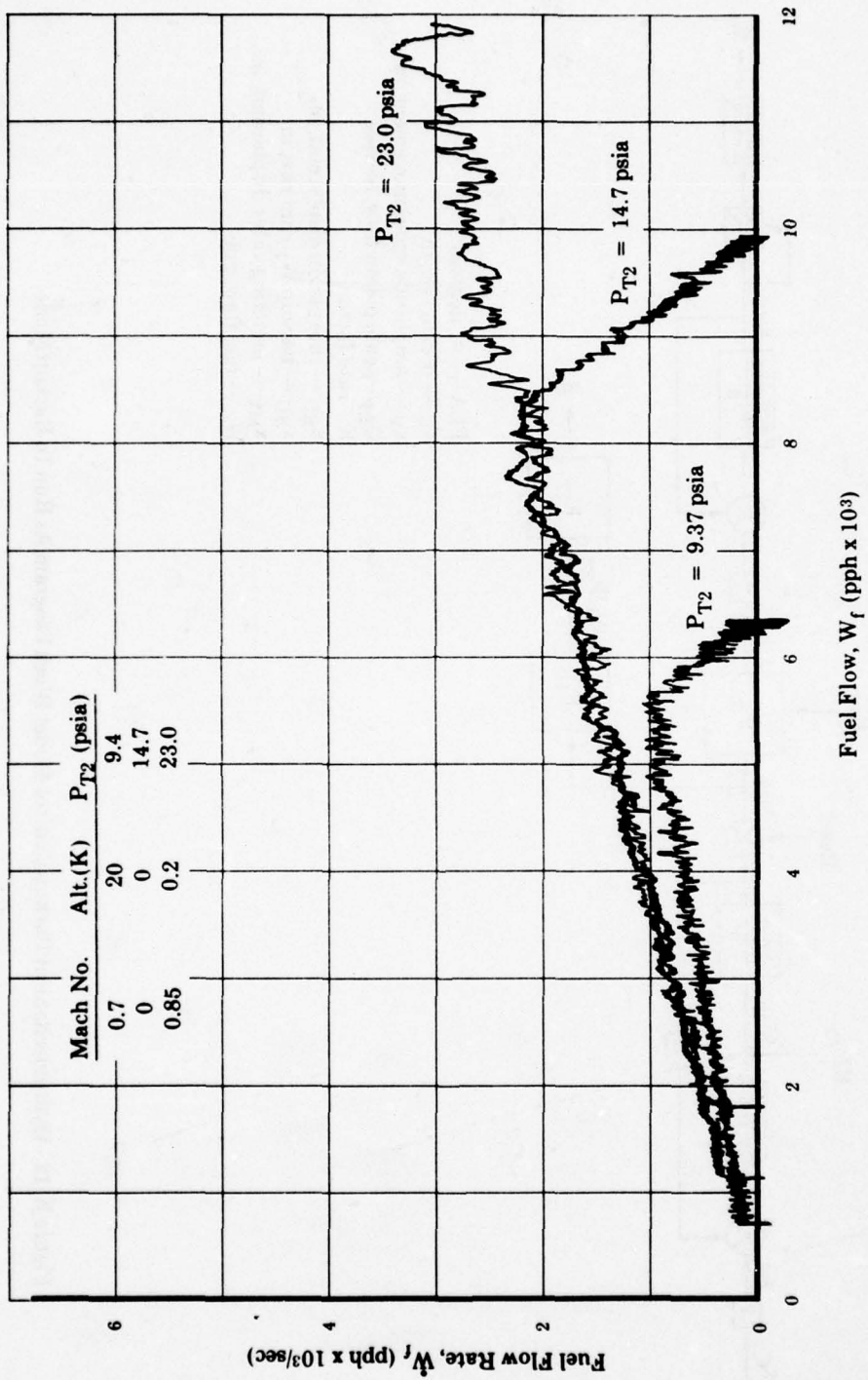


Figure K-13 - Backup Control Fuel Flow Rate Vs Fuel Flow Min To Max Dry Power.

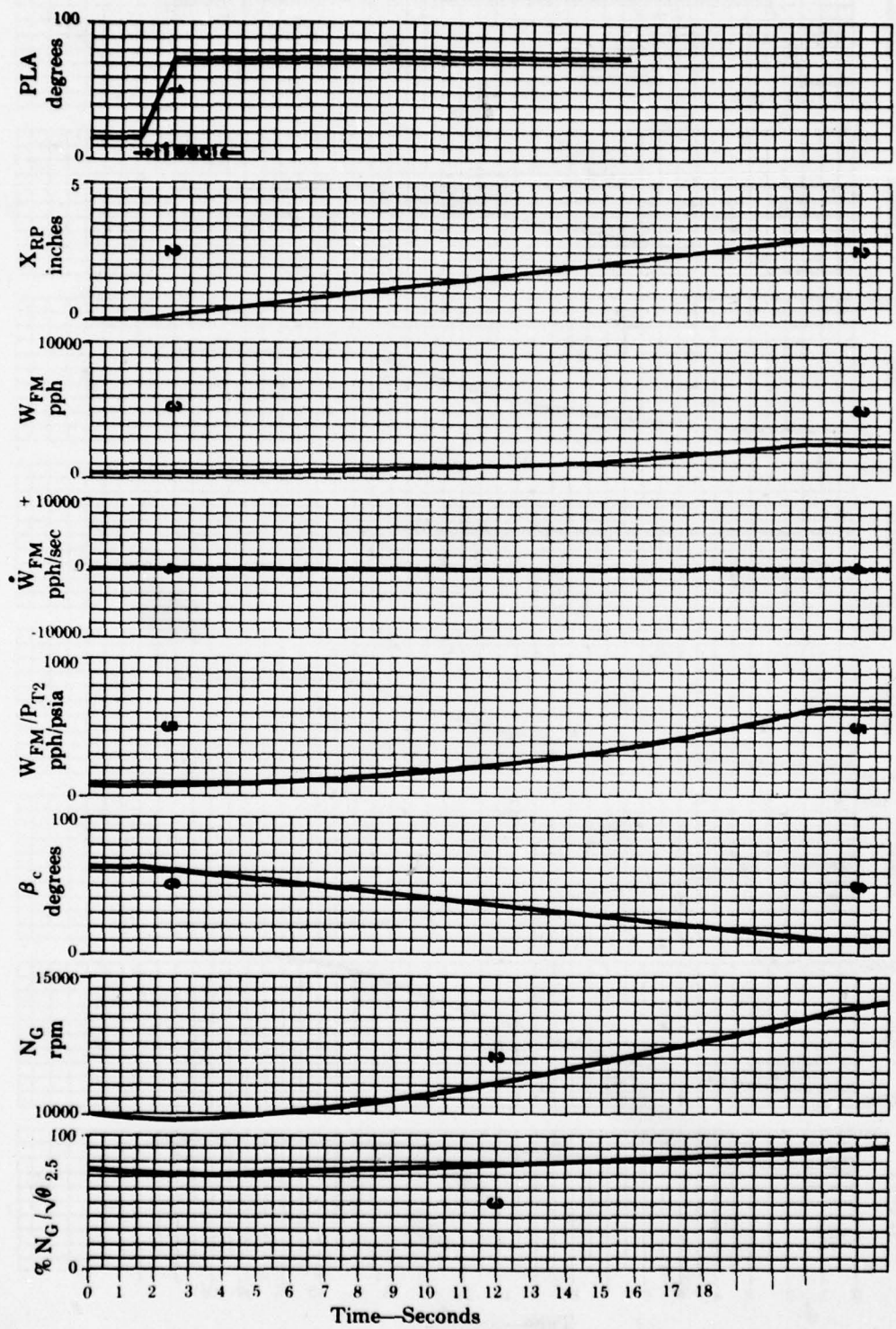


Figure K-14 - Backup Control Model Throttle Burst At P_{T2} = 4.0 PSIA.

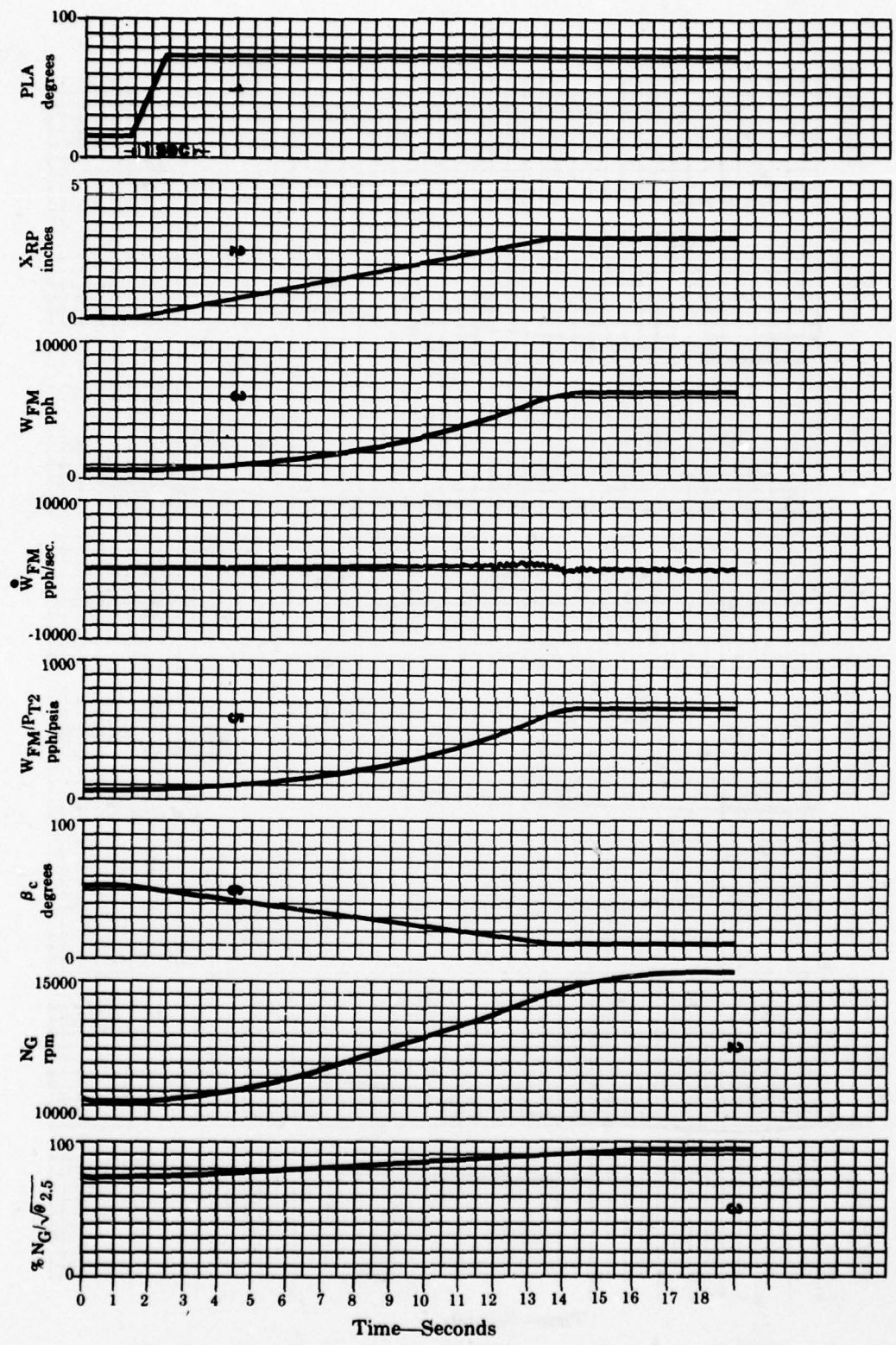


Figure K-15 - Backup Control Model Throttle Burst At P_{T2} = 9.4 PSIA.

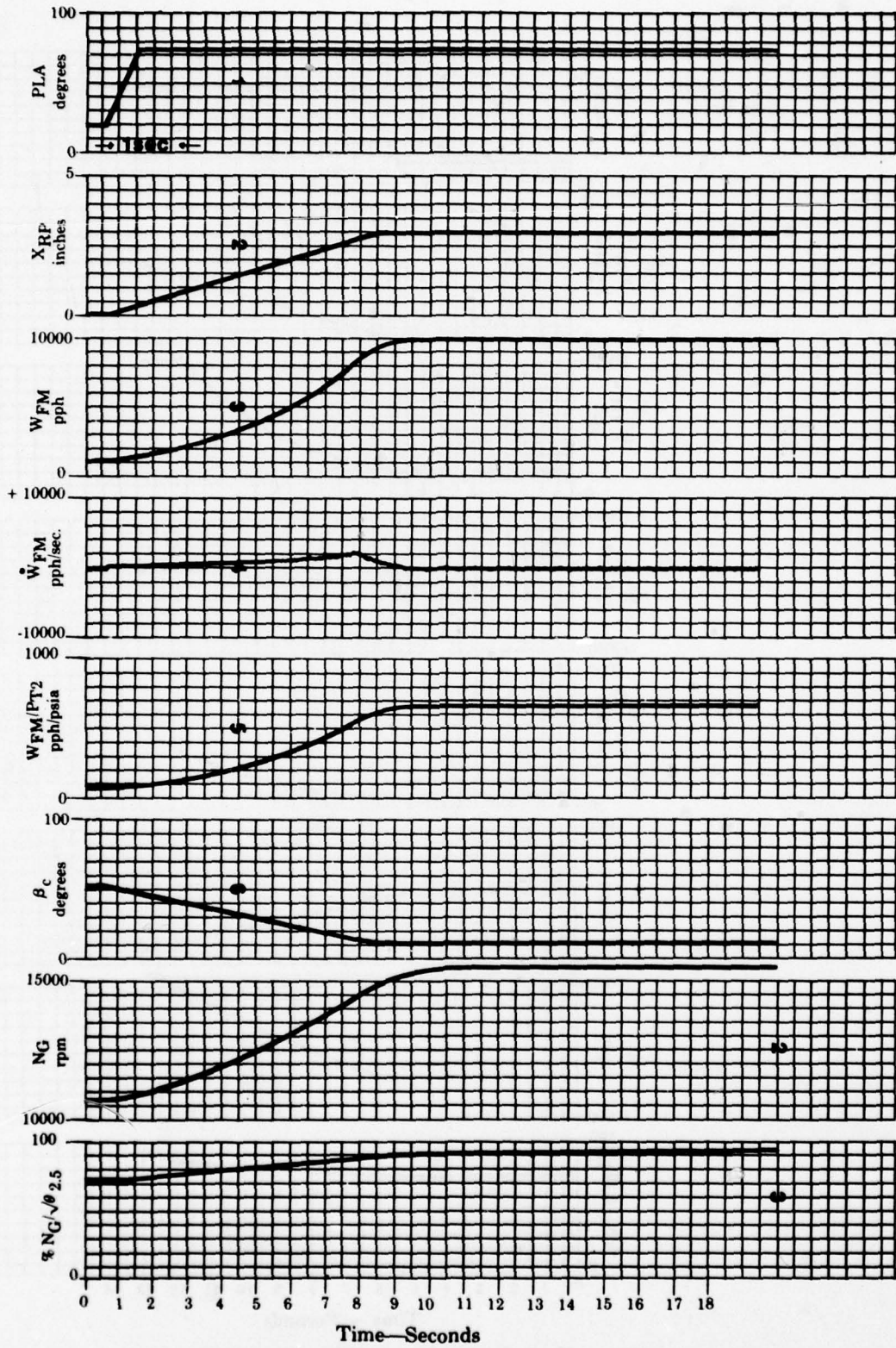


Figure K-16 - Backup Control Model Throttle Burst At SLS Standard Day.

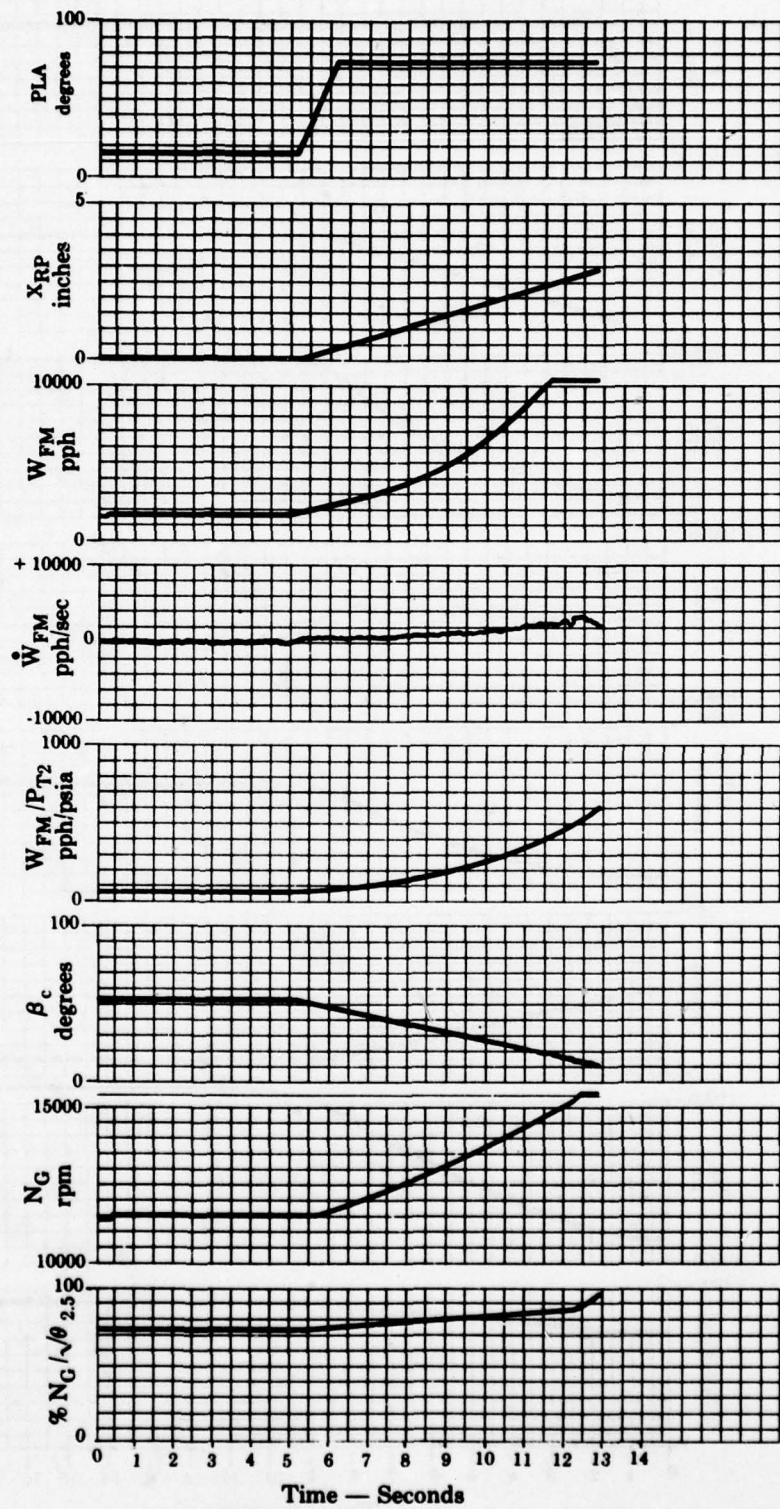


Figure K-17 - Backup Control Model Throttle Burst At $P_{T2} = 23$ PSIA.

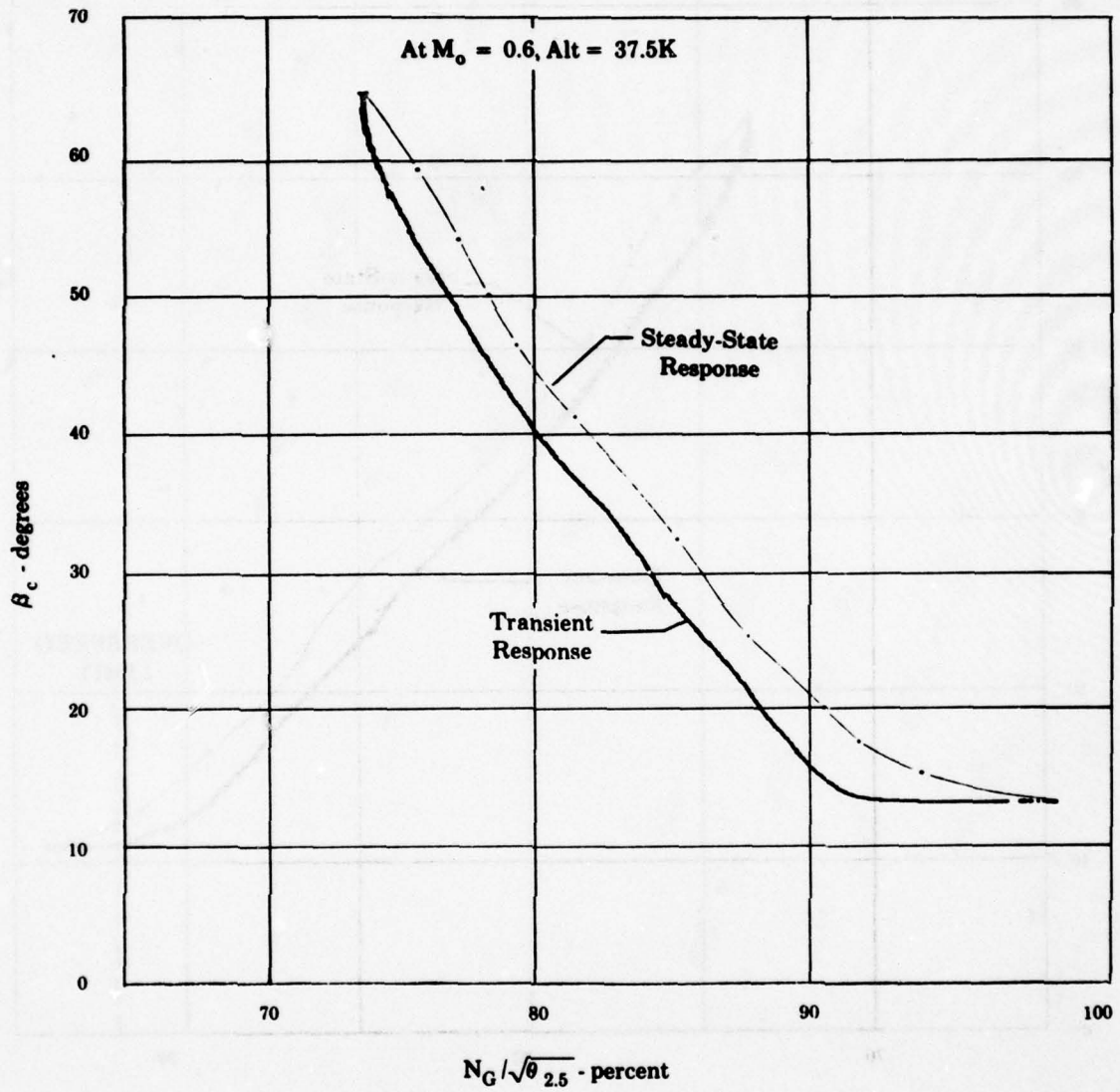


Figure K-18 - β_c Vs. $N_G / \sqrt{\theta}^{2.5}$ Steady-State & Throttle Burst at $P_{T2} = 4.0$ PSIA.

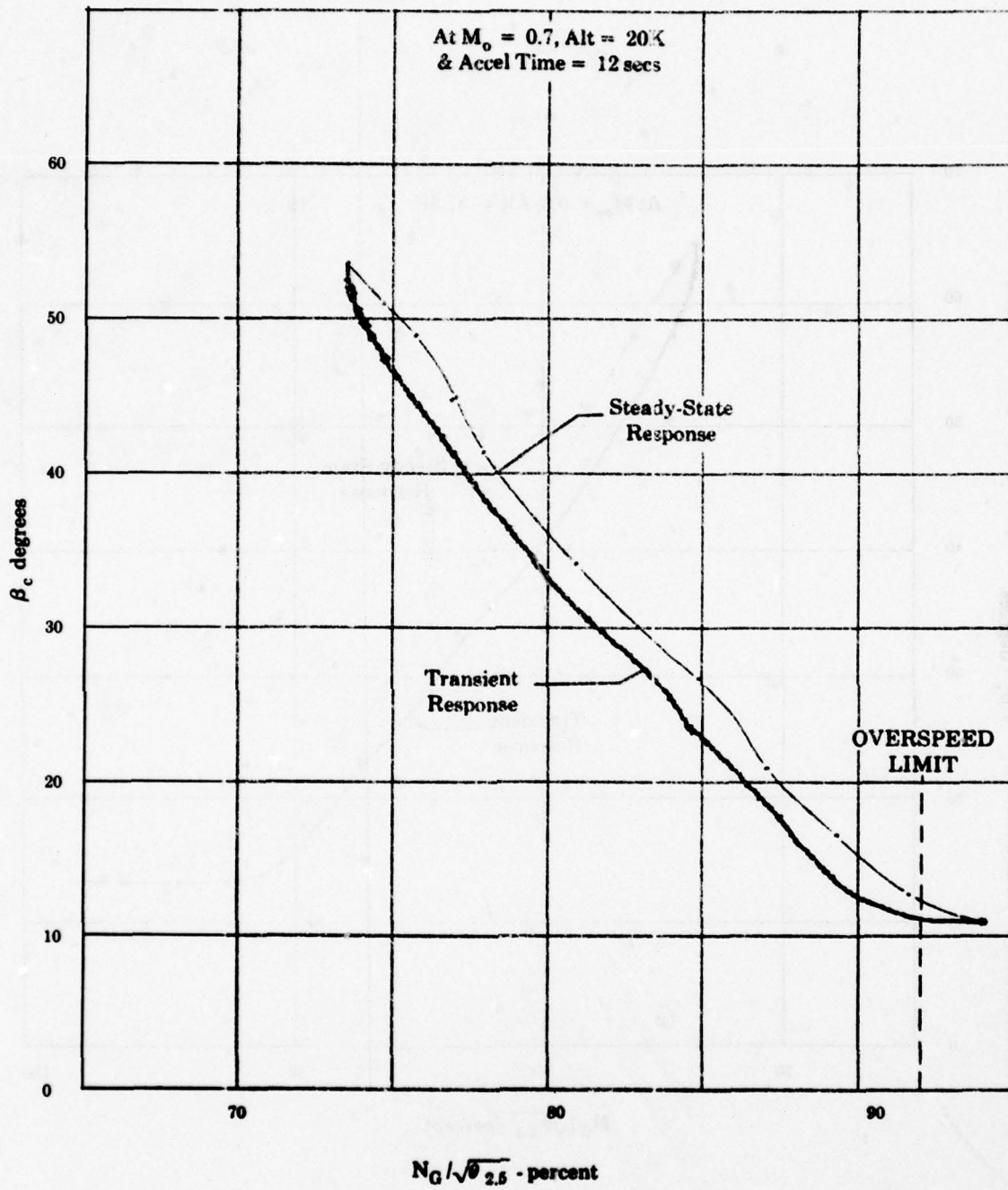


Figure K-19 - β_c Vs $N_G / \sqrt{\theta}^{2.5}$ Steady-State & Throttle Burst at $P_{T2} = 9.37$ PSIA.

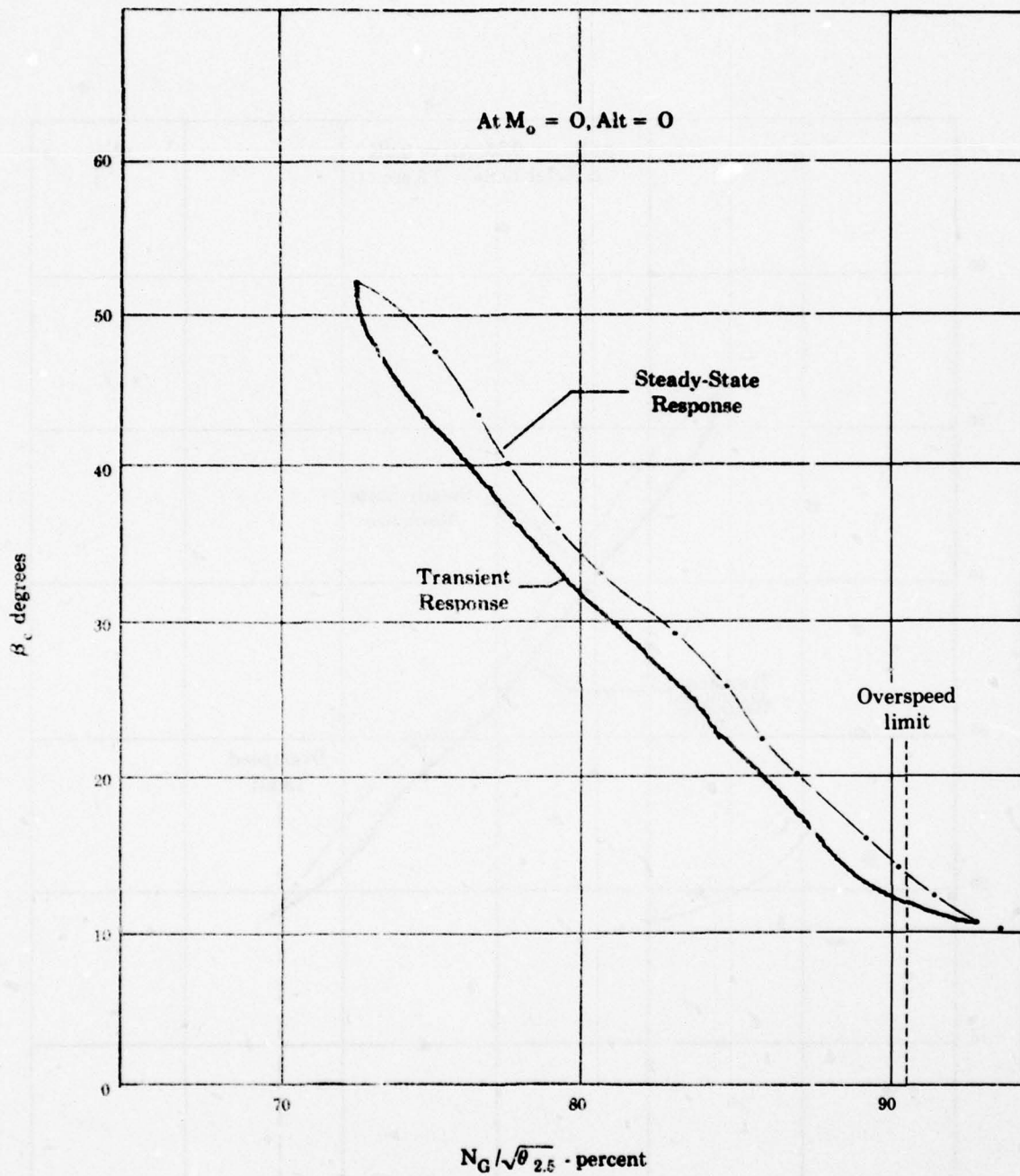


Figure K-20 - β_c Vs. Percent $N_G / \sqrt{\theta}^{2.5}$ Steady-State and Throttle Burst at $F_{T2} = 14.7$ PSIA.

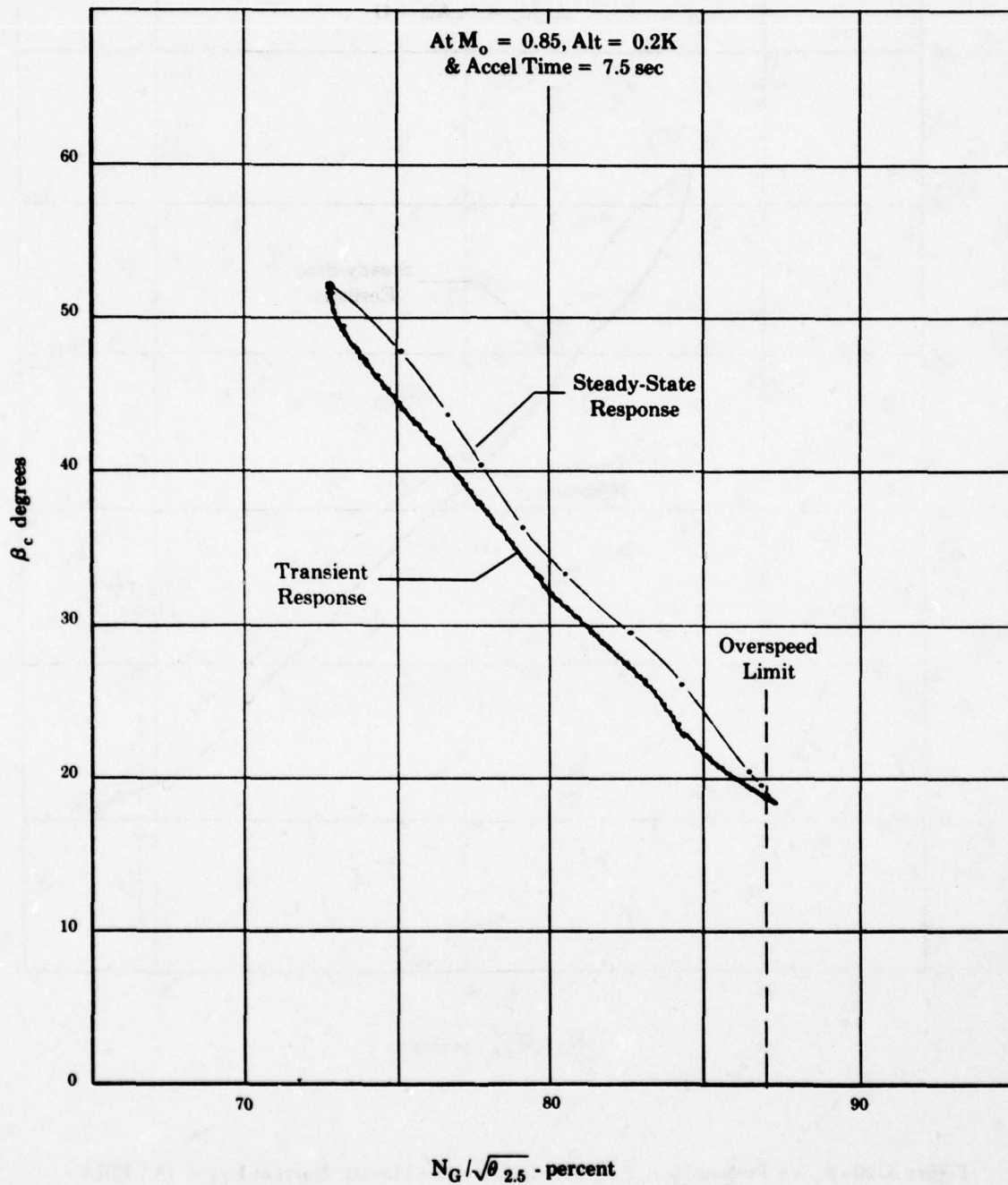


Figure K-21 - β_c Vs. $N_G \sqrt{\theta}^{2.5}$ Steady-State & Throttle Burst at $P_{T2} = 23.0$ PSIA.

5. **VOLUME, WEIGHT AND COST ESTIMATES OF THE COMBINATION ELECTRICAL/HYDROMECHANICAL BACKUP CONTROL**

a. **Volume Estimate**

The combination backup control consists of the components shown in Figure K-6. Most of the volume consists of the hydromechanical portion. This can be estimated from the envelope dimensions given in Figures K-4 and K-5. The overall volume is:

$$7.3 \times 9 \times 7.7 + \frac{\pi}{4} (7.7^2) (0.6) = 534 \text{ in}^3$$

This volume includes some voids and these should be subtracted.

- (1) Void at rear left side as viewed facing large round cover:

$$2.5 \times 2 \times 1.5 = 7.5 \text{ in}^3$$

- (2) Void at lower right side facing cover:

$$0.5 \times 4 \times 3 \times 7.3 = 44 \text{ in}^3$$

- (3) Void at right rear:

$$1 \times 2.5 \times 5 = 12.5 \text{ in}^3$$

The net volume of the hydromechanical portion of the control (less fuel valve) is:

$$534 \text{ in}^3 - 64 \text{ in}^3 = 470 \text{ in}^3$$

The other significant volumes are the power supply and circuits. These volumes are based on Figure N-10. The power supply occupies the major portion of the volume so about 80% was used. The above volumes and the volumes of the remaining components are summed below.

	<u>Cubic Inches</u>
Hydromechanical Portion, Backup	470
Power Source (Separate Winding)	2
Core Speed (N_G) Sensor	2
Power Supply	92
Circuits	30
Rate Transducer	2
Harness	20
Overspeed Servovalve	10
Single Stage Servovalve	7
Linear Variable Phase Transformer (LVPT)	<u>2</u>
Total Estimated Volume	597

b. **Weight Estimate**

The weight of the hydromechanical portion can be found by multiplying the volume by a density factor. The density factor is based on experience with other hydromechanical controls. The value used is 0.06 lbs/in³. The estimated weight of the hydromechanical portion is:

$$470 \text{ in}^3 \times 0.06 \text{ lbs/in}^3 = 28.2 \text{ lbs}$$

The other significant weights are the electrical power supply and the circuits. Here again, the density factor used (0.043 lb/in^3) is based on experience. The estimated weight of the power supply and circuits is:

$$122 \text{ in}^3 \times 0.043 \text{ lb/in}^3 = 5.2 \text{ lbs}$$

The above estimated weights plus those of the remaining components are summed below.

	<u>Lbs</u>
Hydromechanical Portion	28.2
Power Supply and Circuits	5.2
Power Source	0.4
N_G Sensor	0.4
Rate Transducer	0.3
Harness	2.2
Overspeed Servo valve	1.0
Single Stage Servo valve	0.7
LVPT	0.3
P_{T2} Probe and Tube	1.1
	<hr/> 39.8

c. Cost Estimates

The cost estimates are based on 1977 dollars, 1000th unit and an order for 100 units. The estimated costs are:

Servo Pressure Regulator	\$ 195	Covers (12)	\$ 600
Pressure Sensor (P_{T2})	800	Throttle Shaft Seals and Bearings	75
Servo Piston and Sleeve (P_{T2})	300	Rate Valve and Sleeve (P_{T2})	115
3-D Cams, Shaft and Bearings	500	Latch Mechanisms (2)	300
Rate Piston and Sleeve	300	Feedback Shaft, Seals and Bearings	90
Summing Pistons and Sleeves (2)	700	Overspeed Servo valve	1100
Main Housing, Backup Control Portion	1500	Single Stage Servo valve	300
Ball Valve Assemblies (3)	225	Power Source (Alternator Winding)	140
Linkage and Bearings (β_c)	250	Core Speed (N_G) Sensor	100
2-D Cams (2)	150	LVPT	205
Metering Valve Linkage and Bearings	200	Rate Transducer	185
Gears, Rack and Pinion and Supports	150	Power Supply and Circuits	3340
Hydraulic Locks (2)	300	Miscellaneous Hardware	300
Valve and Sleeve (β_c)	150	Assembly and Test	1320
Reset Piston and Sleeve	125	Harness	600
			<hr/> \$14,615

The power supply and circuits are a major cost. For this estimate, 60% of the cost of the electrical backup control power supply and circuits was used (See Appendix N, Paragraph 5.c.). The assembly and test cost is for the hydromechanical portion only.

APPENDIX L - HYDROMECHANICAL BACKUP CONTROL HAVING FUEL FLOW SETTING FUNCTION WITH FUEL RATE LIMITS IN A SERIES CONFIGURATION

This approach explored the advantage of substituting a hydromechanical governor for the electrical overspeed function of combination approach of Appendix K. The hydromechanical portion of the combination system and its electrical feedback sensors were selected. To these were added a hydromechanical governor. An additional servovalve was added to reduce the fuel flow floor at high Mach number operation. This requirement is shown in Appendix K.

The resulting estimated UCR and GHPL are shown in Table L-1. It is concluded that the substitution of the hydromechanical governor for the electrical overspeed function of the combination control of Appendix K results in a small improvement of both UCR and GHPL; however, these improvements do not reach the reliability level of the recommended approach shown in Appendix I.

**TABLE L-1
RELIABILITY SUMMARY FOR THE HYDROMECHANICAL/SERIES/W_f/W_f BACKUP CONTROL**

	UCR Per 10 ⁶ Hrs.	Get Home Power Loss (GHPL) Per 10 ⁶ Hrs.
Combination Electrical/Hydromechanical	63.0	19.2
Hydromechanical Portion Alone	37.7	11.3
Electrical Feedback, Sensors, Cable, etc.	5.2	.53
Hydromechanical Governor	15.0	3.0
Flyweights		
Spool Valve - Rotated		
Spring		
Zero Leak Device		
	57.9	14.83
Override Floor At High M ₀	2.23	1.18
Servovalve and Circuit	60.1	16.01
FADEC	<u>118.4</u>	40.2
Combination UCR	178.5	
Combination FADEC/Backup GHPL:		
Backup GHPL		16.01
Unprotected Primary Valve Signals		<u>2.0</u>
Total GHPL		18.01

**APPENDIX M — HYDROMECHANICAL BACKUP CONTROL HAVING A FUEL FLOW SETTING
FUNCTION WITH FUEL RATE LIMITS IN A PARALLEL CONFIGURATION**

This approach explored the reliability advantage of parallel (standby) configuration. It was derived from the control of Appendix K by first substituting a hydromechanical governor in place of the electrical overspeed limit and the electrical speed sensor. Hydromechanical floors were removed.

A transfer valve for switching fuel valve and stator control servo pressures was added. In addition, a servo pressure sensor was added to force the backup control to precisely track the primary control during primary operation to avoid any fuel flow transient upon transfer from primary to backup. This latter feature, shown on Figure M-1, was renewed with Air Force Aero Propulsion Laboratory. Its necessity was challenged on the basis that the Integrated Propulsion Control Systems program with a similar transfer did not need such tracking device. Further analysis for the chosen system, reported in Appendix I, showed that it was not needed and hence was not included there.

The estimated UCR and GHPL for system are shown in Table M-1. The GHPL of this approach is comparable to the recommended system (Appendix I) but inferior in UCR. In addition, this control is much more complex and not proven so it is not recommended nor was it studied further.

**TABLE M-1
RELIABILITY SUMMARY FOR THE HYDROMECHANICAL PARALLEL/ W_f/\dot{W}_f BACKUP
CONTROL.**

	UCR /10 ⁶ Hrs.	Get Home Power Loss (GHPL) /10 ⁶ Hrs.
Hydromechanical Portion	37.7	11.3
Remove Floors & Summers	- 8.9	- 2.3
Remove Sensors (2)	- 2.4	- .6
Added, High M_o Servo, Harness, etc.	19.2	.0
Add Hydromechanical (H.M.) Governor N_G Limit	15.0	3.0
Flyweights		
Spool Valve - Rotated		
Spring		
Zero Leak Device		
Add ΔP Servo Valve Zero Device	+ 2.4	0.6
2 Bias Pistons	+ 2.4	0.6
Transfer Valve, W_f Tracking, Switch & Power to Valve	9.2	1.5
Total	<hr/> 74.6	<hr/> 14.1
FADEC	118.4	40.2
Combination UCR	<hr/> 193.0	

— Continued —

Table M-1 (Continued)

Combination Power Loss: FADEC & H.M. Fail	.0013/10⁶ Hrs.
FADEC & Transfer Fail	.0008/10⁶ Hrs.
H.M. Fails & Transfer Malfunction	.00003/10⁶ Hrs.
Transfer Sticks Midway	1.5/10⁶ Hrs.
H.M. Overspeed Malfunctions	1.5/10⁶ Hrs.
Total GHPL	<u>3.0/10⁶ Hrs.</u>

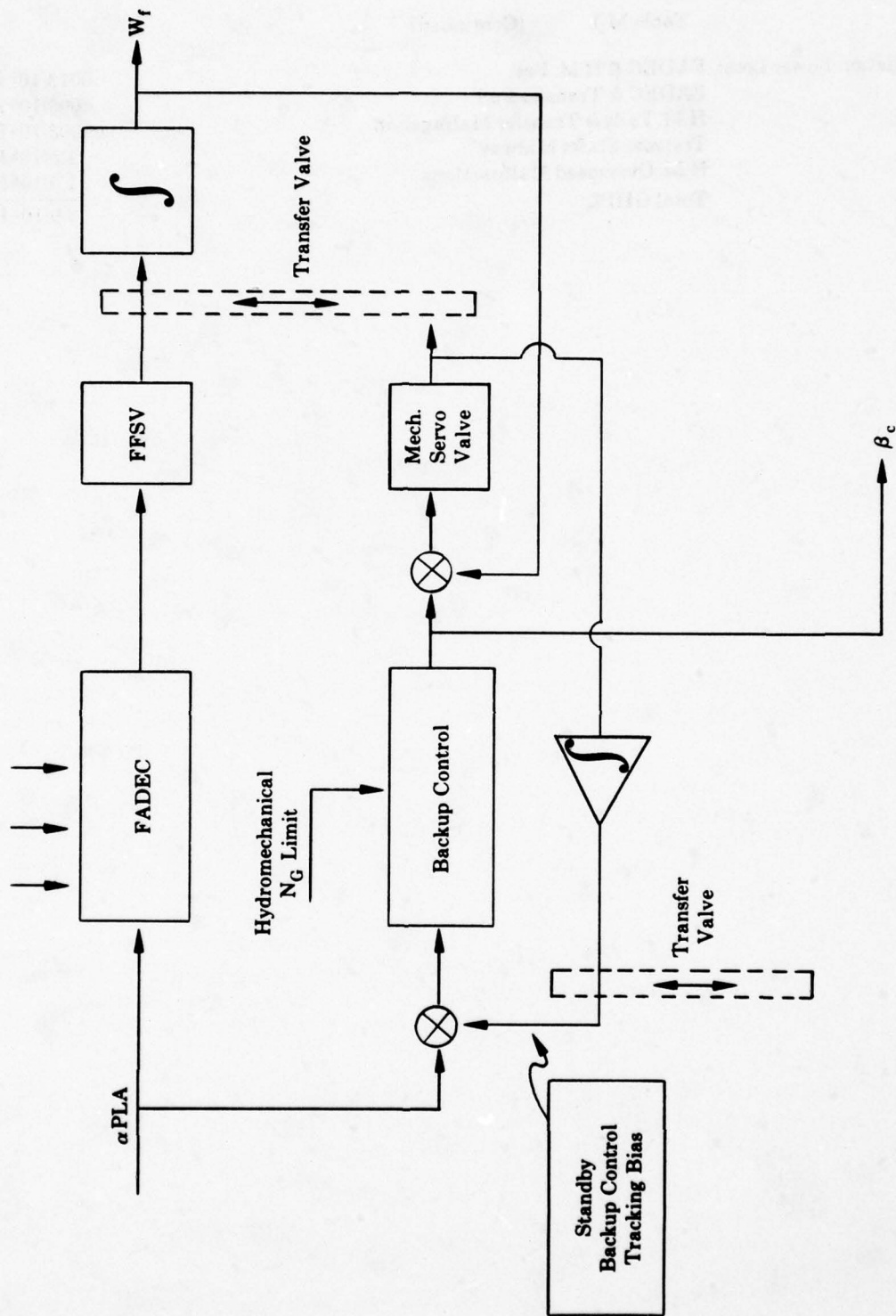


Figure M-1 - Tracking System.

APPENDIX N - ELECTRICAL BACKUP CONTROL HAVING SPEED SETTING WITH SPEED RATE LIMITS IN PARALLEL CONFIGURATION.

1. APPROACH

Speed rate was selected as the accel and decel parameter for the electrical approach. Some reasons were:

- a. Electrical speed sensing does not require a drive pad.
- b. Core speed (N_G) limiting provides overtemperature protection in subsonic and supersonic region (See Figure H-1).
- c. Corrected speed, $N_G / \sqrt{\theta_{2.5}}$, is a satisfactory parameter for β_c scheduling so N_G can be used for both variables.

Several electrical backup control approaches were considered. With the summing concept, used for the combination and fluidic approaches, either the backup or the primary control can cause "loss of power" failures. Since electrical controls do not have the field demonstrated reliability that hydromechanical controls have, the result is more significant. Based on this, the selected electrical approach is the type that is on standby during primary mode operation (see Figure N-1).

The operation of the electrical backup control is discussed in the various modes as follows:

- a. **Primary Mode** — In this mode, the backup control provides only N_G overspeed protection. The objective is to minimize the amount of electronics in use during primary mode operation and, thus, minimize the power loss failures due to backup control. If overspeed occurs, the overspeed detector and latch cause automatic transfer to the backup mode. The backup control integrator tracks N_G actual so its output (N'_{GR}) is essentially N_G actual. A speed error amplifier speeds up the integrator only in this mode. This is necessary so that transfer to backup can occur at steady state or during a transient without a jump in speed error. The output of the backup W_f servovalve is blocked by a transfer valve so that the primary W_f servovalve alone controls the metering valve. The transfer valve (See Figure N-2) is spring and pressure loaded toward the primary mode operation stop. This is to protect against a transfer if backup electrical power is lost. The power source for the backup control and the solenoid are common — a separate winding on the alternator.

The electronics are functioning and computing a rate limited speed request signal (N'_{GR}). A standby β_c schedule is a function of $N_G / \sqrt{\theta_{2.5}}$ is also being computed. This schedule is equivalent to that computed by the primary control. The transfer valve, mechanically coupled to the one causing switching of W_f servovalve output, blocks the backup β_c servovalve and allows only the primary β_c servovalve to control the actuator.

- b. **Transfer to Backup Mode** — Transfer is initiated by either pilot action, loss of electrical power to the primary control, overspeed or by action of the primary control when it senses faulty operation. After initiation, the following occurs:
 - 1) A switch is closed and an 80 ma signal is transmitted to the electrohydraulic transfer valve. The valve strokes to the backup mode stop at which it ports only backup W_f and β_c servovalve flow to the actuators.
 - 2) A switch is opened between the speed error amplifier and the summer. This allows only the signal determined by the function of P_{T2} to be transmitted to the variable saturation limit device.

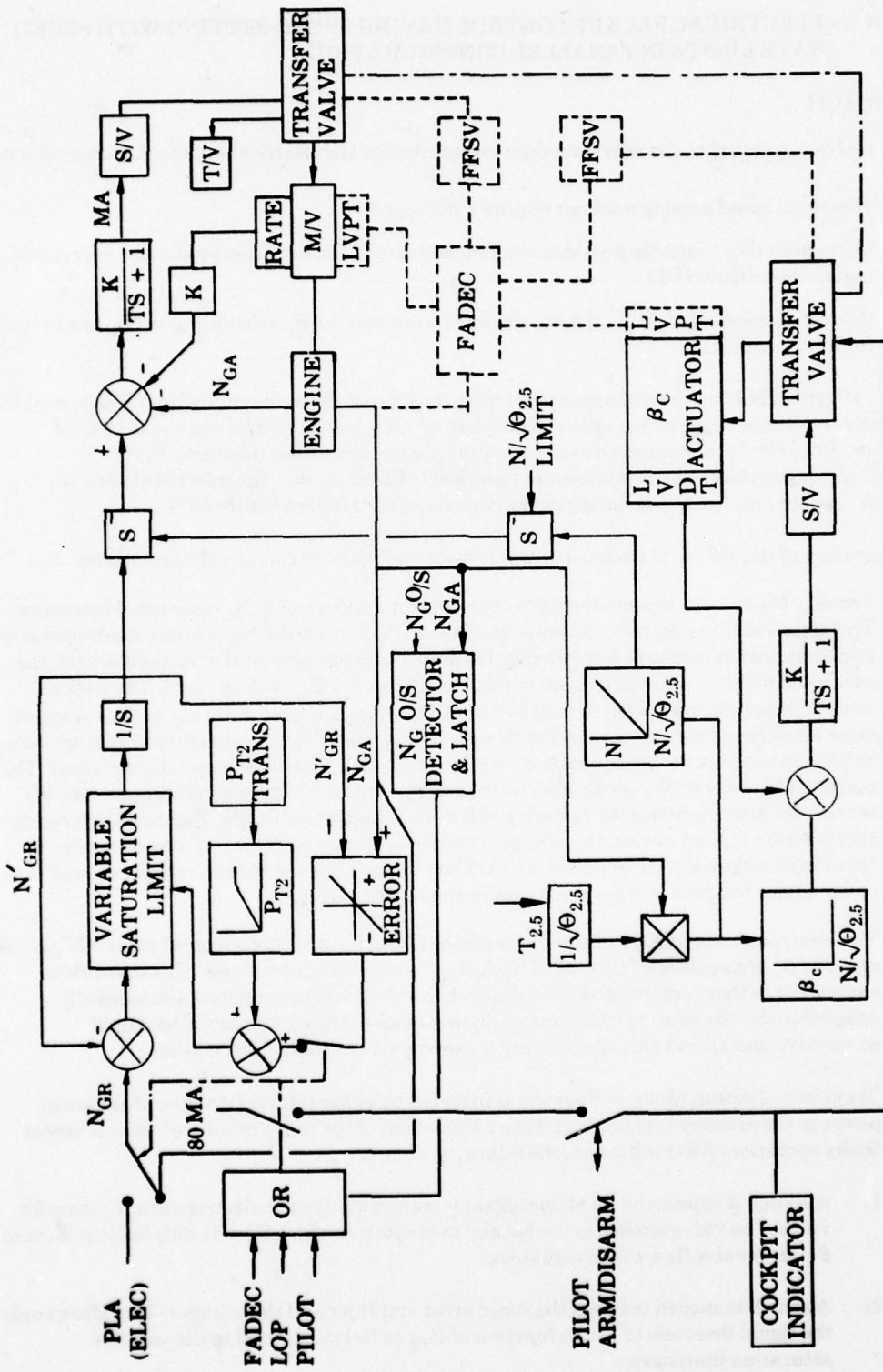
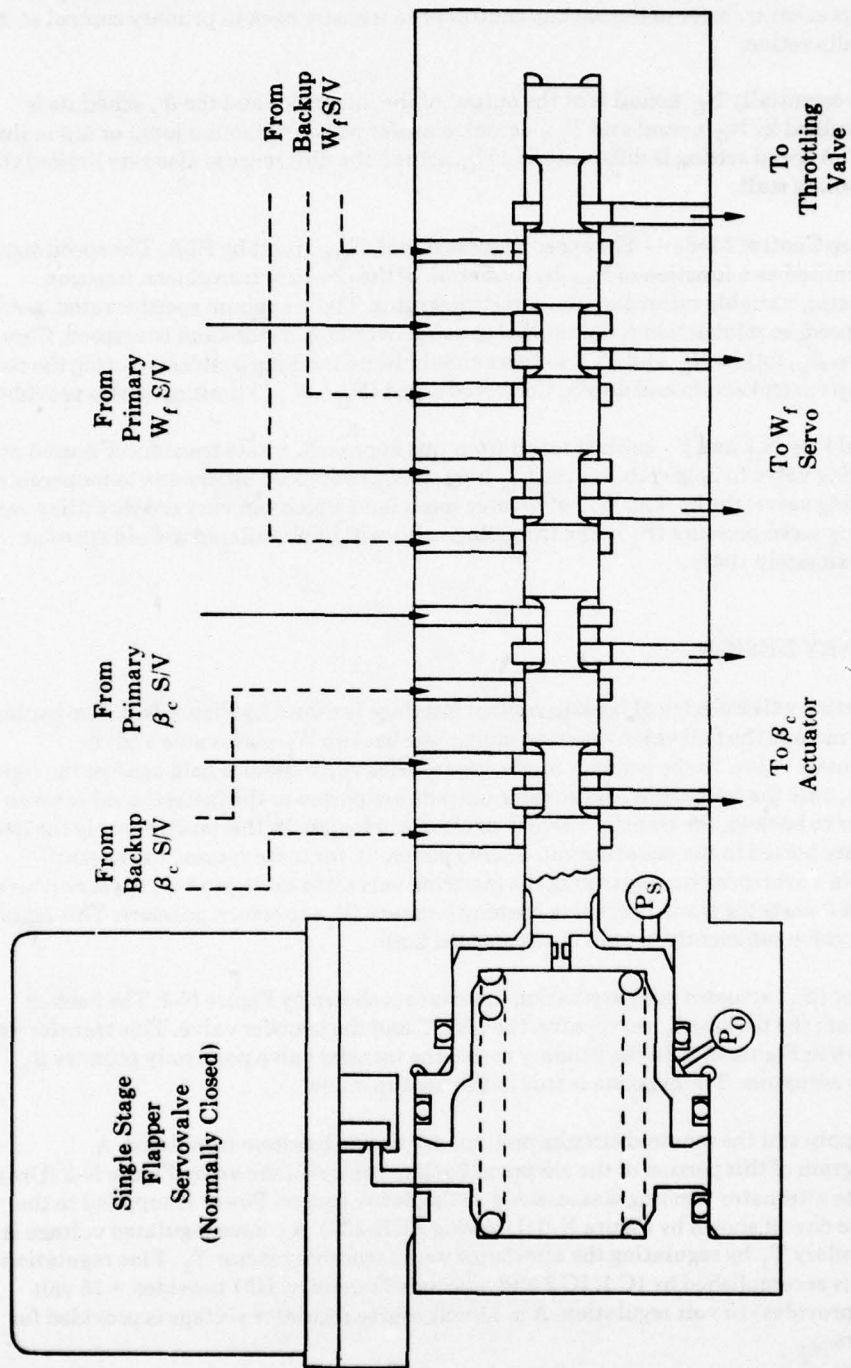


Figure N-1 - Block Diagram for the Electrical Approach.



Scale \approx 2:1

Figure N-2 - Transfer Valve for the Electrical Approach.

- 3) The third switch changes the upstream speed request signal (N_{GR}) from N_G actual to PLA.
- 4) The fourth switch is shown in the line to the transfer valve and allows the pilot to prevent transfer to the backup control or to transfer back to primary control at his discretion.

Since essentially N_G actual is at the output of the integrator and the β_c schedule is determined by N_G actual and $T_{2.5}$ actual, transfer occurs without a jump or dip in thrust. If the PLA speed setting is different than N_G actual, the difference is also rate limited thus preventing stall.

- c. Backup Control Mode — The speed request signal, N_{GR} , is set by PLA. The speed signal is rate limited as a function of P_{T2} by the action of the pressure transducer, function generator, variable saturation limit and integrator. The maximum speed is rated, not 4% overspeed, so pilot action is not needed to avoid overtemperature and overspeed. Core stators, β_c , follow N_G and $T_{2.5}$ so there should be no tracking problems during the slower backup control accels and decels. Corrected speed ($N_G / \sqrt{\theta_{2.5}}$) limiting is also provided.

Closed loop N_G and β_c control result from this approach. A rate transducer is used at the metering valve to help stabilize the N_G loop. If N_G overspeed occurs due to inoperable open metering valve, the backup W_f servovalve has a land which can vary the throttling valve opening servo pressure (P_x). The throttling valve will be modulated to hold speed at approximately 104%.

2. PRELIMINARY DESIGN

The fuel metering valve/electrical backup control interface is shown by Figure N-3. The backup control components include the fuel valve rate transducer, the backup W_f servovalve and the electrohydraulic transfer valve. In the primary mode, the transfer valve spool is held against the right stop. In this position, only the primary W_f servovalve outputs are ported to the metering valve servo piston. Upon transfer to backup, the transfer valve is stroked to left stop. In this position, only the backup servovalve outputs are ported to the metering valve servo piston. If, for some reason, the backup servovalve cannot limit overspeed by controlling the metering valve, the extra land on the servovalve spool is stroked until it ports the throttling valve opening pressure (P_x) to return pressure. This action closes the throttling valve sufficiently to hold the overspeed limit.

The core stator (β_c) actuator primary/backup interface is shown by Figure N-4. The backup control components are the backup β_c servovalve, the LVDT and the transfer valve. This transfer valve is the same one shown in Figure N-2. In the primary mode, the transfer valve ports only primary β_c servovalve output to actuators. The opposite is true in the backup mode.

The power supply and the required circuits preliminary design has been completed. A functional block diagram of this portion of the electrical backup control is shown by Figure N-5 (Drawing ACE-347). A separate alternator winding was selected as the power source. Power is supplied to the backup control by the circuit shown by Figure N-6 (Drawing ACE-338). A coarse regulated voltage is obtained at the secondary T_1 by regulating the alternator with saturable reactor T_2 . Fine regulation of the ± 15 volt supply is accomplished by IC 1, IC 2 and associated circuitry. IC 1 provides +15 volt regulation and IC 2 provides -15 volt regulation. A ± 13 volt coarse regulator voltage is provided for driving torque motors.

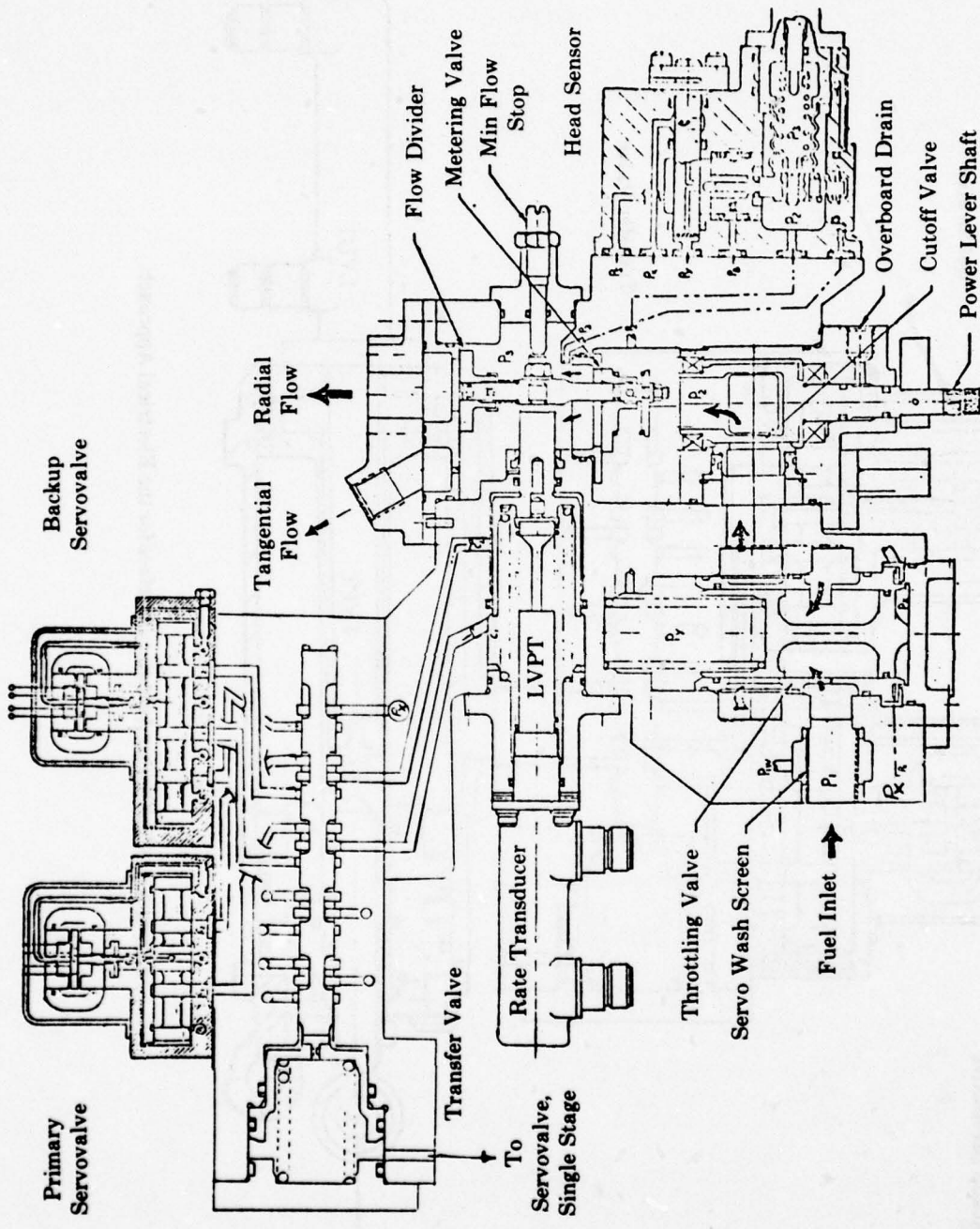


Figure N-3 - Fuel Valve Interface For the Electrical Backup Control.

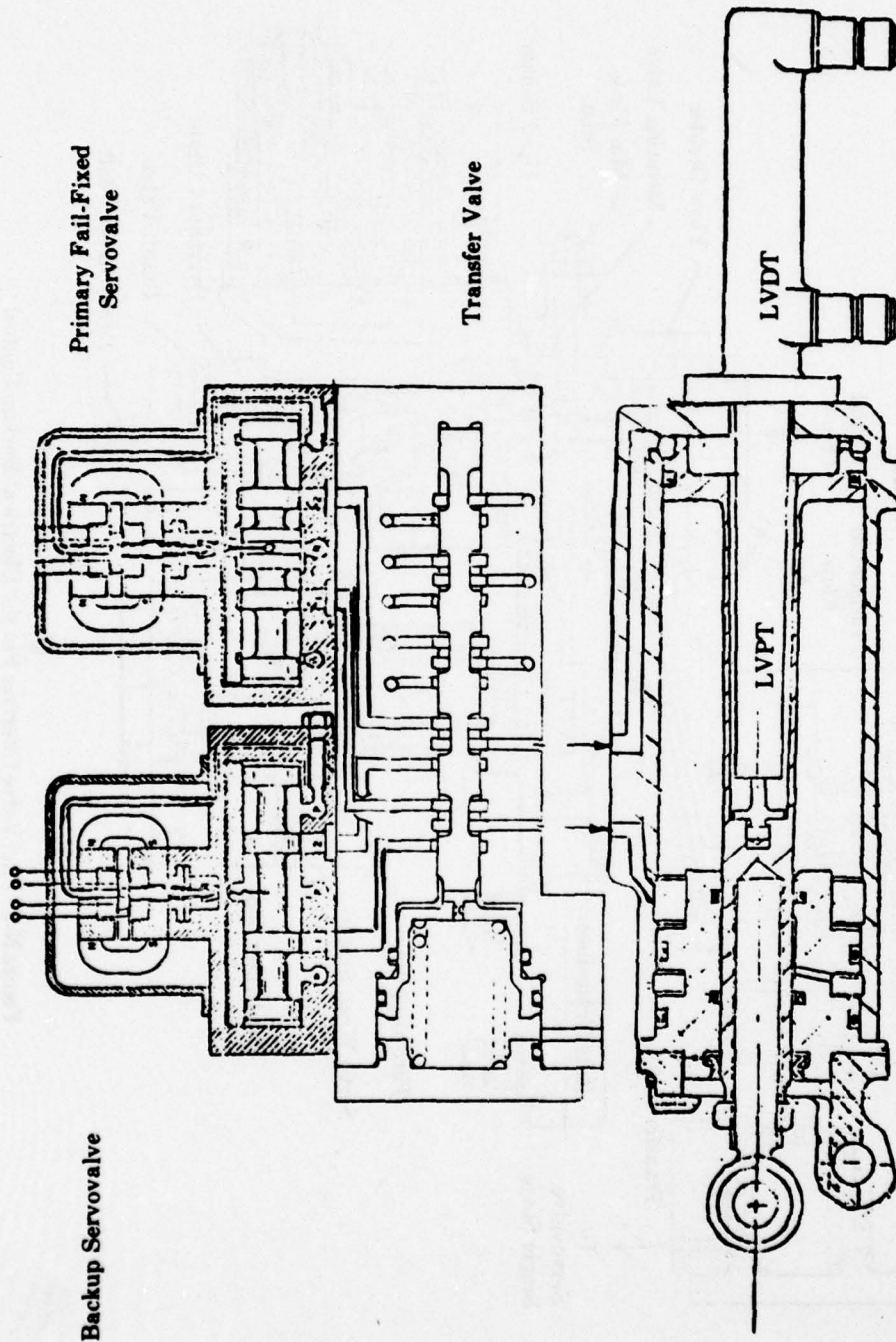


Figure N-4 - Core Stator Actuator Interface for the Electrical Approach.

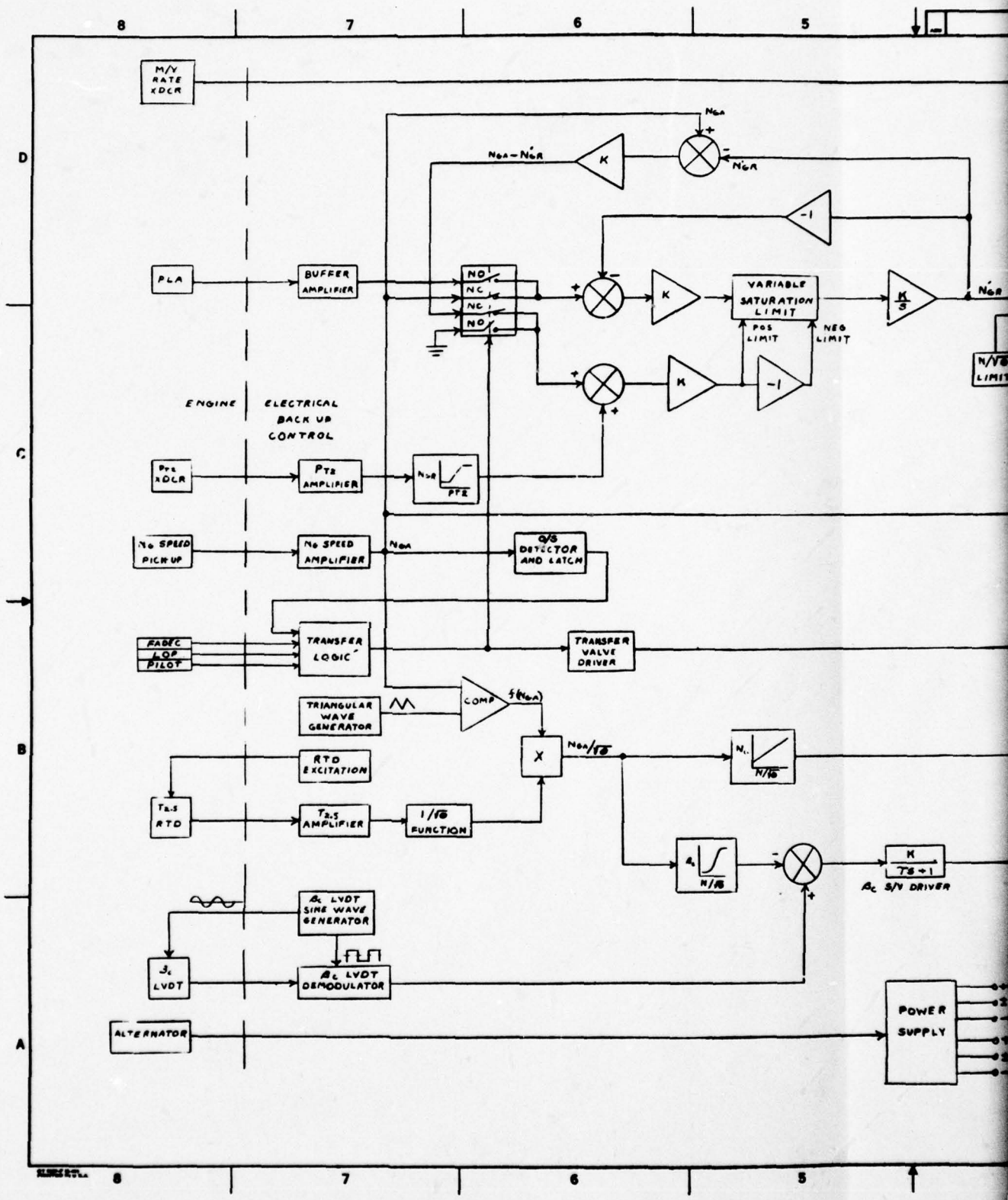
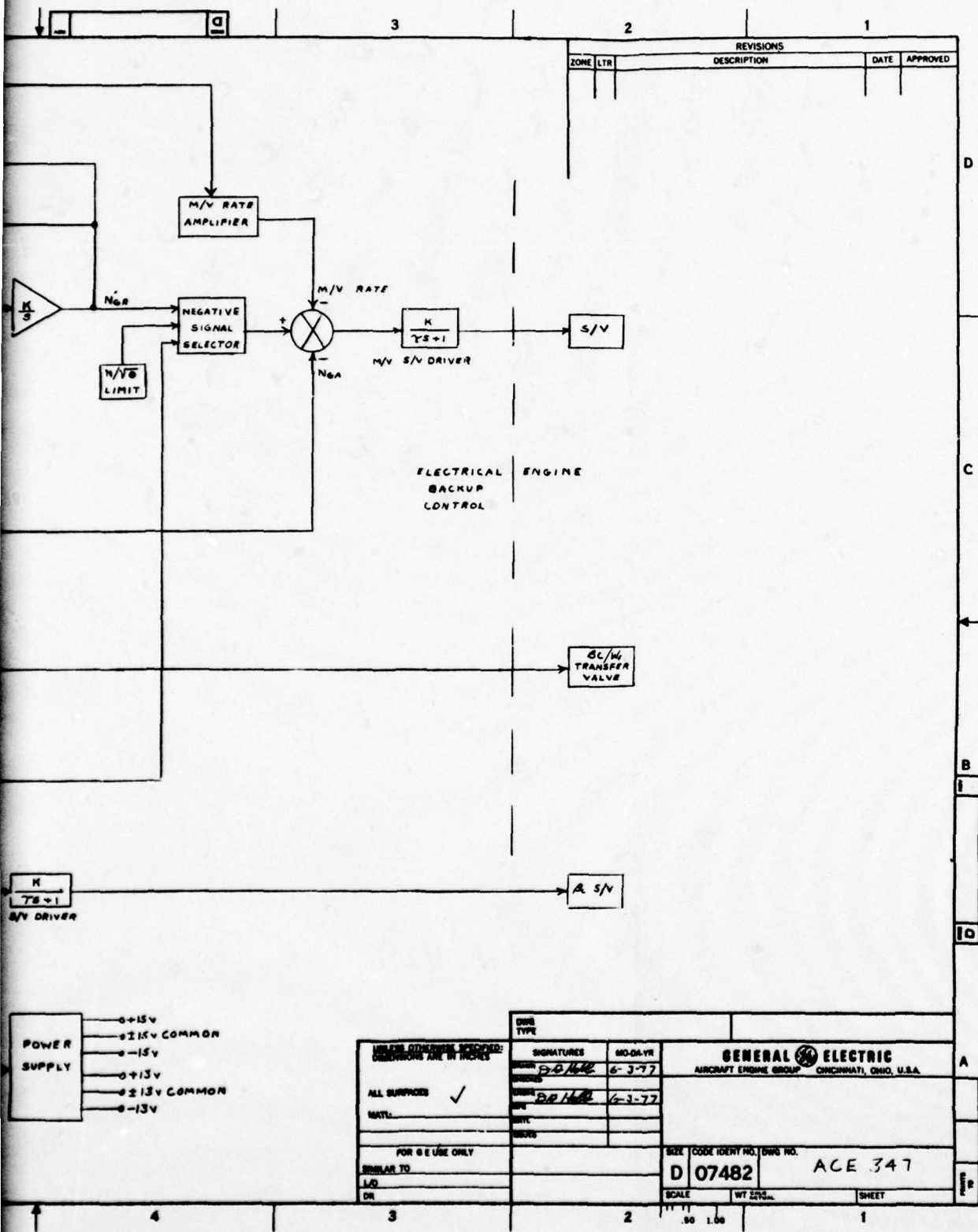


Figure N-5 - Electrical Backup Control



Backup Control Block Diagram.

Excitation for the β_c LVDT is provided by the circuit shown in Figure N-7 (Drawing ACE-339). IC 1 through IC 5 comprise an oscillator circuit. The output of IC 5 is a triangular wave that is fed back to the input of IC 2 which is used as a comparator. A reference voltage is also fed back from IC 4 via IC 1. When the output of IC 5 integrates to a voltage slightly greater than the reference voltage, the output of IC 2 switches causing the output of IC 4 to switch and change the polarity of the integrating voltage at the input to IC 5. The reference voltage to IC 2 is also reversed and switching at the output of IC 2 will again occur when the output of IC 5 is slightly greater than the reference voltage.

The output of IC 5 is fed to the input of IC 9, an active bandpass filter amplifier. The output of IC 9 is a sine wave that is fed to IC 7, IC 10, and IC 11. IC 7 is part of a demodulator and AGC circuit used to control the amplitude of the sine wave. A DC voltage is fed back to IC 3 and IC 4 from IC 8 and is used to control the output amplitude of IC 5.

IC 10 is a comparator that provides a square wave signal for demodulation of the LVDT output. IC 11 is a power amplifier to provide excitation drive to the LVDT.

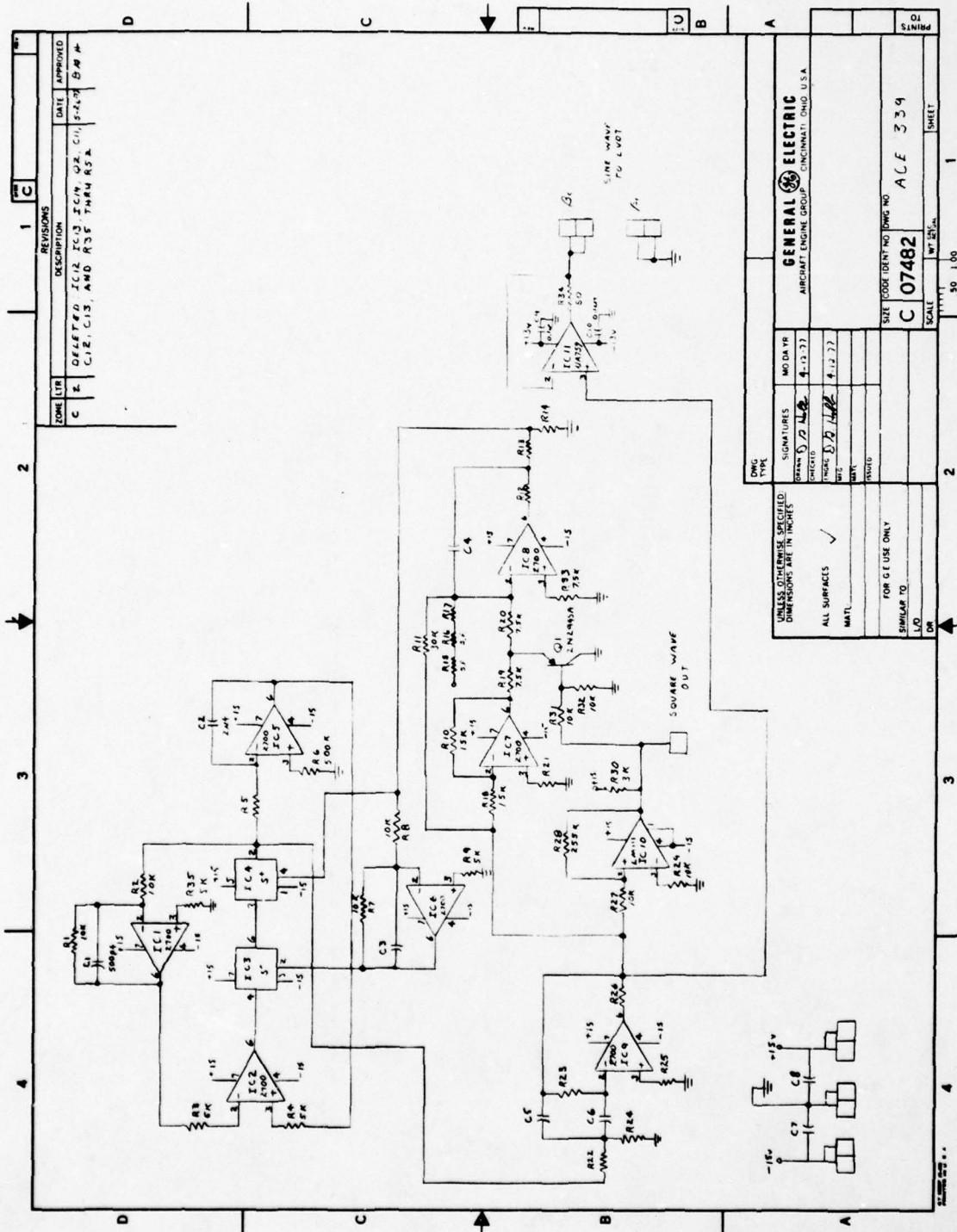
Circuits for the $T_{2.5}$ processing and β_c schedule are shown in Figure N-8 (Drawing ACE-340). IC 1 and IC 8 are amplifiers which provide the RTD temperature sensor excitation and signal processing, respectively. IC 1 provides a constant current to the RTD. The level of current is determined by R3 and feedback resistors R1 and R2, IC 8 amplifies and level shifts the RTD signal. The output of IC 8 is a DC voltage proportional to the desired temperature range.

The output of IC 8 is fed to the inputs of IC's 2, 5, 9 and 13. The outputs of these amplifiers are a four slope approximation of the $1/\sqrt{\theta}_{2.5}$ function and are fed to IC 3.

N_{GA} is a DC voltage proportional to actual N_G signal and is fed to the noninverting input of IC 19, a voltage comparator amplifier. IC's 12, 15, 16, 17, and 18 comprise an oscillator circuit similar to the one in the sine wave generator circuit description. The output of IC 18 is a triangular wave that is fed to the inverting input of IC 19. The triangular wave causes the comparator to switch and the output of IC 19 is a pulse width modulated signal. The pulse width is proportional to N_G actual. This signal is fed to IC 3, a negative selector, whose output is a pulse that has an amplitude proportional to $1/\sqrt{\theta}_{2.5}$ and a pulse width proportional to N_G actual. This multiplies N_{GA} and $1/\sqrt{\theta}_{2.5}$. IC 4 and IC 6 are amplifiers that filter and amplify the $N_{GA}/\sqrt{\theta}_{2.5}$ signal so that the IC 6 output is a dc voltage representing $N_{GA}/\sqrt{\theta}_{2.5}$. This voltage is fed to IC 11 that generates the N_{GR} vs. $N_G/\sqrt{\theta}_{2.5}$ schedule.

The β_c vs. $N_G/\sqrt{\theta}_{2.5}$ schedule circuit is comprised of IC's 10, 14, 20, 21 and 22. These generate a three slope schedule. IC 25 Q 1 and IC 26 form a synchronous demodulator circuit whose inputs are the β_c LVDT secondary signal and the square wave from the sine generator circuit. Demodulation is accomplished by switching Q1 on and off in the proper phase relationship with the β_c LVDT signal. The output of IC 26 is a DC voltage proportional to β_c position. This voltage is fed to IC 24 where it is subtracted from the β_c vs. $N_G/\sqrt{\theta}_{2.5}$ voltage. The output of IC 24 drives the β_c servovalve.

Figure N-9 (Drawing ACE-341) shows the processing circuits for PLA, P_{T2} , N_G and the servovalve driver. An electrical 0 to -10 volt PLA signal is fed to IC 1 a buffer amplifier, whose output goes to IC 25. IC 25 is used to switch from the N_{GA} signal to PLA when the fail signal is activated. The switch output goes to a variable saturation limit and integrator circuit consisting of IC's 2, 3, 4, 5, and 6. IC 4 and IC 5 are positive and negative signal selectors, respectively, and set the limit of the signal being applied to the integrator, IC 6. The limits are determined by the outputs of IC 11, an amplifier that sums N_{GA} - N_{GR} and the P_{T2} signal, and IC 2 (unity gain inverting amplifier). The PLA signal or the N_{GA} signal is applied to the input of IC 3 causing an error at its output. IC 6 will integrate until its output equals the input of IC 3. IC 2 is a unity gain amplifier that inverts the output of IC 6 and feeds this back to the input of IC 3.



REVISIONS		DATE	APPROVED
ZONE	DESCRIPTION		
C	DELETED IC12 IC13 IC14 Q2, C11, S2, S3, S4, S5		
E	C12, C13, AND R55 THROUGH R58		

UNLESS OTHERWISE SPECIFIED, DIMENSIONS ARE IN INCHES		SIGNATURES		NO. DATE	
ALL SURFACES	✓	DESIGNED	D. J. HALL	4-12-77	
		CHECKED	D. B. HALL	4-12-77	
		MATL.			
		ISSUED			
FOR G I USE ONLY		DRAWING NO.		DWG NO.	
SIMILAR TO		C 07482		A L F 3 3 9	
LVD		SCALE		30 1:00	
DW		SHEET		1	

GENERAL ELECTRIC
AIRCRAFT ENGINE GROUP - CINCINNATI, OHIO U.S.A.

Figure N-7 - Electrical Backup Control LVDT Sine Wave Generator.

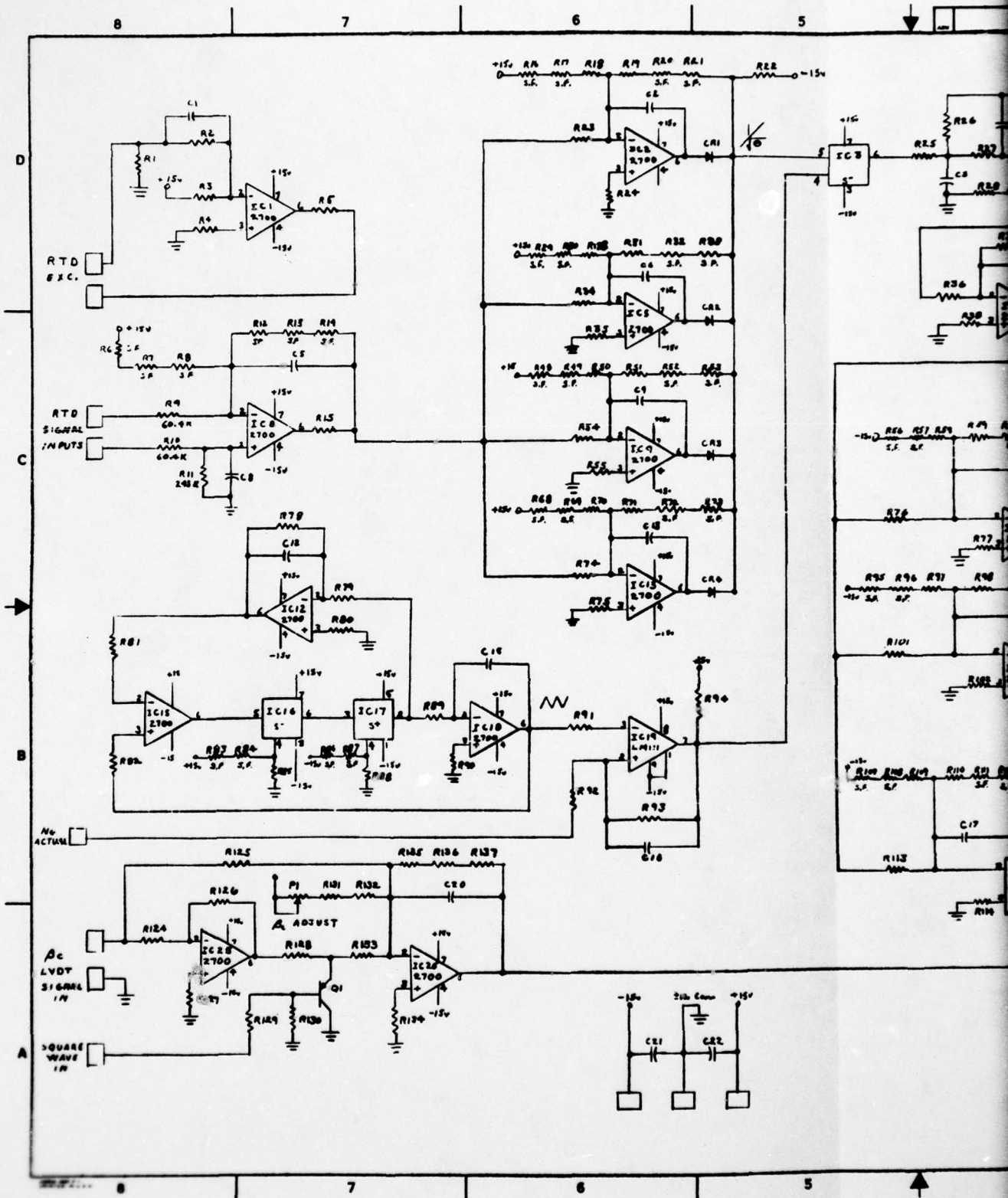
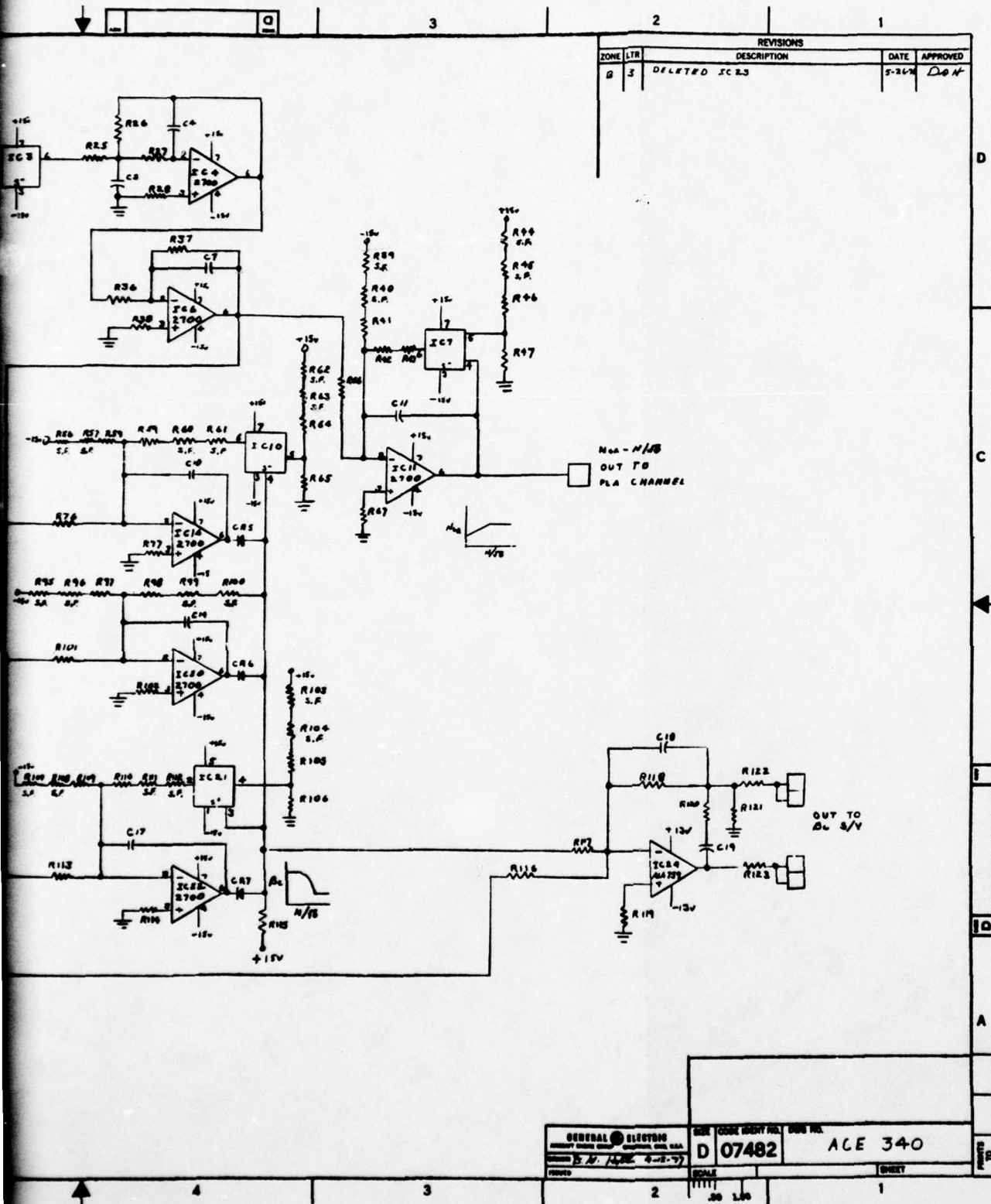


Figure N-8 - Electrical Backup Control T_{2.5}



Backup Control T_{2.5}, β_c Schedule Circuit.

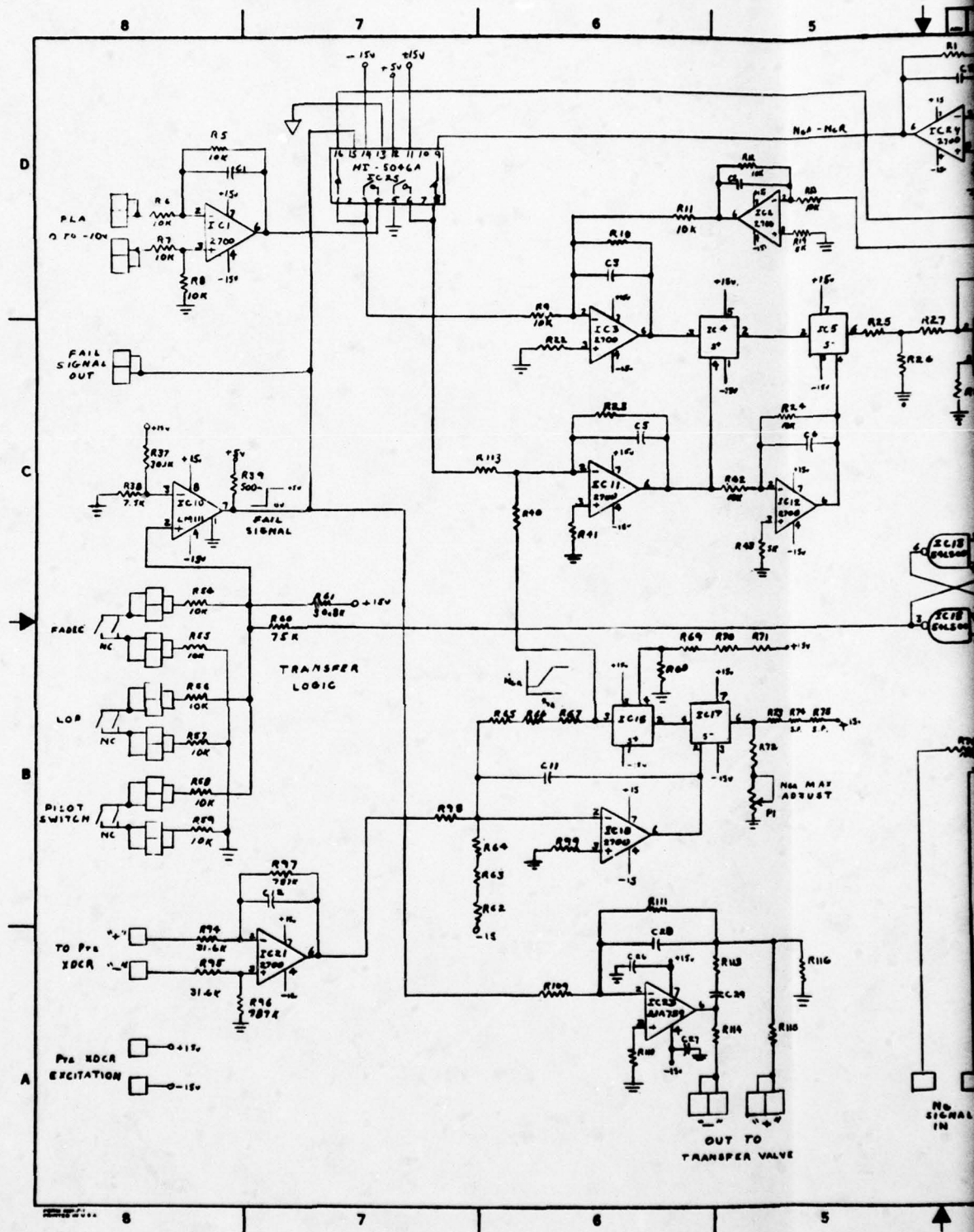
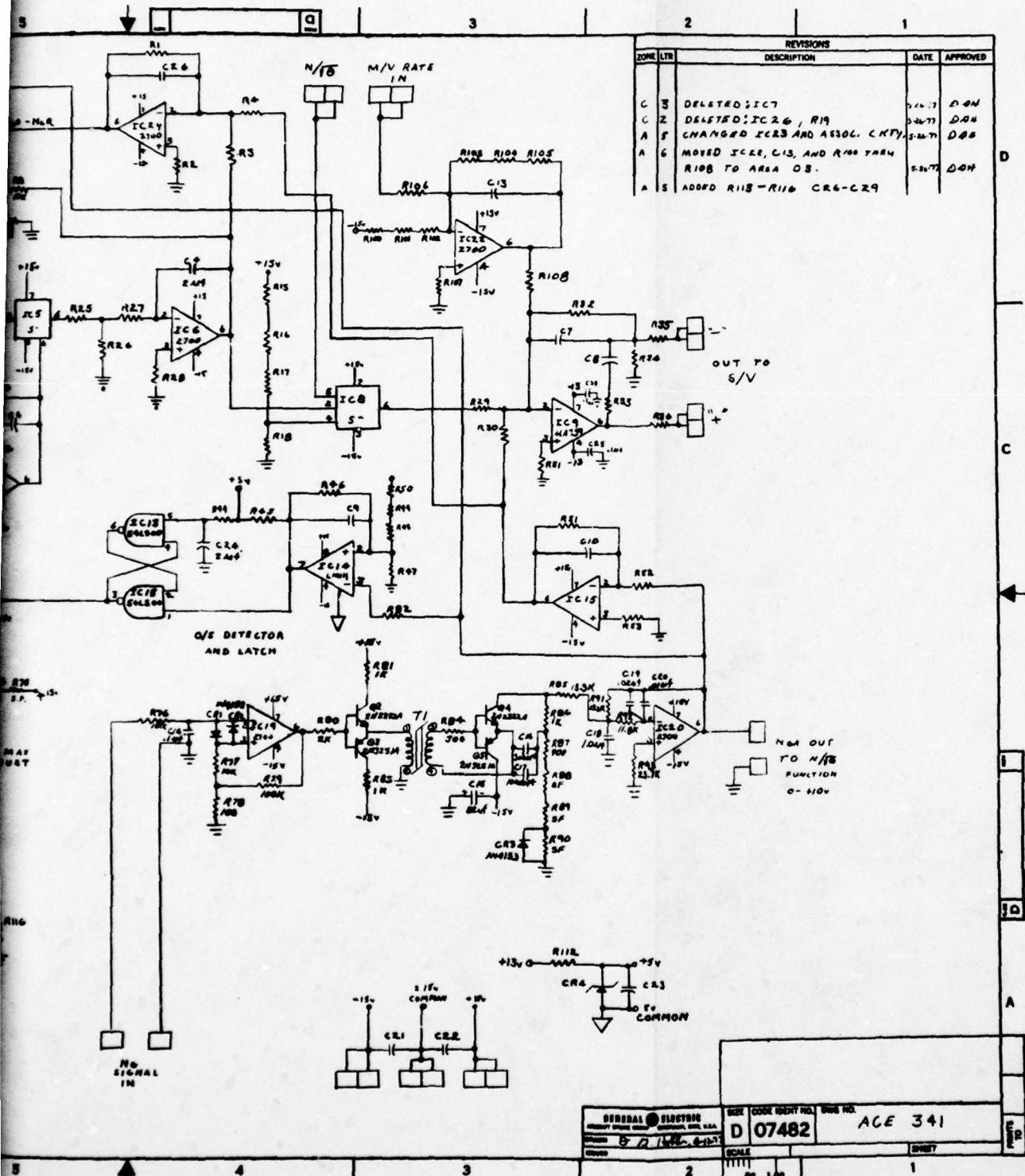


Figure N-9 - Electrical Backup Control



ical Backup Control PLA, P_{T2}, S/V Driver, N_G.

GENERAL ELECTRIC POWER ELECTRONICS DIVISION	SIZE CODE IDENT. NO. D 07482	BASE NO. ACE 341
SCALE 1/100		REVIT

The P_{T2} pressure transducer signal is processed by IC's 16, 17, 18, and 21. IC 18 and IC 21 are operational amplifiers to set the signal gain and IC 16 and IC 17 are signal selectors and set the min and max limits for P_{T2} . The output of IC 16 is fed to IC 11 where it is summed with the $(N_{GA} - N_{GR})$ signal and is used to set the variable saturation limits.

IC's 19 and 20, transistors Q2, Q3, Q4, Q5, and the associated circuitry process the N_G speed signal. The signal from the N_G pickup is fed to IC 19 and is processed by the following circuitry and the output of IC 20 is a DC signal representing N_{GA} . This output goes to four different points. One is to IC 15 where it is inverted and fed to the servovalve (S/V) driver amplifier, IC 9. Another is to switch IC 25 where it is connected to the input of the variable saturation circuit. The third is to the $N_G / \sqrt{\theta}_{2.5}$ function circuit and the fourth is to the overspeed (O/S) detector and latch circuit.

IC 14 is a comparator that is used to detect an overspeed condition. The O/S reference voltage is set by resistors R47 through R50. When an O/S is detected, IC 14 switches and sets the latch comprised of the two NAND gates of IC 13. The latch signal is fed to the fail signal detector, IC 10. This is a comparator amplifier and can also be switched by three other signals: (1) A signal from the digital control (FADEC), (2) a loss of power signal (LOP), and (3) a switch actuated by the pilot. The output of IC 10 actuates switch IC 25 and also provides the signal to IC 23, an amplifier that drives a transfer valve in the β_c and W_f loops.

IC 8 is a negative signal selector and selects the lowest amplitude of three signals: (1) the $N_G / \sqrt{\theta}_{2.5}$ limit voltage set by resistor divider consisting of R15 thru R18, (2) the output of IC 6, the PLA channel integrator, and (3) the $N / \sqrt{\theta}_{2.5}$ function signal. The output of IC 8 goes to IC 9 where it is summed with the N_{GA} signal and the metering valve (M/V) rate signal. IC 22 is an amplifier that scales the output of the M/V rate transducer to the desired value. The output of IC 9 provides the drive to the servovalve.

A preliminary flight weight packaging study was completed on the electrical backup control (see Figure N-10). Sound thermal and mechanical design is required to meet the desired control reliability in the on-engine environment. The packaging design had the following objectives:

- a. Small size and lightweight.
- b. High thermal capacity direct fuel cooling of electrical components with short, high conduction thermal paths from the components to the fuel.
- c. Reliable structural design taking into consideration isolation from high frequency vibrations, handling damage, and inspectability of parts.
- d. Quick and easy access to all the parts and electrical components for assemble, repair, and inspection.
- e. Low cost, high reliability, and minimum weight/space penalty as the result of the above.

An aluminum alloy cold plate provides means of supporting and cooling the hybrid substrates and discreet electrical components. The cold plate is a brazed assembly comprised of a 0.250 inch diameter by 0.030 inch wall serpentine-shaped fuel tube, external fuel port block, spacer rails, and 0.090 inch thick mounting plates. The cold plate is high frequency vibration isolated from the outside panels and control mounts. Vibration isolation is achieved by elastomer strips and grommets located at the points where the cold plate joins to the side panels.

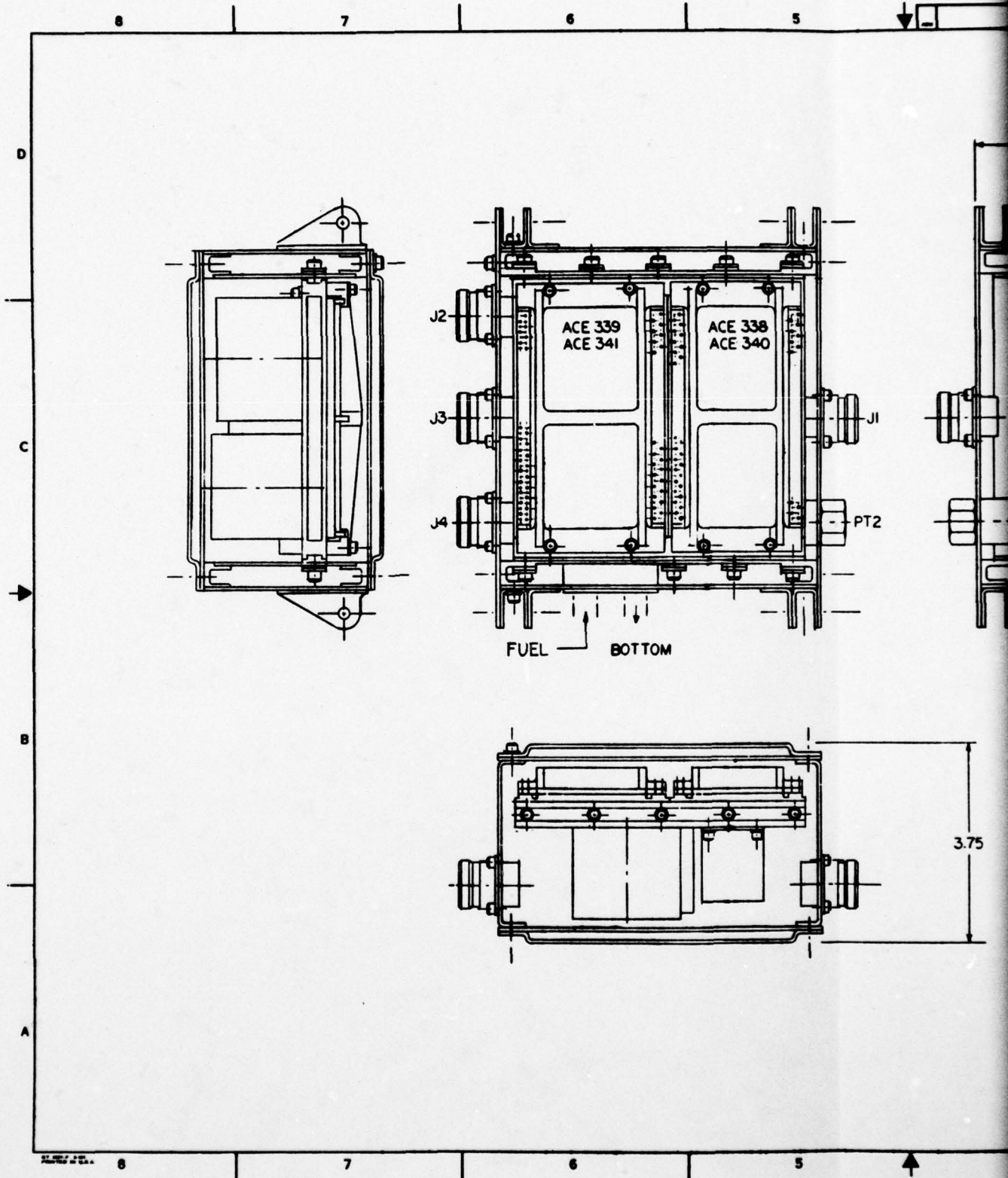
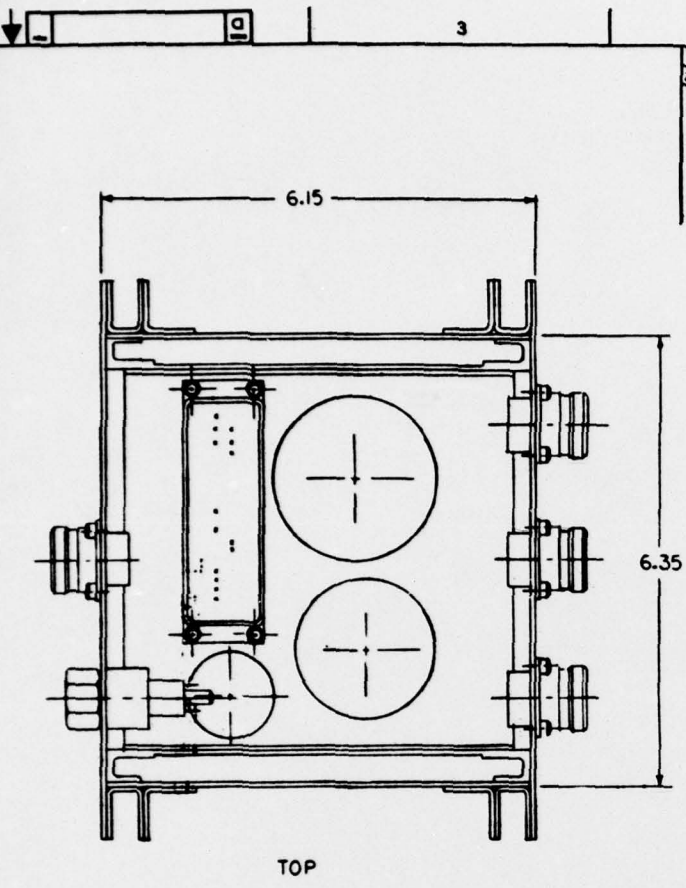


Figure N-10 - Backup Control I



REVISIONS				
ZONE	LTR	DESCRIPTION	DATE	APPROVED

D
 C
 B
 A
 10
 11
 12

3.75

TOP

UNLESS OTHERWISE SPECIFIED: DIMENSIONS ARE IN INCHES		SIGNATURES DESIGNER CHECKED KOFTINBERRY		MO-DA-YR 6-2-77		GENERAL ELECTRIC AIRCRAFT ENGINE GROUP CINCINNATI, OHIO, U.S.A.	
ALL SURFACES <input checked="" type="checkbox"/>		FINISH PAINT COLOR		SIZE D 07482		CODE IDENT NO. DWG NO. 61455L0	
FOR G E USE ONLY		SCALE 1:1		WT 250g		SHEET	

Backup Control Layout.

Double-wall 0.062 inch thick side panels are used to avoid handling damage to internal components and to provide radiation shielding from hot sections of the engine. Both top and bottom cover panels are also double walled and stiffening ribs are formed in the top and bottom cover panel brazed assemblies.

Aluminum precision castings are used to clamp the hybrid substrate boards to the cold plate. Silicone rubber strips are imbedded along the center and edges of these clamps, and the rubber acts as a spring to hold the substrate tightly to the cold plates. Figure N-11 shows design details of the hybrid multilayered boards. Several layers of alumina metallized with tungsten electrical runs will be stacked and fired to form an integral assembly. This type of multilayer substrate is available from several companies including Ceramic Systems, Metalized Ceramics, Minnesota Mining and Manufacturing, LDC Limited and Kyoceram International Incorporated. Multilayer alumina substrates with tungsten metallization are also used in packages for microelectronic devices. The typical board will be 0.060 inch thick. Silicon chips will be bonded to the board and Kovar beam leads will provide electrical connection from the chip to the board. Kovar pins near the edge of the board are used to make a wrap-and-solder joint to the multistrand wire which carries electrical communications to and from the board. Detrimental stresses in the board, chip, and electrical connections are avoided by the following:

- a. Matched low coefficients of thermal expansion;

Alumina board	2.7×10^{-6} in./in. °F
Silicon chip	1.7×10^{-6} in./in. °F
Kovar beam leads and pins	2.8×10^{-6} in./in. °F
Tungsten runs	2.6×10^{-6} in./in. °F
- b. Ductile bonds using lead/tin, indium/lead, or gold/silicon.
- c. Flatness of 0.001 inch over the mounting surface of the board and the surface of the aluminum cold plate.
- d. Special heat treatment of the cold plate to assure dimensional stability.
- e. Uniformly distributed and maximum-load-limited board clamping provided by silicone rubber strips at the board edges and center.
- f. Low shear modules of rubber strips permits the board to slip relative to the cold plate during thermal extremes.

Fuel cooling of the hybrid boards and discreet modules is a very important attribute of the design. The cold plate also serves to provide a rigid, constant-temperature surface on which to clamp the ceramic hybrid boards. Each cold plate is nearly 0.5 inch thick and designed so as to avoid any bending loads or distortion which if transmitted to the hybrid board could lead to electrical failure. General Electric has developed a special heat treatment involving sequential cryogenic and elevated-temperature soaks to achieve thermal/dimensional stability in 6061-T6 aluminum. A flat-face fuel port is provided with a Gask-O-Seal flange external to the control. No fuel joints or seals are used inside the control, and the serpentine-shaped fuel tubes have thick 0.030 inch walls to avoid the possibility of fuel leakage inside the control.

The control is not hermetically sealed. All internal electrical components are either contained in alumina or aluminum enclosures or potted with silicone rubber. All wire connections are potted and all wiring has adequate PVC insulation. Metal parts are either anodized or stainless steel. No fungus

	Plating	Bond (Liquidus)
A	Tungsten to Kovar	Pb/Sn 60/40 (240° C)
B	Copper to Kovar	Pb/Sn 63/37 (228° C)
C	Tungsten to Tungsten	In/Pb 50/50 (320° C)
D	Silicone to Tungsten	Au/Si (435° C)
E	Aluminum to Kovar	T/C (480° C)
F	Kovar to Tungsten	Pb/Sb 98/2 (320° C)

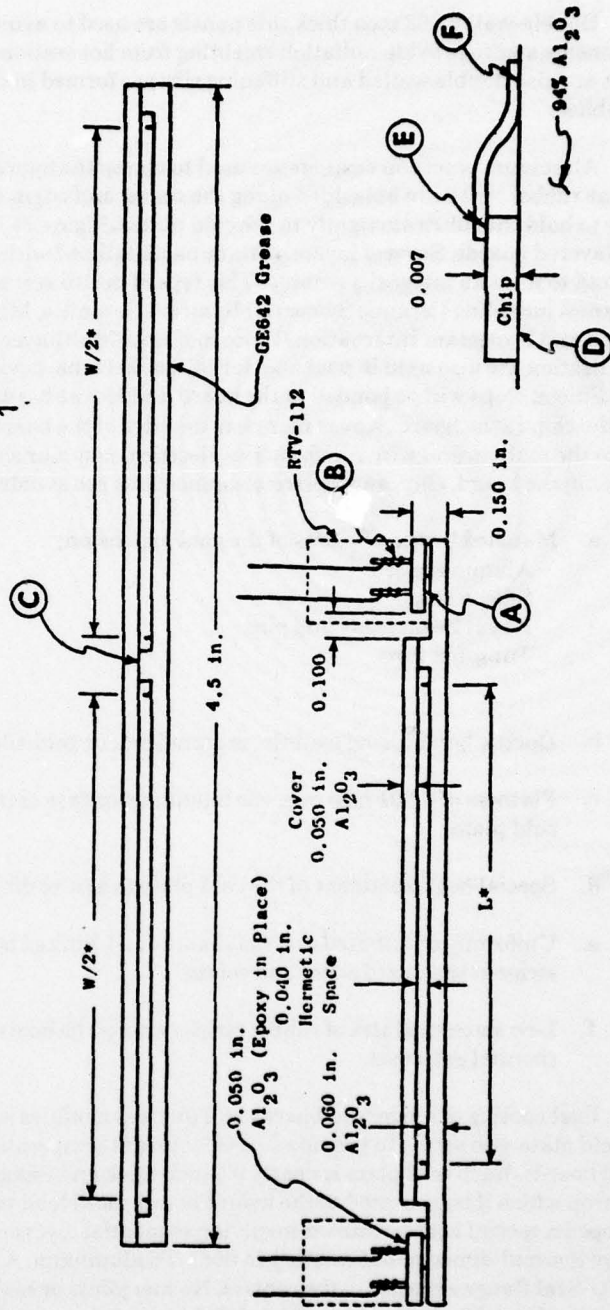
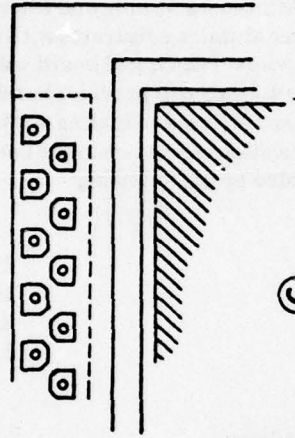


Figure N-11 - FADEC Substrate Cross Section.

supporting materials are used. Hybrid boards have their own integral covers to provide a hermetic seal of circuit elements.

The major concern with vibration is with respect to high frequencies which could produce resonant excitation of the small structures associated with hybrid and other electrical components. Experience (F101 tests, etc.) had shown that silicone rubber potting is an excellent way to eliminate high frequency vibrations in the control. Damping using silicone rubber potting is effective because of the relatively large energy absorption mass of RTV and the high velocities/low displacements of higher frequency vibrations. Although customary vibration test frequencies are below 2000 Hz, it is the frequencies above 2000 Hz which may be most damaging to the very small elements of electrical components. High frequency vibration may be mechanically induced by fan or compressor blade passing frequencies, fluid flow pulsations, or gear meshing frequencies. Noise is another source, and panel resonance of the control box may amplify noise into mechanical vibration. RTV potting is used in all sensitive areas except the hybrid boards. In order that higher frequency vibration does not enter the hybrids, elastomer dampening strips are provided at the point where the cold plate and chassis join at the control side plates. RTV rubber dampening strips are also provided between the clamps and the hybrid boards.

3. RELIABILITY ANALYSIS

a. Analysis Procedural Tools

The electronic circuitry portions of the electrical backup control were analyzed in a manner similar to that used for FADEC. This consisted primarily of utilizing MIL-HDBK-217B, "Military Standardization Handbook Reliability Prediction of Electronic Equipment" reliability prediction procedures for microelectronic devices.

The electronic circuitry is shown by Figures N-6 through N-9. The types of elements and the number of each are shown in Table N-1. The base failure rate for each type of element was calculated per the procedures given in the handbook for a junction temperature of 38°C. The base failure rates due to substrate and film processing, network complexity and substrate area, resistor/resistance tolerance and hybrid package were also calculated. The base failure rates are shown in Table N-1. The base failure rates were multiplied by the following factors to give the modified failure rates also shown in Table N-1:

π_T	- Temperature factor at junction temperature of 85°C	3.75
π_E	- Environmental factor (ground fixed)	1.0
π_Q	- Quality factor (Class A MIL-M-3810)	0.5
π_F	- Circuit function factor (digital hybrids)	0.8

The temperature factor was based on 95% of the time at 79°C and 5% of the time at 98°C. The product of all the factors is 1.5.

Electrical and hydromechanical component failure rates were found by using either the Reliability Analysis Program (RAP) method or by similarity with comparable components from other engine control systems, particularly the FADEC system.

b. Analysis Results

The components included in the electrical backup control are shown in Figure N-12. The Unscheduled Component Removal (UCR) rates for the components are shown in Table N-2. The UCR rates are equivalent to the modified failure rates shown on Table N-1.

Table N-2 gives the estimated Get Home Power Loss (GHPL) rates when primary and backup control are combined. As mentioned previously, the electrical backup control is on standby. In addition, the pilot can block transferring to the backup control or switch back to primary control by means of the override switch. The outputs of the backup W_f and β_c servovalves are blocked during primary mode operation. This combination of features results in that most of the failures will be "loss of protection". Remembering the above, each component was studied in regards to what fraction of the UCR's would result in power loss. Some may feel the GHPL rate is actually lower than the estimate because of the pilot override switch. Also, inadvertant transfer to backup due to an erroneous overspeed signal or a false signal from the primary control does not necessarily mean power loss. It can be seen logically that, when a backup control with these features is combined with the electrical primary control, few GHPL failures will occur.

TABLE N-1
ELECTRICAL BACKUP CONTROL CIRCUITRY PARTS COUNT AND RELIABILITY

Component	Element	Qty.	Base FR/10 ⁶ hrs/ Element	Modified FR/10 ⁶ Hrs.
Power Supply (ACE 338)	Op Amp	2	.0285	Total .268
	Resistor	14	.0005	
	Capacitor	15*	.0004	
	Transistor	6	.0053	
	Diode	16	.0048	
	Transformer	2*	.0267	
LVDT Sine Wave Generator and LVDT Demod- ulator (ACE 339)	Op Amp	12	.0285	Total .553
	Resistor	34	.0005	
	Capacitor	11	.0004	
	Transistor	1	.0053	
T _{2.5} , β_c Schedule Circuits (ACE 340)	Op Amp	25	.0285	Total 1.07
	Resistor	90	.0005	
	Capacitor	22	.0004	
	Transistor	1	.0053	
	Diode	7	.0048	
PLA, P _{T2} , S/V Driver, N _G (ACE 341)	Op Amp	22	.0285	Total 1.248
	Resistors	84	.0005	
	Capacitors	26	.0004	
	Transistor	4	.0053	
	Diode	3	.0048	
	Transformer	1*	.0267	
Hybrid Assemblies	Substrate	2	.04	Total 1.60
	Network	2	.10	
	Tolerance (Resistors)	2	.11	
	Package	2	.82	

*Not available as a chip

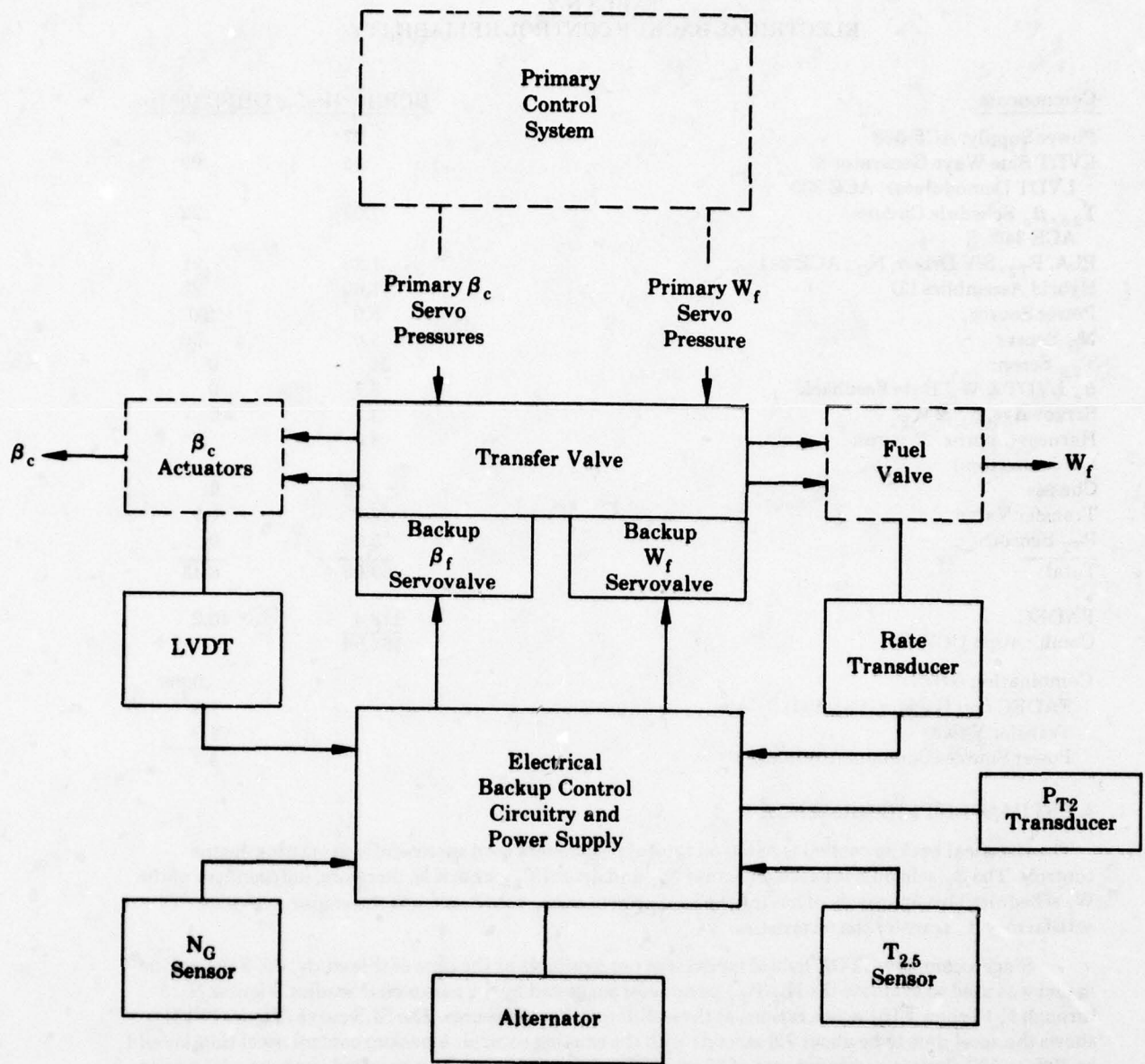


Figure N-12 - Components Included In The Electrical Backup Control.

TABLE N-2
ELECTRICAL BACKUP CONTROL RELIABILITY

<u>Components</u>	<u>UCR/10⁶ Hrs.</u>	<u>GHPL/10⁶ Hrs.</u>
Power Supply; ACE 338	.27	.05
LVDT Sine Wave Generator & LVDT Demodulator; ACE 339	.55	.09
T _{2.5} , β _c Schedule Circuits; ACE 340	1.07	.20
PLA, P _{T2} , S/V Driver, N _G ; ACE 341	1.25	.21
Hybrid Assemblies (2)	1.60	.25
Power Source	5.0	2.9
N _G Sensor	5.0	.50
T _{2.5} Sensor	21	0
β _c LVDT & W _F Rate Feedback	3.7	0
Servo valve, β _c & W _F	3.7	0
Harness (approx. 28 wires, 9 connectors)	8.0	.8
Chassis	.32	0
Transfer Valve	7.2	1.5
P _{T2} Sensor	5.0	0
<u>Total</u>	<u>63.66</u>	<u>6.45</u>
FADEC	118.4	40.2
Combination UCR	<u>182.06</u>	
Combination GHPL:		.0005
FADEC and Backup (Parallel)		1.5
Transfer Valve		2.9
Power Source (Common Alternator)		<u>4.4</u>

4. ESTIMATED PERFORMANCE

The electrical backup control is based on typical parameters used successfully in existing engine controls. The β_c schedule is based on actual N_G and actual T_{2.5} and, it is, therefore, independent of the W_f schedule. This approach, of having the backup control β_c schedule track the engine, provides satisfactory β_c transfer characteristics.

Since a complete JTDE hybrid model was not available at the time of this study, the F101 engine model was used to evaluate the N_G/P_{T2} parameter suggested by the parametric studies. Figures N-13 through N-15 show F101 accelerations at three different P_{T2} pressures. The SLS curve (Figure N-13) shows the accel time to be about 7.8 seconds with the existing control. A backup control accel time should be 30% to 50% longer so a speed rate of 30 rpm/sec/psia was selected. This resulted in about a 10 second accel on the backup control. A fighter engine would have a normal accel time of about 5 seconds so a 7.5 nominal accel time on backup control is expected. A review of the plotted responses indicate the backup control \dot{N}_G (slope) is less than the existing \dot{N}_G at all speeds. The P_{T2} correction factor appears satisfactory at 10.1 psia and conservative at 5.9 psia. It is intended that the speed rate (\dot{N}_G) not increase at P_{T2} greater than 14.7 psia so the margin between the backup \dot{N}_G and existing \dot{N}_G increases as P_{T2} increases. Backup control dynamics, probably of the proportional plus integral type, will compensate for the lag between W_f and N_G. Appendix H provides additional estimated performance data.

The input into the electrical backup control is N_G (actual) during primary mode operation. Again, the N_G portion of the control is tracking the engine. Upon transfer, the input is switched to the N_G requested by PLA. Any difference, however, goes through the \dot{N}_G limit device so acceptable transfer characteristics are expected.

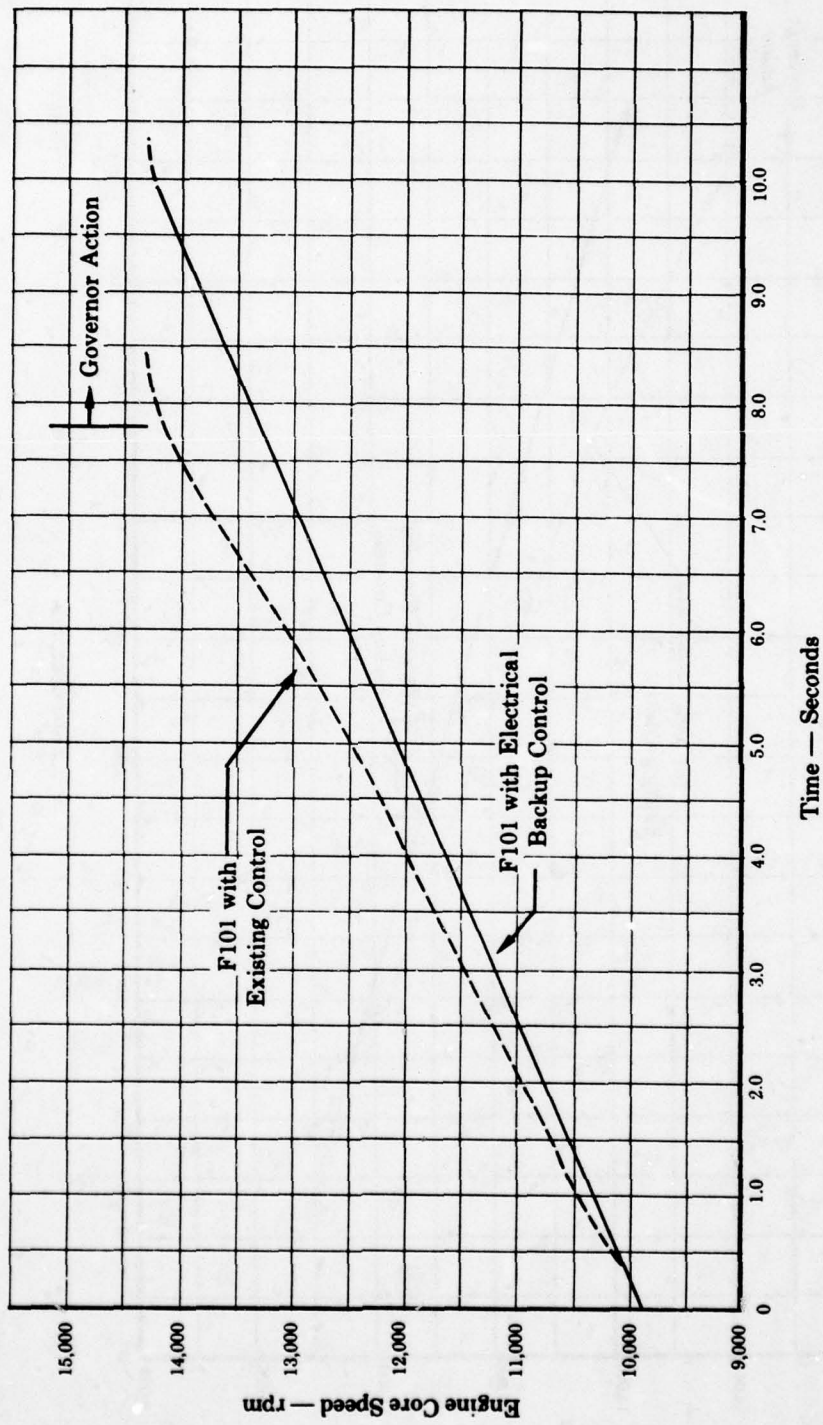


Figure N-13 - Estimated Response of Electrical Backup Control to a Throttle Burst at SLS (\dot{N}_G — 30 rpm/sec/psia).

AD-A055 658

GENERAL ELECTRIC CO CINCINNATI OHIO AIRCRAFT ENGINE GROUP F/G 21/5
BACKUP CONTROL FOR A VARIABLE CYCLE ENGINE.(U)

DEC 77 H B KAST, G L POPPEL, J E HURTLE

F33615-76-C-2086

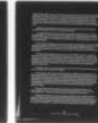
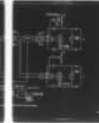
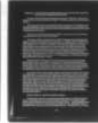
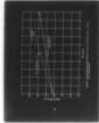
UNCLASSIFIED

77AEG-633

AFAPL-TR-77-92

NL

3 OF 3
ADA
055658



END
DATE
FILMED
8-78
DDC

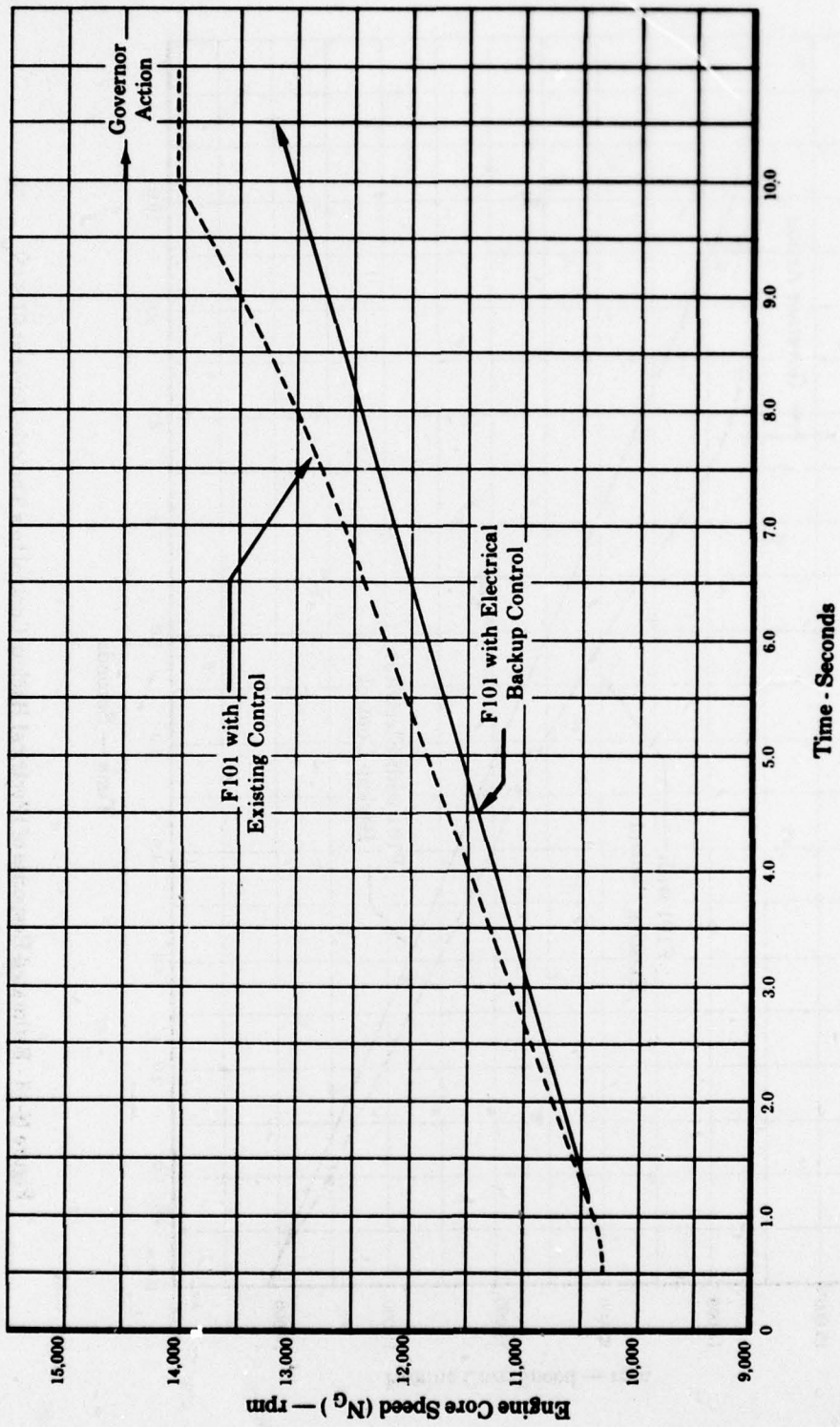


Figure N-14 - Estimated Response of Electrical Backup Control to a Throttle Burst at $P_{T2} = 10.1$ psia ($\dot{N}_G = 30$ rpm/sec/psia).

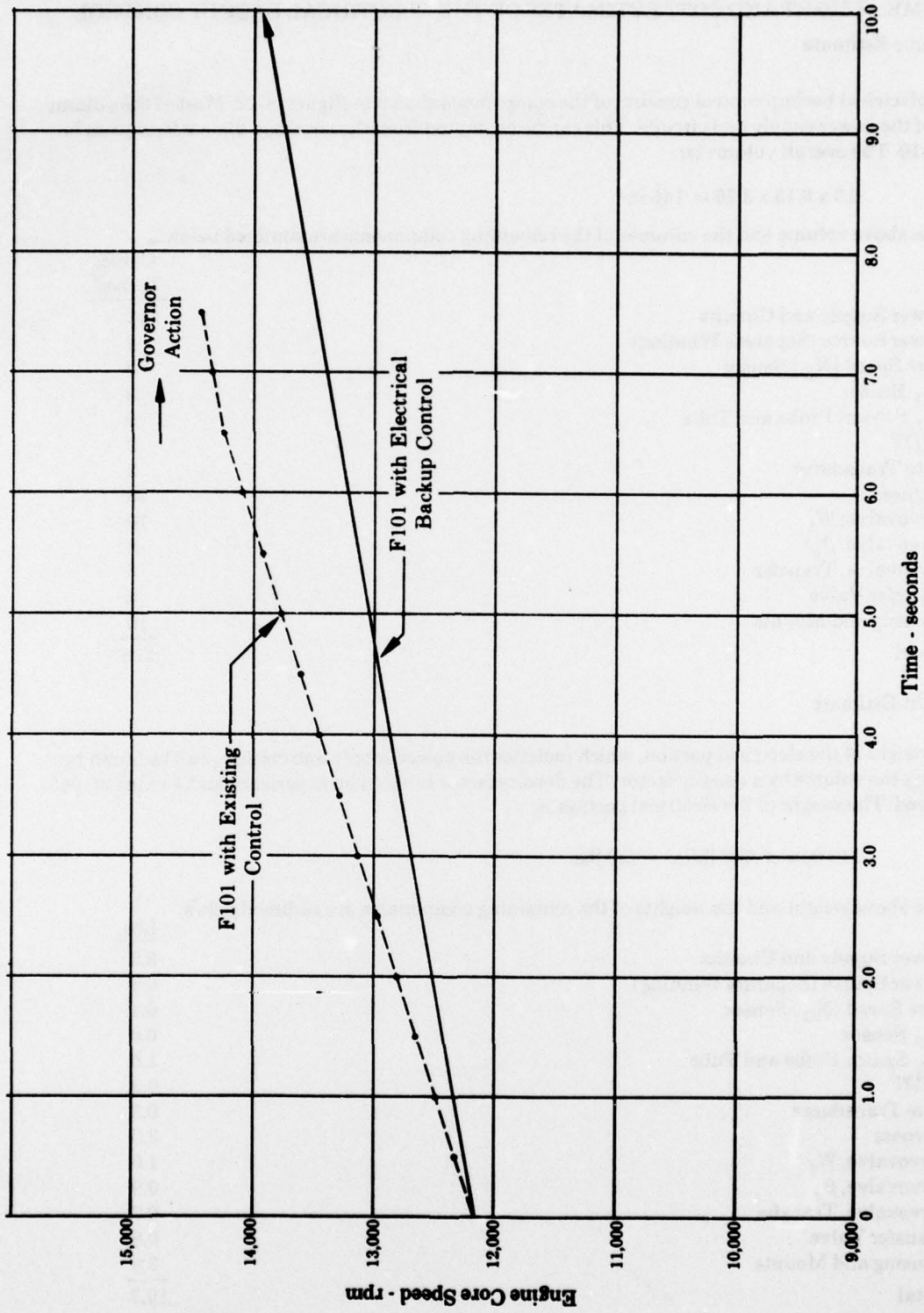


Figure N-15 - Estimated Response of Electrical Backup Control to a Throttle Burst at $P_{T2} = 5.91$ psia ($\dot{N}_G = 30$ rpm/sec/psia).

5. VOLUME, WEIGHT AND COST ESTIMATES OF THE ELECTRICAL BACKUP CONTROL

a. Volume Estimate

The electrical backup control consists of the components shown in Figure N-12. Most of the volume consists of the power supply and circuits. This can be estimated from the envelope dimensions given in Figure N-10. The overall volume is:

$$6.5 \times 6.15 \times 3.75 = 146 \text{ in}^3$$

The above volume and the volumes of the remaining components are summed below:

	<u>Cubic Inches</u>
Power Supply and Circuits	146
Power Source (Separate Winding)	2
Core Speed (N_G) Sensor	2
$T_{2.5}$ Sensor	3
P_{T_2} Sensor, Probe and Tube	9
LVDT	2
Rate Transducer	2
Harness	23
Servo valve, W_f	10
Servo valve, β_c	9
Servo valve, Transfer	6
Transfer Valve	4
Housing and Mounts	<u>10</u>
Total	228

b. Weight Estimate

The weight of the electrical portion, which includes the power supply and circuits, can be found by multiplying the volume by a density factor. The density factor is based on experience and a value of .043 lb/in³ is used. The weight of the electrical portion is:

$$146.0 \text{ in}^3 \times .043 \text{ lb/in}^3 = 6.3 \text{ lbs.}$$

The above weight and the weights of the remaining components are summed below.

	<u>Lbs.</u>
Power Supply and Circuits	6.3
Power Source (Separate Winding)	0.4
Core Speed (N_G) Sensor	0.4
$T_{2.5}$ Sensor	0.6
P_{T_2} Sensor Probe and Tube	1.5
LVDT	0.3
Rate Transducer	0.3
Harness	3.0
Servo valve, W_f	1.0
Servo valve, β_c	0.9
Servo valve, Transfer	0.7
Transfer Valve	0.8
Housing and Mounts	<u>3.5</u>
Total	19.7

c. Cost Estimate

The major portion of the electrical backup control cost is in the power supply and circuits. The estimates can be divided into materials, subcomponents and labor.

Hybrid Boards (2)	\$1200
Chassis and Cover	450
Power Supply	900
Connector Set (4)	240
Miscellaneous Hardware	500
Labor for Board Assembly and Test	800
Wiring and Waterproofing	1400
Final Electrical Checkout	80
Total	\$5570

Again the cost estimates are based on 1977 dollars, 1000th unit and a 100 unit order. The above cost and those of the remaining components are summed below.

Power Supply and Circuits	\$ 5,570
Power Source (Separate Winding)	140
Core Speed (N_G) Sensor	100
$T_{2.5}$ Sensor	300
P_{T_2} Sensor, Probe and Tube	370
LVDI	185
Rate Transducer	185
Servo valve, W_f	1,100
Servo valve, β_c	700
Transfer Valve	700
Harness	700
Housing, Brackets, Fasteners, etc.	800
Servo valve, Transfer	350
Total	\$11,100

APPENDIX O - FLUIDIC BACKUP CONTROL HAVING FUEL FLOW SETTING, WITH FUEL RATE LIMITS IN SERIES CONFIGURATION

A schematic of the fluidic approach of the backup control is shown in Figure O-1. Figure O-2 is a breakdown of the functional blocks identified in Figure O-1. The W_f/P_{T2} parameter was also used for this approach.

The mechanization is based on stock amplifiers, resistors and capacitors. The amplifiers are a mix of standard size amplifiers (0.02 in. nozzle width) and miniature amplifiers (0.01 in. nozzle width). The miniature amplifiers are used where high input-output characteristics plus very fast response are required to mechanize a particular function.

There are two functions in the system which are difficult to mechanize with conventional fluidic components. These are the rate limit and the multiplier.

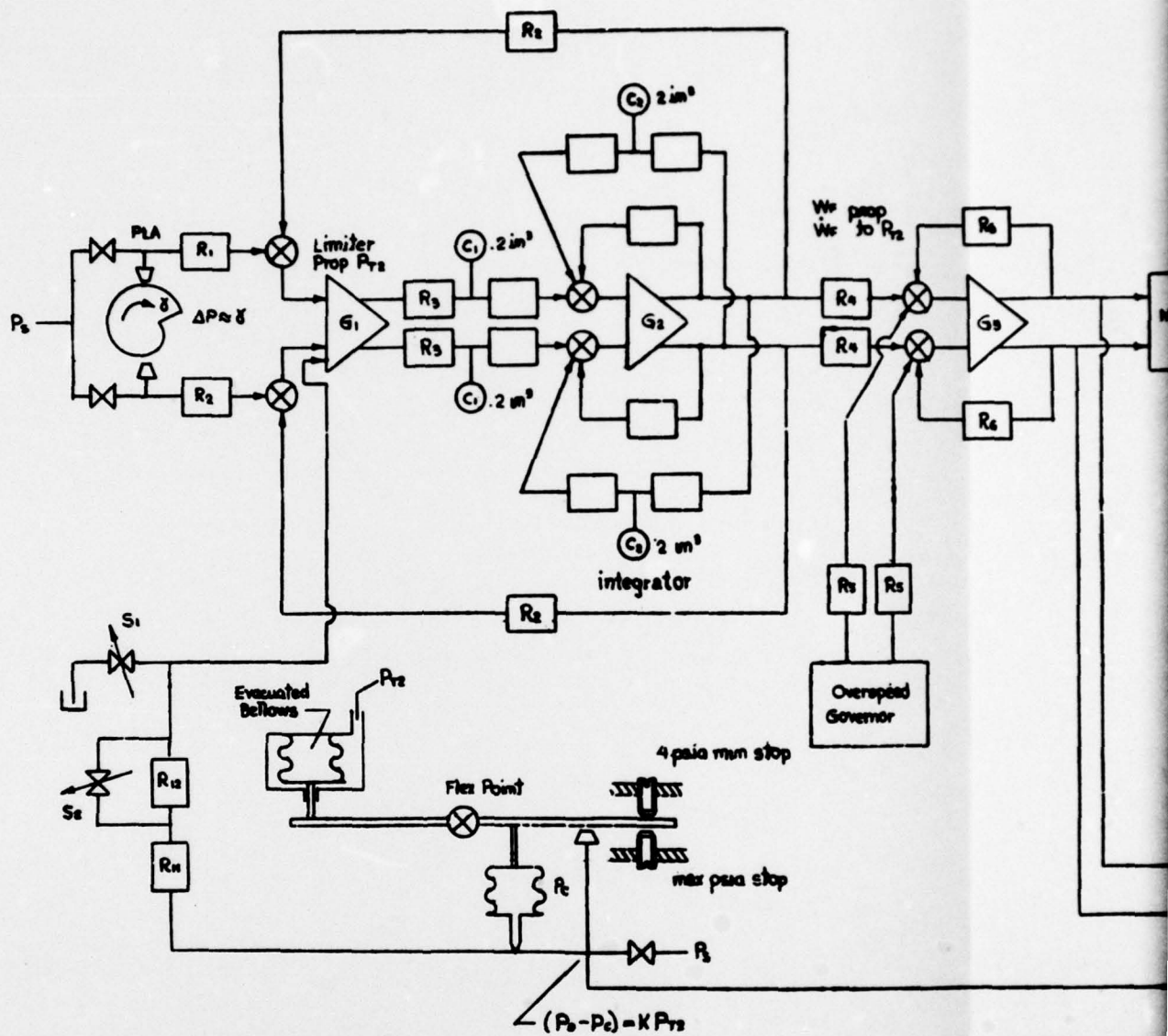
The rate limit requires an integration function. The traditional method of mechanizing a fluidic integrator is basically the same as the electronic counterpart, i.e., a high gain operational amplifier with resistor and capacitors in the feedback. The high gain operational amplifier presents no problem in the fluidic integrator, however, the characteristics of the fluidic resistors and capacitors vary with both ambient temperature and the absolute pressure of the environment. The nominal output rate of the integrator will be inversely proportional to the product of a resistor and capacitance. Typically, if we assume the operating fluid (compressor discharge air) tracks the ambient air temperature, an ambient range of -65 to 400°F will result in a 25% change in rate output. (Rate increases with increasing temperature.) In the mechanization of Figure O-1, the temperature effect is compensated by conditioning the P_{T2} signal. The specified accuracy on rate is $\pm 7\%$, thus compensation is a reasonable approach for taking care of ambient temperature variations.

The resistor/capacitor (RC) product will vary inversely and the output rate directly with the absolute pressure of the air surrounding the components. The conventional method of coping with altitude effects on fluidic components is to put the fluidics in an enclosure and vent all flow to ambient through a choked orifice. This establishes an absolute pressure environment whereby the pressure ratio across amplifiers and other components stays within a workable range. Where only proportional gain or noncritical frequency dependent functions are performed this technique is generally adequate.

In the backup control an absolute pressure regulator will be required to hold the circuit enclosure at an absolute pressure of 5 psia. The multiplier required for this application must have a linear range of approximately 60:1 on the fuel demand input. This range has not been demonstrated on any practical fluidic device. The general approach of using a PDM circuit where pulse width is a direct function of one input and pulse height a function of the second input. This has the potential of achieving the required range. A linear range of 20:1 on pulse width has been demonstrated on a PDM circuit developed for a missile guidance system. The output of this particular PDM was at a high flow and pressure level, requiring large amplifiers. The range was limited by the response time of the amplifiers. Redesign of the basic circuit by miniaturizing the critical amplifiers and reducing the power output levels should extend the range by the 3:1 factor required for the backup system. The PDM oscillator and wave shaping networks also use resistance and capacitive components. Consequently, the multiplier also requires a controlled ambient pressure.

Referring to Figure O-1, operation of the system is as follows:

Throttle position is converted to a push-pull pressure differential by a cam linked to the throttle. The cam varies the skirt area of two nozzles. The nozzles in conjunction with two upstream orifices produce a pressure differential linearly related to cam rotation. This pressure signal is applied through a summing junction to the input of a 3 stage proportional amplifier (G_1). The nozzle supply for the last stage is generated by the P_{T2} sensor, hence the saturated output of G_1 is proportional to P_{T2} . For rapid



S_1 & S_2 ported by primary fuel control servovalve spool
 S_1 - open on decel, closed on backup & accel
 S_2 - open on accel, closed on backup & decel

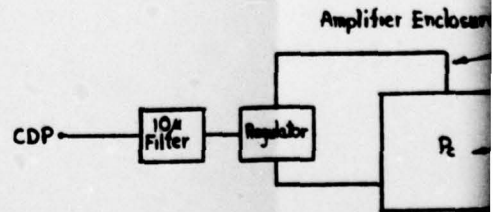
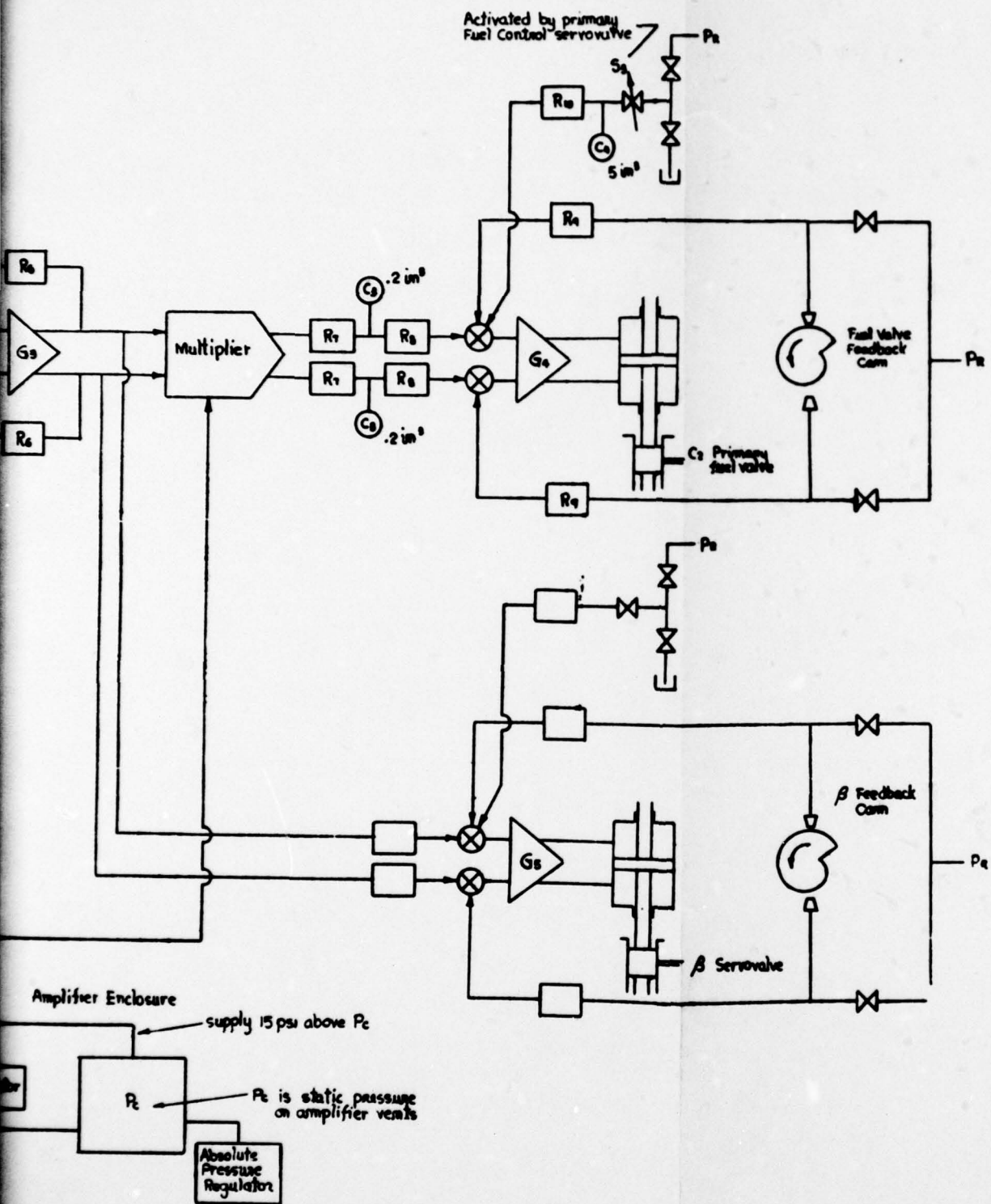


Figure O-1 - Fluidic Backup Control For V



Map Control For Variable Cycle Engine.

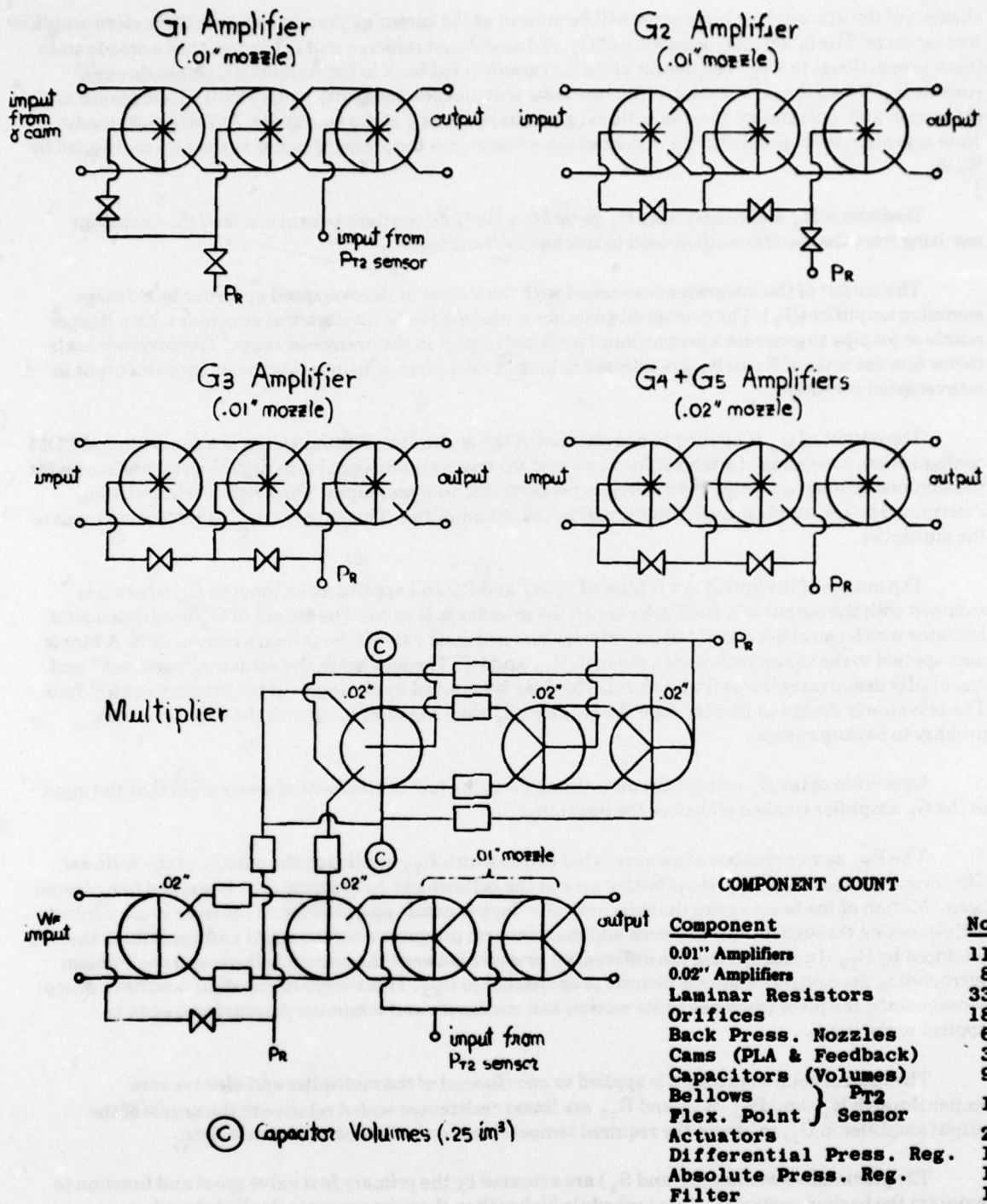


Figure O-2 - Amplifier Stackups.

changes of throttle angle, a large error will be present at the summing junction and the three stage amplifier will saturate. The integrator, consisting of G_2 and associated resistors and capacitors, has a steady state input proportional to P_{T2} . The output of the integrator is fed back to the summing junction through resistor R_2 . When the error signal at the summing junction becomes sufficiently small, G_2 comes out of saturation and operates on the proportional gain characteristic of the amplifiers. At this point steady state operation is achieved and the output of the integrator is the pressure signal at the cam multiplied by R_2/R_1 .

Resistance R_3 and capacitance C_1 generate a lag time constant to cancel a lead time constant resulting from the specific method used to mechanize the integrator.

The output of the integrator is summed with the output of the overspeed governor by a 3 stage summing amplifier (G_3). The overspeed governor is assumed to be an electrical governor with a flapper nozzle or jet pipe to generate a proportional push-pull signal in the overspeed range. The governor scale factor and the ratio of R_5 to R_4 are selected to permit the governor to override the integrator output in an overspeed condition.

The output of G_3 is applied to one channel of the multiplier. The multiplier is a conventional PDM configuration, consisting of a triangular wave and the analog input signal plus digital elements to convert the summed signals to a pulse width directly proportional to signal input. The height of the pulse is determined by the supply pressure to the digital output amplifier. This supply (P_{T2}) is the second input to the multiplier.

The output of the multiplier is filtered by R_7 and C_3 and applied as an input to G_4 where it is summed with the output of a feedback cam on the primary fuel valve. The output of G_4 positions a pilot actuator which can effect control of the primary fuel metering valve if the primary control fails. A bias is also applied to the summing junction through R_{10} and C_4 . The bias holds the actuator "hardover" and essentially deactivates the backup control. This bias is removed by closing S_3 if the primary control fails. The bias slowly decays to zero through the R_{10} and C_4 time constant to smooth the transition from primary to backup control.

Operation of the β_c control circuit is the same as the fuel control with the exception that the input to the G_5 amplifier is taken off before the multiplier.

The P_{T2} sensor consists of an evacuated bellows with P_{T2} applied to the outside of the bellows. The torque generated by P_{T2} , the effective area of the bellows and its moment arm, is applied to a pivoted beam. Motion of the beam varies the skirt area of a flapper nozzle and produces a pressure in the control bellows acting through its effective area and moment arm produces a torque equal and opposite to that produced by P_{T2} . In steady state the differential pressure between the control bellows and the ambient surrounding the control bellows is directly proportional to P_{T2} . This torque summation does have droop; consequently, the pivot beam has finite motion and maximum and minimum pressure stops can be applied to the beam.

The control bellows pressure is applied to one channel of the multiplier and also the rate limiter through R_{11} and R_{12} . R_{11} and R_{12} are linear resistances scaled relative to the nozzle of the output amplifier in G_1 , to obtain the required temperature compensation on the rate limit.

The pneumatic switches (S_1 and S_2) are actuated by the primary fuel valve spool and function to maintain the backup control transient schedule higher than the primary control schedules when on primary control and accelerating, S_2 is open and S_1 is closed. This increases the P_{T2} pressure applied to the G_1 limiter and increases the rate schedule. On decel, S_2 is closed and S_1 is open which decreases the P_{T2} pressure, and consequently, reduces the rate limit. On backup control, both S_1 and S_2 are closed.